A therapeutic roadmap for ovarian cancer using TLR4 MyD88 and MAD2 as prognostic indicators

A thesis submitted to Trinity College,
University of Dublin,
For the degree of
Doctor of Philosophy
November 2015

By Mark Bates

Department of Histopathology and Morbid Anatomy,
Trinity College, Dublin

Trinity College Dublin

The University of Dublin

Under the supervision of
Professor John O'Leary, Dr Sharon O'Toole,
Dr Amanda McCann, Dr Michael Gallagher,
Dr Cathy Spillane and Dr Cara Martin

Declaration

I hereby certify that the work in this thesis has not been submitted for any other degree or diploma at this, or any other university, and that all of the work described herein is entirely my own except where otherwise acknowledged. This thesis may be made available from the library for lending, consulting or copying.

I have read and I understand the plagiarism provisions in the General Regulations of the University Calendar for the current year, found at http://www.tcd.ie/calendar.

I have also completed the Online Tutorial on avoiding plagiarism 'Ready Steady Write', located at http://tcd-ie.libguides.com/plagiarism/ready-steady-write.

_____

Mark Bates

Acknowledgements

This study was funded by a PhD Scholarship from the Royal City of Dublin Hospital Trust, the Emer Casey Foundation and SOCK (Supporting Ovarian Cancer Knowledge). A special thank you goes to our funding bodies for supporting this work.

I would like to give a huge thank you to my supervisors Professor John J. O'Leary, Dr. Sharon O'Toole, Dr. Cathy Spillane, Dr. Michael Gallagher, Dr Cara Martin and Dr. Amanda McCann. Each of you has given me the expertise, guidance and encouragement needed to be able to complete this research project to the highest possible standards. Your help has been invaluable in developing the project and myself to be a more independent and confident researcher. I really appreciate everything you have done for me over the last three years.

A huge thank you to everyone who has passed through the Molecular Pathology Research Lab at the Coombe Hospital and everyone over at the Department of Obstetrics and Gynaecology at the Institute of Molecular Medicine St James' Hospital especially, Claudia Gasch, Anthony Cooney, Gomaa Suliman, Dr. Itunu Soyinbe, Dr. Katherine McAllister, Dr Helen Keegan, Dr Antonino Glaviano, Dr. Lynne Kelly, Dr. Prerna Tewari, Dr. Brendan Ffrench, Dr. Christine White, Dr. Victoria McEneaney and Dr Fiona Martin.

Thanks to everyone over at the Sir Patrick Dunns Research Laboratory over the past years especially, Louise Flynn, Lauren Brady, Steven Busschots and Dr. Paul Smith. I would also like to thank Dr.Gordon Blackshields for all the help and many hours spent working on bioinformatics related analyses. Thanks to Dr. Stephen Smith of the Microbiology Department in the Central Pathology Research Lab, for allowing us to use facilities and equipment.

Thanks to Mrs. Jacqui Barry-O'Crowley of the Histopathology Department at the Coombe hospital for her expert guidance on Immunohistochemical staining.

I would also like to thank Dr. Ciaran O Riain who reviewed and marked all ovarian cancer tumour specimens which were used over the course of this study. Thanks to Dr. Danielle Costigan, Dr. Eimear Lee and Dr. Dorinda Mullen who carried out pathological review and scoring of Immunohistochemically stained sections as part of this project.

Publications

Journal Articles

Charles J. d'Adhemar, Cathy D. Spillane, Michael F. Gallagher, **Mark Bates**, Sharon O'Toole, John J. O'Leary et al 2014. The MyD88+ Phenotype Is an Adverse Prognostic Factor in Epithelial Ovarian Cancer. *PloS one*, 9(6), p.e100816.

Published Abstracts

Bates, M., O'Toole, S., Spillane, C., McCann, A., Gallagher, M., Costigan, D., … O'Leary, J. (2015a). The Role of MAD2 and MyD88 as Prognostic Indicators in Ovarian Cancer. *The Journal of Pathology*, *237*, S1–S52.

Bates, M., O'Toole, S., Spillane, C., McCann, A., Gallagher, M., Costigan, D., … O'Leary, J. (2015b). The Role of the TLR4 Pathway and the Spindle Assembly Checkpoint in Ovarian Cancer Prognosis. *The Journal of Pathology*, *237*, S1–S52.

Conference proceedings

M Bates, SA O'Toole, CD Spillane, A McCann, M Gallagher, JJ O'Leary (2014). A therapeutic roadmap for ovarian cancer using MyD88 and MAD2 as prognostic indicators. Poster presentation at the British Gynaecological Cancer Society Conference, London, July, 2014.

M Bates, SA O'Toole, CD Spillane, A McCann, M Gallagher, JJ O'Leary (2014). A therapeutic roadmap for ovarian cancer using MyD88 and MAD2 as prognostic indicators. Poster presentation at the 9th International cancer conference, 17th-18th September 2014.

M Bates, SA O'Toole, CD Spillane, A McCann, M Gallagher, JJ O'Leary (2014). A therapeutic roadmap for ovarian cancer using MyD88 and MAD2 as prognostic indicators. Poster presentation at the 17th IMM Annual Meeting, 7th November 2014.

M Bates, SA O'Toole, CD Spillane, A McCann, M Gallagher, JJ O'Leary (2014). A therapeutic roadmap for ovarian cancer using MyD88 and MAD2 as prognostic indicators. Poster presentation at the 7th School of Medicine Postgraduate Research Day, Monday 8th December 2014.

M Bates, SA O'Toole, CD Spillane, A McCann, M Gallagher, JJ O'Leary (2015). The role of the TLR4 pathway and the spindle assembly checkpoint in ovarian cancer prognosis. Poster presentation at the United States and Canadian Academy of Pathology Conference, 21st March 2015.

Summary

Ovarian cancer is 4th leading cause of cancer death in woman and the most lethal gynaecological malignancy. Most patients present with advanced disease where the 5 year survival rate is less than 40%. Standard treatment for advanced ovarian cancer includes cytoreductive surgery followed by paclitaxel/carboplatin based chemotherapy. However despite the use of these front-line chemotherapeutic agents, mortality rates for ovarian cancer have remained almost unchanged for the past 30 years. A major reason for this poor prognosis is the development of chemoresistance and recurrent disease. Therefore there is a dire need for prognostic biomarkers which can predict patient response to chemotherapy from the outset and prevent the development of chemoresistant recurrent disease. Currently there are no reliable prognostic markers in routine use for ovarian cancer. In this study we investigated the role of three protein biomarkers TLR4, MyD88 and MAD2 in ovarian cancer. High TLR4 and MyD88 expression and low MAD2 expression have been associated with poor survival and paclitaxel resistance *in-vitro*. The aim of this project was to assess the combined utility of these three markers in predicting patient prognosis and to investigate any potential *in-vitro* link between these three markers and the paclitaxel resistance mechanisms in which they are involved.

Interestingly in this study, siRNA knockdown of MAD2 in A2780 and SKOV-3 ovarian cancer cells resulted in a 3 fold increase in TLR4 mRNA expression demonstrating an *in-vitro* link between these two biomarkers. Knockdown of TLR4 in SKOV-3 was shown to recover chemosensitivity of these cells to paclitaxel. Furthermore knockdown of MAD2 was shown to render SKOV-3 chemoresistant to paclitaxel. This perhaps demonstrates a partial overlap in the paclitaxel resistance mechanisms associated with both markers. Following knockdown of MAD2, SKOV-3 cells displayed an increase in β-galactosidase activity, an enlarged cell phenotype and exhibited an upregulation of a number of senescence associated genes as confirmed by microarray analysis. Microarray analysis of SKOV-3 cells following knockdown of TLR4 identified a number of altered gene pathways which may be responsible for the increase in sensitivity of these cells to paclitaxel. Two novel signalling pathways altered following the knockdown of TLR4 were the olfactory receptor and the ErbB signalling pathways. A number of olfactory receptor genes were downregulated following knockdown of both TLR4 and MAD2. Cross comparison of arrays identified a number of other differentially expressed genes affected following knockdown of TLR4 and MAD2 which may help us to better understand the *in-vitro* relationship between these two biomarkers.

Combined assessment of these three markers in a TMA cohort demonstrated that these markers can be used very successfully in combination to predict patient prognosis. The three markers when used in combination identified different at risk subpopulations of patients. Patients with high TLR4, high MyD88 and low MAD2 expression exhibited the worst prognosis. These patients are unlikely to respond to paclitaxel therapy and in fact paclitaxel therapy may be harmful to these patients. Therefore these patients should instead receive alternative therapies or be directed towards clinical trials. In future patients should be triaged based on the expression of these three markers and should be given more appropriate therapies such as targeted therapies based on the molecular evidence.

Abbreviations

ACOG – American College of Obstetricians and Gynecologists

AP-1 – Activator Protein 1

AP Assay – Acid phosphatase cell proliferation/cytotoxicity assay

ATP – Adenosine Triphosphate

AU – Arbitrary Units

B2M – Beta-2 microglobulin

BAX – BCL-2-associated X protein

BCL2 – B-cell Lymphoma 2

BCL-XL – B-cell Lymphoma extra-large

BRCA – Breast Cancer Associated Gene

C5AR1 – complement component 5a receptor 1

CAIX – Carbonic anhydrase IX

CBLB-Cas-Br-M (murine) ecotropic retroviral transforming sequence b

CCK-8 Assay – Cell Counting Kit-8 cell proliferation/cytotoxicity assay

CCL2 – Chemokine (C-C motif) ligand 2

CCR – Chemokine (C-C motif) receptor

CD – Cluster of differentiation

cDNA – Complementary DNA

CSC – Cancer stem cell

CTC – Circulating tumour cell

CXCL – Chemokine C-X-C motif ligand

DAVID – Database for Annotation, Visualization and Integrated Discovery

DFI – Disease Free Interval

DMSO – Dimethyl Sulfoxide

ECACC – The European Collection of Cell Cultures

ECM – Extra cellular matrix

EGF – Epidermal Growth Factor

EGFR – Epithelial Growth Factor Receptor

EMT – Epithelial-to-Mesenchymal Transition

EOC – Epithelial Ovarian Cancer

ERBB2 – V-Erb-B2 avian erythroblastic leukemia viral oncogene homolog

FBS – Foetal bovine serum

FDA – US Food and Drug Administration

FIGO – The International Federation of Gynaecological Oncologists

GAPDH – Glyceraldehyde-3-phosphate dehydrogenase

HE4 – Human epididymis protein 4

IC – Inhibitory concentration

IGF – Insulin growth factor

IGFBP – Insulin growth factor binding protein

IL – Interleukin

IRAK – Interleukin-1 receptor-associated kinase

LNA – Locked Nucleic Acid

LOC653879 – Similar to complement C3 precursor

LPS – Lipopolysaccharide

KEGG – Kyoto encyclopedia of genes and genomes

MAD2 – Mitotic Arrest deficienct protein 2

MAL – MyD88 Adaptor like

MAPK – Mitogen-activated protein kinase

MCP-1 – Monocyte chemoattractant protein-1

MD-2 – Leukocyte antigen 96

MMP – Matrix metallopeptidase

MTT – 4,5-dimethylthiazol-2-yl-2,5-diphenyltetrazolium bromide

MyD88 – Myeloid differentiation factor 88

mRNA – Messenger RNA

NEMO – NF-κB essential modulator

NFKB – Nuclear factor kappa light chain enhancer of activated B cells

NSAID – Non streodial anti-inflammatory drug

OR – Olfactory receptor

OS – Overall Survival

P21 – Cyclin-dependent kinase inhibitor 1

p53 – Tumour protein p53

PARP – Poly ADP ribose polymerase

PBS – Phosphate buffered saline

PDCD4 – Programmed cell death 4

PFS – Progression Free Survival

PI – Propidium Iodide

PLCO – Prostate, Lung, Colorectal, and Ovarian Cancer Screening Trial

PROS – Protein S

PTX – Paclitaxel

RA – Retinoic Acid

RB – Retinoblastoma

RECIST – Response evaluation criteria in solid tumours

RIPA – Radioimmunoprecipitation

RIN – RNA Integrity Number (RIN)

RMA – Robust multichip average

RNA – Ribonucleic acid

ROMA – Risk of ovarian malignancy algorithm

RT-PCR – Reverse transcription PCR

SAC – Spindle assembly checkpoint

SAHF – Senescence associated heterochromatin foci

SASP – Senescence associated secretory phenotype

siRNA – Small interfering RNA

SNPs – Single nucleotide polymorphisms

STAT – Signal Transducer and Activator of Transcription

STIC – Serous Tubal intra-epithelial carcinoma

STRING – Search Tool for the Retrieval of Interacting Genes/Proteins

TBST – Tris buffered saline with tween

TGF – Transforming growth factor

TIR – Toll interleukin 1 receptor domain

TLR4 – Toll like receptor 4

TMA – Tissue Microarray

TNF – Tumour necrosis factor

TRAIL – Tumour necrosis-related apoptosis-inducing ligand

TRIF – Tir domain containing adaptor inducing interferon-β

TRAF-6 – TNF receptor associated factor 6

TRAM – TRIF-related adapter molecule

UKCTOCS – The United Kingdom Collaborative Trial of Ovarian Cancer Screening

VEGF – Vascular endothelial growth factor

XIAP – X-linked inhibitor of apoptosis

Table of Contents

Table of Figures

Table of Tables

Chapter 1

General Introduction

Trinity College Dublin

The University of Dublin

Chapter 1

General Introduction

1.1 Overview

This chapter provides a brief introduction to ovarian anatomy, ovarian cancer, the three protein biomarkers TLR4, MyD88 and MAD2, the three regulatory microRNA's miR-433, miR-146a and miR-21, the pathways in which they are involved and their respective roles in ovarian cancer.

1.2 Structure and Function of the Ovary

The ovaries are the main female reproductive organs and are responsible for the production of female sex gametes or oocytes commonly referred to as eggs and for the production of female hormones including oestrogen and progesterone **(Figure 1.1)**. Each ovary has an ovoid structure and is around 3cm in diameter. They are located on either side of the uterus in areas known as the ovarian fossae. The ovaries are attached to the uterus and pelvic wall by the ovarian ligament and suspensory ligaments respectively. The surface of the ovary is covered by a layer of simple mesothelium called "germinal epithelium", beneath which lies a layer of dense connective tissue called the tunica albuginea. The interior stromal tissue of the ovary is divided into an outer cortex and inner medulla region. The outer cortex contains oocytes which are housed within specialised structures called ovarian follicles, while the inner medulla consists of various blood vessels such as the ovarian vein and ovarian artery which supply bloodflow to the ovary (Martini *et al*. 2012)**.**

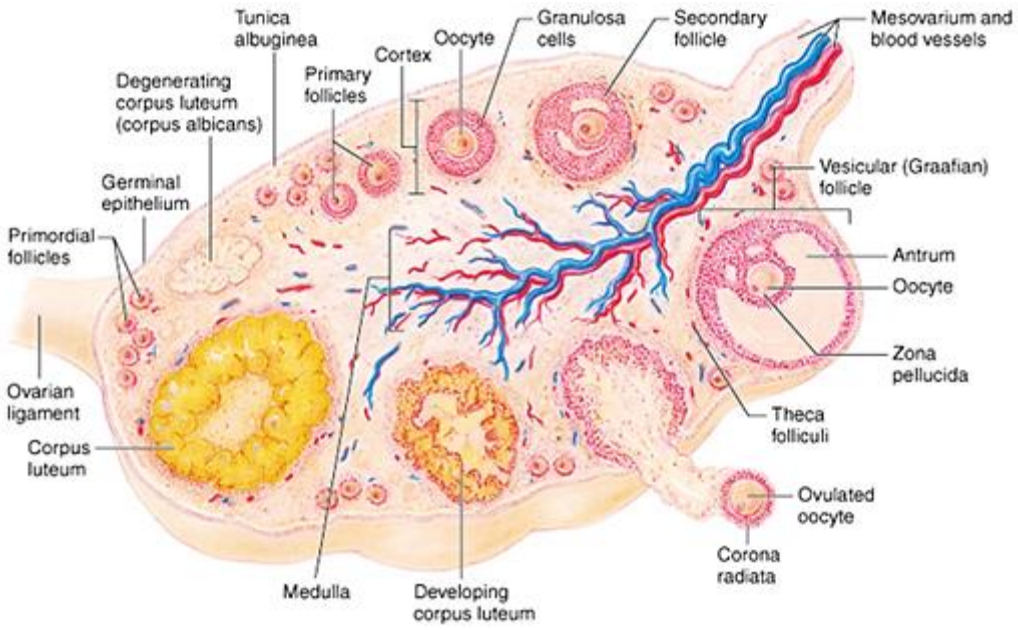

Figure 1.1 The structure of the ovary. The ovary is covered in a single layer of mesothelium “germinal epithelium”. The inner stromal tissue consists of the medulla and cortex. Oocytes commonly referred to as eggs develop in the cortex within follicles which mature until the eggs are released. The residual follicle then degenerates forming corpus lutea and then corpus albicans. Blood flow is supplied by the ovarian vein and ovarian artery (www.colorado.edu 2001).

1.3 Ovarian Cancer

1.3.1 Incidence and mortality

Worldwide, 239,000 new cases of ovarian cancer are diagnosed annually with 152,000 deaths reported each year (IARC). Two thirds of all ovarian cancers had previously been thought to occur in developed countries, likely due to differences in life expectancy, the late age of onset of ovarian cancer and differences in parity (Ferlay *et al*., 2010). Although more recent evidence suggests that ovarian malignancies may be becoming more common in developing countries (Iyoke & Ugwu 2013). Ovarian cancer is the 4th most common cause of cancer death in women worldwide and the most lethal gynaecological malignancy (Siegel et al. 2013). In Ireland, ~370 cases of ovarian cancer were diagnosed and ~270 deaths were reported from the disease per year between 1994-2010 **(Figure 1.2)**. The 5 year survival rate in Ireland rose from 30% to 32% between 1994-2012, but still remains below the EU average of 38%. Ireland has the 7th highest incidence and the 4th highest mortality rate from the disease in Europe (National Cancer Registry 2014) and mortality rates are expected to rise (O'Lorcain & Comber 2006).

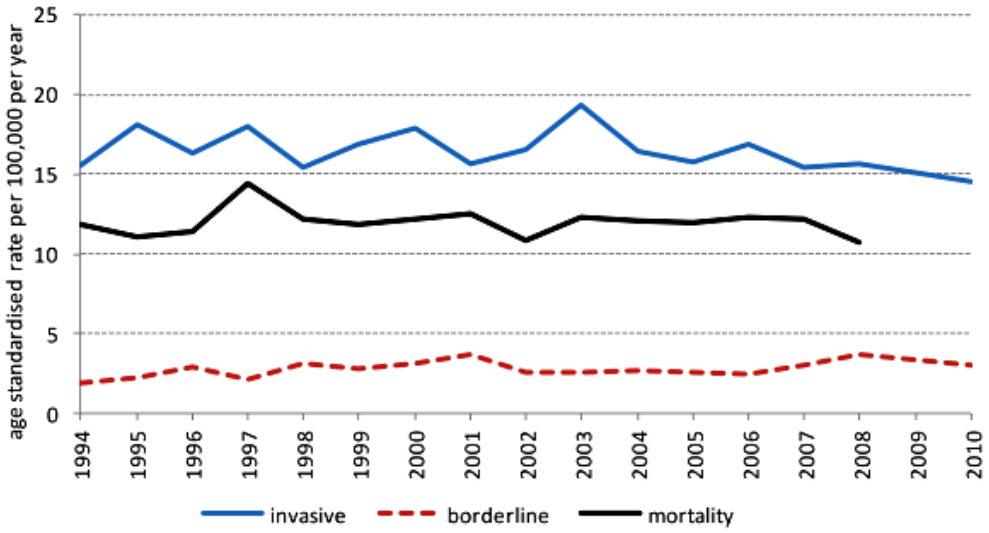

Figure 1.2 Ovarian cancer incidence and mortality rates in Ireland between 1994-2010. During this time the age-standardised incidence rates for invasive ovarian cancer ranged from 15 to 19 cases per 100,000 women per year. Between 2 and 4 borderline cases per 100,000 per year were diagnosed. Mortality rates have remained fairly stable over time, ranging between 11 and 14 deaths per 100,000 women per (National Cancer Registry 2012b).

1.3.2 Aetiology and risk factors

The exact aetiology of ovarian cancer remains unknown, although the induction of menopause and reproductive hormones are thought to play strong roles in its development with approximately 85% of ovarian cancers being diagnosed in post-menopausal women, with an average age of diagnosis of 65 years (Smith & Xu 2008).

1.3.2.1 Hypotheses regarding the aetiology of ovarian cancer

A number of theories surrounding the aetiology of ovarian cancer exist; these include the incessant ovulation, gonadotropin stimulation and the serous tubal intraepithelial carcinoma (STIC) hypotheses.

1.3.2.1.1 The incessant ovulation hypothesis

The incessant ovulation hypothesis was originally proposed in 1971 (Fathalla 1971). This theory proposes that continual damage occurs to the surface epithelium as a result of ovulation and the release of ova from the ovary. This repetitive wounding leads to the accumulation of mutations in surface epithelial cells leading to the formation of an ovarian tumour (Fathalla 2013) **(Figure 1.3).**

1.3.2.1.2 The follicle depletion and gonadotrophin stimulation hypothesis

An interesting theory proposed by (Smith & Xu 2008) which may explain the age dependence/menopause status of ovarian cancer is the follicle depletion hypothesis/gonadotrophin stimulation hypothesis **(Figure 1.3)**. During menopause, levels of the hormone gonadotrophin increases in women, this is due to the lack of a feedback loop which exists in premenopausal women. In pre-menopausal women gonadotrophin is released by the anterior pituitary gland during ovulation and stimulates the production of oestrogen by granulosa cells in ovarian follicles. Gonadotrophins activate cyclo-oxygenases and induce an inflammatory response which supports the release of the ovum from the ovary. Following release of the ovum from the ovary, ovarian follicles degenerate into a structure known as the corpus luteum which is responsible for the production of progesterone *(*Martini *et al*. 2012). Progesterone then serves to negatively regulate gonadotrophin expression following ovulation (Skinner *et al* 1998). However in post-menopausal woman, in which ovarian follicles have been depleted, negative regulation of gonadotrophin levels does not occur. The high long term levels of gonadotropins likely generate an inflammatory environment in the ovary that facilitates transformation of surface epithelial cells and the development of ovarian cancer.

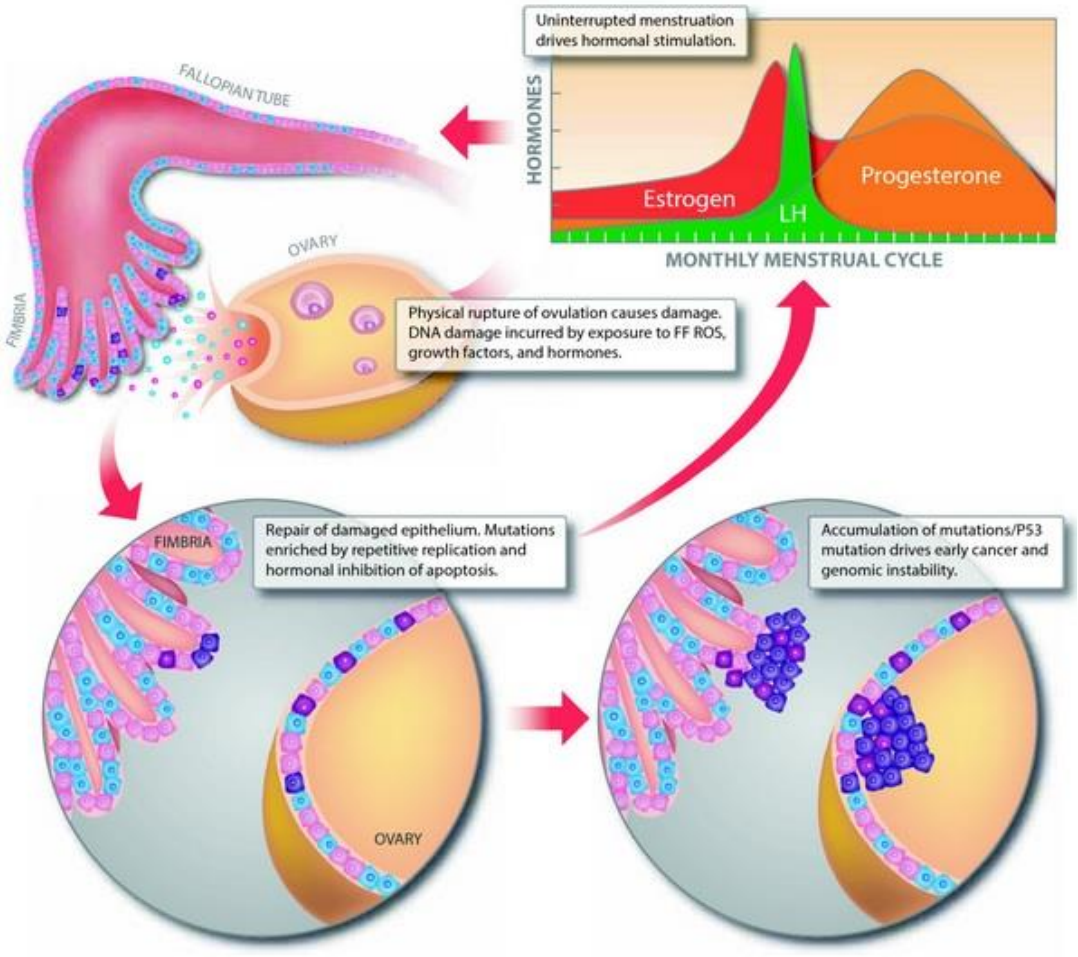

Figure 1.3 The incessant ovulation and gonadoptrophin hypotheses. Monthly physical damage from ovulation necessitates increased cell proliferation during repair, eventually leading to genomic instability. Gonadotrophin hypothesis: Exposure to hormones released during ovulation inhibits natural apoptosis, uninterrupted hormonal fluctuation stimulate differentiation, proliferation, and ultimately malignant transformation (Emori & Drapkin 2014).

1.3.2.1.3 The serous tubal intraepithelial carcinoma (STIC) hypothesis

Recently it has become evident that the distal portion of the fallopian tubes represents a possible source of high grade serous carcinoma, with the precursor lesion being identified as serous tubal intraepithelial carcinoma (STIC) **(Figure 1.4)**. This has challenged previous beliefs that serous ovarian cancer arises from the surface epithelium (Carlson *et al*. 2008; Dietl & Wischhusen 2011; McCluggage 2011; Kurman & Shih 2011; Kessler *et al*. 2013). This recent insight is even reflected in the new International Federation of Gynaecology and Obstetrics (FIGO) staging system for ovarian cancers, with early stages (Stage I and II) no longer merely being considered to be confined to one or more ovaries but also to one or more fallopian tubes (Prat 2014). Mor & Alvero (2013) propose a mechanism whereby migratory cancer stem cells, shed from the surface epithelium and migrate towards the ovarian surface epithelium. These cells are possibly attracted by inflammatory chemokines /cytokines released during ovulation. They are then thought to penetrate the surface epithelium, entering through microwounds created by the ovulatory process. Mor & Alvero (2013) surmise that the surface epithelium may represent a fertile ground that promotes tumour growth. Thus high grade serous ovarian tumours may represent secondary tumour formation and fallopian tube metastasis rather than being the primary site of disease, which may explain the difficulties detecting early disease and why most serous ovarian tumours are at an advanced stage (Smith & Xu 2008). The STIC hypothesis was originally proposed by (Carlson *et al*. 2008) who demonstrated that 47% of patients with serous epithelial ovarian cancer also contain a concomitant serous intraepithelial tubal carcinoma. P53 mutations are detected in 95% high grade serous ovarian cancers (Domcke *et al*. 2013). Interestingly STIC tumours exhibit high levels of p53 accumulation, further supporting a clonal relationship between the two lesions (Shendure & Ji 2008).

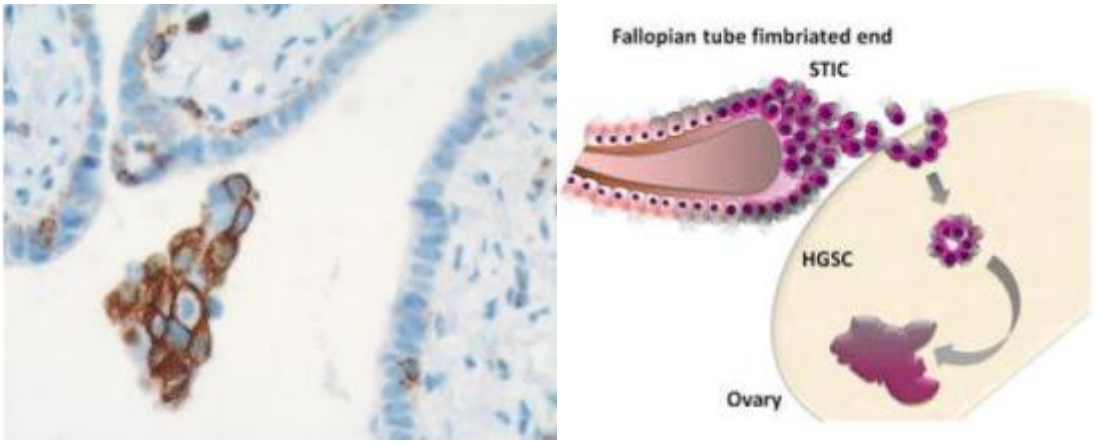

Figure 1.4 Fallopian tube hypothesis on the origin of high-grade serous carcinoma (HGSC). Fallopian tube epithelium (FTE) cells of the fimbriated ends undergo initial neoplastic transformation, becoming serous tubal intraepithelial carcinoma (STIC). STIC cells possess resistance to anoikis that favors settlement and invasion of the ovarian surface. The ovarian microenvironment, rich in hormonal and inflammatory factors, drives the full neoplastic transformation to invasive HGSC (Right) (www.omicsonline.org). CD44-positive cells from the fallopian tube that broke away from the tissue (Mor & Alvero 2013) (Left).

1.3.2.2 Risk factors for ovarian cancer

A number of other factors may also contribute to the development of ovarian cancer including, genetics and family history, mutations in the BRCA1, BRCA2 and TP53 genes, endometriosis, use of hormone replacement therapy, smoking, obesity and infertility (Fasching *et al*. 2009; Moslehi *et al*. 2000; Riman *et al*. 2004; Beral *et al*. 2012; Olsen *et al*. 2007; Bast *et al*. 2009). Certain factors such as tubal ligation, early age of first pregnancy and long term oral contraceptive use may have a protective effect (Riman *et al*. 2004; Ness & Modugno 2006).

1.3.3 Histology of ovarian cancer subtypes

The major classes of ovarian cancers are epithelial, germ cell and sex cord/stromal tumours, with epithelial ovarian cancers (EOC's) making up between 80-90% of all ovarian malignancies. Epithelial ovarian cancers are divided into a number of histological subtypes, these include serous, mucinous, endometrioid and clear cell tumours **(Figure 1.5)**. The majority of EOC's are malignant and invasive and most cases are serous carcinomas (Bell 2005; National Cancer Registry 2012b).

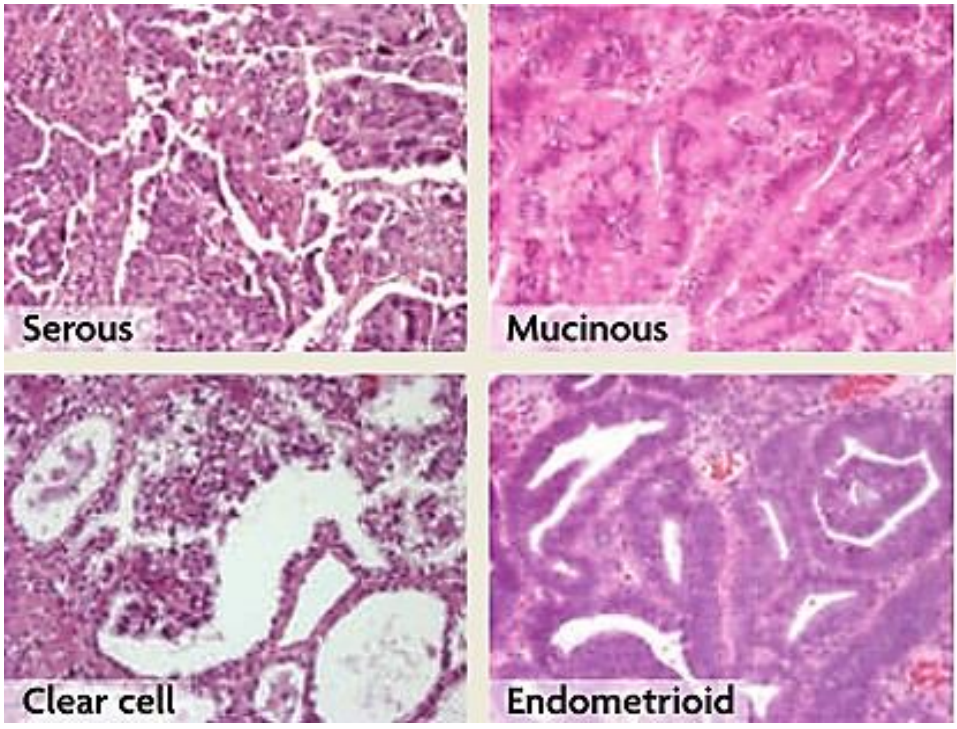

Figure 1.5 Histology of epithelial ovarian cancer subtypes. There are four main subtypes of epithelial ovarian cancer including serous, mucinous, clear cell and endometrioid (Bast *et al*. 2010).

1.3.4 Staging and grading

Ovarian cancers are staged by the FIGO staging system **(Table 1.1)**

Table 1.1 The FIGO staging classification for cancer of the ovary, fallopian tube, and peritoneum (Adapted from Prat 2014).

FIGO Stage	FIGO Classification
I	Growth limited to the ovaries
IA	Tumour limited to 1 ovary or fallopian tube, no tumour on ovarian or fallopian tube surface, (capsule intact), no malignant cells in the ascites or peritoneal washing
IB	Tumour limited to both ovaries (capsule intact) or fallopian tubes; tumour on ovarian of fallopian tube surface, no malignant cells in the ascites or peritoneal washings
IC	Tumour limited to 1 or both ovaries or fallopian tubes with any of the following: IC1: Surgical Spill IC2: Capsule ruptured before surgery or tumour on ovarian or fallopian tube surface IC3: Malignant cells in the ascites or peritoneal washings
II	Growth involving 1 or both ovaries with pelvic extension
IIA	Extension and/or implants on uterus and/or fallopian tubes and or ovaries
IIB	Extension to other pelvic intraperitoneal tissues
III	Tumour involving 1 or both ovaries or fallopian tubes or primary peritoneal cancer, with cytologically or histologically confirmed spread to the peritoneum outside the pelvis and or metastasis to the retroperitoneal lymph nodes
IIIA	Positive retroperitoneal lymph nodes only (cytologically or histological proven) IIIA1(i): Metastasis up 10mm in greatest dimension IIIA1(ii): Metastasis more than 10mm in greatest dimension IIIA2: Microscopic extrapelvic (above the pelvic brim) peritoneal involvement with or without positive retroperitoneal lymph nodes
IIIB	Macroscopic peritoneal metastasis beyond the pelvis up to 2cm in greatest dimension, with or without metastasis to the retroperitoneal

	lymph nodes
IIIC	**Macroscopic peritoneal metastasis beyond the pelvis more than 2cm in greatest dimension, with or without metastasis to the retroperitoneal lymph nodes (includes extension of tumour to capsule of liver and spleen without parenchymal involvement of either organ)**
IV	**Distant metastasis excluding peritoneal metastases**
IVA	**Pleural effusion with positive cytology**
IVB	**Parenchymal metastases and metastases to extra-abdominal organs (including inguinal lymph nodes and lymph nodes outside of the abdominal cavity**

Ovarian cancers are also graded based on the FIGO or WHO classification systems among others, which are based on the degree of differentiation/cellular atypia and the percentage tumour growth compared to surrounding normal glandular architecture (Rosen *et al*. 2010; McCluggage 2011) **(Table 1.2)**.

Table 1.2 The various grades of ovarian cancer.

Grade	Description
Grade 0	**Non-invasive tumours**
Grade 1	**Tumours composed of well differentiated cells, which resemble normal tissue, 5% of solid tumour growth, good prognosis**
Grade 2	**Tumours is composed of moderately well differentiated cells which mostly resemble the normal tissue, 5% to 50% of solid tumour growth , poor prognosis**
Grade 3	**Tumours are composed of poorly differentiated cells, atypical cells which do not resemble normal tissue, more than 50% solid tumour growth, worst prognosis**

1.3.5 Screening and detection

The poor prognosis associated with ovarian cancer makes it the most lethal of the gynaecological malignancies. There are a number of reasons for this, firstly there is no screening programme in place as ovarian cancer is poorly understood and as of yet there is no adequate method of detecting the disease in its early stages, where prognosis rates are much higher. Furthermore most women are asymptomatic and do not display symptoms until advanced stage of disease. Although some women may display non-specific symptoms such as bloating, pelvic pain, difficulty eating and frequent urination, this can indicate a range of various medical conditions (Schorge *et al*. 2010). One of the only biomarkers that is currently being used in early detection of ovarian cancer is CA125, however its role in early detection has been controversial.

1.3.5.1 CA125 and OVA1

Carcinoma Antigen 125 (CA125) was originally identified by (Bast *et al*. 1981) and was so named as it was the antigenic determinant for the 125th antibody produced against the ovarian cancer cell line OVCA433. This high molecular weight glycoprotein was subsequently cloned and found to be encoded by the MUC16 gene (Yin & Lloyd 2001). CA125 provides a protective mucosal barrier against infectious agents on the surface of epithelial cells and the female reproductive tract. It is expressed on ovarian tumour cells and can be secreted into circulation in response to epidermal growth factor. CA125 is frequently analysed in serum samples of patients with ovarian cancer and was originally introduced as a marker for early detection, however its use in early detection is controversial (Schmidt 2011). Around 90% of women with advanced ovarian cancer have elevated levels of CA125, however only 50% express CA125 in the early stages limiting its use in early diagnosis. Various commercial assays are available for its detection (Davelaar *et al*. 1998). The American Congress of Obstetricians and Gynaecologists (ACOG) has recommended against its use in early detection as it is likely to lead to high number of false positive results and unnecessary and invasive procedures which will cause unnecessary anxiety and stress to the patient and additional healthcare costs (ACOG 2013). Furthermore, two large scale screening studies, one in the UK, the UKCTOCS trial (Menon *et al*. 2009) and the PLCO trial in the US (Buys 2011) looked at using a CA-125 blood test along with transvaginal ultrasound to detect early stage ovarian cancer. In these studies, more patients with cancer were identified, with only some in the early stages; however the screened women had no survival benefit as a result of screening. CA-125 lacks

specificity and is upregulated particular in pre-menopausal women where CA-125 levels may be upregulated in a number of benign conditions such as menstruation, endometriosis, pregnancy and pelvic inflammatory disease. Furthermore its sensitivity is only around 50%, with a large number of ovarian cancer patients showing no elevated serum levels of CA-125.

1.3.6 Management and treatment

Standard treatment for advanced ovarian cancer involves optimal surgical debulking which may include hysterectomy, bilateral salpingo-oophorectomy, tubal ligation and removal of the lymphnodes to limit the spread of metastasis, this is usually followed by paclitaxel/carboplatin based chemotherapy. Both chemotherapy drugs are administered intravenously via a picc line into the brachial artery or via a central line into the jugular vein, one after the other. Firstly paclitaxel is given over a period of about 3 hours, followed by carboplatin which is infused over a 1 hour period. Following single administration of the paclitaxel/carboplatin therapy, patients are given a 3 week rest period; this completes 1 cycle of chemotherapy. In total 6-8 cycles of chemotherapy are given over 5-6 months representing a single course of treatment. Neoadjuvant therapy is also becoming more commonly used; this involves shrinking the tumour with chemotherapy drugs prior to surgery. This is used in cases where the patient has significant omental disease and malignant ascites. Complete removal of macroscopic disease is essential, as sub-optimal debulking has been correlated with significantly reduced progression free survival (PFS) and overall survival (OS) **(Figure 1.6)**.

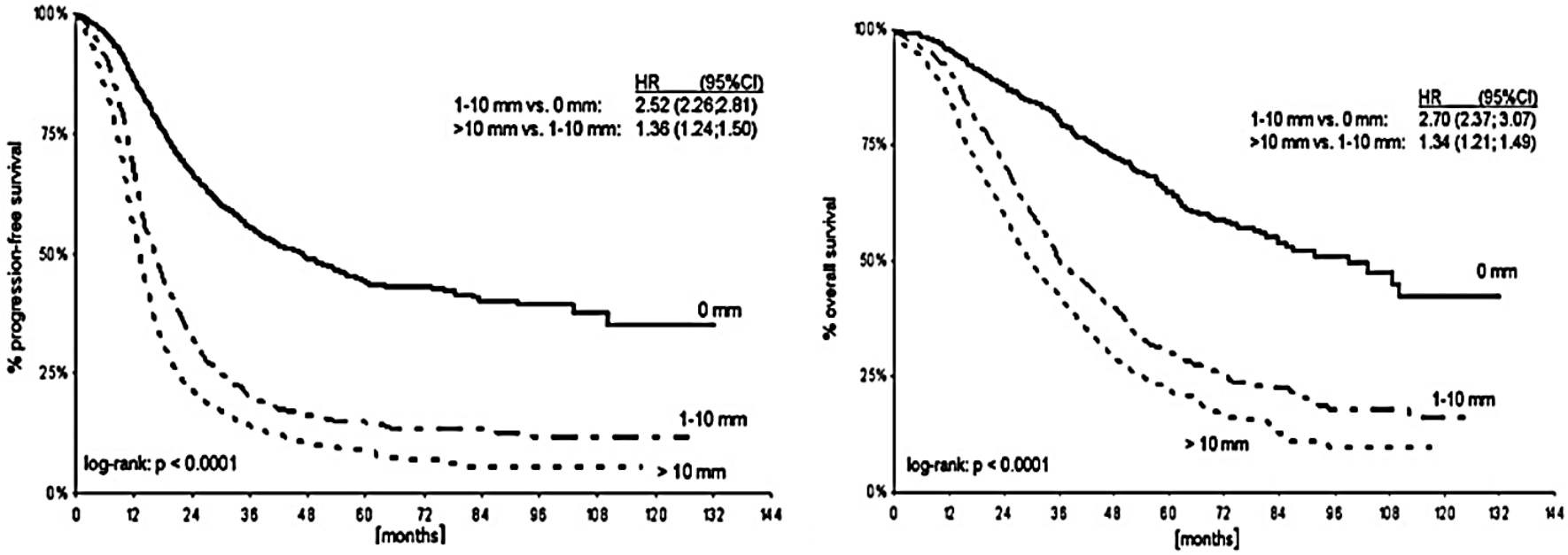

Figure 1.6 Kaplan-Meier curves showing the progression free survival (Left) and Overall survival (Right) of patients who underwent optimal and suboptimal debulking. Significant reduced PFS and OS rates were seen with patients with residual macroscopic disease (1-10mm, >10mm, sub-optimal debulking) and patients with no evidence of residual macroscopic disease (0mm)(du Bois *et al*. 2009).

1.3.6.1 Paclitaxel and Carboplatin

Paclitaxel is a chemotherapeutic agent used to treat various forms of cancer including ovarian cancer. It is a plant derivative of the pacific yew tree and causes the stabilisation of cell microtubules by binding to their β-tubulin subunit, inhibiting their disassembly inducing cell cycle arrest and subsequent apoptosis (Cheng *et al*. 2002). It is sold under the tradename taxol by Bristol-Myers-Squibb. Carboplatin (cis-diammine cyclobutane-1,1-dicarboxylato platinum II) is a platinum anticancer drug used for treating many types of human cancer. It was first developed in the 1970s and was approved for use in 1989 under the trade name (paraplatin) and was found to be less oto-, neuro-, and nephrotoxic than its parent drug cisplatin (Alberts *et al*. 1990; Murray *et al*. 2012). Carboplatin works by binding to guanine bases in DNA to form intra and inter-strand crosslinks, triggering apoptosis (Cheng *et al*. 2002; Di *et al*. 2012). However, despite the use of these frontline anticancer drugs, little has been done to improve upon the poor prognosis rates in ovarian cancer with mortality rates remaining almost unchanged for the past number of decades (National Cancer Registry 2014).

1.3.7 Recurrent disease and chemoresistance

Although initial response rates may be as high as 80%, most patients will develop recurrent disease. This is usually coupled with the development of a chemoresistant phenotype that is less responsive to chemotherapeutic agents. Some patients may not even initially respond well to chemotherapy (A. Kim *et al*. 2012). Patients who progress or have stable disease during first-line treatment or who relapse within 1 month are considered to be chemorefractory. Patients who respond to primary treatment and relapse within 6 months are considered chemoresistant, and patients who relapse more than 6 months after completion of initial therapy are characterized as chemosensitive (Markman *et al*. 1991; A. Kim *et al*. 2012). As of yet, no reliable method of treating recurrent/chemoresistant disease exists. Therefore most ovarian cancer patients will ultimately die as a result of recurrent disease. Recurrent disease may be treated with additional rounds of chemotherapy or with alternative chemotherapeutic agents such as liposomal doxorubicin, toptecan, fluorouracil, gemcitabine or oxaliplatin. But with each successive round, it becomes less effective until eventually the disease is no longer treatable (Ozols 2002; Bruchim *et al*. 2013). Therefore the molecular mechanisms which underlie the development of recurrent disease and chemoresistance need to be elucidated so that more effective treatment modalities can be developed in order to improve patient prognosis.

1.3.8 Ovarian cancer biomarkers

In recent years, a number of new biomarkers have been discovered for ovarian cancer which may help aid diagnostics, prognostics and therapy including HE4, HER3, BRCA1/2, CSC markers and microRNAs. However not all of these have been introduced into routine clinical practice.

1.3.8.1 HE4

Human epididymis protein 4 (HE4) is a low molecular weight glycoprotein that is expressed predominantly in epithelial cells of the epididymis and other tissues throughout the body including the breasts and female genital tract. Human epididymis protein 4 also known as wap four disulphide domain protein 2 is encoded by the WFDC2 gene. HE4 is overexpressed in both early and recurrent ovarian cancer; high preoperative levels of HE4 are associated with advanced disease and poor patient prognosis including reduced overall survival (Drapkin *et al*. 2005; Li *et al*. 2009; Anastasi *et al*. 2010; Kalapotharakos *et al*. 2012; Kong *et al*. 2012). It is overexpressed less often during endometriosis and benign ovarian disease (Kadija *et al*. 2012) than CA-125 and has been found to be expressed in many tumours not expressing CA-125 (Holcomb *et al*. 2011; Granato *et al*. 2015). It displays high sensitivity alone or in combination with CA125 for predicting early disease (Heliström *et al*. 2003; Molina *et al*. 2011;Sandri *et al*. 2013; Ortiz-Muñoz *et al*. 2014). HE4 gained FDA approval as a biomarker for monitoring recurrence and progression in patients with epithelial ovarian cancer in 2011(Andersen *et al*. 2011; Montagnana *et al*. 2011). Recent studies suggest that a Risk of Ovarian Malignancy Algorithm (ROMA) index which incorporates CA125 and HE4 levels in serum, is likely to produce a test of high sensitivity and specificity in identifying ovarian cancer patients (Sandri *et al*. 2013; Ortiz-Muñoz *et al*. 2014).

1.3.8.2 HER3

HER3 is highly expressed on both primary tumours and the surface of circulating tumour cells (CTCs) and its expression has been found to be associated with the development of metastasis, chemoresistance and reduced survival (Tanner *et al*. 2006; Bezler *et al*. 2012; Ocana *et al*. 2013). CTCs are tumour cells released from the primary tumour and enter circulation. These cells travel through the bloodstream and spread to distant target organs, where they propagate, resulting in secondary tumour formation (Cui *et al*. 2015). Therapeutic targeting of HER-3 may therefore lead to improved therapeutic outcomes in ovarian cancer. Blockage of HER3 using a monoclonal antibody or knockdown using siRNA has been shown to reduce tumour growth and metastasis in, *in-vivo* mouse models. Interestingly in a study by (Sheng *et*

al. 2010) It was found that HER3 positive tumours in mice models first metastasise to the omentum before forming distant secondary metastasis. They found that siRNA knockdown of HER3 in cell models did not produce the same results as in mice, leading them to believe that something present in the microenvironment of the omentum was contributing to cancer dependency on HER3. This led them to identify the NRG-1 receptor, which is abundantly expressed in the omentum as a binding partner for HER-3, which helps facilitate HER-3 mediated spread of ovarian cancer. Specifically NRG-1 is thought attract HER-3 positive tumour cells to the omentum. siRNA knockdown of NRG-1 was shown to significantly decrease metastatic spread in mouse models and NRG-1 positive tumours were associated with increased tumour burden.

1.3.8.3 Cancer stem cell markers

Cancer stem cells are cancer cells which have acquired many of the abilities of normal stem cells, including the ability to self-renew and differentiate and are thought to be the only cell type capable of generating a tumour (tumorigenesis)(Moitra 2015). These cells are intrinsically chemoresistant and can also undergo quiescence which allows them to survive therapies which target actively dividing cells. Furthermore they also express high levels of efflux pumps which allow them to resist most cytotoxic therapies (Moitra 2015). As these cells are capable of replicating indefinitely and are able to resist chemotherapy, they are thought to be responsible for the development of chemoresistant and recurrent disease. Cancer stem cells (CSCs) similar to haemotopoietic stem cells may exist as hierarchies within a tumour, and various populations/hierarchies of CSCs may exist within a single tumour due to the acquisition of spontaneous mutations over the lifetime of the cancer stem cell (Ffrench *et al*. 2014). Various markers exist for the detection of cancer stem cells in ovarian cancer, however no one marker may be capable of identifying all cancer stem cells within a tumour. Instead they likely highlight specific populations of cancer stem cells within a given tumour. Cancer stem cells have also been identified in cancer cell lines. Markers which have been identified for the detection of cancer stem cells in ovarian cancer include CD24, CD44, CD117, CD133, ALDH1, HSP, ABCG2, MyD88 (Alvero *et al*. 2011; Ffrench *et al*. 2014) and many studies examining the expression of these markers have been linked them to poor patient prognosis (Kristiansen *et al*. 2002; Silva *et al*. 2011; Steffensen *et al*. 2011; Luo *et al*. 2011; d'Adhemar *et al*. 2014).

1.3.8.4 BRCA1/2

Breast cancer type 1 susceptibility protein (BRCA1) and breast cancer type 2 susceptibility protein (BRCA2) are both involved in the repair of DNA double-strand breaks (DSBs) through the homologous recombination (HR) pathway (Girolimetti *et al*. 2014). Homologous recombination involves copying the sequence information from homologous sister chromatids to repair the damaged sequence. BRCA1 also forms part of a complex with other repair proteins including ATM, RAD50, MRE11, RAD50, MRE11, NBS1, and BLM, MLH1, MSH2, and MSH6 known as the BRCA1-associated genome surveillance complex (BASC)(Wang *et al*. 2000). Under normal circumstances BRCA1/2 repair DSBs, however in patients with a germline mutation in BRCA1/2, ineffective DNA repair occurs, resulting in chromosome instability and aneuploidy. This eventually leads to malignant tumourigenesis due to the accumulation of mutations (Girolimetti *et al*. 2014). However patients with BRCA1/2 mutations are more sensitive to inter-strand DNA crosslinking agents such cisplatin and carboplatin. Although patients with these mutations can also develop resistance to cisplatin and carboplatin. This may be due to the formation of secondary mutations that may re-align the open reading frame, resulting in the formation of a functioning protein and restores the HR pathway (Dhillon *et al*. 2011). Mutations in these key repair proteins increase the risk of developing breast and ovarian cancer. Germline mutations in BRCA1 and BRCA2 occur in 3–6% and 1–3% of ovarian cancers respectively(Fasching *et al*. 2009). Although perhaps of even greater importance than germline mutations is the high incidence of BRCA1/2 mutations that also occur in cases of sporadic ovarian cancer. A study by Hennessy *et al*. (2010) demonstrated that the frequency of sporadic BRCA1/2 mutations in ovarian cancer may be as high as 23%. BRCA1/2 methylation status may also be highly important for patients with sporadic ovarian cancer. BRCA1/2 methylation status has been shown to be associated with reduced survival compared to patients with unmethylated BRCA1/2 in patients with sporadic ovarian cancer (Rice *et al*. 2000; Ben Gacem *et al*. 2012). BRCA1/2 methylation appears to lower the expression of BRCA1/2 protein expression. Methylation of BRCA1/2 results in reduced BRCA1/2 protein formation. Mutation or inactivation of these key DNA repair proteins has a central role in ovarian tumorigenesis and chemoresistance.

1.3.8.5 MicroRNAs

MicroRNAs are a very valuable and huge source of potential biomarkers for ovarian cancer research. MicroRNA profiling may allow us to identify signatures associated with diagnosis, prognosis and response to treatment. In a previous study by our group

(Langhe et al. 2015) microRNA expression was analysed between sample from patients with malignant and benign ovarian disease and four microRNAs were significantly downregulated in cancer patients, these microRNAs are involved in important cancer pathways such as WNT signalling, AKT/mTOR, TLR-4/MyD88 and VEGF signalling pathway. This study among various others demonstrates the massive potentially for microRNAs as serum biomarkers. The ability to distinguish between benign and malignant ovarian disease as was shown in this study could have very important clinically implications such as less radical treatment for benign lesions, preservation of fertility in young women and reserving waiting lists in gynaecological cancer centres for malignant cases.

1.3.9 New therapies and targeted therapy for ovarian cancer

In recent years a number of new targeted therapies have been also been investigated and become available for ovarian cancer.

1.3.9.1 Pertuzumab

Pertuzumab is a monoclonal antibody which targets HER-2 and prevents it from dimerising with other members of the erb family including HER-3. Currently, a clinical trial NCT01684878 is underway which is examining the use of Pertuzumab in combination with standard chemotherapy in women with recurrent platinum-resistant epithelial ovarian cancer (www.clinicaltrials.gov). A number of other therapeutic agents targeting HER-3 are also being investigated in clinical trials (Jiang *et al*. 2012).

1.3.9.2 PARP Inhibitors

Patients with mutation or inactivation of BRCA1/2 aswell as being more susceptible to cisplatin may also be highly susceptible to treatment with Poly ADP-ribose polymerase (PARP) inhibitors. Poly ADP-ribose polymerase is a family of enzymes which catalyse the formation of poly ADP-ribose. PARP family members sense single stranded DNA breaks and synthesise Poly ADP-ribose to signal other repair enzymes to the site of the damaged DNA. Poly ADP ribose is then degraded by Poly ADP-ribose glycohydrolase (PARG) following repair of the DNA strand. In patients with mutation in BRCA1/2, ineffective DNA repair leads to the accumulation of DNA damage and eventually the mutation of an important tumour suppressor/oncogene leading to tumourigenesis. DNA repair still occurs in these patients regardless. DNA repair is ineffective in patients with BRCA1/2 mutations. PARP inhibitors induce further damage resulting in cell apoptosis in these patients. In December 2014 the FDA granted accelerated approval of the first PARP inhibitor Lynparza (olaparib) from AstraZeneca

for the treatment of advanced ovarian cancer in patients harbouring BRCA mutations who have failed on three or more chemotherapy treatments (Nature Publishing Group, 2015). They also approved Myriad genetics BRACAnalysis test as a companion diagnostic tool to identify germline BRCA mutations in patient to be treated with Lynparza (www.genomeweb.com).

1.3.9.3 VEGF inhibitors

Bevacizumab (Avastin) is a VEGF inhibitor sold by Genentech Inc and is approved for the treatment of primary and recurrent platinum resistant ovarian cancer, metastatic colorectal cancer, NSCLC, rectal cancer, metastatic renal cancer, advanced cervical cancer and recurrent glioblastoma in combination with other therapies. Avastin was previously granted accelerated approval for metastatic breast cancer but the FDA subsequently withdrew approval as it was found to have no benefit to PFS and OS (www.fda.gov 2014). Pazopanib (Votrient®) is a targeted therapy drug that, like bevacizumab, helps stop new blood vessels from forming. A study by du Bois *et al*. (2014) found that maintenance therapy with Pazopanib prolonged PFS in patients with advanced ovarian cancer.

1.3.9.4 Aspirin

Metastasis is the main cause of cancer related deaths and constitutes a major clinical management problem for patients with cancer. The transport of CTCs into through the bloodstream and extravasation to distant target organs is a key step in the development of metastasis. Upon entry into the bloodstream CTCs interact with platelets and are shielded from detection from the immune system, a process termed “platelet cloaking”. As well as its role in immune evasion, platelet cloaking of ovarian cancer cell lines has been shown to induce EMT (Spillane *et al*. 2014). Furthermore, both platelets and platelet releasates have been shown to mediate pro-survival and pro-angiogenic signalling (Egan *et al*. 2011). These property of platelets may therefore further enhance metastasis by promoting the development of a more migratory invasive phenotype (Spillane *et al*. 2014). Interestingly Spillane *et al*. (2014) demonstrated that the rate of platelet-ovarian cancer cell adhesion differs depending on the type of cell line. This may reflect surface marker expression and the metastatic potential of different ovarian cells. Further molecular characterisation of the surface markers expressed by CTCs may lead to the development of targeted therapies which prevent metastatic spread by CTCs. Interestingly in recent years, mounting evidence has highlighted a potential role for aspirin in preventing/reducing the development of metastasis in a number of cancers including breast (Johnson *et al*. 2002), colorectal

(Friis *et al*. 2009), pancreatic (Tan *et al*. 2011), non-Hodgkin (Cerhan *et al*. 2003), head and neck (Wilson *et al*. 2013), prostate (Veitonmaki *et al*. 2013) and ovarian (Tsoref *et al*. 2014). Aspirin has been shown to inhibit platelet function through acetylation of the platelet cyclooxygenase (COX)(Schrör 1997). It is through this function that it may help prevent and treat metastasis by preventing platelet cloaking and CTC invasion.

1.3.9.5 Folic acid receptor inhibitors

Folic acid receptor alpha is overexpressed in various epithelial malignancies including ovarian cancer. Two folic acid receptor inhibitors have been tested for ovarian cancer, vintafolide and farletuzumab. Vintafolide was withdrawn by Merck after a late stage trial revealed it was unable to improve progression-free survival (PFS) in patients with platinum-resistant ovarian cancer. Farletuzumab is a drug marketed by morphotek currently under investigation for the treatment of ovarian cancer (www.morphotek.com).

1.3.9.6 Metformin

Metformin sold under the tradename Glucophage is used in the treatment of type 2 diabetes and has also been used to treat polycystic ovarian syndrome. This drug in recent years has also been shown to enhance survival rates in patients with ovarian cancer. Interestingly, Hirsch *et al*. (2013) showed that metformin could selectively target breast cancer stem cells. A further study by Hu et al. (2014) demonstrated that low dose metformin treatment inhibited breast and ovarian cancer *in-vivo* and downregulated cancer stemness markers including CD44 Nanog, Oct-4 and c-myc. Therefore it is thought that metformin may selectively reprogram cancer stem cells into non cancer cells.

1.3.9.7 Catumaxomab

Catumaxomab which is sold under the tradename removab is a new monoclonal antibody developed by Fresenius Biotech which targets CD3 and EPCAM and has shown to be effective at treating and reducing the amount malignant ascites in patients with ovarian cancer (Tsikouras et al. 2013).

However despite the availability of these promising biomarkers and targeted therapies for ovarian cancer the clinical utility of these biomarkers and targeted therapies individually is quite limited. This is due in part to the heterogeneity of ovarian cancer, even within distinct histological subtypes such as high grade serous ovarian cancer. As a result not all patients will exhibit an adequate response to new therapies and analysis of a single biomarker will not always give sufficient information about a patient's

prognosis. Instead panels of reliable biomarkers need to be examined in patients with specific histological subtypes of the disease in order to obtain accurate prognostic information about individual patients and to enhance patient therapy.

In the last number of years breast cancer therapy has been revolutionised with the discovery of human epidermal growth factor receptor 2 (HER-2) and the introduction of personalised medicine; as a result patient prognosis rates have drastically improved (National Cancer Registry 2012a). Breast cancer therapy is now based upon the molecular phenotype of the disease and the expression of various surface receptors including HER-2, oestrogen receptors (OR) and progesterone receptors (PR). By classifying patients by molecular phenotypes, patients can be triaged accordingly and receive the most appropriate treatment (Olopade *et al*. 2008; Oakman *et al*. 2009). Recently MyD88, TLR4 and MAD2 have been shown by our group individually in separate ovarian cancer cohorts to be important markers of prognosis in ovarian cancer (Furlong *et al*. 2012; d'Adhemar *et al*. 2014). What is novel about this project is that the combined utility of these three markers will be investigated within the same patient cohort. Furthermore staining patterns will be assessed in a unique cohort consisting of primary, metastatic and recurrent matched patient samples. *In-silico* analysis predicted no direct interaction or pathway linkage between the TLR4-MyD88 pathway and MAD2. However a relationship may still exist between these important biomarkers and this is explored in future chapters. We see a potential prognostic role for these three protein biomarkers in ovarian cancer. They may be able to predict patient chemoresponse from the outset and better direct patient therapy ultimately improving patient outcomes.

1.4 MyD88 and the TLR4 signalling pathway in cancer

1.4.1 Pathway overview

Toll like receptors are an important part of our innate immune defence against invading pathogens and are expressed by various immune cells. Additionally they are also expressed by skin keratinocytes, glial cells in the brain, paneth cells in digestive tract and in the female reproductive tract e.g. Toll like receptor 4 (TLR4) on the surface epithelium of the ovaries (Zeromski *et al*. 2008; Zhou *et al*. 2009). As well as these different cell types, toll like receptors can also be expressed by cancer cells and become activated by cellular debris generated from both normal and neoplastic cells which may be present in the tumour microenvironment (Sato *et al*. 2009). In recent years, the TLR4-MyD88 signalling pathway has been implicated in a number of different cancers including ovarian cancer (Kelly *et al*. 2006; Hua *et al*. 2009; Doan *et al*. 2009; Szajnik *et al*. 2009; Szczepanski *et al*. 2009; Ikebe *et al*. 2009; Zhang *et al*. 2010; Hsu *et al*. 2011; Sheyhidin *et al*. 2011; Xu *et al*. 2011; Zhang *et al*. 2012; Sun *et al*. 2012; Kim *et al*. 2012; Rajput *et al*. 2013; Eiro *et al*. 2013; Eiró *et al*. 2013; Volk-Draper *et al*. 2014; Yang *et al*. 2014; Haricharan & Brown 2015). It is thought that signalling through this pathway may contribute to the development of an inflammatory microenvironment, which supports tumour growth and indeed the link between inflammation and the development of cancer has been well established in the past number of decades (R. Chen *et al*. 2008; O'Neill 2008; Sato *et al*. 2009). Extracellular recognition of a ligand causes the intracellular toll-interleukin 1 receptor (TIR) domain of TLR4 to bind a similar TIR domain in the adaptor protein MyD88 which forms a protein bridge or scaffold in order to recruit other signalling molecules. MyD88 has a second domain called a death domain which it then uses to recruit two protein kinases IRAK4 and IRAK1 through their death domains. The IRAK complex recruits an E3 ubiquitin ligase called TRAF6 and an E2 ligase called TRICA1 which together generate a scaffold of polyubiquitin chains on TRAF6 itself and on the protein NEMO, that recruits and activates the serine-threonine kinase TAK1. TAK1 in turn activates members of the mitogen activated protein kinase family including c-jun terminal kinase (JNK) and MAPK14 (P38 MAPK) which activate a number of substrates including the transcription factor AP-1 which is involved in cell proliferation, transformation, and cell death. TAK1 also phosphorylates and activates the IKB kinase complex (IKK) which is composed of three proteins, IKKα, IKKβ, and IKKϒ (NEMO). When activated, IKK phosphorylates IκB which then releases nuclear factor kappa-light-chain-enhancer of activated B cells (NF-κB). IκB is then subsequently ubiquitinated and degraded in the proteasome. Once released from its inhibitor, NF-κB moves into the nucleus, where it

directs the activation of gene expression of a number of inflammatory cytokines and chemokines including TNF-α, IL-1β, IL-12, IL-6, IL-10 and CXCL8 (Murphy 2012) **(Figure 1.7)**.

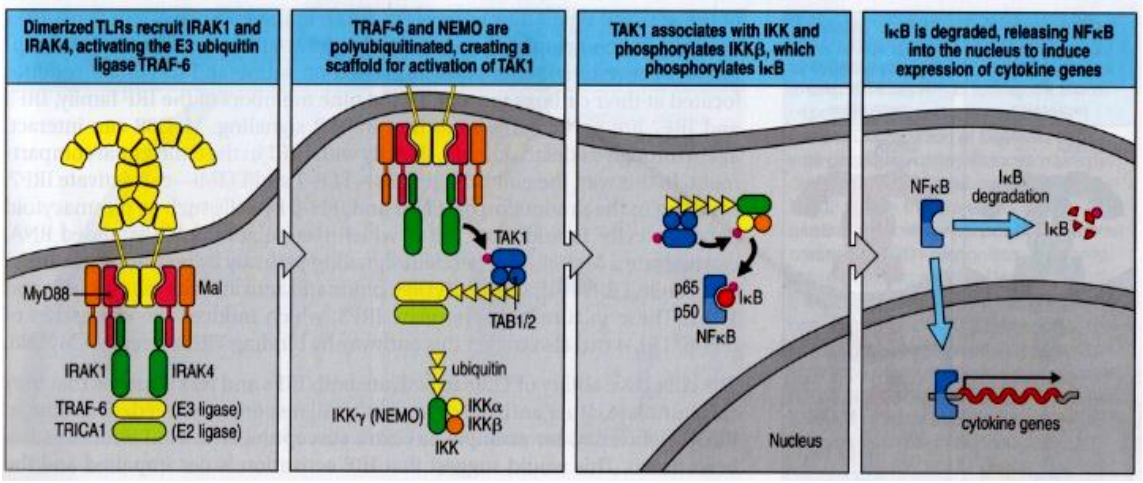

Figure 1.7 An overview of the MyD88 dependent TLR4 pathway. Upon binding of a ligand the TIR domain of TLR4 binds to the TIR domain MyD88 which recruits other downstream signalling molecules culminating in the activation of IKK which phosphorylates IKB allowing NF-κB to enter the nucleus and activate gene expression of various inflammatory cytokines and chemokines (Murphy 2012).

TLR4 is also capable of signalling through a MyD88 independent pathway involving the alternative adaptor protein TRIF, which activates the transcription of type 1 interferons (Murphy 2012) **(Figure 1.8)**.

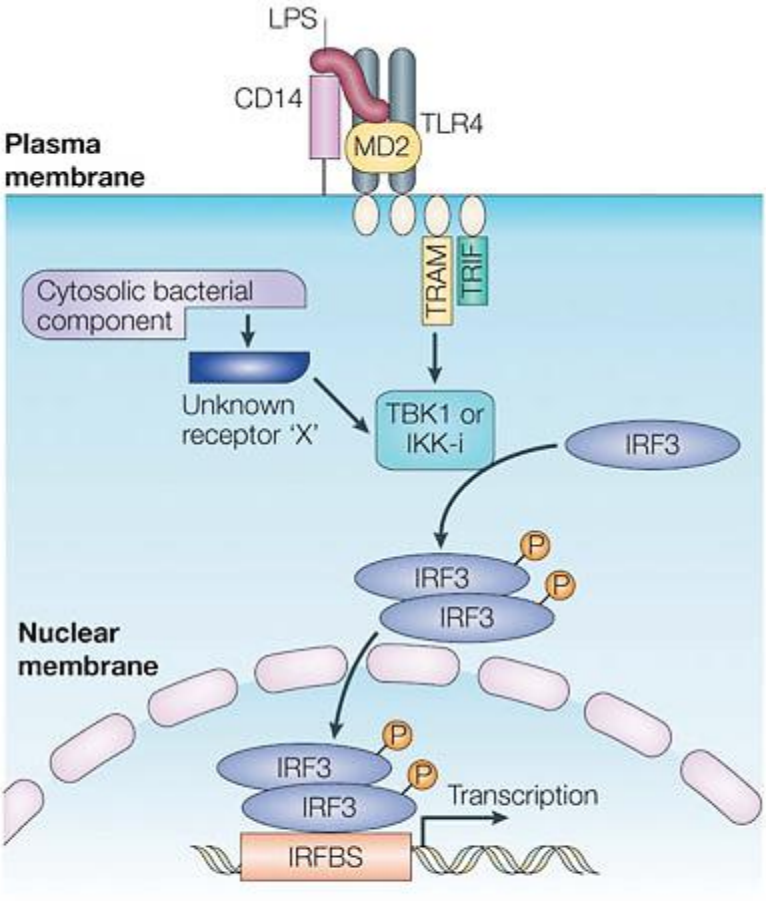

Figure 1.8 The TRIF dependent TLR4 signalling pathway. TLR4 can signal through the adaptor protein MyD88 to activate the production of inflammatory cytokines and chemokines. Additionally, TLR4 can signal through a MyD88 independent pathway involving the adaptor protein TRIF, in order to synthesise type 1 interferons (Decker *et al* 2005).

1.4.2 The TLR4-MyD88 pathway in patient prognosis and chemoresistance

Recently our group and others have shown that high immunohistochemical staining of MyD88 in ovarian cancer cases is associated with poor patient prognosis including reduced PFS (p=0.02), OS (p=0.029) and the development of metastasis (Kim *et al*. 2012; Zhu *et al*. 2012; d'Adhemar *et al*. 2014) **(Figure 1.9 B&D)**. Additionally MyD88 was shown to be a highly specific marker for ovarian cancer, as it does not stain normal ovarian epithelium. Furthermore our group demonstrated that high immunohistochemical staining of TLR4 in ovarian cancer cases was associated with reduced PFS (p=0.016) **(Figure 1.9A)**.

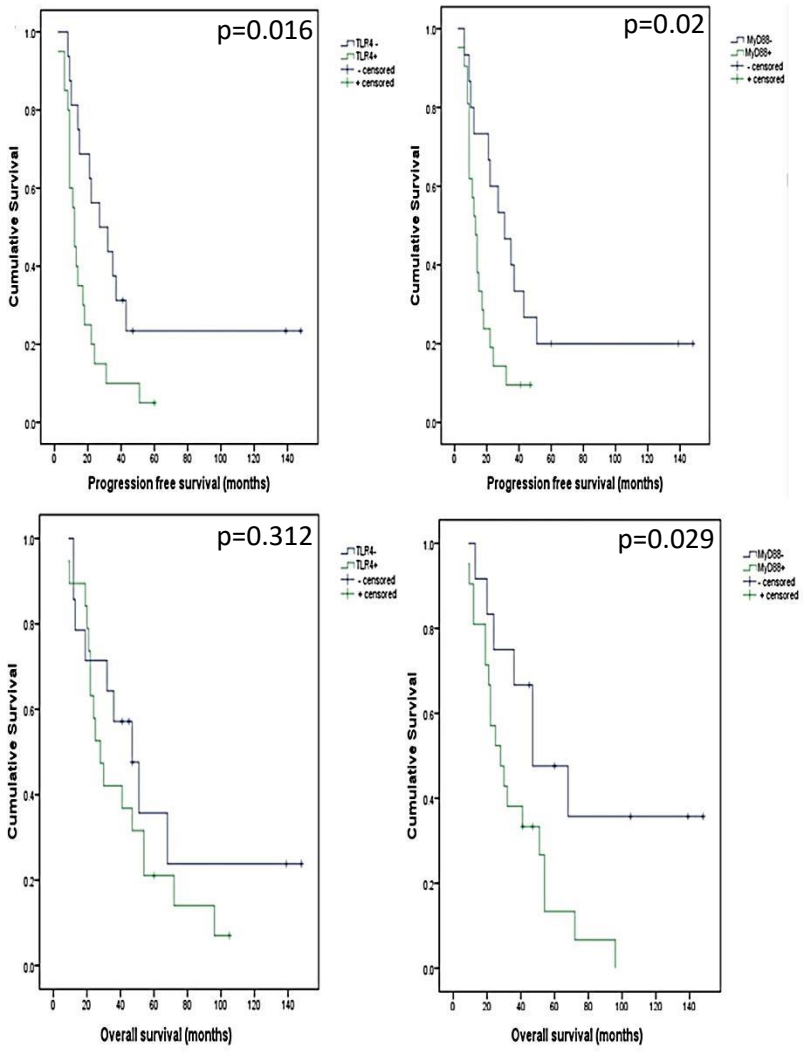

Figure 1.9 TLR4 and MyD88 expression and progression free survival and overall survival. Following immunostaining for MyD88 and TLR4, immunostaining result were correlated with patient survival using Kaplan-Meier analysis. High MyD88 expression was correlated with a reduction in PFS (B) and OS (D). High TLR4 expression was correlated with reduced PFS (A) but not a reduction in OS (C), n=69, p<0.05 (d'Adhemar *et al*. 2014).

,MyD88 has also been implicated in a range of other cancers including leukaemia and lymphoma (Nowicki *et al*. 2003; Ngo *et al*. 2011; Treon *et al*. 2012; Puente *et al*. 2011; Gonzalez-Aguilar *et al*. 2012; Choi *et al*. 2013), intestinal (Rakoff-Nahoum & Medzhitov 2007), gastric and colon (Kennedy *et al.* 2014; Coste *et al*. 2010; Kfoury *et al*. 2013), breast (Egunsola *et al*. 2012), liver (Naugler *et al*. 2007), skin (Cataisson *et al*. 2012), lung (Xu *et al*. 2011; Egunsola *et al*. 2012) and pancreatic cancers (Liang *et al*. 2013). Moreover MyD88 has been shown to be a marker of ovarian cancer stem cells (Alvero *et al*. 2011).

1.4.3 MyD88 as a marker of ovarian cancer stem cells

Cancer stem cells (CSCs) or tumour initiating cells (TICs) are cancerous cells which share various properties with normal stem cells, including the ability to self-renew and differentiate (Foster *et al*. 2012). These cells are thought to be the only type of cell capable of generating a tumour (tumourigenesis) (Moitra 2015). CSCs similar to normal stem cells may be organised into stem-progenitor-differentiated cell hierarchies, with the most powerful CSC in a dormant quiescent state at the apex of the hierarchy (Ffrench *et al*. 2014). The apex CSC can be activated to produce actively dividing progenitor cells which in turn give rise to differentiated cells which form the bulk of the tumour. Once progenitor cells are produced then the apex CSC can return to a quiescent state, long periods of quiescence likely protect CSCs from the stress associated with cell division. This hierarchical organisation may augment the tumours ability to overcome therapeutic insults. CSCs are thought to be intrinsically chemoresistant and those cells in a quiescent state may be further protected from anti-mitotic chemotherapies which target actively dividing cells. Therefore these cells are thought to recapitulate the tumour following completion of chemotherapy leading to recurrent disease and chemoresistance. Direct targeting of CSCs may therefore be needed to successfully eliminate a tumour (Reya *et al*. 2001) **(Figure 1.10)**.

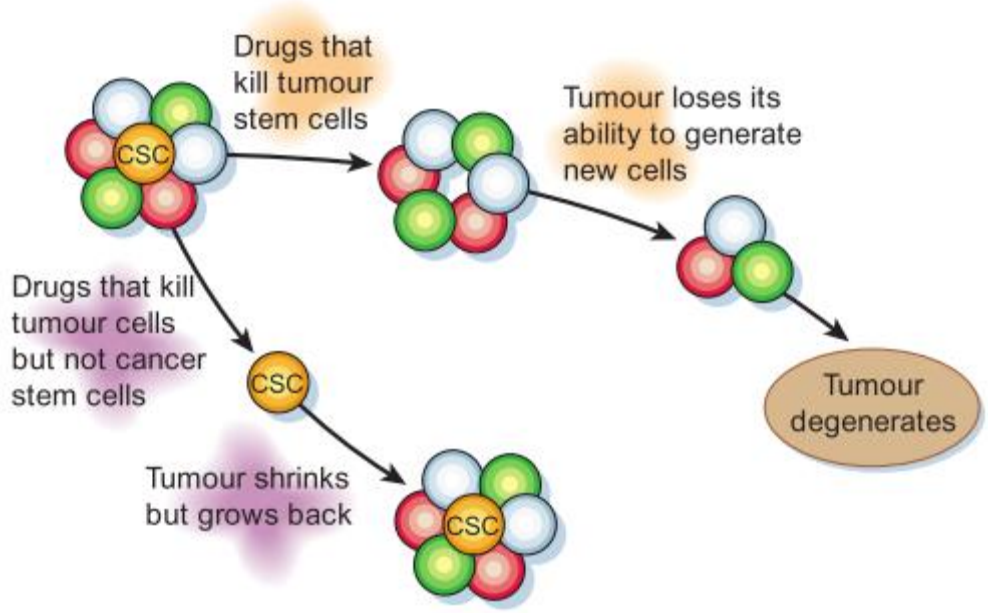

Figure 1.10 Cancer stem cells lead to recurrent disease and chemoresistance. CSCs are not eliminated by conventional chemotherapy and are thought to regenerate the tumour following completion of chemotherapy leading to recurrent disease and chemoresistance, therefore CSCs need to be targeted in order successfully eliminate the tumour (Reya *et al*. 2001).

Our group has demonstrated that MyD88 is a very important gene in differentiation in the embryonal carcinoma model, 2102Ep (Sulaiman 2015). Indeed it may be an important regulator of differentiation in all pluripotent stem cells including CSCs. Suppression of MyD88 in 2102Ep cells facilitates differentiation following retinoic acid treatment. If MyD88 is not supressed then differentiation does not occur, even in response to retinoic acid treatment. Interestingly MyD88 downregulation does not result in spontaneous differentiation, but instead induces a “primed undifferentiated state” which if given the correct stimulus such as retinoic acid allows differentiation to occur. This may have important implications for future CSC therapy. CSCs are thought to only be capable of generating tumours when in an undifferentiated state, while differentiated cells have no tumourigenic potential (Ffrench *et al*. 2014). Therefore forced differentiation of CSCs is an attractive option for CSC therapy. Forced differentiating CSCs, may reduce/reverse their tumourigenic potential leading to more successful cancer therapies and the prevention of chemoresistant and recurrent disease. We believe the work performed in the 2102Ep cell model supports the hypothesis that EOC MyD88 positive cells may be stem-like due to their MyD88 expression pattern. Therefore targeting MyD88 may potentially act as type of enforced differentiation therapy.

Furthermore Alvero *et al* (2011)**,** isolated a population of ovarian cancer stem cells which were MyD88^{+} and CD44^{+}. These cells, unlike their MyD88^{-} CD44^{-} counterparts, were resistant to paclitaxel induced apoptosis. Furthermore, paclitaxel was shown to induce signalling through the TLR4-MyD88 pathway and activate expression of various inflammatory chemokines and cytokines in these MyD88^{+} CSCs. Interestingly, our group and others have also shown that blockage or knockdown of TLR4 in SKOV-3 cells (a paclitaxel resistant ovarian cancer cell line), renders these cells more sensitive to paclitaxel therapy. These cells have an active TLR4-MyD88 pathway and constitutively express various inflammatory cytokines and chemokines. Paclitaxel treatment was shown to further upregulate cytokine expression in these cells, while blockage of this pathway supressed cytokine secretion (Szajnik *et al*. 2009; d'Adhemar *et al*. 2014; Huang *et al*. 2014; A. C. Wang *et al*. 2009). Paclitaxel is a known ligand for TLR4 (Byrd-Leifer *et al*. 2001), therefore in some patients paclitaxel treatment may not only have little benefit for these patients, it may in fact be harmful. Therefore for certain patient's alternative treatments such as CSC therapy or blockage of the TLR4-MyD88 pathway using an inhibitor prior to paclitaxel treatment may lead to more successful disease outcomes.

1.5 MAD2 and the spindle assembly checkpoint

During M phase of the cell cycle there is a crucial cell cycle checkpoint known as the spindle assembly checkpoint (SAC). The spindle assembly checkpoint prevents the cell from entering anaphase until all chromosomes have successfully attached to the mitotic spindle. This ensures proper segregation of sister chromatids. Proper chromosome segregation is essential for correct cell division. Improper chromosome segregation (aneuploidy) often results in cell death and is a major hallmark of cancer. During spindle assembly, microtubules from each spindle pole attach to the kinetochores of each chromosome ensuring that the sister chromatids are segregated to opposite poles of the cell. This ensures that equal copy numbers of each chromosome segregate into both the mother and daughter cell. Sister chromatids are joined together by a molecule called cohesin. During anaphase, cohesin is degraded by the enzyme separase which for most of the cell cycle is bound and inhibited by the protein securin. However during the metaphase-anaphase transition, the anaphase promoting complex/cyclosome (APC)/C is activated by Cdc20. APC/C is a ubiquitin ligase and acts on securin, signalling its degradation by the proteasome releasing separase. This allows it to carry out separation of chromosomes by degrading cohesin, the molecule which keeps sister chromatids together (Liu *et al*. 2010). A number of proteins are required for maintaining the spindle assembly checkpoint, until correct attachment of chromosomes has occurred. These include members of the mitotic arrest deficiency (Mad) protein family (Mad1, Mad2, Mad3) and the budding uninhibited by benzimidazoles (Bub) family (Bub1, BubR1, Bub3) of proteins which were first identified in budding yeast (Li & Murray 1991; Hoyt *et al*. 1991). These proteins conglomerate at the kinetochores, generating a wait signal, and prevent Cdc20 from activating the APC until microtubules have successfully attached to the kinetochores **(Figure 1.11)**. Mad2 and Bub1 are the main members from each family involved in the SAC. Correct function of these two proteins in the SAC pathway is essential for the prevention of aneuploidy and as such their dysregulation has been implicated in a number of cancers (Antoni *et al*. 2005)**.**

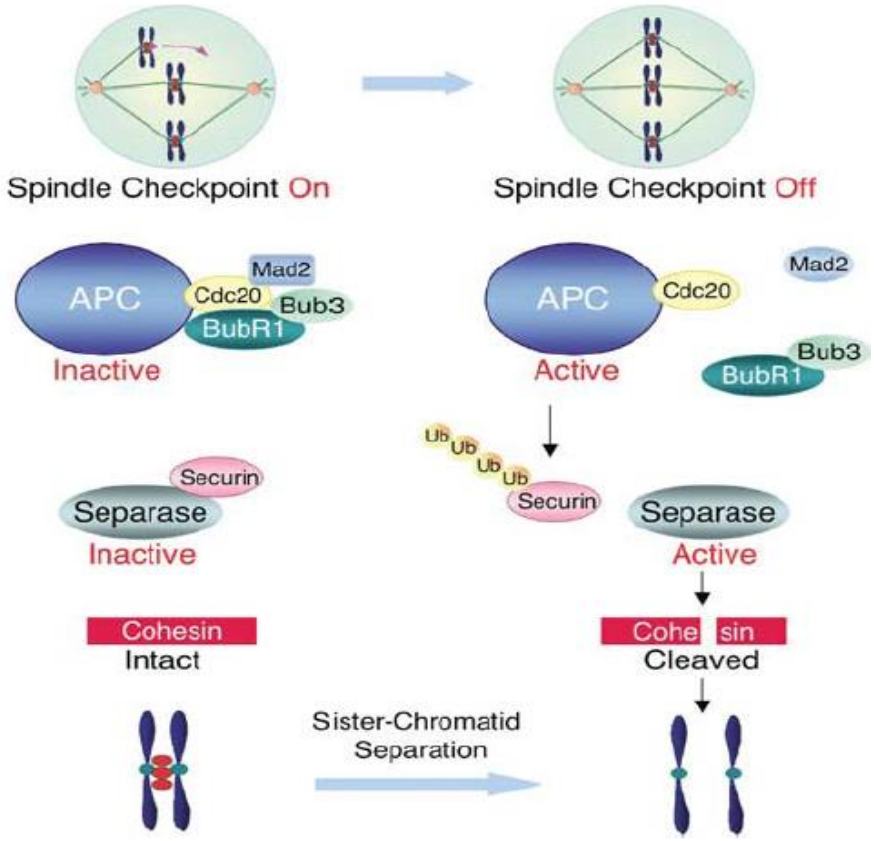

Figure 1.11 The spindle assembly checkpoint (SAC) and the role of MAD2 in correct chromosome separation. MAD2, Bub3 and BubR1 prevent the onset of anaphase by inhibiting the APC/Cdc20 complex until all spindle microtubules have correctly aligned with the kinetochores of each chromatid, thus ensuring correct chromosomal separation prior to cell division and preventing the onset of aneuploidy and cancer (Bharadwaj & Yu 2004).

Aberrant MAD2 expression has been reported in a wide range of different cancers including colon (Rimkus *et al*. 2007), gastric (Kim *et al*. 2005; Du *et al*. 2006; L. Wang *et al*. 2009), ovarian (Wang *et al*. 2002; Sudo 2004; Hao *et al*. 2010; Furlong *et al*. 2012), nasopharyngeal (Wang *et al*. 2000), soft tissue sarcoma (Hisaoka *et al*. 2008), testicular germ cell (Fung *et al*. 2007), hepatocellular (Chen *et al*. 2002; Jeong *et al*. 2004; Zhang *et al*. 2008), prostate (Prencipe *et al*. 2010), breast (Percy *et al*. 2000; Prencipe *et al*. 2009) and lung cancers (Gemma *et al*. 2001; Kato *et al*. 2011). A number of studies have also shown that downregulation of MAD2 increases resistance to chemotherapeutic agents; cisplatin (Cheung *et al*. 2005; Fung *et al*. 2006) and paclitaxel (Sudo 2004; Prencipe *et al*. 2009). Interestingly, a study by (Wang *et al*. 2004) showed that MAD2 also contains a binding motif for the DNA repair protein, Breast and Ovarian Cancer Susceptibility Protein 1 (BRCA1).Thus BRCA1 acts as a positive regulator of MAD2 transcription. Previously our group demonstrated that

MAD2 was downregulated during hypoxia in a number of cell models and that downregulation or knockdown of MAD2 was shown to induce senescence and paclitaxel resistance *in-vitro* (Prencipe *et al*. 2009; Prencipe *et al*. 2010; Furlong *et al*. 2012). Furthermore, our group also showed that MAD2 was downregulated in hypoxic tumour regions. Therefore MAD2 downregulation and the induction of senescence may be a method exploited by cancerous cells in the hypoxic tumour microenvironment to become chemoresistant. Our group also identified that low MAD2 IHC staining in patients with high grade serous ovarian cancer was associated with significant reduction in their PFS (p = 0.0003) **(Figure 1.12)**.

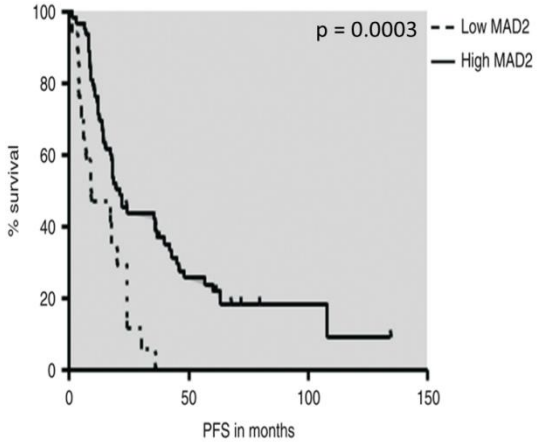

Figure 1.12 MAD2 IHC staining intensity is associated with progression-free survival (PFS) in high-grade serous EOC. Low MAD2 IHC staining intensity was correlated with progression-free survival (PFS) in patients with high-grade serous EOC. Multivariate Cox's regression hazard analysis (adjusted for stage, tumour grade and optimum surgical debulking < 1cm) showed a significant correlation between low MAD2 IHC staining intensity and PFS (p = 0.0003; HR 4.689, n=82).

1.6 MicroRNA regulation of the TLR4-MyD88 pathway and MAD2

MicroRNAs are small non-coding RNAs around 22nts in length which are capable of regulating gene expression. MicroRNAs regulate gene expression, either by binding to and inhibiting mRNA or by tagging the promoter region of target genes for methylation by DNA methyltransferases (Baley & Li 2012). Over 1000 MicroRNAs have been identified to date and are known to regulate gene expression of a number of important signalling pathways involved in DNA repair, proliferation and apoptosis and indeed a single microRNA may be capable of regulating hundreds of gene targets. Aberrant microRNA expression occurs in various disease states including cancer and aberrant microRNA expression may also be contributing to the development of the chemoresistant phenotype and recurrent disease (Gao *et al*. 2010).

1.6.1 MicroRNAs as biomarkers in ovarian cancer

MicroRNAs are frequently detected in both solid tumours (Volinia *et al*. 2006) and the sera of cancer patients (X. Chen *et al*. 2008; Langhe *et al*. 2015) and more recently in circulating tumour exosomes (Taylor & Gercel-Taylor 2008). MicroRNA profiling may allow us to identify signatures associated with diagnosis, prognosis and response to treatment of human tumours. There are a variety of methods available for the detection of microRNAs including RT-PCR, microRNA array based methods (Szafranska *et al*. 2008). They can also be detected *in-situ* using locked nucleic acid (LNA) probes (Nuovo 2008; Yamamichi *et al*. 2009) or detected by newer sequencing technologies such as nanostring counting (Alder *et al*. 2012; Fabbri *et al*. 2012; Kolbert *et al*. 2013) In this study, three microRNAs miR-433, miR-146a and miR-21 were analysed in ovarian cancer cell lines.

1.6.2 miR-146a and miR-21

A number of microRNAs are known to regulate the TLR4-MyD88 pathway including miR-155,147,125b, 21, 7e, 21, 146a (Liston *et al*. 2010; Tang *et al*. 2010; Sheedy *et al*. 2010; O'Neill *et al*. 2011). miR-21 is an oncomir, and is aberrantly expressed in numerous cancers. It serves to negatively regulate the inflammatory response to lipopolysaccharide (LPS). Specifically, miR-21 induction decreases the expression of PDCD4, in turn causing the upregulation of the IL-10 driven anti-inflammatory response, while also supressing the NF-κB driven pro-inflammatory response (Quinn & O'Neill 2011). miR-146a is one member of the miR-146 family of microRNAs which consists of miR-146a and miR-146b. miR-146 serves to negatively regulate downstream members of the MyD88 pathway specifically TNF receptor-associated factor (TRAF-6) and IL-1 receptor-associated kinase 1(IRAK-1) to inhibit activation of NF-κB and the release of cytokines. Under normal circumstances miR-146 serves to downregulate expression of inflammatory molecules released during inflammation thus preventing cellular damage from long term activation of inflammatory pathways and serves as part of a negative feedback loop in conjunction with miR-155 and miR-21. miR-146a is upregulated by NF-κB and other factors such as interleukin 1 and tumour necrosis factor-alpha (Quinn & O'Neill 2011). It has been identified as a key molecule involved in endotoxin tolerance and is implicated in a number of inflammatory and immune disorders such as osteoarthritis. Interestingly in a study by (Fabbri 2012) it was proposed that microRNAs secreted in exosomes from cancerous cells may be capable of activating TLRs. Further evidence has shown that the expression of miR-21 and miR-146a is inversely linked to the expression of both TLR4 and MyD88 and some studies have shown that they are able to directly target both TLR4 and MyD88 (Yang *et al*. 2011; Zhao *et al*. 2012; Lario *et al*. 2012; Chen *et al*. 2013). Previously our group performed microRNA qPCR on a small subset of MyD88 negative and MyD88 positive EOC cases (d'Adhemar *et al*. 2014). It was found that expression of miR-21 and miR-146a was upregulated in all MyD88 negative EOCs. Expression of these two microRNAs was also assessed in a number of ovarian cancer cell lines and their chemoresistant counterparts. Variable changes in the expression of these two regulatory microRNAs was observed between each cell model and their chemoresistant counterparts (d'Adhemar *et al*. 2014). There was a 6.5 fold increase in miR-146a in A2780cis cells compared to MyD88-negative A2780 cells. IGROV-1CDDP cells showed a 1.2 fold increase in miR-146a relative to the chemosensitive IGROV-1 cells, however this change was not statistically significant ($p=0.4557$). A2780cis cells showed a 1.5 fold decrease in miR-21 compared to A2780, however this change was

not statistically significant (p=0.5958). A 2 fold increase in miR-21 was detected in the chemoresistant IGROV-1CDDP cells relative to IGROV-1 cells.

1.6.3 miR-433

miR-433 was shown to target MAD2 previously by (Furlong *et al*. 2012) using a luciferase reporter assay. Within this study, it was also shown that overexpression of miR-433 caused down regulation of MAD2 and induced senescence and paclitaxel resistance in A2780 cells. Analysis of miR-433 in patient tumour samples also revealed that patients expressing high levels miR-433 had a significantly reduced PFS (p=0.024) **(Figure 1.13)**. In a subsequent paper by (Weiner-Gorzel *et al*. 2015), it was demonstrated that miR-433 induces senescence by downregulating expression of cyclin-dependent kinase 6, preventing the phosphorylation of pRB and blocking continuation through the cell cycle. miR-433 was also predicted to target three other senescence associated genes including MAPK14, E2F3, and CDKN2A. Interestingly miR-433 was detected in exosomes isolated from the growth culture media of A2780, PEO1 and PEO4 cells. The authors conclude that miR-433 enriched cells may affect their environment and could potentially induce senescence in neighbouring cells using miR-433 incorporated into vesicles.

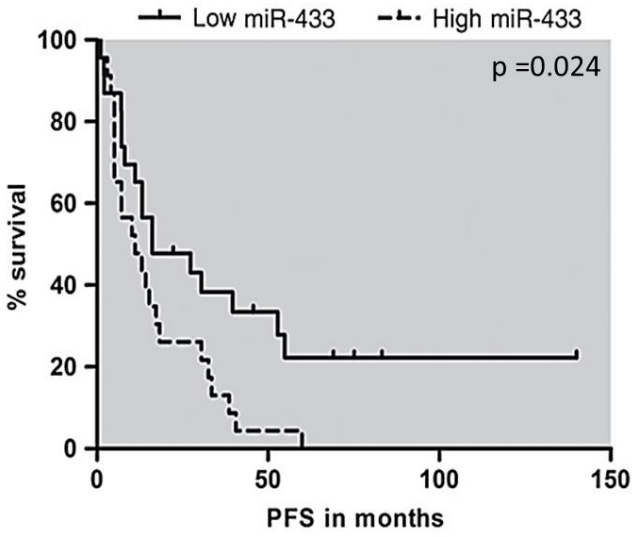

Figure 1.13 miR-433 expression and PFS. miR-433 was analysed by RT–PCR and normalized to U6 (microRNA endogenous control). The median expression level was 1.07. For statistical analysis, patient samples were grouped into low (< 1.8) and high (>1.8) miR-433 expression categories. Kaplan–Meier survival curve and log rank analysis revealed that high miR-433 expression in patients with high grade serous EOC was associated with reduced PFS, p<0.05, n=45.

TLR4, MyD88 and MAD2 have shown great promise individually as prognostic biomarkers in ovarian cancer and are involved in paclitaxel resistance in ovarian cancer. Additionally the regulatory microRNAs miR-146a, miR-21 and miR-433 may have an important role in ovarian cancer. Therefore the aim of this study was to assess the *in-vitro* relationship between the three protein biomarkers and the three microRNA biomarkers and further assess their respective roles in paclitaxel resistance. Another major aim was to assess the combined utility of MAD2, TLR4 and MyD88 in predicting patient prognosis as individually they are reliable prognostic indicators. The ultimate aim of this is to identify patients who are least likely to respond to paclitaxel based chemotherapy and whether biomarker triage may allow more appropriate patient treatment.

1.7 Hypotheses

1) The combined assessment of TLR4, MyD88 and MAD2 may more accurately predict chemoresponse and outcome for women presenting with ovarian cancer.
2) An *in-vitro* relationship may exist between the TLR4-MyD88 pathway and the spindle assembly checkpoint protein MAD2.
3) The regulatory microRNAs miR-146a, miR-21 and miR-433 may play a role in ovarian cancer and paclitaxel resistance.

1.8 Aims and objectives

1) To assess the *in-vitro* relationship between TLR4, MyD88 and MAD2.
2) To further assess the mechanism by which MAD2 and the MyD88/TLR4 play a role in chemoresistance.
3) To assess ability of MyD88, TLR4 and MAD2 to predict patient prognosis in cohort of high grade serous ovarian cancer and determine whether they can be used in combination to more accurately predict patient outcomes.
4) To further assess the role of the regulatory microRNAs miR-146a, miR-21 and miR-433 in ovarian cancer and paclitaxel resistance.

1.9 References

1) Akira, S. & Takeda, K., 2004. Toll-like receptor signalling. *Nature reviews. Immunology*, 4(7), pp.499–511. Available at: http://www.ncbi. nlm.nih. gov /pubmed/15229469 [Accessed July 10, 2014].
2) Alberts, D.S., Canetta, R. & Mason-Liddil, N., 1990. Carboplatin in the first-line chemotherapy of ovarian cancer.,
3) Alder, H. *et al*., 2012. Dysregulation of miR-31 and miR-21 induced by zinc deficiency promotes esophageal cancer. *Carcinogenesis*, 33(9), pp.1736–1744.
4) Alison, M.R. et al., 2002. An introduction to stem cells. The Journal of pathology, 197(4), pp.419–23.
5) Alvero, A.B. *et al*., 2011. Molecular phenotyping of human ovarian cancer stem cells unravel the mechanisms for repair and chemo-resistance. *Cell Cycle*, 8(1), pp.158–166.
6) Anastasi, E. et al., 2010. HE4: A new potential early biomarker for the recurrence of ovarian cancer. Tumor Biology, 31(2), pp.113–119.
7) Andersen, M.R. et al., 2011. Use of a Symptom Index, CA125 and HE4 to predict ovarian cancer. , 116(3), pp.1–13.
8) Antoni, A. De *et al*., 2005. The Mad1 / Mad2 Complex as a Template for Mad2 Activation in the Spindle Assembly Checkpoint University of North Carolina at Chapel Hill. , 15, pp.214–225.
9) Baley, J. & Li, J., 2012. MicroRNAs and ovarian function. *Journal of ovarian research*, 5(1), p.8.
10) Bast, R.C. *et al*., 1981. Reactivity of a monoclonal antibody with human ovarian carcinoma. *The Journal of clinical investigation*, 68(5), pp.1331–1337.
11) Bast, R.C., Hennessy, B. & Mills, G.B., 2010. The biology of ovarian cancer : new opportunities for translation. *Nature Reviews Cancer*, 9(6), pp.1–28.
12) Bast, R.C., Hennessy, B. & Mills, G.B., 2009. The biology of ovarian cancer: new opportunities for translation. *Nature reviews. Cancer*, 9(6), pp.415–28. Available at: http://www.pubmedcentral.nih.gov/article rend er.fcgi?artid=2814299&tool=pmcentrez&rendertype=abstract [Access ed July 9, 2014].
13) Behrens, B.C. *et al*., 1987. Characterization of a cis Diamminedichloro-platinum (II) -resistant Human Ovarian Cancer Cell Line and Its Use in Evaluation of Platinum Analogues. , (Ii), pp.414–418.
14) Bell, D. a, 2005. Origins and molecular pathology of ovarian cancer. *Modern pathology : an official journal of the United States and Canadian Academy of Pathology, Inc*, 18 Suppl 2(August 2004), pp.S19–32. Available at: http://www.ncbi.nlm.nih.gov/pubmed/157614 64 [Accessed March 28, 2013].
15) Ben Gacem, R. et al., 2012. Contribution of epigenetic alteration of BRCA1 and BRCA2 genes in breast carcinomas in Tunisian patients. Cancer Epidemiology, 36(2), pp.190–197.
16) Beral, V. *et al*., 2012. Ovarian cancer and smoking: individual participant meta-analysis including 28,114 women with ovarian cancer from 51 epidemiological studies. *The lancet oncology*, 13(9), pp.946–56. Available at: http://www.pubmedcentral.nih.gov/articlerender.fcgi? Artid =3431503 &tool=pmcentrez&rendertype=abstract [Accessed Nov -ember 11, 2012].
17) Bezler, M., Hengstler, J.G. & Ullrich, A., 2012. Inhibition of doxorubicin-induced HER3-PI3K-AKT signalling enhances apoptosis of ovarian cancer

cells. Molecular Oncology, 6(5), pp.516–529. Available at: http://dx.doi.org/10.1016/j.molonc.2012.07.001.
18) Bharadwaj, R. & Yu, H., 2004. The spindle checkpoint, aneuploidy, and cancer. *Oncogene*, 23(11), pp.2016–27. Available at: http://www.ncbi.nlm.nih.gov/pubmed/15021889 [Accessed October 29, 2012].
19) Bruchim, I., Jarchowsky-Dolberg, O. & Fishman, A., 2013. Advanced (>second) line chemotherapy in the treatment of patients with recurrent epithelial ovarian cancer. *European journal of obstetrics, gynecology, and reproductive biology*, 166(1), pp.94–8. Available at: http:// www.ncbi.nlm.nih.gov/pubmed/23088893 [Accessed March 18, 2013].
20) Buys, S.S., 2011. Effect of Screening on Ovarian Cancer Mortality: The Prostate, Lung, Colorectal and Ovarian (PLCO) Cancer Screening Randomized Controlled Trial *JAMA: The Journal of the American Medical Association*, 305(22), p.2295.
21) Byrd-Leifer, C. a *et al*., 2001. The role of MyD88 and TLR4 in the LPS-mimetic activity of Taxol. *European journal of immunology*, 31(8), pp.2448–57. Available at: http://www.ncbi.nlm.nih.gov/pubmed/1150 0829.
22) Carlson, J.W. *et al*., 2008. Serous tubal intraepithelial carcinoma: Its potential role in primary peritoneal serous carcinoma and serous cancer prevention. *Journal of Clinical Oncology*, 26(25), pp.4160–4165.
23) Cataisson, C. *et al*., 2012. IL-1R-MyD88 signaling in keratinocyte transformation and carcinogenesis. *The Journal of experimental medicine*, 209(9), pp.1689–702. Available at: http://www.pub med central.nih.gov /articlerender.fcgi?artid= 3428947& tool=pmcentrez& rendertype=abstract [Accessed May 22, 2014].
24) Cerhan, J.R. et al., 2003. Association of aspirin and other non-steroidal anti-inflammatory drug use with incidence of non-Hodgkin lymphoma. International Journal of Cancer, 106(5), pp.784–788.
25) Chen, J. et al., 2012. A restricted cell population propagates glioblastoma growth after chemotherapy. Nature, 488(7412), pp.522–6.
26) Chen, R. *et al*., 2008. Cancers take their Toll--the function and regulation of Toll-like receptors in cancer cells. *Oncogene*, 27(2), pp.225–33. Available at: http://www.ncbi.nlm.nih.gov/pubmed/18176 604 [Accessed October 29, 2012].
27) Chen, X. *et al*., 2008. Characterization of microRNAs in serum: a novel class of biomarkers for diagnosis of cancer and other diseases. *Cell research*, 18(10), pp.997–1006.
28) Chen, X. *et al*., 2002. Gene Expression Patterns in Human Liver Cancers. , 13(June), pp.1929–1939.
29) Chen, Y., Chen, J., Wang, H., Shi, J., Wu, K., Liu, S., … Wu, J. (2013). HCV-Induced miR-21 Contributes to Evasion of Host Immune System by Targeting MyD88 and IRAK1. *PLoS Pathogens*, *9*(4), e1003248. doi:10.1371/journal.ppat.1003248
30) Cheng, J.Q. *et al*., 2002. Role of X-linked inhibitor of apoptosis protein in chemoresistance in ovarian cancer: possible involvement of the phosphoinositide-3 kinase/Akt pathway. *Drug resistance updates : reviews and commentaries in antimicrobial and anticancer chemotherapy*, 5(3-4), pp.131–46. Available at: http://www.ncbi.nlm. nih.gov/pubmed/12237081.
31) Cheung, H.W. *et al*., 2005. Mitotic arrest deficient 2 expression induces chemosensitization to a DNA-damaging agent, cisplatin, in nasopharyngeal carcinoma cells. *Cancer research*, 65(4), pp.1450–8. Available at: http://www.ncbi.nlm.nih.gov/pubmed/15735033 [Accessed November 23, 2012].
32) Choi, J.-W. *et al*., 2013. MYD88 expression and L265P mutation in diffuse large B-cell lymphoma. *Human pathology*, 44(7), pp.1375–81. Available at

http://www.ncbi.nlm.nih.gov/pubmed/23380077 [Accessed February 20, 2014].
33) Chuthapisith, S., 2007. Cancer Stem Cells and Chemoresistance. Cancer Stem Cells in practice and theory.
34) Coste, I. *et al*., 2010. Dual function of MyD88 in RAS signaling and inflammation , leading to mouse and human cell transformation. , 120(10), pp.3663–3667.
35) Cui, L., Kwong, J. & Wang, C.C., 2015. Prognostic value of circulating tumor cells and disseminated tumor cells in patients with ovarian cancer: a systematic review and meta-analysis. Journal of Ovarian Research, 8(38). Available at: http://dx.doi.org/10.1186/s13048-015-0168-9.
36) d'Adhemar, C.J. *et al*., 2014. The MyD88+ Phenotype Is an Adverse Prognostic Factor in Epithelial Ovarian Cancer. *PloS one*, 9(6), p.e100816. Available at: http://www.ncbi.nlm.nih.gov/pubmed/24977 712 [Accessed July 2, 2014].
37) Davelaar, E.M. *et al*., 1998. Comparison of seven immunoassays for the quantification of CA 125 antigen in serum. *Clinical Chemistry*, 44(7), pp.1417–1422.
38) Decker, T., Müller, M. & Stockinger, S., 2005. The yin and yang of type I interferon activity in bacterial infection. *Nature reviews. Immunology*, 5(9), pp.675–87. Available at: http://www.ncbi.nlm.nih.gov/pubmed/ 16110316.
39) Dhillon, K.K., Swisher, E.M. & Taniguchi, T., 2011. Secondary mutations of BRCA1/2 and drug resistance. Cancer Science, 102(4), pp.663–669.
40) Di, A.J., Goodisman, J. & Dabrowiak, J.C., 2012. Understanding how the platinum anticancer drug carboplatin works : From the bottle to the cell. *Inorganica Chimica Acta*, 389, pp.29–35. Available at: http://dx.doi.org /10.1016/j.ica.2012.01.028.
41) Dietl, J. & Wischhusen, J., 2011. The forgotten fallopian tube. *Nature reviews. Cancer*, 11(3), p.227; author reply 227. Available at: http:// www.ncbi.nlm.nih.gov/pubmed/21326326 [Accessed March 11, 2014].
42) Doan, H.Q. et al., 2009. Toll-like receptor 4 activation increases Akt phosphorylation in colon cancer cells. Anticancer research, 29(7), pp.2473–8. Available at: http://www.pubmedcentral.nih.gov/article render. fcgi?artid=2901163&tool=pmcentrez&rendertype=abstract.
43) Domcke, S. *et al*., 2013. Evaluating cell lines as tumour models by comparison of genomic profiles. *Nature communications*, 4, p.2126. Available at: http://www.pubmedcentral.nih.gov/articlerender.fcgi? artid =3715 866&tool=pmcentrez&rendertype=abstract [Accessed January 28, 2014].
44) Drapkin, R. et al., 2005. Human epididymis protein 4 (HE4) is a secreted glycoprotein that is overexpressed by serous and endometrioid ovarian carcinomas. Cancer Research, 65(6), pp.2162–2169.
45) Du Bois, A. *et al*., 2009. Role of surgical outcome as prognostic factor in advanced epithelial ovarian cancer: a combined exploratory analysis of 3 prospectively randomized phase 3 multicenter trials: by the Arbeits-gemeinschaft Gynaekologische Onkologie Studiengruppe Ovarialkarzin. *Cancer*, 115(6), pp.1234–44. Available at:http://www. ncbi. nlm.nih. gov /pubmed/19189349 [Accessed July 24, 2014].
46) Du Bois, a. et al., 2014. Incorporation of Pazopanib in Maintenance Therapy of Ovarian Cancer. Journal of Clinical Oncology, 32(30), pp.3374–3382. Available at: http://jco.ascopubs.org/cgi/doi/10.1200/ JCO.2014.55.7348.
47) Du, Y. *et al*., 2006. Depression of MAD2 inhibits apoptosis of gastric cancer cells by upregulating Bcl-2 and interfering mitochondrion pathway. *Biochemical and biophysical research communications*, 345(3), pp.1092–8.

Available at: http://www.ncbi.nlm.nih.gov/pubmed/ 16714000 [Accessed October 24, 2012].
48) Egan, K. et al., 2011. Platelet adhesion and degranulation induce pro-survival and pro-angiogenic signalling in ovarian cancer cells. PLoS ONE, 6(10).
49) Egunsola, A.T. *et al*., 2012. Growth, metastasis, and expression of CCL2 and CCL5 by murine mammary carcinomas are dependent upon Myd88. *Cellular immunology*, 272(2), pp.220–9. Available at: http://www.ncbi. nlm.nih.gov/pubmed/22088941 [Accessed October 29, 2012].
50) Eiro, N. et al., 2013. Expression of TLR3, 4, 7 and 9 in cutaneous malignant melanoma: relationship with clinicopathological characteristics and prognosis. Archives of dermatological research, 305(1), pp.59–67.
51) Eiró, N. et al., 2013. Toll-like receptors 3, 4 and 9 in hepatocellular carcinoma: Relationship with clinicopathological characteristics and prognosis. Hepatology research : the official journal of the Japan Society of Hepatology, pp.1–10. Available at: http://www. ncbi.nlm .nih.gov/pubmed/23742263.
52) Emori, M.M. & Drapkin, R., 2014. The hormonal composition of follicular fluid and its implications for ovarian cancer pathogenesis. *Reproductive biology and endocrinology : RB&E*, 12(1), p.60. Available at: http://www. pubmedcentral.nih.gov/articlerender.fcgi?artid=410512 8&tool=pmcentrez&rendertype=abstract.
53) Fabbri, M. *et al*., 2012. MicroRNAs bind to Toll-like receptors to induce prometastatic inflammatory response. *Proceedings of the National Academy of Sciences of the United States of America*, 109(31), pp.E2110–6. Available at: http://www.pubmedcentral.nih. gov/article render.fcgi?artid =3412003&tool=pmcentrez&rendertype=abstract [Acc essed November 26, 2012].
54) Fabbri, M., 2012. TLRs as miRNA Receptors. *Cancer research*, pp.6333–6337. Available at: http://www.ncbi.nlm.nih.gov/ pubmed/23 222301 [Accessed December 13, 2012].
55) Fasching, P. a *et al*., 2009. Role of genetic polymorphisms and ovarian cancer susceptibility. *Molecular oncology*, 3(2), pp.171–81. Available at: http://www.ncbi.nlm.nih.gov/pubmed/19383379 [Accessed October 25, 2012].
56) Fathalla, M., 2013. Incessant ovulation and ovarian cancer–a hypothesis re-visited. *Facts, views and vision in Obgyn*, 5(4), pp.292–297. Available at: http://www.fvvo.be/assets/407/07-Fathalla.pdf.
57) Fathalla, M.F., 1971. Incessant ovulation--a factor in ovarian neoplasia? *Lance*, 2(7716), p.163. Available at: http://www.thelancet. com/journals /a/article/PIIS0140-6736(71)92335-X/fulltext.
58) Ferlay, J. et al., 2010. Estimates of worldwide burden of cancer in 2008: GLOBOCAN 2008. International Journal of Cancer, 127(12), pp.2893–2917.
59) Foster, R., Buckanovich, R.J. & Rueda, B.R., 2012. Ovarian cancer stem cells: Working towards the root of stemness. Cancer letters. Available at: http://www.ncbi.nlm.nih.gov/pubmed/23138176 [Accessed November 27, 2012].Fung, M.K.L. *et al*., 2006. Role of MEK/ERK pathway in the MAD2-mediated cisplatin sensitivity in testicular germ cell tumour cells. *British journal of cancer*, 95(4), pp.475–84.
60) Friis, S. et al., 2009. Aspirin and other non-steroidal anti-inflammatory drugs and risk of colorectal cancer: a Danish cohort study. Cancer causes & control : CCC, 20(5), pp.731–740.

61) Fung, M.K.-L. *et al*., 2007. MAD2 expression and its significance in mitotic checkpoint control in testicular germ cell tumour. *Biochimica et biophysica acta*, 1773(6), pp.821–32.
62) Furlong, F. *et al*., 2012. Low MAD2 expression levels associate with reduced progression-free survival in patients with high-grade serous epithelial ovarian cancer. *The Journal of pathology*, 226(5), pp.746–55. Available at: http://www.ncbi.nlm.nih.gov/pubmed/22069160 [Accessed February 23, 2013].
63) Gao, W. *et al*., 2010. Deregulated expression of miR-21, miR-143 and miR-181a in non-small cell lung cancer is related to clinicopathologic characteristics or patient prognosis. *Biomedicine & pharmacotherapy = Biomédecine & pharmacothérapie*, 64(6), pp.399–408. Available at: http://www.ncbi.nlm.nih.gov/pubmed/20363096 [Accessed October 29, 2012].
64) Gemma, a *et al*., 2001. Genomic structure of the human MAD2 gene and mutation analysis in human lung and breast cancers. *Lung cancer (Amsterdam, Netherlands)*, 32(3), pp.289–95. Available at: http://www.ncbi.nlm.nih.gov/pubmed/11390010.
65) Girolimetti, G. et al., 2014. BRCA-Associated Ovarian Cancer : From Molecular Genetics to Risk Management. BioMed research international, 2014.
66) Globocan,iarc.fr 2012, International agency for research on cancer Globocan 2012:Estimated cancer incidence and mortality and prevalence worldwide in 2012
67) Gonzalez-Aguilar, A. *et al*., 2012. Recurrent mutations of MYD88 and TBL1XR1 in primary central nervous system lymphomas. *Clinical cancer research : an official journal of the American Association for Cancer Research*, 18(19), pp.5203–11. Available at: http://www.ncbi. nlm.nih. gov/pubmed/22837180 [Accessed February 20, 2014].
68) Granato, T. et al., 2015. HE4 in the differential diagnosis of ovarian masses. Clinica Chimica Acta, 446, pp.147–155. Available at: http://linkinghub.elsevier.com/retrieve/pii/S0009898115002004.
69) Greaves, M. & Maley, C.C., 2012. Clonal Evolution in Cancer. , 481(7381), pp.306–313.
70) Group, N.P., 2015. PARP inhibitor approved, despite vote. Nature Biotechnology, 33(2), pp.116–116.
71) Gupta, P.B. et al., 2009. Identification of selective inhibitors of cancer stem cells by high-throughput screening. Cell, 138(4), pp.645–59. Available at: http://www.ncbi.nlm.nih.gov/pubmed/19682730 [Accessed October 30, 2012].
72) Hao, X. *et al*., 2010. Effect of Mad2 on paclitaxel-induced cell death in ovarian cancer cells. Journal of Huazhong University of Science and Technology. Medical sciences = Hua zhong ke ji da xue xue bao. Yi xue Ying De wen ban = Huazhong keji daxue xuebao. Yixue Yingdewen ban, 30(5), pp.620–5. Available at: http://www.ncbi .nlm.nih.gov/pubmed /21063845 [Accessed March 12, 2014].
73) Haricharan, S. & Brown, P., 2015. TLR4 has a TP53-dependent dual role in regulating breast cancer cell growth. Proceedings of the National Academy of Sciences, 2015, p.201420811.
74) Heliström, I. et al., 2003. The HE4 (WFDC2) protein is a biomarker for ovarian carcinoma. Cancer Research, 63(13), pp.3695–3700.
75) Hennessy, B.T.J. et al., 2010. Somatic mutations in BRCA1 and BRCA2 could expand the number of patients that benefit from poly (ADP ribose) polymerase inhibitors in ovarian cancer. Journal of Clinical Oncology, 28(22), pp.3570–3576.

76) Hirsch, H. a, Iliopoulos, D. & Struhl, K., 2013. Metformin inhibits the inflammatory response associated with cellular transformation and cancer stem cell growth. Proceedings of the National Academy of Sciences of the United States of America, 110(3), pp.972–7. Available at: http://www.ncbi.nlm.nih.gov/pubmed/23277563 [Accessed May 28, 2013].
77) Hisaoka, M., Matsuyama, A. & Hashimoto, H., 2008. Aberrant MAD2 expression in soft-tissue sarcoma. *Pathology international*, 58(6), pp.329–33. Available at: http://www.ncbi.nlm.nih.gov/pubmed/18477 210 [Acc essed October 29, 2012].
78) Holcomb, K. et al., 2011. Human epididymis protein 4 offers superior specificity in the differentiation of benign and malignant adnexal masses in premenopausal women. American Journal of Obstetrics and Gynecology, 205(4), pp.358.e1–358.e6.
79) Hoyt, M. a, Totis, L. & Roberts, B.T., 1991. S. cerevisiae genes required for cell cycle arrest in response to loss of microtubule function. *Cell*, 66(3), pp.507–17. Available at: http://www.ncbi.nlm.nih. gov/ pub med/ 1651171.
80) Hsu, R.Y.C. et al., 2011. LPS-induced TLR4 signaling in human colorectal cancer cells increases B1 integrin mediated cell adhesion and liver metastasis. Cancer Research, 71(5), pp.1989–1998.
81) Hu, T. et al., 2014. Reprogramming ovarian and breast cancer cells into non-cancerous cells by low-dose metformin or SN-38 through FOXO3 activation. Scientific reports, 4, p.5810. Available at: http://www. pubmed central.nih.gov/articlerender.fcgi?artid=4108946&tool=pmcentrez&renderty pe=abstract.
82) Hua, D. et al., 2009. Small interfering RNA-directed targeting of Toll-like receptor 4 inhibits human prostate cancer cell invasion , survival , and tumorigenicity. , 46, pp.2876–2884.
83) Huang, J.-M. *et al*., 2014. Atractylenolide-I sensitizes human ovarian cancer cells to paclitaxel by blocking activation of TLR4/MyD88-dependent pathway. *Scientific reports*, 4, p.3840.
84) Ikebe, M. et al., 2009. Lipopolysaccharide (LPS) increases the invasive ability of pancreatic cancer cells through the TLR4/MyD88 signaling pathway. Journal of Surgical Oncology, 100(8), pp.725–731.
85) Iyoke, C.A. & Ugwu, G.O., 2013. Burden of gynaecological cancers in developing countries. World journal of obstetrics and gynaecology, 2(1), pp.1–7.
86) Janssens, S. & Beyaert, R., 2002. A universal role for MyD88 in TLR/IL-1R-mediated signaling. *Trends in biochemical sciences*, 27(9), pp.474–82. Available at: http://www.ncbi.nlm.nih.gov/ pubmed/12217 523.
87) Jeong, S.-J. *et al*., 2004. Transcriptional abnormality of the hsMAD2 mitotic checkpoint gene is a potential link to hepatocellular carcinogenesis. *Cancer research*, 64(23), pp.8666–73. Available at: http://www.ncbi.nlm.nih.gov /pubmed/15574775 [Accessed November 23, 2012].
88) Jiang, N., Saba, N.F. & Chen, Z.G., 2012. Advances in Targeting HER3 as an Anticancer Therapy. Chemotherapy research and practice, 2012, p.817304. Available at: http://www.pubmedcentral.nih.gov/articlerender. fcgi?artid=3502787&tool=pmcentrez&rendertype=abstract.
89) Johnson, T.W. et al., 2002. Association of aspirin and nonsteroidal anti-inflammatory drug use with breast cancer. Cancer epidemiology, biomarkers & prevention : a publication of the American Association for Cancer Research, cosponsored by the American Society of Preventive Oncology, 11(12), pp.1586–1591.
90) Kadija, S. et al., 2012. The Utility of Human Epididymal Protein 4, Cancer Antigen 125, and Risk for Malignancy Algorithm in Ovarian Cancer and

Endometriosis. International Journal of Gynecological Cancer, 22(2), pp.238–244.
91) Kalapotharakos, G. et al., 2012. High preoperative blood levels of HE4 predicts poor prognosis in patients with ovarian cancer. Journal of Ovarian Research, 5(1), p.20.
92) Kato, T. *et al*., 2011. Overexpression of MAD2 predicts clinical outcome in primary lung cancer patients. *Lung cancer (Amsterdam, Netherlands)*, 74(1), pp.124–31. Available at: http://www.ncbi.nlm.nih. gov/pubmed/ 213 76419 [Accessed October 24, 2012].
93) Kelly, M.G. et al., 2006. TLR-4 signaling promotes tumor growth and paclitaxel chemoresistance in ovarian cancer. Cancer research, 66(7), pp.3859–68. Available at: http://www.ncbi.nlm.nih.gov/pubmed/16585 214 [Accessed October 22, 2012].
94) Kennedy, C.L. *et al*., 2014. Differential role of MyD88 and Mal/TIRAP in TLR2-mediated gastric tumourigenesis. *Oncogene*, 33(19), pp.2540–6. Available at: http://www.ncbi.nlm.nih.gov/ pubmed/ 23728 346 [Accessed May 19, 2014].
95) Kessler, M., Fotopoulou, C. & Meyer, T., 2013. The molecular fingerprint of high grade serous ovarian cancer reflects its fallopian tube origin. *International journal of molecular sciences*, 14(4), pp.6571–96. Available at: http://www.pubmedcentral. nih.gov/article render.fcgi? artid=36456 55& tool=pmcentrez&rendertype=abstract [Acc essed January 28, 2014].
96) Kfoury, A. *et al*., 2013. MyD88 in DNA repair and cancer cell resistance to genotoxic drugs. *Journal of the National Cancer Institute*, 105(13), pp.937–46. Available at: http://www.ncbi.nlm.nih.gov/pubmed/ 237665 30 [Accessed February 20, 2014].
97) Kim, A. et al., 2012. Therapeutic strategies in epithelial ovarian cancer. *Journal of experimental & clinical cancer research : CR*, 31(1), p.14. Available at: http://www.pubmed central.nih.gov/articlerender. fcgi? artid=33 09949&tool=pmcentrez&rendertype=abstract [Accessed Oct ober 10, 2012].
98) Kim, H.-S. *et al*., 2005. Frequent mutations of human Mad2, but not Bub1, in gastric cancers cause defective mitotic spindle checkpoint. *Mutation research*, 578(1-2), pp.187–201. Available at: http://www. ncbi.nlm. nih.gov/ pubmed/16112690 [Accessed October 24, 2012].
99) Kim, K.H. *et al*., 2012. Expression and significance of the TLR4/MyD88 signaling pathway in ovarian epithelial cancers. *World journal of surgical oncology*, 10(1), p.193. Available at: http://www pubmedcentr al.nih.gov /articlerender.fcgi ?artid=3539 930& tool=pm centrez &rend ertype=abstract [Accessed March 12, 2014].
100) Kolbert, C.P. *et al*., 2013. Multi-Platform Analysis of MicroRNA Expression Measurements in RNA from Fresh Frozen and FFPE Tissues. *PLoS ONE*, 8(1).
101) Kong, S.-Y. et al., 2012. Serum HE4 Level is an Independent Prognostic Factor in Epithelial Ovarian Cancer. Annals of Surgical Oncology, 19(5), pp.1707–1712.
102) Kristiansen, G. et al., 2002. CD24 is expressed in ovarian cancer and is a new independent prognostic marker of patient survival. The American journal of pathology, 161(4), pp.1215–1221.
103) Kurman, R.J. & Shih, I.-M., 2011. Molecular pathogenesis and extraovarian origin of epithelial ovarian cancer--shifting the paradigm. *Human pathology*, 42(7), pp.918–31. Available at: http://www.pub medcentral.nih. gov/article render.fcgi?artid =31480 26&tool=pmcen trez&rendertype=abstract [Accessed January 28, 2014].

104) Langhe, R. *et al*., 2015. A novel serum microRNA panel to discriminate benign from malignant ovarian disease. *Cancer Letters*, 356(2), pp.628–636. Available at: http://linkinghub.elsevier.com/retrieve/pii/ S0304383514005989.
105) Lario, S., Ramírez-Lázaro, M. J., Aransay, a M., Lozano, J. J., Montserrat, a, Casalots, Á., … Calvet, X. (2012). microRNA profiling in duodenal ulcer disease caused by Helicobacter pylori infection in a Western population. *Clinical Microbiology and Infection : The Official Publication of the European Society of Clinical Microbiology and Infectious Diseases*, *18*(8), E273–82. doi:10.1111/j.1469-0691.2012.03849.x
106) Li, J. et al., 2009. HE4 as a biomarker for ovarian and endometrial cancer management. Expert review of molecular diagnostics, 9(6), pp.555–566.
107) Li, R. & Murray, a W., 1991. Feedback control of mitosis in budding yeast. *Cell*, 66(3), pp.519–31. Available at: http://www.ncbi.nlm.nih. gov/pubmed/1651172.
108) Liang, B. *et al*., 2013. Myeloid differentiation factor 88 promotes growth and metastasis of human hepatocellular carcinoma. *Clinical cancer research : an official journal of the American Association for Cancer Research*, 19(11), pp.2905–16. Available at: http://www.ncbi.nlm. nih.gov/pubmed/23549880 [Accessed February 20, 2014].
109) Liston, A., Linterman, M. & Lu, L.-F., 2010. MicroRNA in the adaptive immune system, in sickness and in health. *Journal of clinical immunology*, 30(3), pp.339–46. Available at: http://www.ncbi.nlm.nih. gov/pubmed /20191314 [Accessed December 17, 2012].
110) Liu, Q. *et al*., 2010. Nek2 targets the mitotic checkpoint proteins Mad2 and Cdc20: a mechanism for aneuploidy in cancer. *Experimental and molecular pathology*, 88(2), pp.225–33.
111) Luo, L. et al., 2011. Ovarian cancer cells with the CD117 phenotype are highly tumorigenic and are related to chemotherapy outcome. Experimental and molecular pathology, 91(2), pp.596–602. Available at: http://www.ncbi.nlm.nih.gov/pubmed/21787767 [Accessed October 19, 2012].
112) Ma, J. *et al*., 1998. Abrogated energy-dependent uptake of cisplatin in a cisplatin-resistant subline of the human ovarian cancer cell line IGROV-1. *Cancer Chemotherapy and Pharmacology*, 41(3), pp.186–192.
113) Markman, M. *et al*., 1991. Responses to second-line cisplatin-based intraperitoneal therapy in ovarian cancer: Influence of a prior response to intravenous cisplatin. *Journal of Clinical Oncology*, 9(10), pp.1801–1805.
114) Martini, F.H., Nath, J.L. & Batholomew, E.F., 2012. Fundamentals of Anatomy & Physiology 9th edition Pearson Education Inc,
115) McCluggage, W.G., 2011. Morphological subtypes of ovarian carcinoma: a review with emphasis on new developments and pathogenesis. *Pathology*, 43(5), pp.420–32. Available at: http://www. ncbi.nlm.nih.gov/pubmed/21716157 [Accessed October 8, 2012].
116) Menon, U. *et al*., 2009. Sensitivity and specificity of multimodal and ultrasound screening for ovarian cancer, and stage distribution of detected cancers: results of the prevalence screen of the UK Collaborative Trial of Ovarian Cancer Screening (UKCTOCS). *The Lancet Oncology*, 10(4), pp.327–340.
117) Moitra, K., 2015. Overcoming Multidrug Resistance in Cancer Stem Cells. BioMed Research International.
118) Molina, R. et al., 2011. HE4 a novel tumour marker for ovarian cancer: comparison with CA 125 and ROMA algorithm in patients with gynaecological diseases. Tumor Biology, pp.1–9.

119) Montagnana, M. et al., 2011. HE4 in ovarian cancer: From Discovery to clinical application. Advances in Clinical Chemistry, 55, pp.1–20.
120) Mor, G. & Alvero, A., 2013. The Duplicitous Origin of Ovarian Cancer. *Rambam Maimonides Medical Journal*, 4(1), pp.1–7. Available at: http://www.rmmj.org.il/(S(yyhzy155o0hfqu55wj5w1smm))/Pages/Article.aspx?manuId=255 [Accessed March 20, 2013].
121) Moslehi, R. *et al*., 2000. BRCA1 and BRCA2 mutation analysis of 208 Ashkenazi Jewish women with ovarian cancer. *American journal of human genetics*, 66(4), pp.1259–72. Available at: http://www.pub medcentral.nih gov/articlerender.fcgi?artid=1288193&tool=pmcentrez &rendertype=abstract
122) Murphy, K., 2012. *Janeway's Immunobiology,* 8th ed., Garland Science, Taylor & Francis Group, LLC.
123) Murray, S. *et al*., 2012. Taxane resistance in breast cancer: mechanisms, predictive biomarkers and circumvention strategies. *Cancer treatment reviews*, 38(7), pp.890–903. Available at: http://www. ncbi.nlm.nih.gov/ pubmed/22465195 [Accessed October 29, 2012].
124) National Cancer Registry, 2012a. Breast Cancer Incidence , Mortality , Treatment and Survival in Ireland : 1994-2009 European Network of Cancer Registries.
125) National Cancer Registry, 2012b. Cancer Trends No 14. Cancers of the ovary.
126) National Cancer Registry Ireland. Cancer in Ireland 1994-2012: Annual Report of the National Cancer Registry.
127) Naugler, C.T., 2010. Population genetics of cancer cell clones: possible implications of cancer stem cells. Theoretical biology & medical modelling, 7(1), p.42.
128) Naugler, W.E. *et al*., 2007. Gender disparity in liver cancer due to sex differences in MyD88-dependent IL-6 production. *Science (New York, N.Y.)*, 317(5834), pp.121–4. Available at: http://www.ncbi.nlm.nih. gov/ pubmed/17615358 [Accessed January 24, 2014].
129) Ness, R.B. & Modugno, F., 2006. Endometriosis as a model for inflammation-hormone interactions in ovarian and breast cancers. *European journal of cancer (Oxford, England : 1990)*, 42(6), pp.691–703. Available at: http://www.ncbi.nlm.nih.gov/pubmed/16531042 [Accessed October 29, 2012].
130) Ngo, V.N. *et al*., 2011. Oncogenically active MYD88 mutations in human lymphoma. *Nature*, 470(7332), pp.115–9. Available at: http:// www.ncbi.nlm.nih.gov/pubmed/21179087 [Accessed February 20, 2014].
131) Nowak, D. et al., 2013. Differentiation therapy of leukemia : 3 decades of development Review article Differentiation therapy of leukemia : 3 decades of development. , pp.3655–3665.
132) Nowicki, M.O. *et al*., 2003. Chronic myelogenous leukemia molecular signature. *Oncogene*, 22(25), pp.3952–63. Available at:http://www.ncbi .nlm.nih.gov/pubmed/12813469 [Accessed April 9, 2014].
133) Nuovo, G.J., 2008. In situ detection of precursor and mature microRNAs in paraffin embedded, formalin fixed tissues and cell preparations. *Methods*, 44(1), pp.39–46.
134) Ocana, A. et al., 2013. HER3 overexpression and survival in solid tumors: A meta-analysis. Journal of the National Cancer Institute, 105(4), pp.266–273.
135) O'Lorcain, P. & Comber, H., 2006. Mortality predictions for Ireland, 2001-2015: cancers of the breast, ovary and cervix and corpus uteri. *International journal of gynecological cancer*, 16 supplem(1), pp.1–10.

136) O'Neill, L. a J., 2008. Toll-like receptors in cancer. *Oncogene*, 27(2), pp.158–160. Available at: http://www.nature.com/doifinder /10.1038/sj .onc.1210903 [Accessed November 22, 2012].
137) O'Neill, L. a, Sheedy, F.J. & McCoy, C.E., 2011. MicroRNAs: the fine-tuners of Toll-like receptor signalling. *Nature reviews. Immunology*, 11(3), pp.163–75. Available at: http://www.ncbi.nlm.nih.gov/ pubmed/ 21331081 [Accessed October 30, 2012].
138) Oakman, C. *et al*., 2009. Recent advances in systemic therapy: new diagnostics and biological predictors of outcome in early breast cancer. *Breast cancer research : BCR*, 11(2), p.205. Available at: http://www .pubmedcentral.nih.gov/articlerender.fcgi?artid=2688942&tool=pmcentrez& rendertype=abstract [Accessed January 30, 2013].
139) Olopade, O.I. *et al*., 2008. Advances in breast cancer: pathways to personalized medicine. *Clinical cancer research : an official journal of the American Association for Cancer Research*, 14(24), pp.7988–99. Available at: http://www.ncbi.nlm.nih.gov/pubmed/19088015 [Accessed March 4, 2013].
140) Olsen, C.M. *et al*., 2007. Obesity and the risk of epithelial ovarian cancer: a systematic review and meta-analysis. *European journal of cancer (Oxford, England : 1990)*, 43(4), pp.690–709. Available at:http://www .ncbi.nlm.nih.gov/pubmed/17223544 [Accessed October 29, 2012].
141) Ortiz-Muñoz, B. et al., 2014. HE4, Ca125 and ROMA algorithm for differential diagnosis between benign gynaecological diseases and ovarian cancer. Tumor Biology, 35(7), pp.7249–7258.
142) Ozols, R.F., 2002. Recurrent ovarian cancer: evidence-based treatment. *Journal of clinical oncology : official journal of the American Society of Clinical Oncology*, 20(5), pp.1161–3. Available at: http://www.ncbi.nlm.nih .gov/pubmed/11870155.
143) Percy, M.J. *et al*., 2000. Expression and mutational analyses of the human MAD2L1 gene in breast cancer cells. *Genes chromosomes cancer*, 29(4), pp.356–362. Available at: http://www.ncbi.nlm.nih.gov/ pubmed/11066082.
144) Prat, J., 2014. Staging classification for cancer of the ovary, fallopian tube, and peritoneum. International journal of gynaecology and obstetrics: the official organ of the International Federation of Gynaecology and Obstetrics, 124(1), pp.1–5. Available at: http://www.ncbi.nlm.nih.gov /pubmed/24219974 [Accessed January 26, 2014].
145) Prencipe, M. *et al*., 2009. Cellular senescence induced by aberrant MAD2 levels impacts on paclitaxel responsiveness in vitro. *British journal of cancer*, 102(11), pp.1900–8. Available at: http://www.pub medcentral. nih.gov/articlerender.fcgi?artid=2788249&tool=pmcentre z&rendertype=abstract [Accessed November 10, 2012].
146) Prencipe, M. *et al*., 2010. MAD2 downregulation in hypoxia is independent of promoter hypermethylation. *Cell Cycle*, 9(14), pp.2856–2865. Available at: http://www.landesbioscience.com/jour nals/cc/ article/12362/ [Accessed October 29, 2012].
147) Puente, X.S. *et al*., 2011. Whole-genome sequencing identifies recurrent mutations in chronic lymphocytic leukaemia. *Nature*, 475(7354), pp.101–5. Available at: http://www.pubmedcentral.nih.gov/ articlerender.fcgi?artid =3322590&tool=pmcentrez&rendertype=abstr act [Accessed February 20, 2014].
148) Quinn, S.R. & O'Neill, L. a., 2011. A trio of microRNAs that control Toll-like receptor signalling. *International Immunology*, 23(7), pp.421–425.
149) Rajput, S., Volk-Draper, L.D. & Ran, S., 2013. TLR4 is a novel determinant of the response to paclitaxel in breast cancer. Molecular cancer therapeutics, 12(8), pp.1676–87.

150) Rakoff-Nahoum, S. & Medzhitov, R., 2007. Regulation of spontaneous intestinal tumorigenesis through the adaptor protein MyD88. *Science (New York, N.Y.)*, 317(5834), pp.124–7. Available at:http://www.ncbi. nlm.nih.gov/pubmed/17615359 [Accessed January 27, 2014].
151) Reya, T. *et al*., 2001. Stem cells, cancer, and cancer stem cells. *Nature*, 414(6859), pp.105–11. Available at: http://www.ncbi.nlm. nih.gov/pubmed /11689955.
152) Rice, J.C. et al., 2000. Methylation of the BRCA1 promoter is associated with decreased BRCA1 mRNA levels in clinical breast cancer specimens. Carcinogenesis, 21(9), pp.1761–1765.
153) Riman, T., Nilsson, S. & Persson, I.R., 2004. Review of epidemiological evidence for reproductive and hormonal factors in relation to the risk of epithelial ovarian malignancies. *Acta obstetricia et gynecologica Scandinavica*, 83(9), pp.783–95. Available at: http:// www.ncbi.nlm.nih. gov/pubmed/15315588.
154) Rimkus, C. *et al*., 2007. Expression of the mitotic checkpoint gene MAD2L2 has prognostic significance in colon cancer. *International journal of cancer. Journal international du cancer*, 120(1), pp.207–11. Available at: http://www.ncbi.nlm.nih.gov/pubmed/17044027 [Accessed November 22, 2012].
155) Rosen, D.G. *et al*., 2010. Morphological and molecular basis of ovarian serous carcinoma. *Journal of biomedical research*, 24(4), pp.257–63. Available at: http://www.pubmedcentral.nih.gov/articlerender. fcgi?artid =3596590&tool=pmcentrez&rendertype=abstract [Accessed August 10, 2014].
156) Sandri, M.T. et al., 2013. Comparison of HE4, CA125 and ROMA algorithm in women with a pelvic mass: Correlation with pathological outcome. Gynecologic Oncology, 128(2), pp.233–238. Available at: http://dx.doi.org/10.1016/j.ygyno.2012.11.026.
157) Sankaranarayanan, R. & Ferlay, J., 2006. Worldwide burden of gynaecological cancer: The size of the problem. *Best Practice and Research: Clinical Obstetrics and Gynaecology*, 20(2), pp.207–225.
158) Sato, Y. *et al*., 2009. Cancer Cells Expressing Toll-like Receptors and the Tumor Microenvironment. *Cancer microenvironment : official journal of the International Cancer Microenvironment Society*, 2 Suppl 1, pp.205–14.
159) Schmidt, C., 2011. CA-125: A biomarker put to the test. *Journal of the National Cancer Institute*, 103(17), pp.1290–1291.
160) Schorge, J.O. *et al*., 2010. SGO White Paper on ovarian cancer: etiology, screening and surveillance. *Gynecologic oncology*, 119(1), pp.7–17. Available at: http://www.ncbi.nlm.nih.gov/pubmed/20692025 [Accessed November 20, 2012].
161) Schrör, K., 1997. Aspirin and platelets: the antiplatelet action of aspirin and its role in thrombosis treatment and prophylaxis. Seminars in Thrombosis and haemostasis, 23(4), pp.349–56.
162) Sell, S., 2005. Leukemia: stem cells, maturation arrest, and differentiation therapy. Stem cell reviews, 1(3), pp.197–205. Available at: http://www.ncbi.nlm.nih.gov/pubmed/17142856.
163) Shackleton, M., 2010. Normal stem cells and cancer stem cells: similar and different. Seminars in cancer biology, 20(2), pp.85–92. Available at: http://www.ncbi.nlm.nih.gov/pubmed/20435143 [Accessed October 29, 2012].
164) Sheedy, F.J. *et al*., 2010. Negative regulation of TLR4 via targeting of the proinflammatory tumor suppressor PDCD4 by the microRNA miR-21. *Nature immunology*, 11(2), pp.141–7. Available at: http:// www.ncbi.nlm .nih.gov/pubmed/19946272 [Accessed October 4, 2012].

165) Shen, D.W. *et al*., 1986. Human multidrug-resistant cell lines: increased mdr1 expression can precede gene amplification. *Science (New York, N.Y.)*, 232(4750), pp.643–645.
166) Shendure, J. & Ji, H., 2008. Next-generation DNA sequencing. *Nature Biotechnology*, 26(10), pp.1135–1145. Available at: http://www.ncbi .nlm .nih.gov/pubmed/18846087.
167) Sheng, Q. et al., 2010. An Activated ErbB3 / NRG1 Autocrine Loop Supports In Vivo Proliferation in Ovarian Cancer Cells. Cancer Cell, 17(3), pp.298–310. Available at: http://dx.doi.org/10.1016/j.ccr. 2009.12.047.
168) Sheyhidin, I. et al., 2011. Overexpression of TLR3, TLR4, TLR7 and TLR9 in esophageal squamous cell carcinoma. World journal of gastroenterology : WJG, 17(32), pp.3745–51. Available at: http://www.pubmedcentral.nih.gov/articlerender.fcgi?artid=3181461&tool=pmcentrez&rendertype=abstract [Accessed February 3, 2013].
169) Siegel, R., Naishadham, D. & Jemal, A., 2013. Cancer Statistics , 2013. , 63(1), pp.11–30.
170) Silva, I. a et al., 2011. Aldehyde dehydrogenase in combination with CD133 defines angiogenic ovarian cancer stem cells that portend poor patient survival. Cancer research, 71(11), pp.3991–4001. Available at: http://www.pubmedcentral.nih.gov/articlerender.fcgi?artid=3107359&tool=pmcentrez&rendertype=abstract [Accessed May 27, 2014].
171) Skinner, D.C. *et al*., 1998. The negative feedback actions of progesterone on gonadotropin-releasing hormone secretion are transduced by the classical progesterone receptor. *Proceedings of the National Academy of Sciences of the United States of America*, 95(18), pp.10978–10983.
172) Smith, E.R. & Xu, X.-X., 2008. Ovarian ageing, follicle depletion, and cancer: a hypothesis for the aetiology of epithelial ovarian cancer involving follicle depletion. *The lancet oncology*, 9(11), pp.1108–11. Available at: http://www.pubmedcentral.nih.gov/articlerender.fcgi? artid =2713057&tool =pmcentrez&rendertype=abstract [Accessed October 29, 2012].
173) Spillane, C.D. et al., 2014. Abstract 4951: Platelet cloaking of CTCs is a universal phenomenon, which drives metastasis. Cancer Research, 74.
174) Steffensen, K.D. et al., 2011. Prevalence of epithelial ovarian cancer stem cells correlates with recurrence in early-stage ovarian cancer. Journal of oncology, 2011, p.620523.
175) Stordal, B. *et al*., 2012. Resistance to paclitaxel in a cisplatin-resistant ovarian cancer cell line is mediated by P-glycoprotein. *PLoS ONE*, 7(7).
176) Sudo, T., 2004. Dependence of Paclitaxel Sensitivity on a Functional Spindle Assembly Checkpoint. *Cancer Research*, 64(7), pp.2502–2508. Available at: http://cancerres.aacrjournals.org/cgi/doi/10.1158/ 0008-5472.CAN-03-2013 [Accessed November 10, 2012].
177) Sulaiman, G., 2015. The Role Of MyD88 in Embryonal Carcinoma Stem Cells. *Unpublished Thesis*.
178) Sun, Z. et al., 2012. Role of toll-like receptor 4 on the immune escape of human oral squamous cell carcinoma and resistance of cisplatin-induced apoptosis. Molecular cancer, 11(1), p.33.
179) Szafranska, A.E. *et al*., 2008. Accurate molecular characterization of formalin-fixed, paraffin-embedded tissues by microRNA expression profiling. *The Journal of molecular diagnostics : JMD*, 10(5), pp.415–423.
180) Szajnik, M. *et al*., 2009. TLR4 signaling induced by lipopolysacharide or paclitaxel regulates tumor survival and chemoresistance in ovarian cancer. *Oncogene*, 28(49), pp.4353–4363.
181) Szczepanski, M.J. et al., 2009. Triggering of toll-like receptor 4 expressed on human head and neck squamous cell carcinoma promotes tumor

development and protects the tumor from immune attack. Cancer Research, 69(7), pp.3105–3113.
182) Tan, X.L. et al., 2011. Aspirin, nonsteroidal anti-inflammatory drugs, acetaminophen, and pancreatic cancer risk: A clinic-based case-control study. Cancer Prevention Research, 4(11), pp.1835–1841.
183) Tang, B. *et al*., 2010. Identification of MyD88 as a novel target of miR-155, involved in negative regulation of Helicobacter pylori-induced inflammation. *FEBS letters*, 584(8), pp.1481–6. Available at:http://www .ncbi.nlm. nih.gov/ pubmed/20219467 [Accessed October 22, 2012].
184) Tanner, B. et al., 2006. ErbB-3 predicts survival in ovarian cancer. Journal of Clinical Oncology, 24(26), pp.4317–4323.
185) Taylor, D.D. & Gercel-Taylor, C., 2008. MicroRNA signatures of tumor-derived exosomes as diagnostic biomarkers of ovarian cancer. *Gynecologic oncology*, 110(1), pp.13–21. Available at:http://www.ncbi .nlm.nih.gov/pubmed/18589210 [Accessed January 30, 2014].
186) The American College of Obstetricians and Gynecologists, 2013. Five Things Physicians and Patients Should Question.
187) Treon, S.P. *et al*., 2012. MYD88 L265P somatic mutation in Waldenström's macroglobulinemia. *The New England journal of medicine*, 367(9), pp.826–33. Available at: http://www.ncbi.nlm.nih .gov/pubmed/22931316 [Accessed February 20, 2014].
188) Tsikouras, P. et al., 2013. The contribution of catumaxomab in the treatment of malignant ascites in patients with ovarian cancer: A review of the literature. Archives of Gynecology and Obstetrics, 288(3), pp.581–585.
189) Tsoref, D., Panzarella, T. & Oza, A., 2014. Aspirin in prevention of ovarian cancer: Are we at the tipping point? Journal of the National Cancer Institute, 106(2), pp.1–2.
190) Veitonmaki, T. et al., 2013. Use of aspirin, but not other non-steroidal anti-inflammatory drugs is associated with decreased prostate cancer risk at the population level. Eur J Cancer, 49(4), pp.938–945. Available at: http://www.ncbi.nlm.nih.gov/pubmed/23079475.
191) Volinia, S. *et al*., 2006. A microRNA expression signature of human solid tumors defines cancer gene targets. *Proceedings of the National Academy of Sciences of the United States of America*, 103(7), pp.2257–2261.
192) Volk-Draper, L. et al., 2014. Paclitaxel Therapy Promotes Breast Cancer Metastasis in a TLR4-Dependent Manner. Cancer Research, 74(19), pp.5421–5434.
193) Wang, A.C. *et al*., 2009. Role of TLR4 for paclitaxel chemotherapy in human epithelial ovarian cancer cells. *European journal of clinical investigation*, 39(2), pp.157–64. Available at:http://www.ncbi.nlm.nih .gov/pubmed/19200169 [Accessed January 30, 2013].
194) Wang, L. *et al*., 2009. MAD2 as a key component of mitotic checkpoint: A probable prognostic factor for gastric cancer. *American journal of clinical pathology*, 131(6), pp.793–801. Available at: http://www. ncbi.nlm .nih.gov/pubmed/19461085 [Accessed October 29, 2012].
195) Wang, R.-H., Yu, H. & Deng, C.-X., 2004. A requirement for breast-cancer-associated gene 1 (BRCA1) in the spindle checkpoint. *Proceedings of the National Academy of Sciences of the United States of America*, 101(49), pp.17108–13.
196) Wang, X. *et al*., 2000. Correlation of defective mitotic checkpoint with aberrantly reduced expression of MAD2 protein in nasopharyngeal carcinoma cells. *Carcinogenesis*, 21(12), pp.2293–7. Available at: http:// www. ncb i.nlm.nih.gov/pubmed/11133821.

197) Wang, X. *et al*., 2002. Significance of MAD2 Expression to Mitotic Checkpoint Control in Ovarian Cancer Cells Significance of MAD2 Expression to Mitotic Checkpoint Control in Ovarian. , pp.1662–1668.
198) Weiner-Gorzel, K. *et al*., 2015. Overexpression of the microRNA miR-433 promotes resistance to paclitaxel through the induction of cellular senescence in ovarian cancer cells. *Cancer Medicine*, p.n/a–n/a. Available at: http://doi.wiley.com/10.1002/cam4.409.
199) Wilson, J.C. et al., 2013. Non-steroidal anti-inflammatory drug and aspirin use and the risk of head and neck cancer. British journal of cancer, 108(5), pp.1178–81. Available at: http://www.ncbi.nlm.nih.gov/ pubmed/23449358.
200) www.clinicaltrials.gov
201) www.colorado.edu, 2001. The Structure of an Ovary.
202) www.fda.gov, 2014
203) www.genomeweb.com
204) www.morphotek.com
205) www.omicsonline.org
206) Xu, Z. *et al*., 2011. Nickel promotes the invasive potential of human lung cancer cells via TLR4/MyD88 signaling. *Toxicology*, 285(1-2), pp.25–30. Available at: http://www.ncbi.nlm.nih.gov/pubmed/21473897 [Accessed January 28, 2013].
207) Yamamichi, N. *et al*., 2009. Locked nucleic acid in situ hybridization analysis of miR-21 expression during colorectal cancer development. *Clinical cancer research : an official journal of the American Association for Cancer Research*, 15(12), pp.4009–4016.
208) Yang, H. et al., 2014. Toll-Like Receptor 4 Prompts Human Breast Cancer Cells Invasiveness via Lipopolysaccharide Stimulation and Is Overexpressed in Patients with Lymph Node Metastasis. PLoS ONE, 9(10), p.e109980. Available at: http://dx.plos.org/10.1371/journal. pone. 0109980.
209) Yang, K., He, Y. S., Wang, X. Q., Lu, L., Chen, Q. J., Liu, J., … Shen, W. F. (2011). MiR-146a inhibits oxidized low-density lipoprotein-induced lipid accumulation and inflammatory response via targeting toll-like receptor 4. *FEBS Letters*, *585*(6), 854–860. doi:10.1016/j.febslet.2011.02.009
210) Yin, B.W.T. & Lloyd, K.O., 2001. Molecular cloning of the CA125 ovarian cancer antigen: Identification as a new mucin, MUC16. *Journal of Biological Chemistry*, 276(29), pp.27371–27375.
211) Zeromski, J., Mozer-Lisewska, I. & Kaczmarek, M., 2008. Significance of toll-like receptors expression in tumor growth and spreading: a short review. Cancer microenvironment : official journal of the International Cancer Microenvironment Society, 1(1), pp.37–42. Available at: http://www.pubmedcentral.nih.gov/articlerender.fcgi?artid=2654361&tool=pmcentrez&rendertype=abstract [Accessed October 18, 2012].
212) Zhang, J.J. et al., 2010. Expression and significance of TLR4 and HIF-1α in pancreatic ductal adenocarcinoma. World Journal of Gastroenterology, 16(23), pp.2881–2888.
213) Zhang, S.-H. *et al*., 2008. Clinicopathologic significance of mitotic arrest defective protein 2 overexpression in hepatocellular carcinoma. *Human pathology*, 39(12), pp.1827–34. Available at: http://www.ncbi. nlm. nih.gov/pubmed/18715617 [Accessed October 29, 2012].
214) Zhao, J., Xu, G., Jia, W., Dong, W., Zhang, Y., Zhao, Z., & Wei, J. (2012). Construction of a recombined adenovirus vector carrying pri-miR-21 gene and research on it's target gene TLR4. *Journal of Cellular and Molecular Immunology*, *2*, 153–155.

215) Zhang, Y. et al., 2012. Toll-like receptor 4 ligation confers chemoresistance to docetaxel on PC-3 human prostate cancer cells. Cell Biology and Toxicology, 28(4), pp.269–277.
216) Zhu, Y. *et al*., 2012. Prognostic significance of MyD88 expression by human epithelial ovarian carcinoma cells. *Journal of translational medicine*, 10(1), p.77.

Chapter 2

Materials and Methods

Chapter 2

Materials and Methods

2.1 Overview

In this chapter, a number of methods employed in this study are described. A number of the techniques used in this chapter are used in a number of chapters. Where this occurs, the full description of the technique is restricted to this chapter.

2.2 Cell culture

2.2.1 Cell lines

The human epithelial ovarian cancer cell lines A2780 and SKOV-3 **(Figure 2.1)** were purchased from the European Collection of Cell Cultures (ECACC, UK) and stored in cryovials (Thermo Scientific™) in liquid nitrogen until required. The A2780 cell line was derived from a primary untreated and paclitaxel sensitive cancer (Behrens *et al* 1987) and the SKOV3 cell line was derived from the ascites of a patient with advanced, metastatic ovarian cancer and is resistant to most cytotoxic drugs, including paclitaxel (Cuello *et al* , 2001). All cell culture was performed inside a laminar flow hood (Airstream® Class II Biological Safety Cabinet, ESCO, Singapore).

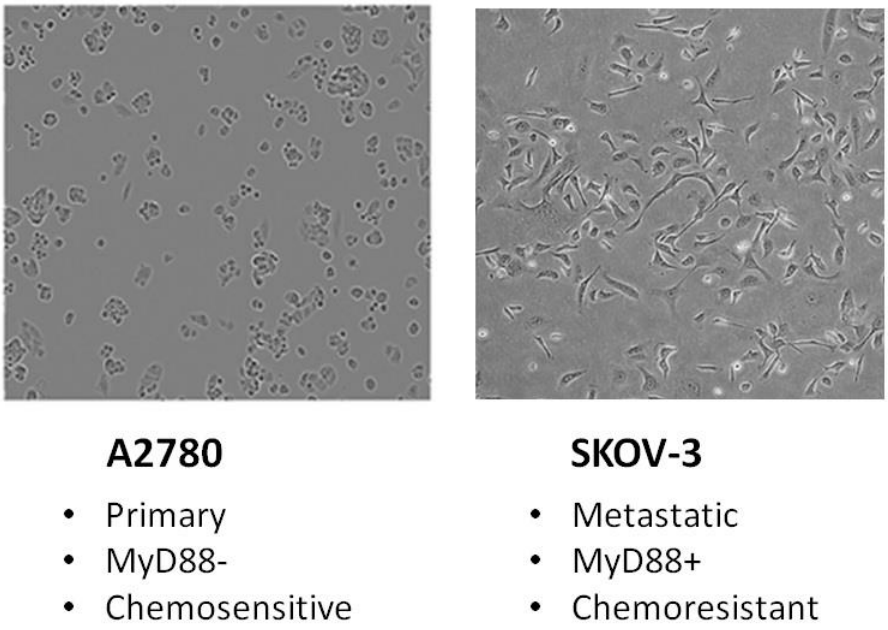

Figure 2.1 A2780 cells (Left) and SKOV-3 cells (Right). A2780 and SKOV-3 cells were cultured for 72 hours and images were taken at 4X magnification. Below each image is a list of the different properties of these two ovarian cancer cell models including MyD88 status, chemoresponsiveness and the tumour site from which the cell lines were derived.

2.2.2 Resuscitation of stocks from liquid nitrogen

Cryovials taken from liquid nitrogen were quickly thawed at room temperature. Vials were opened inside a laminar flow hood and the thawed cell suspension was then immediately transferred to pre-warmed media (37°C) in a T25 flask (Sarstedt, Germany) and incubated overnight at 37°C in a humidified atmosphere (5% CO2).

2.2.3 Routine culture of mammalian cells

A2780 cells and SKOV-3 cells were cultured in RPMI 1640 medium (Sigma, USA) and McCoys modified 5A medium respectively, supplemented with 10% foetal bovine serum (FBS) (Sigma, USA) and 5000IU penicillin/streptomycin (Sigma, USA). A2780 cells were routinely maintained in T75 flasks, while SKOV-3 cells were maintained in T175 flasks. All cell culture was carried out in the laminar flow hood. Cells were checked regularly for bacterial and fungal contamination.

2.2.4 Subculture of cell lines

Cells were routinely cultured until 70-80% before passaging. A2780 cells were cultured in T75 flasks and routinely passaged at a ratio of 1:5-1:8 depending on the confluency of the cells. SKOV-3 cells were in T175 flasks and were routinely passaged 1:2-1:4 as required.

2.2.5 Preparation of liquid nitrogen stocks

After purchasing a cell line, stocks of each cell line were prepared and stored in liquid nitrogen. To prepare stocks, flasks of cells were trypsinized and pelleted at 1000xg. The supernatant was then discarded and cells were then resuspended in an appropriate volume of 1x DMSO serum free cell freezing medium (C6295, Sigma, USA). Next 1ml of cell suspension was then transferred to a 1.8ml nunc cryovial (368632, Thermoscientific). Cryovials were then placed in a polystyrene box and stored overnight at -80°C (Hetofrig CL410, Richmond Scientific, UK). The following day stocks were placed in a labelled tray and transferred to liquid nitrogen for long term storage.

2.2.6 Cell counting

Many applications including cell culture require use of suspensions of cells, therefore it is necessary to determine cell concentration. A device used for determining the number of cells per unit volume of a suspension is called a counting chamber **(Figure 2.2)**. The most widely used type of chamber is called a haemocytometer, since it was originally designed for performing blood cell counts. A haemaocytometer also known as a neubauer counting chamber is a specialized microscope slide which has 3 features:

1. It has been etched with a grid over a defined area
2. There are 2 counting chambers each containing a separate grid
3. It has a thickened quartz coverslip. When this is placed on the haemocytometer, the haemocytometer is sealed so that the chamber contains a defined height from the grid (0.1mm)

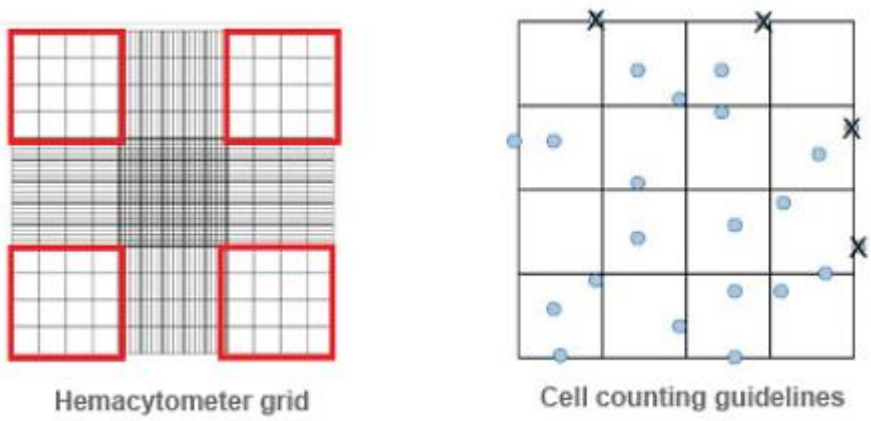

Figure 2.2 A haemocytometer grid (Left) and cell counting guide (Right). Cells within the 4x4 gridded areas marked by red boxes are counted to determine the number of cells/ml in a cell suspension. The cell counting guide displays the most appropriate way to perform a cell count.

In order to perform a cell count, cells were resuspended in an appropriate volume of media, (The appropriate dilution will result in a cell concentration that gives 50-100 cells per square in the haemocytometer), next 50µl of the cell suspension was mixed with 50µl of sterile media and 100µl of sterile trypan blue (Sigma Aldrich). Trypan blue is cell viability dye; this dye is taken up by dead cells which no longer have an intact plasma membrane and is excluded from live cells. Thus dead cells will appear blue under the microscope while live cells appear colourless. Next 10µl of diluted samples were loaded into the haemocytometer and the number cells counted at 10X magnification, dead cells were excluded from the count. Based on the count obtained the total number of cells in the cell suspension was then calculated. Each of the 4 large squares counted each contain a surface area of 1mm2. The depth of the chamber is 0.1mm, giving each square a volume of 0.1mm3 or 0.0001mls. The average count of the 4 squares therefore was multiplied by the dilution factor and a factor of 10,000 to determine the number of cells/ml.

2.2.7 Aseptic technique

Contamination of cells by fungal/yeast/bacteria and mycoplasma can be prevented through aseptic technique and the addition of antibiotics to cell culture medium including penicillin streptomycin, Amphoterecin B or primocin (invivogen). Cells should be routinely examined for bacterial/fungal contamination and mycoplasma testing should be routinely carried out. Bacterial and fungal contamination are easily recognizable, usually result in a change in the PH of cell culture mediums supplemented phenol red indicator which turn from red to a bright yellow, their presence can also be confirmed microscopically using high magnification. However mycoplasma contamination is harder to recognize and does not result in a PH change, therefore detection is more complicated and colorimetric assays such as the MycoAlert™ PLUS Mycoplasma detection kit are required **(Figure 2.3)**.

2.2.8 MycoAlertTM Plus Mycoplasma Detection Kit

For this assay media from cultured cells is removed and cellular debris from the media is then removed by centrifugation. 100µl of media is then added to a 96 well plate and mixed with 100µl of MycoAlert® Reagent and incubated at room temperature for 5 minutes. An initial absorbance reading is taken at this point using a luminometer (Wallac, Perkin Elmer, Ireland). Next 100µl of MycoAlert® Substrate is added to the well and incubated at room temperature for 10 minutes after which, a second reading is obtained. The presence of mycoplasma is then determined based on the ratio of the two luminometer readings. Positive and negative controls for mycoplasma are provided within the kit and tested during each sample run. If the ratio of Reading 2/Reading 1 is ≤1 this indicates that the sample is negative for mycoplasma. A ratio >1 indicates contamination with mycoplasma.

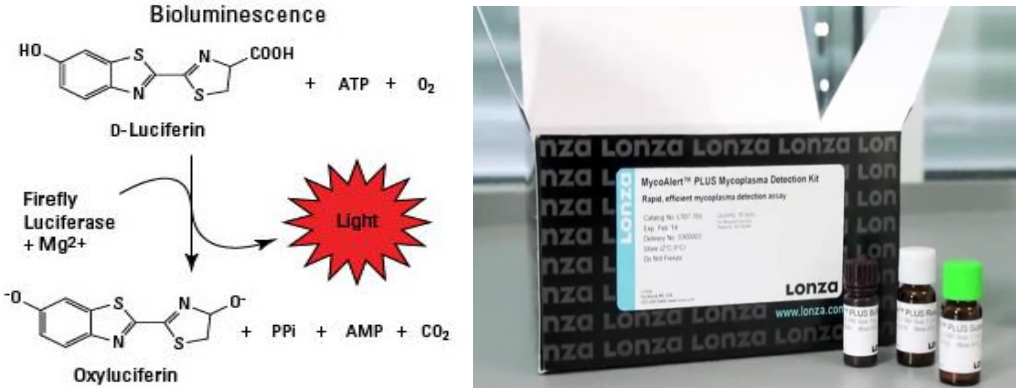

Figure 2.3 The bioluminescence reaction which occurs during mycoplasma detection (Left) and the MycoAlert™ PLUS Mycoplasma Detection Kit (Lonza)(Right). The MycoAlert™ PLUS Mycoplasma Detection Kit (Lonza) can be used for the detection of most of the 180 species of mycoplasma in cell culture reagents including media, media supplements, water aswell as the supernatant of cultured cells. The MycoAlert™ PLUS assay detects the activity of mycoplasmal enzymes which are not expressed in eukaryotic cells. It is a 2 step reagent kit, first mycoalert reagent lyses viable mycoplasma cells and background ATP levels are measured using a luciferase reaction. D-luciferin in the presence of ATP is converted by luciferase to oxyluciferin producing AMP and will emit light at 560nm which can be read using a luminometer. Afterwhich the mycoalert substrate is added which will catalyse the conversion of ADP to ATP in the presence of mycoplasma enzymes released from lysed mycoplasma cells. After incubation with the substrate a second luminescence reading is taken and the ratio of the two readings is obtained. If mycoplasma is present it will give a high luminescenct signal, due to activity of the mycoplasma enzymes which generate increased levels of ATP which can participate in the luciferase reaction.

2.3 Plasmid transfections

2.3.1 Plasmids

A MyD88 over-expression plasmid was purchased from IMAgenes. The plasmid constitutively expressed MyD88 through a pDEST26 vector, which is part of the gateway system **(Figure 2.4)**. Initially no suitable negative control was available for the MyD88 overexpression plasmid. Therefore the decision was made to artificially construct a negative control plasmid. It was decided to cut out a functional group from the MyD88 plasmid. The target that was chosen was the toll-interleukin 1 receptor (TIR) domain, which allows MyD88 to bind to TLRs. This plasmid which had the TIR domain of the MyD88 gene excised was designated the "–TIR negative control plasmid". Some of the initial optimisation experiments used the –TIR plasmid as a negative control.

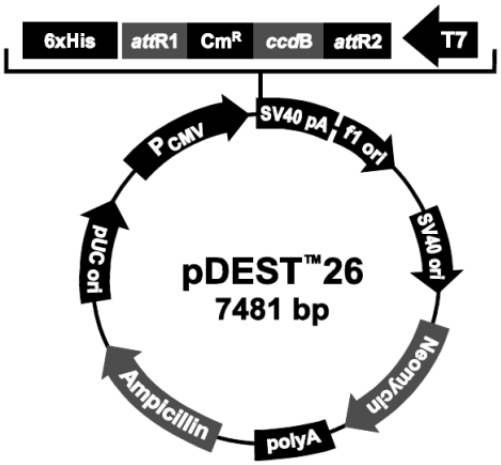

Figure 2.4 The pDEST plasmid vector map. The MyD88 overexpression plasmid is composed of the MyD88 gene inserted into the pDEST 26 vector. This commercially available plasmid (IMAgenes) was used in transfection experiments. The above image displays the vector map for this plasmid including regions encoding ampicillin resistance for antibiotic selection and a CMV and SV40 promoter region for expressing the target gene of interest.

The –TIR negative control plasmid was constructed using restriction enzyme digestion. For this, sequence information was first identified for the MyD88 gene and the TIR domain from the National Center for Biotechnology Information (NCBI) website. The TIR domain lies at nucleotides 513-927 of the MyD88 gene **(Figure 2.5)**. Restriction enzyme sites which would allow the TIR domain to be excised were then identified via restrictionmapper.org. The restriction enzyme NcoI was identified as a suitable restriction enzyme for the digestion as it could cleave sequences above and below the

TIR domain in the MyD88 ORF of the MyD88 OE plasmid. Specifically it would cleave the sequence CCATGG located at nucleotides 17-22 and 2307-2312 **(Figure 2.5)**.

Figure 2.5 Sequence information for the MyD88 gene. Sequence information for the MyD88 gene and the MyD88 TIR domain was identified on the NCBI website. This then allowed the identification of restriction enzyme sites. Restriction digest was then performed in order to excise the TIR domain and create the –TIR negative control plasmid. The TIR domain is highlighted in blue and the restriction enzyme sites are highlighted in red.

NcoI was subsequently purchased from Invitrogen and used in a restriction enzyme digestion reaction as per (**Table 2.1)**.

Table 2.1 Restriction enzyme digestion reaction

Component	Concentration	Volume (µl)
10X Buffer	10X	2.0
dH20	--------	To 20
BSA	10µg/ul	0.2
DNA	1µg	As needed
Enzyme	10U	0.5
Total	--------	20

Digested sample was then resolved using a 1% agarose gel. In the digested well two bands were present, one containing the open plasmid at a high MW and and one at a much lower MW which was the excised TIR domain. The high MW band was subsequently cut out of the gel and DNA was purified using the QIAquick Gel Extraction Kit from Qiagen. Next a ligation reaction was carried out as per **(Table 2.2)** with T4 DNA ligase (Promega) at room temperature for 3 hours. Successful ligation was confirmed as only ligated plasmid DNA could be successfully transfected into E.*coli* cells and be selectively grown on ampicillin plates **(See section 2.3.2)**. Sequence testing was performed by Eurofins scientific, who confirmed the removal of the TIR domain.

Table 2.2 DNA ligation reaction components

Component	Concentration	Volume (µl)
10X Ligase Buffer	10X	1.0
Nuclease-Free Water	--------	To 10
DNA	100ng	As needed
T4 DNA Ligase	0.1-1U	As needed
Total	--------	10

Later a more suitable negative control plasmid designated as the empty vector negative control plasmid (eV Control) became available. This plasmid contains the pDEST 26 vector only and does not constitutively express any gene target.

2.3.2 Preparation of bacterial plasmids and isolation of plasmid DNA

All three plasmid were transfected into Transform One Shot® DH5α chemically competent *E. coli* cells which were supplied as part of the TOPO® TA Cloning® Kit (Invitrogen). After transformation, cells which took up the plasmid efficiently selectively grew on LB plates containing ampicillin and were later grown in LB broth culture containing 100µg/µl ampicillin. From these LB cultures, glycerol stocks for routine use were prepared and plasmid DNA was also isolated (Sambrook *et al*. 1989). Plasmid DNA was isolated from LB cultures using the QIAprep® Spin miniprep kit from Qiagen.

2.3.3 Plasmid transfection procedure

A2780 cells were transfected with the MyD88 overexpression plasmid (MyD88 OE), the –TIR negative control (-TIR) or the empty vector (eV) control negative control, with non-transfected cells serving as an additional controls. 30,000 or 400,000 A2780 cells were seeded into each well of a 24 well or 6 well plates respectively, and transfected with plasmid DNA and lipofectamine RNAiMAX **(See table 2.3)**. For each transfection, plasmid DNA and lipofectamine was first diluted in Opti-MEM® I reduced serum medium. Following 5 minutes incubation, an appropriate volume of cell suspension containing the required number of cells was added to each well. All transfections were carried out using media not containing antibiotics.

Table 2.3 Plasmid Transfection Reagent Protocol

Component	24 well	6 well
Plasmid DNA concentration (ng)	600	3000
Lipofectamine concentration (µl)	0.5	2.5
Opti-MEM® I (µl)	100	500
Serum containing media (mls)	0.5	2.5

2.4 Small interfering RNA (siRNA) transfection

2.4.1 Preparation of siRNA

siRNA targeting MyD88 (siMyD88), TLR4 (siTLR4) and silencer select negative control #1 siRNA (siNeg) were purchased from Invitrogen and On target plus MAD2L1 siRNA (siMAD2) and On target plus Non targeting siRNA (Scr siRNA) were purchased from Dharmacon. siRNA is supplied as a dry pellet at a concentration of 5nmol/l and is reconstituted in 1ml of nuclease free water to create a working concentration of 5µM.

2.4.2 siRNA transfection procedure

SKOV-3 protocol

25,000 or 125,000 SKOV-3 cells were transfected into 24 or 6 well plates respectively, **(See table 2.4)**. Cells were transfected with lipofectamine RNAiMAX reagent and siRNA targeting MyD88, TLR4 or MAD2 at a final concentration of 1nM per well based on optimisation work carried out in Section 3.6 and Section 5.5. For each transfection siRNA and lipofectamine was first diluted in Opti-MEM® I reduced serum medium. Following a 5 minute incubation, an appropriate volume of cell suspension containing the required number of cells was added to each well. All transfections were carried out using media not containing antibiotics.

A2780 Protocol

30,000 or 400,000 A2780 cells were transfected into 24 or 6 well plates respectively, **(See table 2.4)**. Cells were transfected with lipofectamine RNAiMAX reagent and siRNA targeting MAD2 at a final concentration of 30nM per well diluted in Opti-MEM® I reduced serum medium. The 30nM concentration was selected based on optimisation work carried out in Section 5.5.

Table 2.4 siRNA Transfection Reagent Protocol

Component	24 well	6 well
siRNA	As required	As required
Lipofectamine concentration (µl)	1	5
Opti-MEM® I (µl)	100	500
Serum containing media (mls)	0.5	2.5

2.5 RNA isolation and TaqMan RT-PCR

Total RNA was isolated as per the manufacturer's instructions using the *mir*Vana™ miRNA Isolation Kit (Applied Biosystems, Foster City, CA, USA). RNA concentration was determined using the nanodrop 2000c spectrophotometer. Reverse transcription was carried out using the High Capacity cDNA Reverse Transcription Kit (Applied Biosystems, Foster City, CA, USA) or MicroRNA reverse transcription kit (Applied Biosystems, Foster City, CA, USA) on the Gene Amp PCR System 9600 (Perkin Elmer). TaqMan RT-PCR was then performed using the 7900HT Real-Time PCR System (Applied Biosystems, Foster City, CA, USA). Primers and probes for miR-146a, miR-21, miR-146a, MyD88, TLR4, MAD2 and the endogenous controls, glyceraldehyde 3-phosphate dehydrogenase (GAPDH), Beta-2 microglobulin (B2M) RNU6B and miR-16 were obtained from Applied Biosystems (Foster City, CA, USA). These are supplied as commercial pre-designed primer and probe mixes (20X). mRNA expression and microRNA expression levels following transfection were calculated using the ΔΔCT method relative to B2M, GAPDH, RNU6B or miR-16 endogenous controls respectively (Livak & Schmittgen 2001; Schmittgen & Livak 2008). A significant change in mRNA or microRNA expression was considered to be present if at least a 2-fold change (above 200% expression or below 50% expression) in mRNA or microRNA expression was observed, with a p value of ≤0.05 compared to untreated cells and/or negative control cells.

2.6 Protein extraction and western blot analysis

For protein extraction, transfected cells were first trypsinised from 6 well plates using 300µl of trypsin for 5 minutes and the trypsin was neutralised using an equal volume of serum containing media. Cell suspensions were then transferred to multiple pre-chilled eppendorfs and samples from then on were kept on ice. Cells were then pelleted at 1000xg at 4^0C and media was removed. Cells were then resuspended in 1ml of ice cold PBS and repelleted at 1000xg at 4^0C. All PBS was then carefully removed and then the cell pellets were resuspended in 50µl of RIPA lysis buffer (Santa Cruz), modified with phenylmethanesulfonyl fluoride (PMSF) (200mM), a protease inhibitor cocktail, and sodium orthovanadate (100mM) also supplied by Santa Cruz as part of the RIPA lysis buffer system. Cell suspensions were then briefly vortexed and stored at -80^0C until sonication. Cells were later sonicated to ensure complete lysis using the soniprep 150 (MSE Labs, UK). Protein concentration was then determined using the Pierce™ BCA Protein Assay Kit (Thermoscientific). 50µg of diluted protein samples were mixed with 6X laemali buffer and heated to 95^0C for 10mins to ensure complete

denaturation of the protein samples. (For a detailed list of the western blotting buffers and reagents used and their preparation see supplementary information). Denatured protein samples were then resolved by SDS-PAGE on 4-12% Bis-Tris NuPage gels at room temperature (RT) for 50mins at 200V using pre-chilled 1X mops gel running buffer. Proteins were resolved using the XCell SureLock® Mini-Cell SDS PAGE rig (Invitrogen). Resolved proteins were then transferred at RT for 120mins at 30V using pre-chilled 1X tris-glycine transfer buffer to 0.2µM PVDF membranes using the XCell II™ Blot Module (Invitrogen). Following transfer membranes were blocked using either 5% w/v milk protein or 5% BSA (A2153, Sigma) diluted in 1X tris buffered saline with tween (TBST), depending on the antibody **(See Table 2.5)** and incubated at RT for 1 hour on an orbital shaker (Gyrorocker, stuart scientific) to block non-specific binding sites. Next membranes were immersed in primary antibody diluted to the required concentration **(See Table 2.5)** and incubated at 4^0C overnight on an orbital shaker. Primary antibodies were obtained for MyD88 (1:500, D80F5 Cell Signalling), TLR4 (1:500, Ab47093), MAD2 (1: 1000, 610679 BD Biosciences) and GAPDH (1:10,000, Ab9485). Following overnight incubation with the primary antibody, the membranes were rinsed quickly 3 times with 1X TBST to remove most of the residual antibody, then 3x5min washes in 1X TBST were performed. Next the membranes were incubated with the required secondary antibody **(See Table 2.5)** for 1 hour at RT and then the membranes were rinsed quickly 3 times and an additional 3x5min washes were carried out. Following the application of the primary and secondary antibodies, a detection reagent luminol (SC-2048, Santa Cruz) was applied to blots for 1min and membranes were placed between two plastic sheets and excess moisture was removed. Chemiluminescence images were then developed using a Fujifilm LAS-4000 luminescent image analyser and files were saved in 8 bit colour .tif format. Following assessment of individual proteins, blots were stripped with Restore Plus Western Stripping Buffer (Thermoscientific), then 3x5min washes in 1X TBST were performed and blots were then blocked and probed with additional antibodies. Densitometry was then carried out using Quantity One software (Biorad). Abundance of protein in arbitrary units was normalised to GAPDH. The mean density ratio of triplicate bands for each condition was then determined.

Table 2.5 Western blot antibody details

Antibody	Clone No.	Company	Dilution	Diluent	Band Size
MyD88	D80F5	Cell signalling	1:1000	BSA	33kDa
MAD2	61067	BD Bioscience	1:1000	Marvel	24kDa
TLR4	Ab47093	Abcam	1:250	Marvel	95kDa
GAPDH	Ab9485	Abcam	1:10,000	Marvel	37kDa
Anti-Mouse 2^0	-	Jackson Immunoresearch	1:1000	Marvel	-
Anti-Rabbit 2^0	-	Jackson Immunoresearch	1:1000	Marvel	-
Anti-Rabbit 2^0	7074	Cell Signalling	1:1000	Marvel	-

2.7 Drug and vehicle formation and cell viability analysis

Paclitaxel and its vehicle DMSO were purchased from Sigma Aldrich. Paclitaxel was diluted in DMSO to a concentration of 50g/l (58.6mM) based on recommendations by the manufacturer. It was then aliquoted and stored at -20^0C while DMSO was kept at room temperature. Both were wrapped in tinfoil for storage to protect them from light in accordance with the manufacturers' instructions. Aliquots of paclitaxel/DMSO were freshly diluted with media for each experiment to the desired working concentration. Following drug treatments and dose response experiments, the effect on cell viability was then determined using the cell counting kit 8 (CCK-8), the (4,5-dimethylthiazol-2-yl)-2,5-diphenyltetrazolium bromide (MTT) and alkaline phosphatase (AP) assay. Percentage cell viability for each condition was calculated as % of non-transfected cells, which were left untreated. Growth curves were plotted using GraphPad Prism 5.

2.8 Statistical analysis

A student's t-test was performed on all qPCR, densitometry and cell viability data to assess statistical significance of gene silencing experiments and differences in cell viability between drug treated versus untreated and vehicle control groups. A statistically significant difference was considered to be present at $p \leq 0.05$. Statistical analysis was performed using Microsoft excel 2010.

2.9 *In-silico* analysis

In-silico analysis was performed in order to identify any potential interaction between the TLR4-MyD88 pathway and MAD2. *In-silico* analysis was performed using the Search Tool for the Retrieval of Interacting Genes/Proteins (STRING) ver 10 software which is freely available at (http://string-db.org/). This free online bioinformatics resource identifies protein-protein interactions through both direct (physical) as well as indirect (functional) associations (Szklarczyk *et al*., 2015).

Interactions are derived from multiple sources including:

1) Known experimental data from primary interaction databases
2) Pathway information from manually curated databases
3) Automated text-mining technologies which search abstracts and full-text articles
4) Predictive algorithms which utilise genomic information and co-expression analyses
5) Interactions that are observed in one organism which are systematically transferred to other organisms, via pre-computed orthology relations.

2.10 Microarray analysis

2.10.1 Assessment of RNA integrity using the Agilent 2100 bioanalyser

Prior to analysing RNA samples using Affymetrix microarrays, the quality of RNA samples was assessed using the Agilent 2100 Bioanalyzer. Samples were run on Chips from the RNA 6000 Nano kit (Agilent Technologies) and an RNA Integrity Number (RIN) was obtained. Samples with RIN values above 7 were deemed suitable for gene expression analysis.

2.10.2 Affymetrix GeneChip® human gene 2.0 ST arrays

250ng of each RNA sample was converted into sense strand cDNA using the GeneChip® WT PLUS Reagent Kit. Each cDNA samples was then hybridised to Affymetrix GeneChip® human gene 2.0 ST arrays. Arrays were washed using the Affymetrix GeneChip® fluidics station 450 and scanned using the Affymetrix GeneChip® Scanner 3000. Arrays were examined using quality control methods, which are outlined in the quality assessment white paper (Affymetrix, 2007).

2.10.3 Analysis of gene array data

Gene array data was analysed using Bioconductor software libraries (www.bioconductor.org) and the RMA method (Irizarry, Hobbs, *et al*. 2003; Irizarry, Bolstad, *et al*. 2003; Bolstad *et al*. 2003; Carvalho & Irizarry 2010). Differential expression analysis across all the arrays was carried out using RankProd (Breitling *et al*. 2004). DAVID analysis, a free bioinformatics resource available at (http://david.abcc.ncifcrf.gov) was used to characterise differentially expressed genes in order to identify molecular function and biological process-related genes through gene ontology.

2.11 References

1) Affymetrix, 2007. Quality Assessment of Exon and Gene Arrays. *Whitepaper*, pp.1–18.
2) Bolstad, B.M. et al., 2003. A comparison of normalization metholds for high density oligonucleotide array data based on variance and bias. *Bioinformatics*, 19(2), pp.185–193.
3) Breitling, R. et al., 2004. Rank products: A simple, yet powerful, new method to detect differentially regulated genes in replicated microarray experiments. *FEBS Letters*, 573(1-3), pp.83–92.
4) Carvalho, B.S. & Irizarry, R. a., 2010. A framework for oligonucleotide microarray preprocessing. *Bioinformatics*, 26(19), pp.2363–2367.
5) http://david.abcc.ncifcrf.gov
6) http://string-db.org
7) Irizarry, R. a, Hobbs, B., et al., 2003. Exploration, normalization, and summaries of high density oligonucleotide array probe level data. *Biostatistics (Oxford, England)*, 4(2), pp.249–264.
8) Irizarry, R. a, Bolstad, B.M., et al., 2003. Summaries of Affymetrix GeneChip probe level data. *Nucleic acids research*, 31(4), p.e15.
9) Lifetechnologies, 2013. Lipofectamine 2000 reagent protocol.
10) Livak, K.J. & Schmittgen, T.D., 2001. Analysis of relative gene expression data using real-time quantitative PCR and the 2(-Delta Delta C(T)) Method. *Methods (San Diego, Calif.)*, 25(4), pp.402–408.
11) Sambrook, J., Fritsch, E.F. & Maniatis, T., 1989. Molecular Cloning: A Laboratory Manual. Cold Spring Harbor laboratory press,
12) Schmittgen, T.D. & Livak, K.J., 2008. Analyzing real-time PCR data by the comparative C(T) method. *Nature protocols*, 3(6), pp.1101–1108.
13) Szklarczyk, D., Franceschini, A., Wyder, S., Forslund, K., Heller, D., Huerta-Cepas, J., … von Mering, C. (2015). STRING v10: protein-protein interaction networks, integrated over the tree of life. *Nucleic Acids Research*, *43*(Database issue), D447–52. doi:10.1093/nar/gku1003
14) www.bioconductor.org
15) www.restrictionmapper.org

Chapter 3

The effect of siRNA knockdown of MyD88 and TLR4 on the expression of MAD2

Trinity College Dublin

The University of Dublin

Chapter 3

The effect of siRNA knockdown of MyD88 and TLR4 on the expression of MAD2

3.1 Overview

This chapter describes the effect of siRNA knockdown of TLR4 and MyD88 in SKOV-3 cells on chemoresponsiveness to paclitaxel, MAD2 gene and protein expression and the expression of the regulatory microRNAs miR-21, miR-146a and miR-433.

3.2 Introduction

SKOV-3 cells are an epithelial ovarian cell line derived from the ascites of a patient with metastatic cystadenocarcinoma (www.phe-culturecollections.org.uk). They are resistant to most cytotoxic drugs including paclitaxel (PTX) (Behrens *et al*. 1987; Cuello *et al*. 2001) and express both MyD88 and TLR4 protein (Szajnik *et al*. 2009; d'Adhemar *et al*. 2014). Previously our group (d'Adhemar *et al*. 2014) and others (Silasi *et al*. 2006; Kelly *et al*. 2006; Kim & Yoon 2010; Zhu *et al*. 2012) demonstrated that high MyD88 immunohistochemical (IHC) staining intensity was associated with reduced progression free survival (PFS) (p=0.02) and reduced overall survival (OS) (p=0.029) in high grade serous ovarian cancer (Section 1.4). Additionally, our group demonstrated that high TLR4 IHC staining intensity was associated with reduced PFS (p=0.016) in high grade serous ovarian cancer (Section 1.4). Previous work by Szajnik *et al*. (2009) had also demonstrated that knockdown of TLR4 sensitises SKOV-3 cells to paclitaxel. One of the objectives of the current study was to reproduce these findings and assess global changes in gene expression that are responsible for this change in paclitaxel chemoresponsiveness using microarray analysis. Furthermore MyD88 knockdown was also investigated as it was hypothesised that MyD88 dependent TLR4 signalling was responsible for the increased paclitaxel sensitivity in these cells following knockdown of TLR4 rather than the alternative TRIF dependent arm of the TLR4 signalling pathway. In addition, MyD88 had also been shown to be a marker of

ovarian cancer stem cells (Alvero *et al*. 2011; Craveiro *et al*. 2013). Therefore, it was hypothesised that knockdown of MyD88 may selectively target these cells. MyD88 was also shown to be a more reliable prognostic biomarker in ovarian cancer than TLR4 as it is not expressed in normal ovarian surface epithelium and therefore warranted further investigation (d'Adhemar *et al*. 2014).

The second aim of the project was to assess any potential relationship between TLR4, MyD88 and MAD2 and the mechanisms involved in modulating paclitaxel sensitivity following knockdown of TLR4 and MAD2 (Szajnik *et al*. 2009; Furlong *et al*. 2012). Although there is no established relationship between MAD2 and TLR4 or MyD88, these three markers had individually been shown to independently characterise ovarian cancer patients into poor and good responders (Furlong *et al*. 2012 (MAD2); d'Adhemar *et al*. 2014 (TLR4, MyD88)). Therefore, it was hypothesised that these three proteins may act as independent biomarkers in ovarian cancer and that triage assessment of these markers may predict chemoresistance in ovarian cancer.

Three microRNA biomarkers were also investigated as part of this study miR-433, miR-146a and miR-21. miR-433 had been shown to directly target MAD2 and overexpression of miR-433 was shown to induce paclitaxel resistance in ovarian cancer cell lines (Furlong *et al*. 2012; Weiner-Gorzel *et al*. 2015). Furthermore, high miR-433 expression in patient samples was associated with reduced PFS (Furlong *et al*. 2012). The other two microRNAs, miR-146a and miR-21 serve as part of a negative feedback loop to downregulate the NF-κB mediated inflammatory response. miR-21 decreases the expression of programmed cell death protein 4 (PDCD4), in turn causing the upregulation of the IL-10 driven anti-inflammatory response, while also suppressing the NF-κB driven pro-inflammatory response (Quinn & O'Neill 2011). miR-146a serves to negatively regulate downstream members of the MyD88 pathway. Specifically, it downregulates the expression of TNF receptor-associated factor (TRAF-6) and IL-1 receptor-associated kinase 1(IRAK-1) to inhibit activation of NF-κB and cytokine release. Previously our group performed miRNA qPCR on a small subset of MyD88 negative and MyD88 positive EOC cases (d'Adhemar *et al*. 2014) and found that expression of miR-21 and miR-146a was upregulated in all MyD88 negative EOCs. Expression of these two miRNAs was also assessed in the ovarian cancer cell lines A2780 and IGROV-1, as well as their chemoresistant daughter cells A2780cis (cisplatin-resistant) (Behrens *et al*. 1987) and IGROV-1CDDP (cisplatin & paclitaxel-resistant) (Ma *et al*. 1998; Stordal *et al*. 2012). Variable expression of these two regulatory miRNAs was seen between each cell model and their chemoresistant counterparts (Section 1.6). Some studies have shown that they are also able to directly

target both TLR4 and MyD88 (Yang *et al*. 2011; Zhao *et al*. 2012; Lario *et al*. 2012; Chen *et al*. 2013).

The third aim of the project was to assess the expression of these regulatory microRNAs following gene silencing of MyD88 or TLR4. It was hypothesised that knockdown of TLR4 or MyD88 might alter the expression of these microRNAs and perhaps suggest a potential role for miR-146a and miR-21 in paclitaxel chemoresistance. Moreover it was hypothesised that alteration in the expression of miR-433 following knockdown of TLR4 or MyD88 may also establish a potential link between the MAD2 and TLR4-MyD88 mediated paclitaxel chemoresistance mechanisms.

3.2.1 Hypothesis

siRNA knockdown of MyD88 or its receptor TLR4 in the ovarian cancer cell line SKOV-3, may impact on the expression levels of MAD2, render SKOV3 cells chemosensitive to paclitaxel therapy and alter the expression of the regulatory microRNAs miR-146a, miR-21 and miR-433.

3.2.2 Aims

1) To confirm previous data that siRNA knockdown of MyD88 and TLR4 levels was also achieved at the protein level.
2) To assess the impact of knockdown of MyD88 and TLR4 on paclitaxel sensitivity.
3) To assess the impact of knockdown of MyD88 or TLR4 on MAD2 expression levels.
4) To investigate the effect of knockdown of TLR4 or MyD88 on the expression of the regulatory microRNAs miR-146a, miR-21 and miR-433.
5) To identify deregulated genes and pathways following knockdown of TLR4 in SKOV-3 cells using microarray analysis

3.3 Methods

3.3.1 Small-interfering RNA transfection

SKOV-3 cells were cultured as described previously (Section 2.1). Transfections were carried out in both 24 and 6 well plate formats as described (Section 2.4), with lipofectamine RNAiMAX and siRNA targeting TLR4, MyD88 or a negative control siRNA diluted with Opti-MEM® I reduced serum medium. Cells were transfected with siRNA at a final concentration of 1nM. Cell lines were routinely checked for mycoplasma and were mycoplasma-free (Section 2.2)

3.3.2 RNA extraction and TaqMan RT-PCR

Total RNA was isolated using the mirVana™ miRNA Isolation Kit and TaqMan RT-PCR was performed as described (Section 2.5) using commercially available primers and probe sets for miR-146a, miR-21, miR-433, MyD88, TLR4, MAD2, Beta-2 microglobulin (B2M) (mRNA endogenous control) RNU6B and miR-16 (microRNA endogenous controls). Gene expression and microRNA expression levels following transfection were calculated, RNU6B using the ΔΔCT method (Schmittgen & Livak 2008), relative to B2M or miR-16 endogenous controls respectively. A significant change in gene expression was considered to be present if at least a 2-fold change (above 200% expression or below 50% expression) in gene expression was observed, with a p value of ≤0.05 compared to untreated cells and/or negative control cells.

3.3.3 Western blot analysis

Protein was isolated and western blot analysis was performed as described (Section 2.6). Blots were probed with antibodies directed against MyD88 (1:1000, D80F5, Cell Signalling), TLR4 (1:100, Ab47093, Abcam), MAD2 (1: 1000, 610679, BD Biosciences) and GAPDH (1:10,000, Ab9485, Abcam). Chemiluminescence images were developed using a Fujifilm LAS-4000 luminescent image analyser and densitometry was then carried out using Quantity One software (Biorad) as described previously (Section 2.6).

3.3.4 Paclitaxel dose response

Two thousand SKOV-3 cells were seeded in triplicate in a 96 well plate for 72 hours and then treated with concentrations of paclitaxel ranging from 4pM to 80μM for a further 48 hours. After 48 hours cell viability was assessed using the cell cycle kit 8 (CCK-8) assay, the (4,5-dimethylthiazol-2-yl)-2,5-diphenyltetrazolium bromide (MTT) and Alkaline phosphatase (AP) assay (Section 2.7). Percentage cell viability for each

condition was calculated as % of non-transfected cells, which were left untreated. Growth curves were plotted using GraphPad Prism 5.

3.3.5 Drug treatment and assessment of cell viability following siRNA transfection

Following transfection for 72 hours, SKOV-3 cells were either left untreated, treated with 0.00006% DMSO (vehicle control) or 3.5nM of paclitaxel (IC_{25}) for 48 hours. Forty-eight hours post treatment, cell viability was assessed by the cell cycle kit 8 (CCK-8) assay. Absorbance values were read at 450nm using the Sunrise™ microplate reader (Tecan Trading AG, Switzerland). Cell viability for each condition/drug treatment was calculated as a % of non-transfected cells which were left untreated.

3.3.6 In-silico analysis

In-silico analysis was performed in order to identify any potential interaction between the TLR4-MyD88 pathway and MAD2. *In-silico* analysis was performed using the Search Tool for the Retrieval of Interacting Genes/Proteins (STRING) ver 10 software which is freely available at http://string-db.org.

3.3.7 Microarray analysis

RNA samples were converted into single stranded cDNA using the GeneChip® WT PLUS Reagent Kit and hybridised to Affymetrix GeneChip® Human Gene 2.0 ST Arrays (Section 2.10). Microarray analysis was performed using three biological replicates of SKOV-3 cells transfected with either the negative control siRNA or siRNA targeting TLR4. A 1.5 fold change in gene expression and a p value of ≤0.05 was set as the threshold for a significantly upregulated/ downregulated gene, this threshold is in line with recent published works (Landi *et al*. 2008; Volchenboum *et al*. 2010; Minning *et al*. 2014; David *et al*. 2014; Sabe *et al*. 2015; Vathipadiekal *et al*. 2015; Wang *et al*. 2015)

3.3.8 Statistical analysis

A student's t-test was performed on RT-PCR results and cell viability data to assess statistical significance of gene silencing experiments and differences in cell viability between drug treated versus untreated and vehicle control groups. A statistically significant difference was considered to be present at p≤0.05. Statistical analysis was performed using Microsoft excel 2010.

3.4 Results

Prior to commencement of this work, initial optimisation of the siRNA knockdown conditions for TLR4 and MyD88 was performed by Brian Flood, as part of a 3 month laboratory project. Results from this work identified 1nM of siRNA as a suitable concentration for knockdown of both MyD88 and TLR4 at 72 hours. A successful knockdown was considered to be achieved if at least a 2-fold change in gene expression was observed, with a p value of ≤0.05 compared to untreated cells and/or negative control cells.

3.4.1 Optimisation of the TLR4 and MyD88 knockdown protocol in SKOV-3 cells

Prior to carrying out any experimental work into the effect of silencing TLR4 or MyD88, optimal transfection conditions for SKOV-3 cells needed to be established. One of the main criteria for a successful knockdown is introducing a high enough concentration of siRNA into the cell without inducing any off target effects, such as induction of an inflammatory response. To assess the appropriate concentration of siRNA to use with the SKOV-3 cells, three concentrations were evaluated, 1nM, 5nM and 10nM. The cells were transfected with either a negative control siRNA (siNeg), a positive control siRNA (targeting GAPDH; siGAPDH) or a TLR4 targeting siRNA (siTLR4) at these concentrations (n=1). After 72 hours the mRNA expression levels of TLR4 and GAPDH were assessed by TaqMan RT-PCR **(Figure 3.1)**. When SKOV-3 cells were transfected with siRNA targeting GAPDH, a 94.7%, 98.3% and 97.5% knockdown of GAPDH was achieved using 1nM, 5nM and 10nM of siRNA respectively. When SKOV-3 cells were transfected with siRNA targeting TLR4, a 77.7%, 80.2% and 74.1% knockdown of TLR4 was achieved using 1nM, 5nM and 10nM of siRNA respectively. Therefore, for future gene silencing experiments, 1nM of siRNA was used to transfect cells, as this gave efficient knockdown of TLR4 and GAPDH and the low connection minimised the potential of any off target effects from gene silencing experiments.

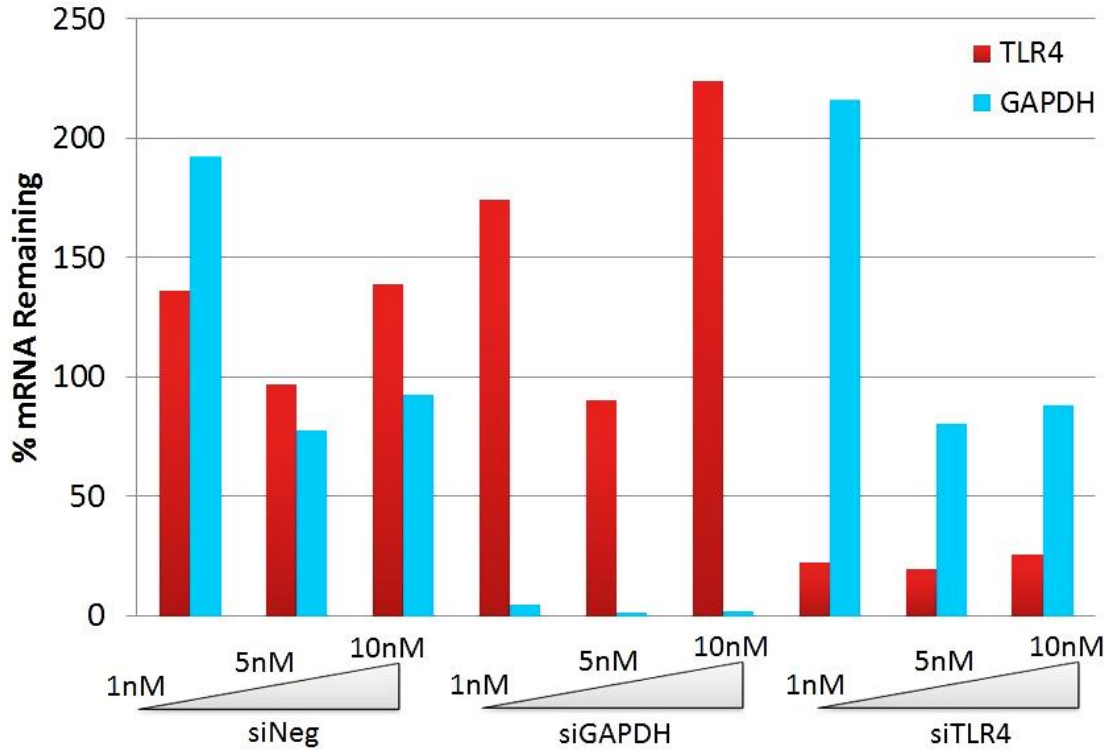

Figure 3.1 Optimisation of SKOV-3 gene silencing protocol. SKOV-3 cells were transfected with 1nM, 5nM or 10nM of Silencer® Select Negative Control No. 1 siRNA (siNeg), Silencer® select GAPDH siRNA (siGAPDH) and a pre-designed siRNA targeting TLR4 (siTLR4) or were left untreated for 72 hours. After 72 hours RNA was harvested using the mirVana™ miRNA Isolation Kit and mRNA expression levels were analysed using TaqMan RT-PCR.TLR4 and GAPDH mRNA expression levels were normalised to the endogenous control B2M and calibrated to that of untreated cells to establish the relative change in mRNA expression (% mRNA remaining) (n=1).

3.4.2 Validation of the TLR4 and MyD88 knockdown protocol in SKOV-3 cells

Following this initial optimisation, siRNA targeting MyD88 was also purchased from Invitrogen. SKOV-3 cells were subsequently transfected with siRNA targeting MyD88, GADPDH and TLR4 (n=3) to fully validate the successfulness of the gene silencing protocol for TLR4 and to validate the gene silencing protocol for MyD88. SKOV-3 cells were transfected with 1nM of siRNA based on previous optimisation results **(Figure 3.1)**, which demonstrated that 1nM of siRNA was effective at silencing both TLR4 and GAPDH mRNA expression. Therefore, the 1nM concentration was also selected as an appropriate starting concentration for gene silencing of MyD88. When transfected with 1nM of siRNA targeting MyD88, TLR4 or GAPDH, significant knockdown of MyD88, TLR4 and GAPDH were achieved compared to both untreated SKOV-3 cells and SKOV-3 cells transfected with the negative control siRNA **(Figure 3.2)**. An 82.1%, 79.8% and 94% knockdown of MyD88, TLR4 and GAPDH mRNA expression were achieved respectively, relative to untreated SKOV-3 cells. TLR4 expression was significantly upregulated in the negative control cells and cells transfected with siRNA targeting MyD88 **(Figure 3.2)**. There was a trend towards an increase with siRNA targeting GAPDH but it was not significant. These differences in expression were not observed when TLR4 expression levels in the cells transfected with siRNA targeting GAPDH and MyD88 were compared to those of the negative control. Furthermore the increase in expression of TLR4 that had been observed at RNA level was not seen at the protein level **(Figure 3.4)**, therefore the result was not considered a significant result and therefore, wasn't further investigated

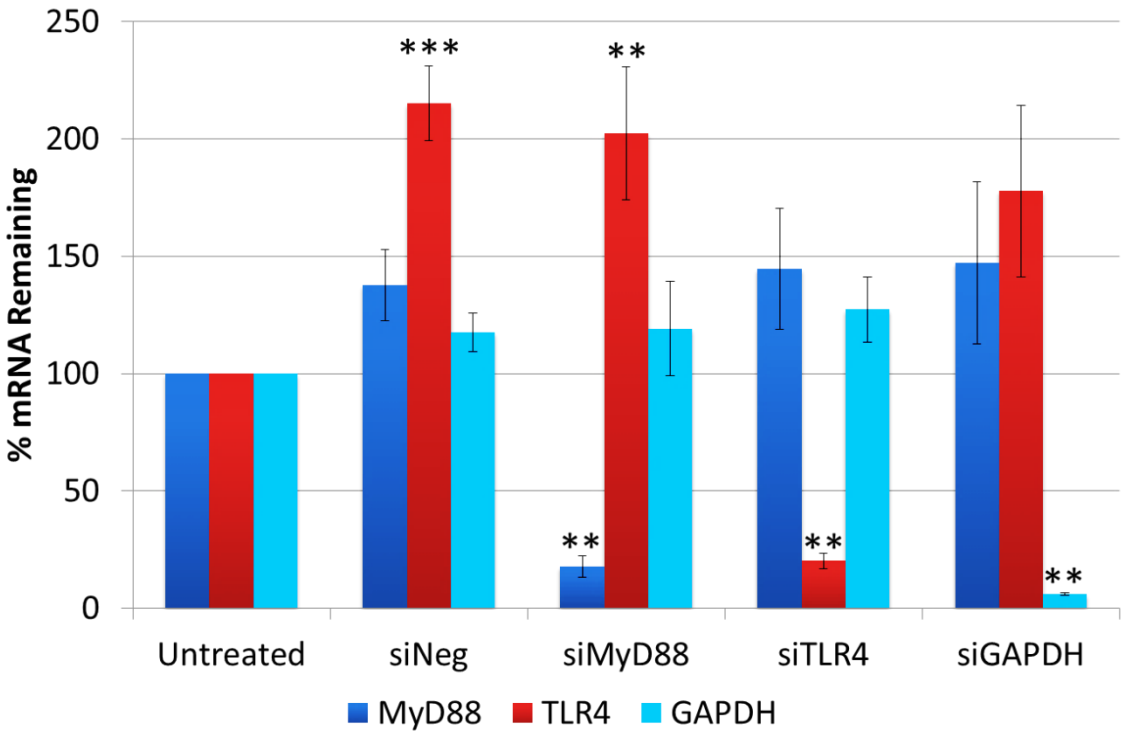

Figure 3.2 Assessment of SKOV-3 gene silencing protocol on TLR4, MyD88 and GAPDH mRNA expression. SKOV-3 cells were transfected with 1nM of siRNA targeting MyD88 (siMyD88), TLR4 (siTLR4), GAPDH (siGAPDH), a negative control siRNA (siNeg) or were left untreated for 72 hours. After 72 hours RNA was isolated using the mirVana™ miRNA Isolation Kit and mRNA expression levels were analysed using TaqMan RT-PCR. TLR4, MyD88 and GAPDH mRNA expression levels were normalised to the endogenous control B2M and calibrated to that of untreated cells to establish the relative change in mRNA expression (% mRNA remaining). Results are expressed as mean +/-SD, n=3; *p<0.05, **p<0.01, ***p<0.001 (Student's t-test).

To further evaluate the potency of this concentration of siRNA knockdown of TLR4 and MyD88 in SKOV-3 cells was also carried out at 24 and 48 hours. When transfected with 1nM of siRNA targeting MyD88 or TLR4, significant knockdown of MyD88 and TLR4 was achieved compared to both untreated SKOV-3 cells and SKOV-3 cells transfected with the negative control siRNA **(Figure 3.3)**. A 92.6 % and 78.5% knockdown of MyD88 and TLR4 was achieved respectively at 24 hours, 92.9 % and 80.5% knockdown of MyD88 and TLR4 was achieved respectively at 48 hours. Therefore, at all time points examined there was significant level of knockdown and there were no significant differences in the level achieved over the time period.

.

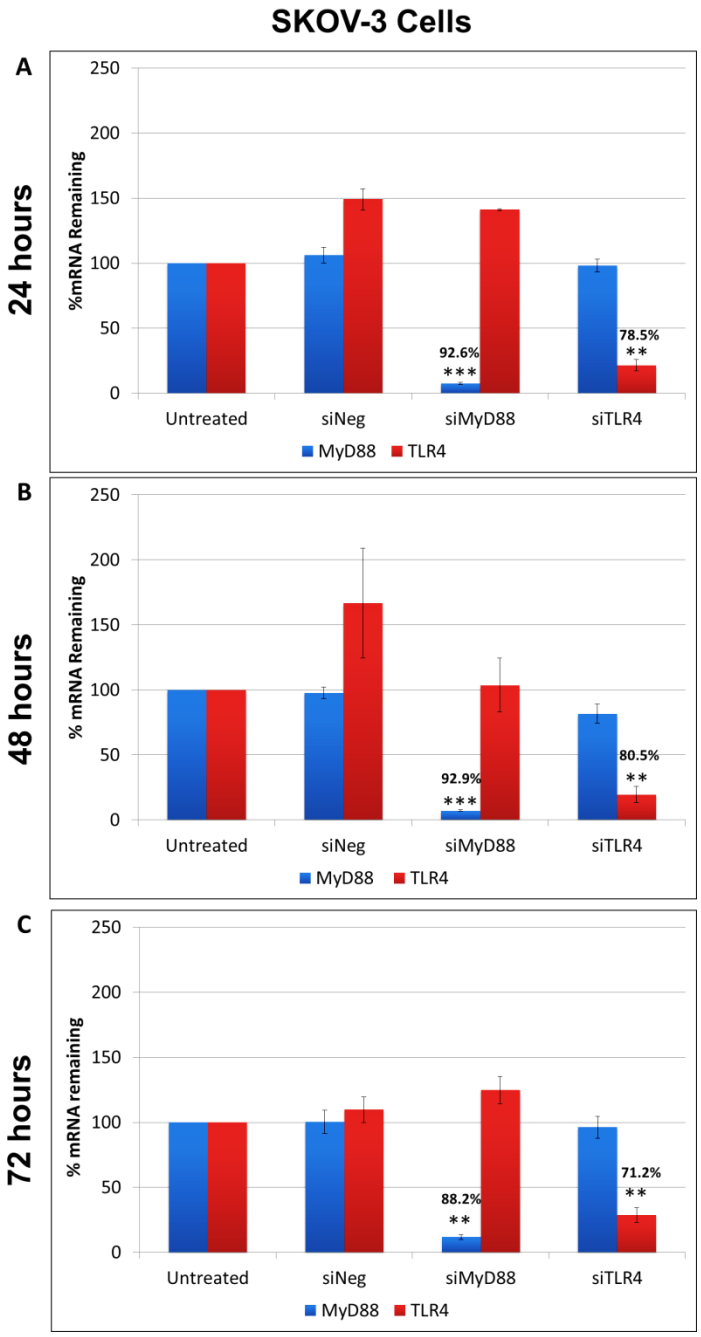

Figure 3.3 Assessment of SKOV-3 gene silencing protocol on TLR4 and MyD88 mRNA expression. SKOV-3 cells were transfected with 1nM of siRNA targeting MyD88 (siMyD88), TLR4 (siTLR4), a negative control siRNA (siNeg) or were left untreated for 24 hours (A) 48 hours (B) and 72 hours (C). After each timepoint RNA was isolated using the mirVana™ miRNA Isolation Kit and mRNA expression levels were analysed using TaqMan RT-PCR. TLR4 and MyD88 mRNA expression levels were normalised to the endogenous control B2M and calibrated to that of untreated cells to establish the relative change in mRNA expression (% mRNA remaining). The results demonstrate that 1nM of siRNA is capable of inducing significant knockdown of both MyD88 and TLR4. Results are expressed as mean +/-SD, at least n=3; *p<0.05, **p<0.01, ***p<0.001 (Student's t-test).

Following validation of the knockdown procedure for MyD88 and TLR4 at the gene level, western blot analysis and densitometry was performed to validate the knockdown of MyD88 and TLR4 at the protein level. Validation of the TLR4 and MyD88 knockdown protocol was essential for the completion and publication of the d'Adhemar *et al* (2014) paper. Western blot analysis and densitometry was performed following knockdown of both TLR4 and MyD88 for 72 hours. Successful knockdown of both MyD88 and TLR4 at the protein level was confirmed at this timepoint **(Figure 3.4)**.

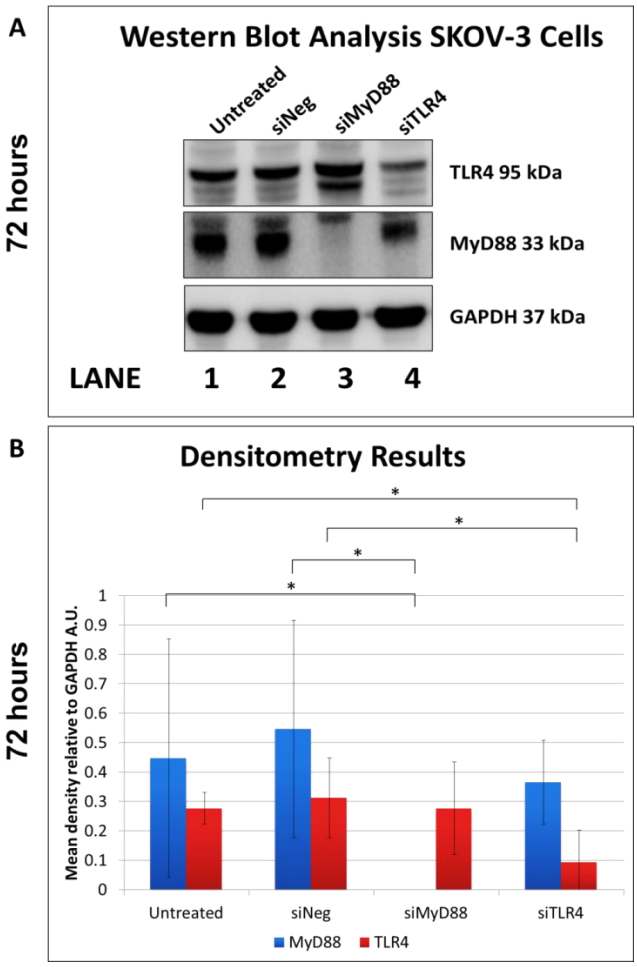

Figure 3.4 Assessment of TLR4 and MyD88 protein expression following knockdown of TLR4 and MyD88 in SKOV-3 cells. SKOV-3 cells were transfected with 1nM siRNA targeting MyD88 (siMyD88), TLR4 (siTLR4), a negative control siRNA (siNeg) or were left untreated for 72 hours. After 72 hours, protein was harvested using RIPA lysis buffer and then western blot analysis was performed for MyD88, TLR4 and GAPDH. Chemiluminescence images were developed using a Fujifilm LAS-4000 luminescent image analyser. Densitometry was then carried out using Quantity One software (Biorad). Protein expression is represented as the mean density normalised to GAPDH in arbitrary units (A.U.) for each condition. The results demonstrate that TLR4 and MyD88 were successfully knocked down at the protein level. Results are expressed as mean +/-SD, n=4; *p<0.05(Student's t-test).

3.4.3 Assessment of the effect of knockdown of MyD88 and TLR4 on the chemoresponsiveness of SKOV-3 cells to paclitaxel

Following validation of the knockdown of TLR4 and MyD88, it was decided to assess the effect of knockdown of TLR4 and MyD88 on paclitaxel sensitivity in these cells. Prior to this assessment the response of untreated SKOV-3 to paclitaxel was evaluated. SKOV-3 cells were treated with concentrations of paclitaxel ranging from (4pM to 80 µM) for 48 hours to ensure an accurate measurement of SKOV-3 chemoresponsiveness. Cell viability was assessed by three different assays, the MTT, AP and CCK-8 assays **(Figure 3.5)**. The reason three methods were assessed was that the MTT assay was standardly used, however it was found with the SKOV-3 cells that the slope of the curve was very steep and that it didn't translate the 100% kill rate observed visually when cells were treated with higher doses of paclitaxel. Therefore, the AP and CCK-8 assays were also used to validate the results observed with the MTT assay. None of the assays were able to detect 100% cell death, the remaining cell viability rates that were observed were attributed to background signal. The slope for all three assays was steep, which made it difficult to accurately differentiate between the IC_{50} from IC_{25} and IC_{75}. For this reason these values were determined using all three assays and were found to be roughly similar. The average of these values was then determined, therefore increasing the accuracy of the results. From this analysis we also noted that the CCK-8 had the lowest standard deviation between replicates and it's absorbance values gave the greatest separation between non-toxic and highly toxic doses. Thus, it was determined that future experiment would be performed with this assay. In order to assess the effect of knockdown of TLR4 and MyD88 on chemoresponsiveness, a dose was required that was not highly toxic to the cells because it was hypothesised that knockdown of TLR4 and MyD88 would increase the chemosensitivity of these cells paclitaxel. The IC_{25} value was subsequently chosen as it should give around a 25% reduction in cell viability. Using all three assays the paclitaxel IC_{25} for SKOV-3 was determined to be 3.5nM

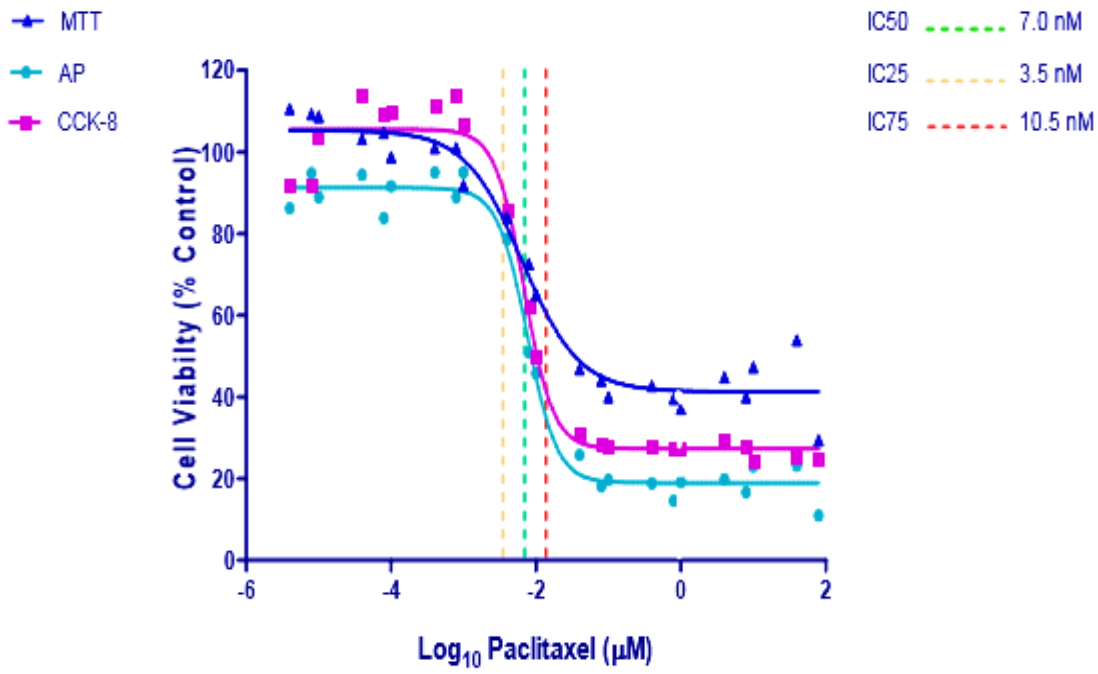

Figure 3.5 SKOV-3 paclitaxel dose response. Two thousand SKOV-3 cells were seeded into a 96 well plate for 72hours and then treated with doses of paclitaxel ranging from (4pM to 80 µM) for 48 hours. Cell viability was assessed by three different assays, the cell counting kit 8 (CCK-8), the (4,5-dimethylthiazol-2-yl)-2,5-diphenyltetrazolium bromide (MTT) and Alkaline phosphatase (AP) assay.

3.4.4 Knockdown of TLR4 but not MyD88 sensitises SKOV-3 cells to paclitaxel

Following determination of the IC_{25}, SKOV-3 cells were transfected with siRNA targeting TLR4, MyD88 the negative control siRNA or were left untreated for 72 hours. After 72 hours SKOV-3 cells were incubated with 3.5nM paclitaxel (IC_{25}), DMSO or were left untreated for a further 48 hours. After 48 hours of drug treatment cell viability was assessed using the CCK-8 assay **(Figure 3.6)**. Following treatment with the IC_{25}, cells transfected with siRNA targeting TLR4 experienced a 23% decrease in cell viability compared to untreated cells which also received treatment with the IC25 ($p=0.02$). This demonstrates that knockdown of TLR4 increases the sensitivity of SKOV-3 cells to paclitaxel therapy. No change in cell viability was observed between cells transfected with siRNA targeting MyD88. This suggests that TLR4 alone modulates SKOV-3 paclitaxel sensitivity.

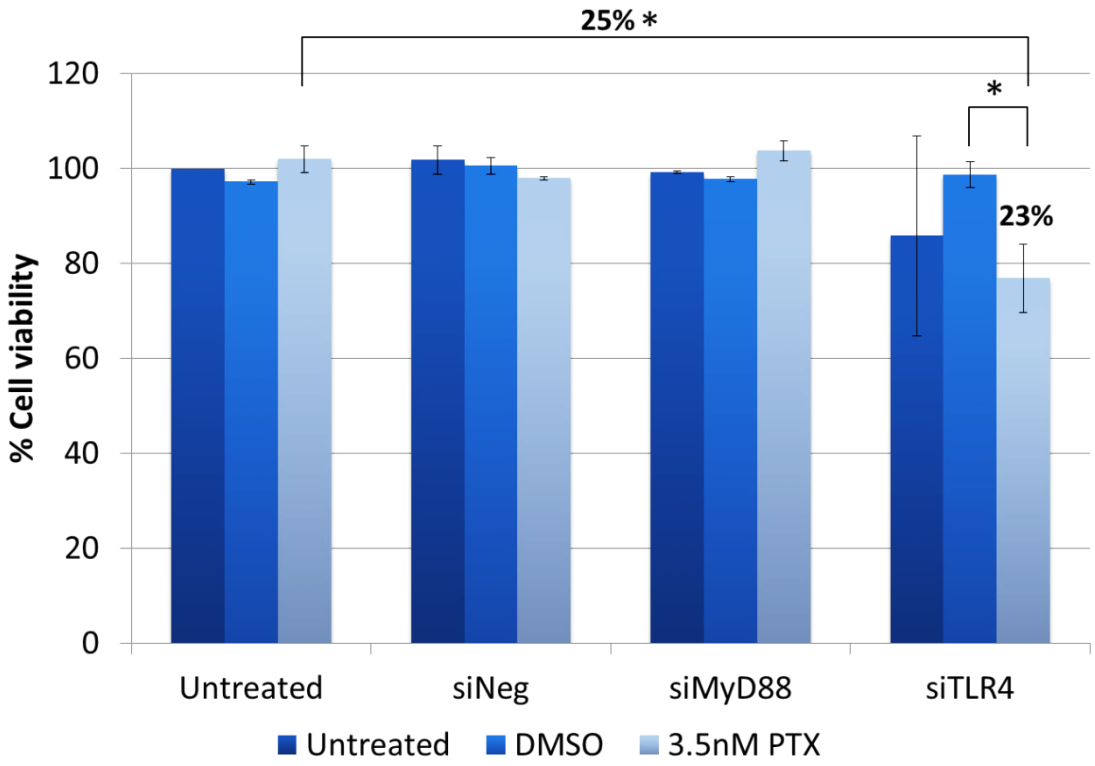

Figure 3.6 Assessment of SKOV-3 chemoresponsiveness to paclitaxel following knockdown of TLR4 or MyD88. SKOV-3 cells were transfected with 1nM siRNA targeting either TLR4 (siTLR4), MyD88 (siMyD88), a negative control siRNA (siNeg) or were left untreated. After 72 hours cells were either left untreated, incubated with DMSO or treated with 3.5nm paclitaxel (IC_{25}) and incubated for a further 48 hours. After 48 hours, cell viability was assessed using the CCK-8 assay. Cell viability rates were then calculated by comparing the absorbance rates under each condition to absorbance values for non-transfected SKOV-3 cells which were left untreated. The results demonstrate that knockdown of TLR4, but not MyD88 sensitises SKOV-3 cells to paclitaxel. Following knockdown of TLR4 and treatment with the IC_{25}, SKOV-3 cells exhibited a 23% or 25% decrease in cell viability compared to the DMSO control or untreated cells treated with 3.5nM paclitaxel respectively. Results are expressed as mean +/-SD, n=3, *$p<0.05$, (Student's t-test).

3.4.5 The expression of the TLR4-MyD88 pathway regulatory microRNAs miR-146a and miR-21 are not affected by loss of TLR4 or MyD88 expression

The regulatory microRNAs miR-146a and miR-21 are known to negatively regulate the TLR4-MyD88 pathway and have also been shown to directly target and downregulate TLR4 and MyD88. In addition, miR-146a and miR-21 have been shown to be upregulated in a number of MyD88 negative tumours. Therefore, it was thought that the expression of these regulatory microRNAs may be altered following knockdown of TLR4 and MyD88 and that this in turn may suggest a potential role for these microRNAs in paclitaxel chemoresistance. In order to investigate this, miR-21 and miR-146a expression was analysed in SKOV-3 cells following knockdown of TLR4 and MyD88 at 24, 48 and 72 hours **(Figure 3.7)**. No significant changes in miR-21 and miR-146a were detected at 24 and 48 hours following knockdown of either TLR4 or MyD88. However, at 72 hours miR-146a was significantly upregulated following knockdown of TLR4 compared to untreated cells but was downregulated compared to the negative control. As this seemed like a potentially interesting result and one that might warrant further evaluation, we decided to repeat the experiment at this time point. This was felt necessary to ensure the accuracy of the results, due to the low level of expression of miR-146a and the conflicting results when compared to the untreated and negative controls. This re-evaluation was done with new samples and a second endogenous control, RNU6B. Unfortunately when these samples were analysed with the RNU6B endogenous control, no significant change in miR-146a was detected **(Figure 3.8)**. Therefore, we concluded that no effect on miR-146a and miR-21 was observed in SKOV-3 despite significant knockdown of MyD88 and TLR4 at any of the time points analysed. This demonstrates that down-regulation of MyD88 and TLR4 has no effect on the expression patterns of these two regulatory microRNAs.

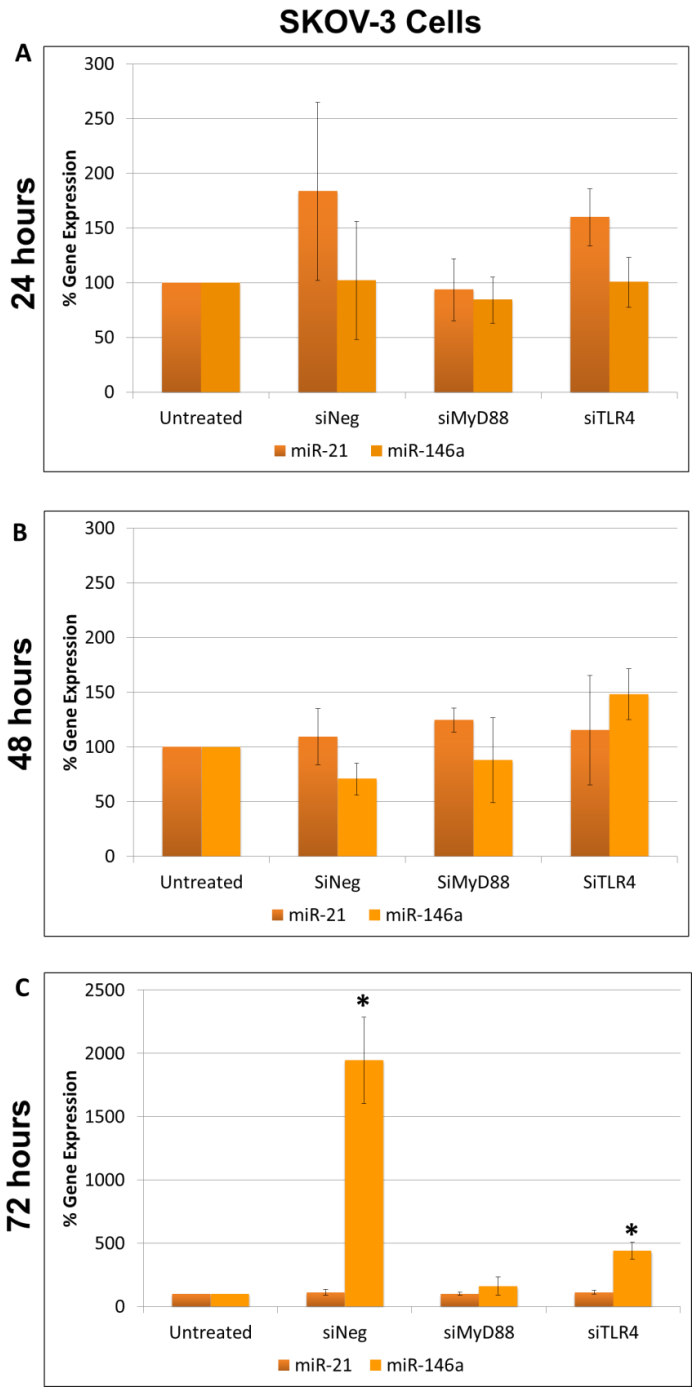

Figure 3.7 Analysis of miR-146a and miR-21 expression 24, 48 and 72 hours following transfection with siRNA targeting MyD88 and TLR4. SKOV-3 cells transfected with siRNA targeting MyD88 (siMyD88), TLR4 (siTLR4), a negative control siRNA (siNeg) or were left untreated for 24 hours (A) 48 hours (B) and 72 hours (C). Following confirmed knockdown of MyD88 and TLR4 at each timepoint, miR-146a and miR-21 expression was assessed using TaqMan RT-PCR. miR-146a and miR-21 expression levels were normalised to the endogenous control miR-16 and calibrated to that of untreated cells in order to determine the relative change in gene expression (%Gene Expression). Results are expressed as mean +/-SD, n=3; *p<0.05 (Student's t-test).

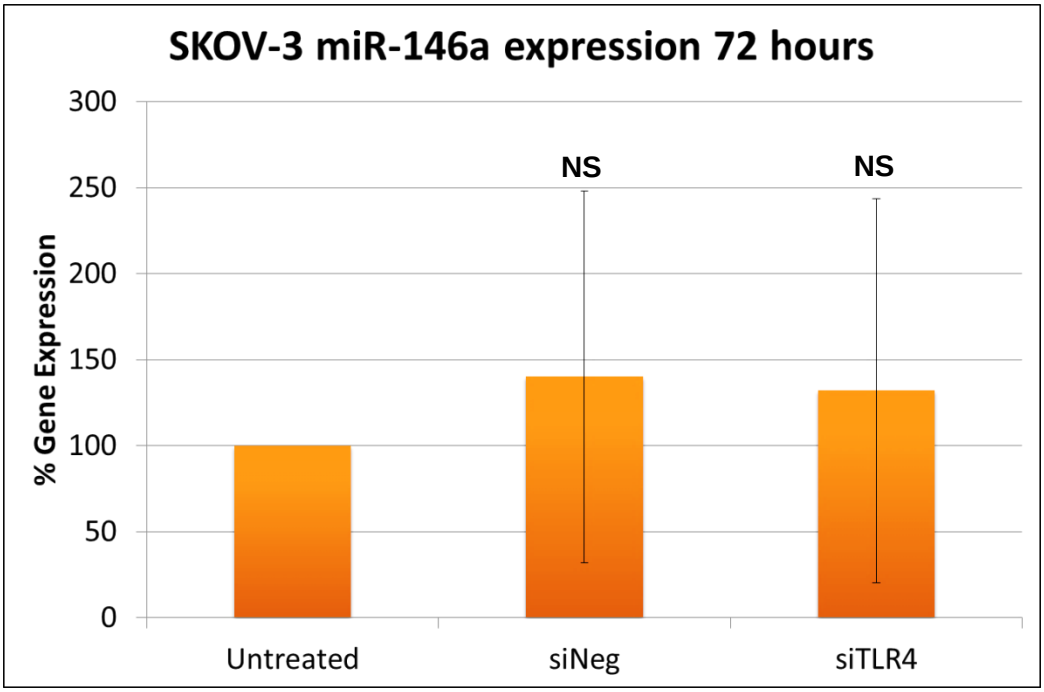

Figure 3.8 Analysis of SKOV-3 miR-146a expression following knockdown of TLR4. SKOV-3 cells transfected with siRNA targeting TLR4 (siTLR4), a negative control siRNA (siNeg) or were left untreated for 72 hours. Following confirmed knockdown of MyD88 and TLR4 at each timepoint, miR-146a, expression levels were measured using TaqMan RT-PCR. miR-146a expression levels were normalised to the endogenous control RNU6B and calibrated to that of untreated cells to establish the relative change in gene expression (% Gene Expression). The results demonstrate that there was no change in miR-146a expression following knockdown of TLR4. Results are expressed as mean +/-SD, n=3, NS-not significant (Student's t-test).

3.4.6 Silencing of TLR4 or MyD88 expression has no effect on the expression of MAD2 or its regulatory microRNA miR-433

Following confirmation of successful knockdown of TLR4 and MyD88 at the gene and protein level, it was important to demonstrate what effect this was having on MAD2 gene and protein expression. Therefore, MAD2 gene expression was analysed following successful knockdown of MyD88 and TLR4 at 24, 48 and 72 hours **(Figure 3.9)**. Loss of MyD88 or TLR4 was found to have no significant impact on MAD2 gene expression at any of the time points analysed. Analysis of MAD2 protein expression at 72 hours post knockdown of MyD88 and TLR4 supported these results, as there was also no change at the protein level **(Figure 3.10)** This indicates that MyD88 and TLR4 do not influence MAD2 gene expression, suggesting that MAD2 may act independently from TLR4 and MyD88 and contribute to paclitaxel resistance through a separate mechanism than TLR4.

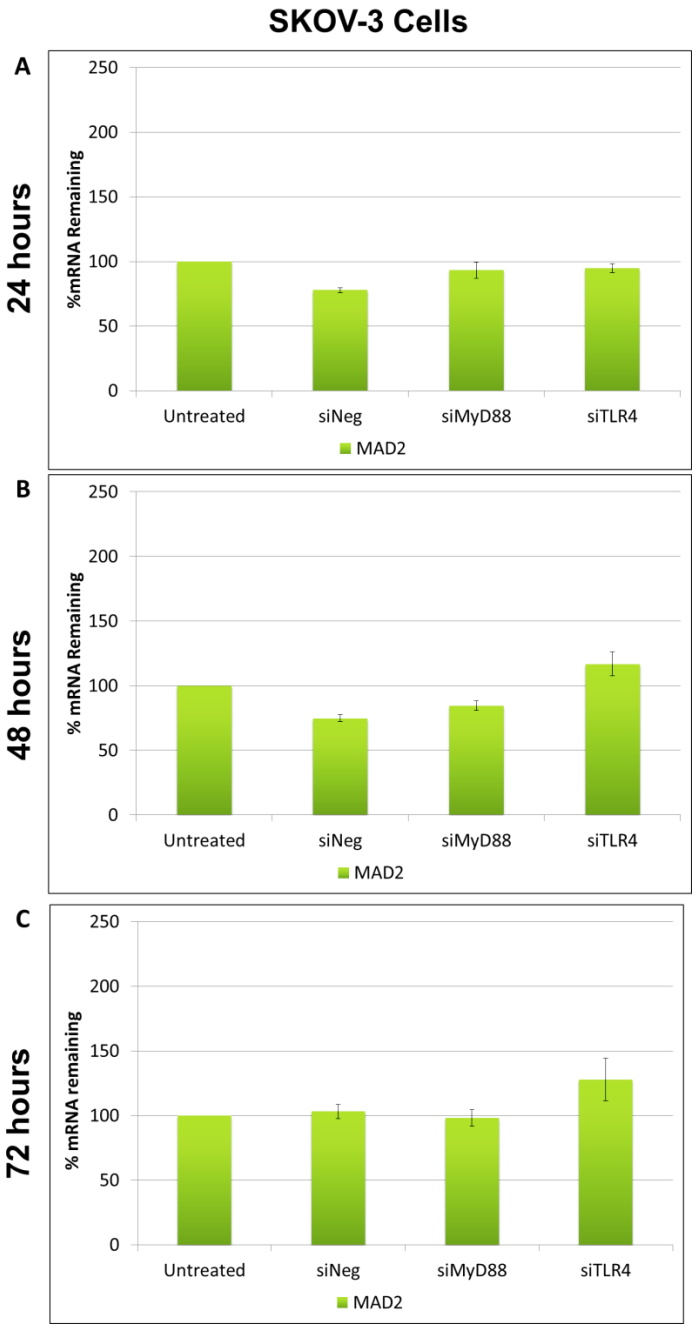

Figure 3.9 Assessment of MAD2 gene expression 24, 48 and 72 hours after transfection with siRNA targeting MyD88 and TLR4. SKOV-3 cells were transfected with 1nM siRNA targeting MyD88 (siMyD88), TLR4 (siTLR4), a negative control siRNA (siNeg) or were left untreated for 24 hours (A) 48 hours (B) or 72 hours (C). After each timepoint RNA was harvested and then mRNA expression levels were analysed using TaqMan RT-PCR. MAD2 mRNA expression levels were normalised to the endogenous control B2M and calibrated to that of untreated cells to establish the relative change in mRNA expression (% mRNA remaining). The results demonstrate that knockdown of MyD88 and TLR4 does not impact on MAD2 gene expression levels. Results are expressed as mean +/-SD n=3.

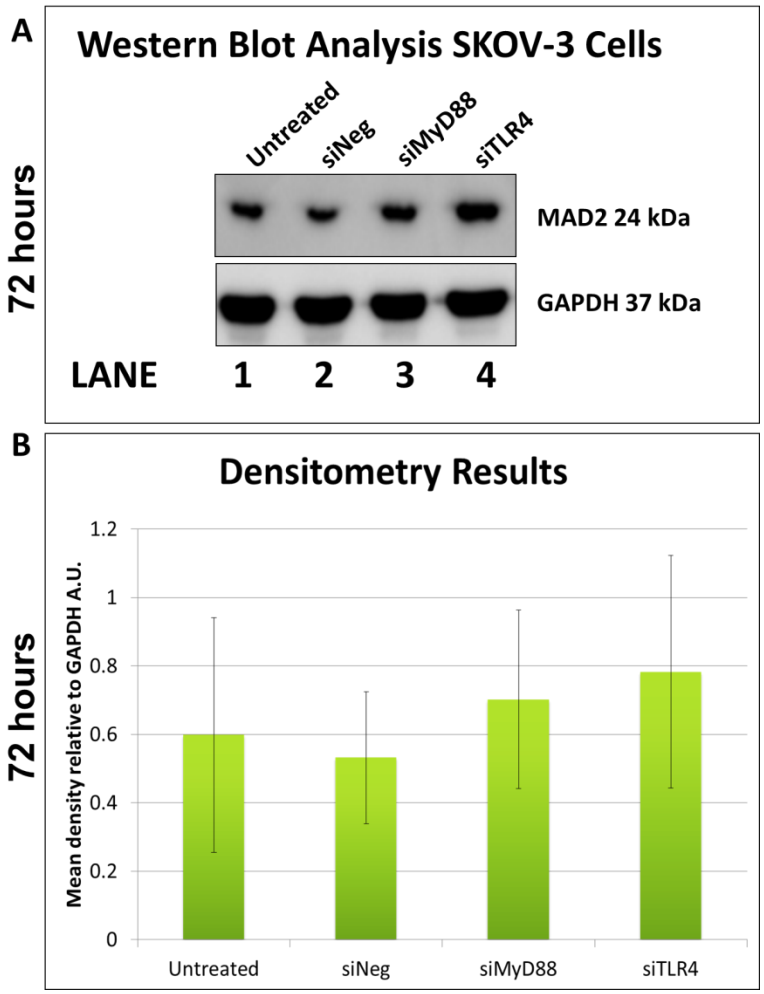

Figure 3.10 Assesment of MAD2 protein expression following knockdown of TLR4 and MyD88 in SKOV-3 cells. SKOV-3 cells were transfected with 1nM siRNA targeting MyD88 (siMyD88), TLR4 (siTLR4), a negative control siRNA (siNeg) or were left untreated for 72 hours. After 72 hours, protein was harvested using RIPA lysis buffer and then western blot analysis was performed for MAD2 and GAPDH. Chemiluminescence images were developed using a Fujifilm LAS-4000 luminescent image analyser. Densitometry was then carried out using Quantity One software (Biorad). Protein expression is represented as the mean density normalised to GAPDH in arbitrary units (A.U.) for each condition. The results demonstrate that knockdown of TLR4 and MyD88 had no effect on MAD2 protein expression levels. Results are expressed as mean +/-SD, n=4.

Following assessment of MAD2 expression at the gene and protein level, it was decided to examine the expression of miR-433. miR-433 has been shown to directly target MAD2 and induce its down-regulation (Furlong *et al*. 2012). Furthermore, overexpression of miR-433 has been shown to induce paclitaxel resistance in the ovarian cancer cell lines A2780 and PEO1 (Furlong *et al*. 2012; Weiner-Gorzel *et al*. 2015). High expression of miR-433 in tumour sections had also been associated with reduced PFS in a high grade serous ovarian cancer cohort (p=0.024) (Furlong *et al*. 2012). Therefore, it was decided to examine miR-433 expression following knockdown of TLR4 and MyD88 in order to discern whether there was any potential link between MAD2 and the TLR4-MyD88 pathway through miR-433, and consequently a link between the miR-433-MAD2 and TLR4 mediated paclitaxel resistance mechanisms. Therefore, miR-433 expression was analysed in SKOV-3 cells following knockdown of TLR4 at 24, 48 and 72 hours **(Figure 3.11)**. Due to the low expression levels of miR-433, which was detected between 35-43 Cts, the expression levels of miR-433 is represented by its Delta Ct values under each condition. No change in miR-433 expression levels were detected following knockdown of TLR4 and MyD88, giving further evidence to suggest that TLR4 and MyD88 have no *in-vitro* relationship with MAD2.

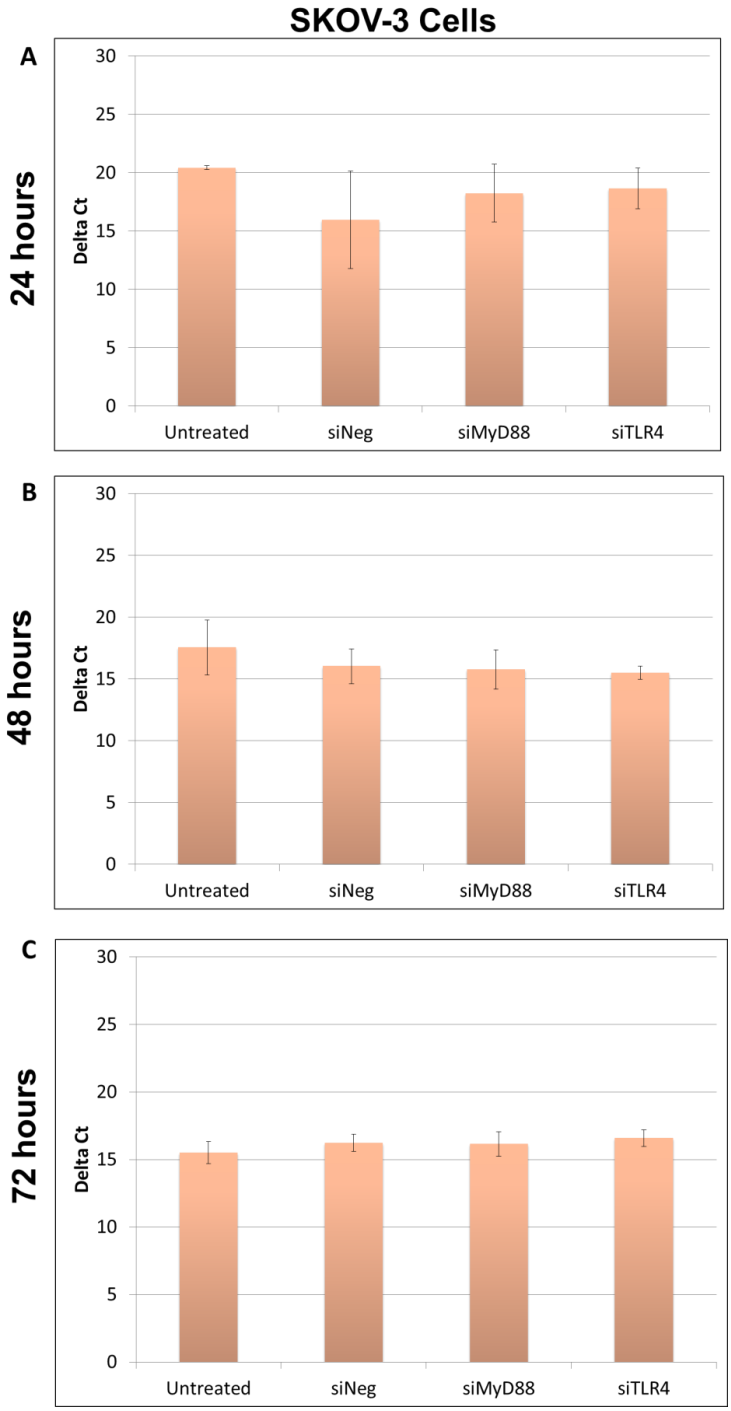

Figure 3.11 Analysis of miR-433 expression 24, 48 and 72 hours after transfection with a siRNA targeting MyD88 or TLR4. SKOV-3 cells transfected with 1Nm siRNA targeting MyD88 (siMyD88), TLR4 (siTLR4), a negative control siRNA (siNeg) or were left untreated for 24 hours (A) 48 hours (B) and 72 hours (C). Following confirmed knockdown of MyD88 and TLR4 at each timepoint, miR-433 expression levels were measured using TaqMan RT-PCR. The Delta Ct values for miR-433 under each condition are displayed on the y axis of each graph. The results demonstrate that knockdown of either TLR4 or MyD88 has no effect on the expression of miR-433. Results are expressed as mean +/-SD, n=3.

3.4.7 *In-silico* analysis does not predict any interaction between MAD2 and TLR4 or MyD88

In parallel with the *in-vitro* work carried out in this study, *in-silico* analysis was performed in order to identify any potential interaction between the TLR4-MyD88 pathway and MAD2. *In-silico* analysis was performed using Search Tool for the Retrieval of Interacting Genes/Proteins (STRING) ver 10 software which is freely available at http://string-db.org/ (Section 2.9). When queried using the STRING database no association was seen between MAD2 and TLR4 or MyD88 **(Figure 3.12A)**. Even when parameters were relaxed and additional proteins known to interact with MAD2, TLR4 and MyD88 were incorporated into the analysis, no interaction was observed **(Figure 3.12B)**. TLR4 and MyD88 and their interactants segregated into a different cluster than MAD2 and its interactants. The *in-silico* analysis predicts that MAD2 does not interact with either TLR4 or MyD88.

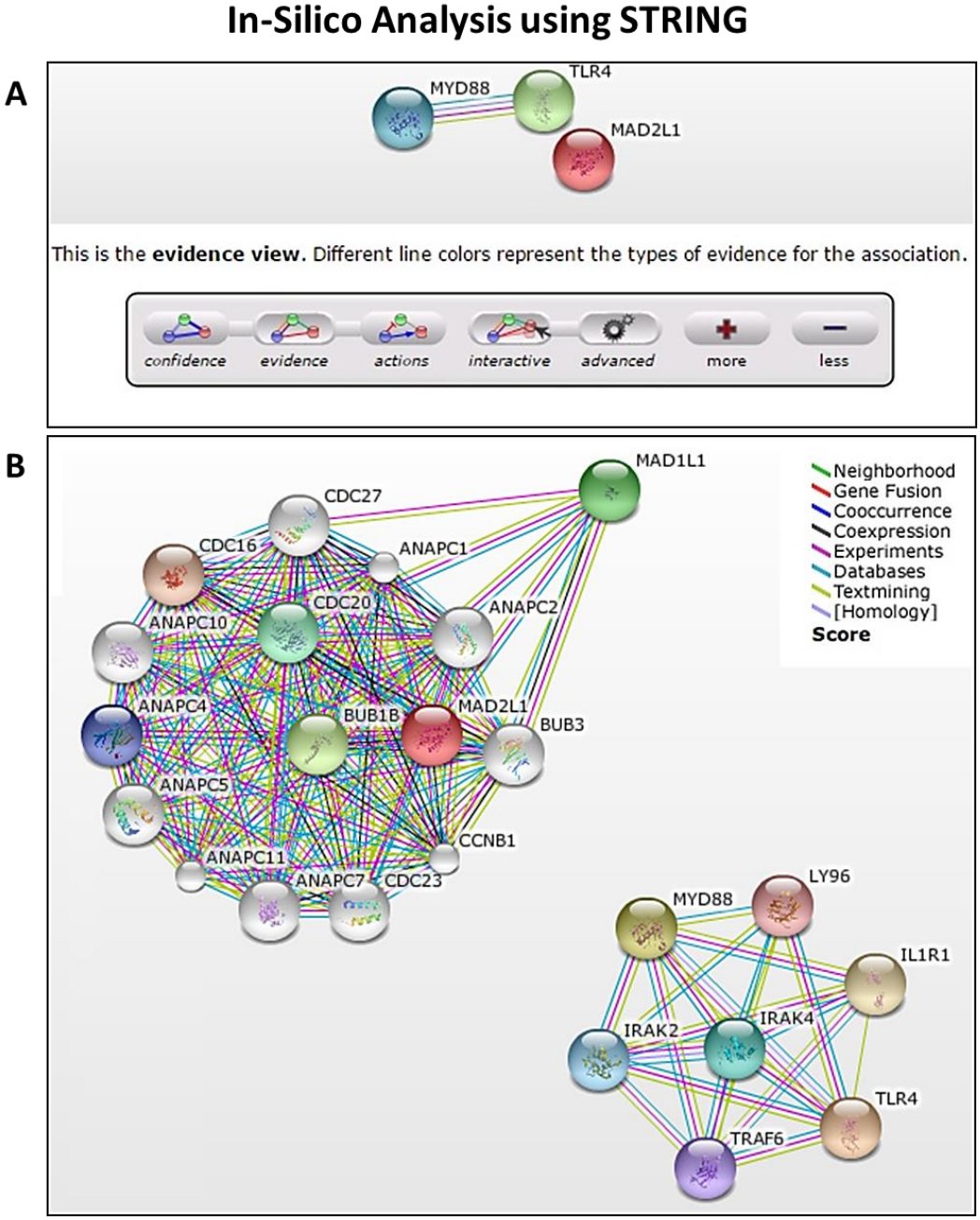

Figure 3.12 The STRING network view. Combined screenshots from the STRING website, which was queried for MyD88, TLR4 and MAD2. Coloured lines between the proteins indicate the various types of interaction evidence. (A) Additional nodes were also incorporated into the analysis and still no interaction between MAD2 and TLR4 or MyD88 was observed. (B) The in silico analysis predicts that there is no direct interaction between MAD2 and TLR4 or MyD88

3.4.8 Microarray analysis of transcriptome changes following knockdown of TLR4 in SKOV-3 cells

To understand how the knockdown of TLR4 was increasing the sensitivity of SKOV-3 cells to paclitaxel **(Section 3.4.2)**, it was decided to assess transcriptome wide changes in gene expression patterns post knockdown of TLR4 using microarray analysis. Affymetrix GeneChip® Human Gene 2.0 ST Arrays were used to analyse changes in gene expression in SKOV-3 cells 72 hours following transfection with siRNA targeting TLR4. Knockdown of TLR4 was first confirmed at the gene level by RT-PCR **(Figure 3.2)** and at the protein level by western blot analysis **(Figure 3.4)**, prior to microarray analysis. Microarray analysis was performed using three biological replicates of SKOV-3 cells transfected with either the negative control siRNA or siRNA targeting TLR4. A 1.5 fold change in gene expression and a p value of $\leq$0.05 was set as the threshold for a significantly upregulated/ downregulated gene, this threshold is in line with recent published works (Vathipadiekal *et al*. 2015). A total of 166 protein coding targets were found to be significantly upregulated and 286 targets found to be significantly downregulated following knockdown of TLR4. The top 20 upregulated and top 20 downregulated genes identified following knockdown of TLR4 are displayed in **Table 3.1** and **Table 3.2**, respectively.

Table 3.1 Top 20 genes upregulated following knockdown of TLR4 for 72 hours in SKOV-3 cells

Ensemble Gene ID	Description	Fold Change	P-Value
ENSG00000117525	Coagulation factor III (thromboplastin, tissue factor)	2.4	0.00001
ENSG00000175592	FOS-like antigen 1	2.2	0.00008
ENSG00000105976	Met proto-oncogene	2.2	0.00008
ENSG00000170616	Scratch family zinc finger 1	2.1	0.00013
ENSG00000144583	Membrane-associated ring finger (C3HC4) 4, E3 ubiquitin protein liga	2.1	0.00021
ENSG00000136155	Sciellin	2.0	0.00024
ENSG00000091409	Integrin, alpha 6	2.0	0.00029
ENSG00000266292	Carboxypeptidase A5	2.0	0.00031
ENSG00000135318	5'-nucleotidase, ecto (CD73)	2.0	0.00041
ENSG00000197646	Programmed cell death 1 ligand 2	2.0	0.00042
ENSG00000058085	Laminin, gamma 2	2.0	0.00043
ENSG00000145220	Ly1 antibody reactive	2.0	0.00045
ENSG00000160352	Zinc finger protein 714	2.0	0.00051
ENSG00000259680	Uncharacterized protein	1.9	0.00082
ENSG00000196944	Olfactory receptor, family 2, subfamily T, member 4	1.9	0.00086
ENSG00000128595	Calumenin	1.9	0.00088
ENSG00000188305	Chromosome 19 open reading frame 35	1.9	0.00122
ENSG00000113070	Heparin-binding EGF-like growth factor	1.9	0.00138
ENSG00000134057	Cyclin B1	1.9	0.00145
ENSG00000205090	Transmembrane protein 240	1.8	0.00166

Ensemble Gene ID - Unique gene ID, **Description -** Gene name, **P-value** - the significance value of the expression change observed. **Fold change** - indicates the degree of expression change. The fold change indicates the degree of expression change. A 1.5 fold change in gene expression and a p value of ≤0.05 was set as the threshold for a significant alteration in gene expression.

Table 3.2 Top 20 genes downregulated following knockdown of TLR4 for 72 hours in SKOV-3 cells

Ensemble Gene ID	Description	Fold Change	P-Value
ENSG00000137745	Matrix metallopeptidase 13 (collagenase 3)	3.9	0.00000
ENSG00000125730	Complement component 3	3.3	0.00000
ENSG00000052802	Methylsterol monooxygenase 1	3.1	0.00000
ENSG00000131203	Indoleamine 2,3-dioxygenase 1	2.7	0.00000
ENSG00000001630	Cytochrome P450, family 51, subfamily A, polypeptide 1	2.6	0.00000
ENSG00000169067	Actin, beta-like 2	2.5	0.00000
ENSG00000135535	CD164 molecule, sialomucin	2.5	0.00000
ENSG00000125968	Inhibitor of DNA binding 1, dominant negative helix-loop-helix protein	2.5	0.00000
ENSG00000205336	G protein-coupled receptor 56	2.4	0.00001
ENSG00000150593	Programmed cell death 4 (neoplastic transformation inhibitor)	2.4	0.00001
ENSG00000159720	ATPase, H+ transporting, lysosomal 38kDa, V0 subunit d1	2.3	0.00002
ENSG00000150347	AT rich interactive domain 5B (MRF1-like)	2.3	0.00003
ENSG00000164125	Family with sequence similarity 198, member B	2.2	0.00003
ENSG00000103485	Quinolinate phosphoribosyltransferase	2.2	0.00004
ENSG00000121858	Tumor necrosis factor (ligand) superfamily, member 10	2.2	0.00004
ENSG00000108395	Tripartite motif containing 37	2.2	0.00005
ENSG00000099194	Stearoyl-CoA desaturase (delta-9-desaturase)	2.2	0.00006
ENSG00000164211	StAR-related lipid transfer (START) domain containing 4	2.1	0.00013
ENSG00000105198	Lectin, galactoside-binding, soluble, 13	2.1	0.00014
ENSG00000186480	Insulin induced gene 1	2.1	0.00014

Ensemble Gene ID - Unique gene ID, **Description -** Gene name, **P-value** - the significance value of the expression change observed. **Fold change** - indicates the degree of expression change. The fold change indicates the degree of expression change. A 1.5 fold change in gene expression and a p value of ≤0.05 was set as the threshold for a significant alteration in gene expression.

3.4.8.1 Gene ontology analysis

The significantly differentially expressed genes identified following knockdown of TLR4 were analysed using the online gene ontology database DAVID, in order to identify pathways and biological processes that were over-represented among this data set. Eight pathways were identified as significantly over-represented, including pathways involved in steroid biosynthesis and metabolism, complement and coagulation cascades, ErbB signalling, focal adhesion and ECM-receptor interaction **(Table 3.3)**.

Table 3.3 Significantly over-represented pathways identified by the DAVID & KEGG databases following knockdown of TLR4 for 72 hours in SKOV-3 cells

Pathways	Count	%	P-Value
Pathways in cancer	21	5	0.00057
ErbB signaling pathway	8	1.9	0.00960
Steroid biosynthesis	4	0.9	0.01000
Complement and coagulation cascades	7	1.7	0.01100
Focal adhesion	12	2.8	0.02200
ECM-receptor interaction	7	1.7	0.02700
Renal cell carcinoma	6	1.4	0.04300
Pancreatic cancer	6	1.4	0.04700

Pathways – The different pathways over-represented following knockdown of TLR4 are represented in column 1. **P-value –** the significance value of the expression change observed, a p value of ≤0.05 was set as the threshold for a significant alteration in pathway expression. **Count** – The number of genes involved in a particular pathway which was found to be over-represented. **% –** Percentage of genes affected out of the total number of genes altered following knockdown of TLR4.

In addition one hundred biological processes were significantly over-represented in this data set. The top 30 biological processes identified are displayed in **Table 3.4**. Among the biological processes affected included those processes involved in regulation of cell death, cell adhesion and sterol metabolism and biosynthesis. The olfactory receptor family although it was not found to be over-represented by DAVID analysis, had a large number of family members deregulated following knockdown of TLR4 **(Supplementary table S1)**.

Table 3.4 The top 30 significantly over-represented biological processes identified by the DAVID database following knockdown of TLR4 in SKOV-3 cells

Biological Process	Count	%	P-Value
Regulation of programmed cell death	41	9.7	0.00001
Regulation of cell death	41	9.7	0.00001
Regulation of apoptosis	40	9.4	0.00001
Regulation of cell adhesion	13	3.1	0.00008
Epidermis development	15	3.5	0.00010
Wound healing	15	3.5	0.00015
Regulation of cell proliferation	36	8.5	0.00017
Ectoderm development	15	3.5	0.00023
Positive regulation of apoptosis	23	5.4	0.00045
Positive regulation of programmed cell death	23	5.4	0.00050
Positive regulation of cell death	23	5.4	0.00053
Sterol biosynthetic process	6	1.4	0.00120
Cell division	17	4	0.00150
Regulation of cell-cell adhesion	5	1.2	0.00150
Negative regulation of programmed cell death	19	4.5	0.00180
Negative regulation of cell death	19	4.5	0.00190
Mitosis	14	3.3	0.00190
Nuclear division	14	3.3	0.00190
M phase of mitotic cell cycle	14	3.3	0.00230
Transmembrane receptor protein tyrosine kinase signaling pathway	14	3.3	0.00230
Enzyme linked receptor protein signaling pathway	18	4.2	0.00270
Organelle fission	14	3.3	0.00270
Response to wounding	24	5.7	0.00300
Negative regulation of cell adhesion	6	1.4	0.00300
Negative regulation of T cell proliferation	5	1.2	0.00330
Cell cycle phase	20	4.7	0.00370
Negative regulation of apoptosis	18	4.2	0.00380
Phosphoinositide-mediated signaling	8	1.9	0.00430
Blood coagulation, extrinsic pathway	3	0.7	0.00510
Regulation of MAP kinase activity	10	2.4	0.00560

Biological Process – The different biological processes over-represented following knockdown of TLR4 are represented in column 1. **P-value** – the significance value of the expression change observed, a p value of ≤0.05 was set as the threshold for a significant alteration in in a biological process. **Count** – The number of genes involved in a particular biological process which was found to be over-represented. **%** – Percentage of genes affected out of the total number of genes altered following knockdown of TLR4.

3.5 Discussion

High MyD88 IHC staining intensity is associated with reduced PFS (p=0.02) and OS (p=0.029) and high TLR4 IHC staining intensity is associated with reduced PFS (p=0.016) in patients with high grade serous ovarian cancer (d'Adhemar *et al*. 2014). In this study, TLR4 knockdown was shown to restore chemosensitivity to paclitaxel in SKOV-3 cells. This is consistent with a number of other publications, which have demonstrated that inhibition or silencing of TLR4 expression in SKOV-3 cells restores chemosensitivity to paclitaxel (Szajnik *et al*. 2009; Wang *et al*. 2009; Huang *et al*. 2014; Wang *et al*. 2014). Furthermore, high TLR4 IHC staining intensity is associated with reduced survival in breast and oesophageal cancer (Sheyhidin *et al*. 2011; Ma *et al*. 2014). Additionally, overexpression of TLR4 using a plasmid vector in the breast cancer cell line, HCC1806, has been shown to induce paclitaxel resistance (Rajput *et al*. 2013).

Paclitaxel is an established ligand for TLR4 (Byrd-Leifer *et al*. 2001) and binding of paclitaxel to TLR4 likely contributes to paclitaxel chemoresistance in ovarian cancer by upregulating the expression of various pro-tumourigenic inflammatory cytokines and pro-survival proteins (Kelly *et al*. 2006; Wang *et al*. 2009; Szajnik *et al*. 2009; Huang *et al*. 2014). The blockage of this pathway in the SKOV-3 cell model using a peptide inhibitor or suppression of this pathway using siRNA has been shown to prevent the activation of inflammatory cytokines and pro-survival proteins enhancing the effect of paclitaxel therapy (Wang *et al*. 2009; Szajnik *et al*. 2009; Huang *et al*. 2014).

The cytokines and pro-survival proteins known to be upregulated by paclitaxel ligation to TLR4 include IL-6, IL-8, VEGF, MCP-1, TNF-α XIAP, pAKt, BCL-2 and BCL-XL (Szajnik *et al*. 2009; Rajput *et al*. 2013; Huang *et al*. 2014; Zhan *et al*. 2015). Each of these respective cytokines and anti-apoptotic/pro-survival proteins have been shown to play a role in ovarian cancer tumourigenesis and chemoresistance (Holcik *et al*. 2001; *Cheng et al*. 2002; Szlosarek *et al*. 2006; Rabinovich *et al*. 2007; Lukaszewicz *et al*. 2007; Yip & Reed 2008; Weng *et al*. 2009; Zhang *et al*. 2010; Niu & Chen 2010; Wang *et al*. 2011; Guo *et al.* 2012; Rajput *et al*. 2013). However, targeting a single cytokine or pro-survival protein may not be sufficient to induce a substantial change in patient outcomes. Instead targeting the entire cytokine network may be a highly effective strategy moving forward for ovarian cancer treatment. TLR4 as it appears to be a master regulator of these various cytokines and pro-survival proteins is a very attractive target for ovarian cancer therapy. The work performed in this study suggests that targeting TLR4 will support paclitaxel based therapy and lead to more successful

therapeutic outcomes for patients with ovarian cancer. Therapeutic targeting of TLR4 is discussed further in chapter 7.

A number of studies, which have targeted MyD88 in different cancer models, including breast, lung, liver and colon cancer, have demonstrated that MyD88 is capable of modulating the chemosensitivity of cells to paclitaxel and other therapeutic agents, such as cisplatin (Egunsola *et al*. 2012; Liang *et al*. 2013; Kfoury *et al*. 2013; G. Liu *et al*. 2014; Xiang *et al*. 2014), however, this study is the first to examine the effect of targeting MyD88 on paclitaxel sensitivity in ovarian cancer cells. While the knockdown of TLR4 was observed to increase the sensitivity of SKOV-3 cells to paclitaxel therapy a similar result was not observed with the knockdown of MyD88. This is an interesting result, as TLR4 is known to signal through both MyD88 and an alternative adaptor protein called TRIF **(Figure 1.8)**. The fact that silencing of TLR4 but not MyD88 restores chemosensitivity of SKOV-3 cells to paclitaxel suggests a role for the TRIF dependent pathway in paclitaxel chemoresistance.

It was hypothesised that the knockdown or suppression of the TLR4-MyD88 pathway by silencing MyD88 or TLR4 gene expression may alter the expression levels of miR-146a and miR-21, which are known to negatively regulate this pathway (Quinn & O'Neill 2011) and have been shown to directly target MyD88 and TLR4 (Yang *et al*. 2011; Zhao *et al*. 2012; Lario *et al*. 2012; Chen *et al*. 2013). The rationale behind this theory was that in addition to TLR4 and MyD88 they were thought to be involved in the paclitaxel chemoresistance mechanism, as they had been demonstrated to be differentially expressed in a number of ovarian cancer cell lines compared to their chemoresistant counterparts (d'Adhemar *et al*. 2014). Furthermore, their expression was upregulated in a subset of MyD88 negative tumours (d'Adhemar *et al*. 2014). Knockdown of MyD88 or TLR4 in SKOV-3 cells had no effect on the expression levels of the regulatory microRNA's miR-21 and miR-146a at any of the time points analysed.

A possible explanation for why no changes in miR-21 and miR-146a was observed is that although microRNAs are known to influence the expression of multiple genes, altering the expression of a single gene target may not be sufficient to exert an effect on the expression of the microRNAs (Vencken *et al*. 2014; Pasquinelli 2012; Aalaei-andabili & Rezaei 2013). miR-146a and miR-21 are known to negatively regulate a number of proteins involved in TLR4-MyD88 dependent signalling, therefore, targeting TLR4 or MyD88 alone may not necessarily influence the expression of miR-146a and miR-21 *in-vitro*, despite the reciprocal expression patterns observed in patient tumour samples (d'Adhemar *et al*. 2014). Overexpressing these two regulatory microRNAs

may give further insight into their role in ovarian cancer, the regulation of MyD88 and TLR4 and any potential role in modulating paclitaxel sensitivity. Interestingly Xie *et al*. (2013) showed that treatment of paclitaxel resistant ovarian cancer cells with miR-21 inhibitors increased their sensitivity to paclitaxel. A study by Echevarría-Vargas *et al*. (2014) also demonstrated that miR-21 is upregulated in cisplatin resistant ovarian cancer cells. Conversely, overexpression of miR-146a has been shown to reduce the invasiveness of gastric (Yao *et al*. 2013), breast (Bhaumik *et al*. 2008; Hurst *et al*. 2009), thyroid (Zhang *et al*. 2014), Glioma (Mei *et al*. 2011) and pancreatic cancer cells (Li *et al*. 2010; Ali *et al*. 2014).

While high TLR4 and MyD88 IHC staining intensity has been associated with poor patient prognosis, low MAD2 IHC staining intensity has been associated with reduced PFS in patients with high grade serous ovarian cancer (p=0.0003)(Furlong *et al*. 2012). Additionally, knockdown of MAD2 has been shown to mediate paclitaxel resistance through the induction of senescence in both MCF-7 breast and A2780 ovarian cancer cell lines (Prencipe *et al*. 2009; Furlong *et al*. 2012). Although MyD88, TLR4 and MAD2 contribute to paclitaxel resistance and poor prognosis in ovarian cancer, no known relationship has been previously described between them. Knockdown of TLR4 or MyD88 in SKOV-3 cells had no effect on the expression levels of MAD2 at either the gene expression or protein level at any of the time points analysed. This suggests that MAD2 acts independently of MyD88 and TLR4 and supports results from *in-silico* analysis, which showed that there was no direct interaction or pathway linkage between TLR4, MyD88 and MAD2. These results would seem to indicate that these proteins contribute to chemoresistance through separate mechanisms. Analysis of miR-433, a MAD2 regulatory microRNA, following knockdown of TLR4 and MyD88 further supports this theory. As like MAD2, miR-433 expression was unaffected following transfection despite its known role in paclitaxel resistance, suggesting that these paclitaxel resistance mechanisms also do not intersect (Furlong *et al*. 2012; Weiner-Gorzel *et al*. 2015).

Knockdown of TLR4 rendered SKOV-3 cells more sensitive to paclitaxel based therapy and this mechanism was independent of MAD2 related chemoresistance and also the MyD88 arm of its signalling pathway. Therefore, to attempt to understand what genes and gene pathways were affected following knockdown of TLR4 and, which may result in this enhanced chemosensitivity whole transcriptome analysis was performed. From this analysis 452 protein coding genes were identified, which were significantly deregulated following knockdown of TLR4. Gene ontology analysis highlighted a number of cellular processes and pathways in which these genes are involved,

including steroid metabolism and biosynthesis, the ERBB signalling pathway, cell death and cell adhesion.

Regulation of apoptosis and programmed cell death was the most significantly altered biological process following knockdown of TLR4. Thirty-eight genes involved in the regulation of apoptosis were affected following knockdown of TLR4 in SKOV-3 cells. This gene list is available in supplementary table **(Table S2)**. Thirteen of nineteen negative regulators of apoptosis were downregulated and 5 of 19 positive regulators of apoptosis were upregulated. The deregulation of so many regulators of apoptosis could indicate that the TLR4 knockdown is rendering the SKOV-3 cells more susceptible to cell death and/or preventing the upregulation of pro-survival genes that contribute to paclitaxel resistance. This may explain why the cells exhibited increased sensitivity to paclitaxel.

Eight genes involved in steroid metabolism and steroid biosynthesis were downregulated following knockdown of TLR4 **(Table S3)**. These genes are involved in the synthesis of cholesterol and play various roles in lipogenesis and glucose homeostasis (Jiang et al. 2005; Krapivner et al. 2007; Dong & Tang 2010; Roongta et al. 2011; Park et al. 2014). This may indicate that SKOV-3 cells due to their TLR4 positivity display enhanced metabolism of lipids and cholesterol. Cancerous cells often display alterations in lipid metabolism, these alterations can affect the availability of structural lipids for the synthesis of membranes, the synthesis and degradation of lipids that contribute to energy homeostasis and the abundance of lipids with signalling functions. Changes in lipid metabolism can affect numerous cellular processes, including cell growth, proliferation, differentiation and motility. Through its role in these various processes, lipid metabolism plays a key role in tumourigenesis and may contribute to chemoresistance (Santos & Schulze 2012). Thus, knockdown of TLR4 in the SKOV-3 cell model may lead to reduced availability and mobilisation of lipid and may have contributed to the increased sensitivity of these cells to paclitaxel.

Gene ontology analysis highlighted focal adhesion, cell adhesion and ECM receptor binding as being over-represented **(Table S4)**. Seven of the thirteen genes involved in these processes were downregulated. A possible explanation for this is that the cells are transitioning between epithelial and mesenchymal phenotypes. Epithelial cells act as surface barrier cells and form tight junctions with adjacent cells and to the basement membrane. Whereas, mesenchymal cells are stem-like cells, which serve as scaffolding or anchoring cells and have multifunctional roles in tissue repair and wound healing. Epithelial-mesenchymal transition (EMT) is a process whereby epithelial cells,

lose their polarity, exhibit loss of cell adhesion and become migratory and invasive, adopting the phenotype of mesenchymal cells (Kalluri & Weinberg 2009). The reverse of this process can also occur where cells lose their mesenchymal characteristics and gain epithelial-like features, this is known as mesenchymal-epithelial transition (MET). Ovarian cancer cells displaying a mesenchymal phenotype have been shown to be more resistant to paclitaxel therapy (Kajiyama *et al*. 2007). Among the genes downregulated was the mesenchymal cell marker fibronectin-1. While important genes involved in the formation of tight junctions, including P-cadherin, integrin alpha 6, laminin beta 2, laminin gamma 3, claudin 1 and claudin 9, were upregulated, demonstrating that these cells are becoming more epithelial and less mesenchymal like..Thus potentailly making them more susceptible to paclitaxel chemotherapy.

Gene ontology analysis of the 452 significantly altered genes also highlighted the ERBB signalling pathway as being significantly over-represented **(Table 3.3)**. Eight genes within this pathway were found to be deregulated following knockdown of TLR4. v-erb-b2 erythroblastic leukemia viral oncogene homolog 2 (Erbb2), commonly known as HER2, Cas-Br-M (murine) ecotropic retroviral transforming sequence b (CBLB), phosphoinositide-3-kinase catalytic beta polypeptide (PIK3CB) and phosphoinositide-3-kinase catalytic regulatory subunit 1 (PIK3R1) were downregulated. While, Amphiregulin (AR), heparin bound epidermal growth factor (HB-EGF), transforming growth factor alpha (TGF-α) and v-crk sarcoma virus CT10 oncogene homolog (CRK) were upregulated. This work establishes a novel link between TLR4, HER2 and other members of the ERBB signalling network in ovarian cancer. Some recent studies have also shown a relationship between TLR4 and a number of these members of the ERBB signalling pathway individually (Bachmaier *et al*. 2007; Bergin *et al*. 2008; Laird *et al*. 2009; Hsu *et al*. 2010; Hackam *et al*. 2013; Chattopadhyay *et al*. 2015; De *et al*. 2015). These studies provide further evidence supporting a link between TLR4 and ERBB signalling in ovarian cancer. Each of these ERBB signalling genes possibly contribute to chemoresistance and tumourigenesis through their various roles in proliferation, migration, adhesion, angiogenesis, apoptosis, and differentiation (Umekita et al. 2000; Soares et al. 2000; Citri & Yarden 2006; Busser et al. 2011; Iqbal & Iqbal 2014).

The olfactory receptor (OR) family although not highlighted by DAVID, had a large number of family members affected following knockdown of TLR4. One of its member's olfactory receptor, family 2, subfamily T, member 4 was one of the top 20 genes upregulated following knockdown of TLR4, therefore, this gene family was deemed of particular interest. Fourteen members of the OR family were downregulated and two members were upregulated following knockdown of TLR4 **(Table S1)**. Among the ORs affected were members of the OR families 1, 2, 4, 5, 6, 7, 8, 51 and 56. ORs are the key smell receptors, which are involved in the processing of detected odour and pheromone signals for transmission to the brain (DeMaria & Ngai 2010). ORs are a large family whose mechanism is well-described in olfactory tissues. In recent years, ORs have been shown to be widely expressed in several non-sensory tissues, such as the testis and sperm, kidneys, prostate, erythroid cells and notochord (Barnea *et al*., 2004; Kaupp, 2010; Li 2013). A previous study by Ward *et al*. (2015) described a relationship between ORs and TLR signalling in Drosophila. In non-sense cells ORs may serve to detect exogenous danger signals within the extracellular environment and thus, help to protect the cell from perceived hostile environment, such as therapeutic insults. OR downregulation following knockdown of TLR4 may therefore, have also contributed to the increased paclitaxel sensitivity of SKOV-3 cells. Interestingly our group has shown that OR downregulation occurs during differentiation of the embryonal carcinoma 2102Ep cell line (Unpublished Manuscript, Sulaiman 2015). Differentiated cells are less tumourigenic and more susceptible to chemotherapy, this may again explain why the SKOV-3 cells were more susceptible to paclitaxel therapy following knockdown of TLR4.

3.6 Conclusion

The siRNA knockdown of TLR4 was shown to increase the sensitivity of SKOV-3 ovarian cancer cells to paclitaxel. This change in paclitaxel resistance did not alter the expression of MAD2 supporting *in-silico* analysis that there is no relationship between the TLR4-MyD88 pathway and MAD2. This suggests that there may be no *in-vitro* relationship between these markers and that they may act as independent biomarkers in ovarian cancer and contribute to paclitaxel resistance through entirely separate mechanisms. The three regulatory microRNAs similarly remained unaffected by siRNA knockdown of TLR4 and MyD88 and may act independently of TLR4 and MyD88 and may serve as additional independent prognostic biomarkers in ovarian cancer. The novel key findings of this study are that the effect of the TLR4 knockdown on the paclitaxel chemoresponse of SKOV3 cells may perhaps be independent of the MyD88 arm of the pathway as the knockdown of MyD88 did not affect the chemoresponse of SKOV-3 cells to paclitaxel. Microarray analysis also highlighted a number of novel downstream pathways which may be involved in this process and which may potentially be targetable such as steroid biosynthesis and ErbB signalling. Olfactory receptors were also a novel family of receptors which were highlighted and may also be involved in the response of SKOV-3 cells to paclitaxel.

3.7 References

1) Aalaei-andabili, S.H. et al., 2013. Toll like receptor (TLR)-induced differential expression of microRNAs (MiRs) promotes proper immune response against infections: A systematic review. *Journal of Infection*, 67(4), pp.251–264. Available at: http://dx.doi.org/10.1016/j. jinf. 2013. 07.016.
2) Ali, S. et al., 2014. Deregulation of miR-146a expression in a mouse model of pancreatic cancer affecting EGFR signaling. *Cancer Letters*, 351(1), pp.134–142. Available at: http://dx.doi.org/10.1016/j.canlet. 2014. 05.013.
3) Alvero, A. et al., 2011. Molecular phenotyping of human ovarian cancer stem cells unravel the mechanisms for repair and chemo-resistance. *Cell Cycle*, *8*(1), 158–166.
4) Bachmaier, K. et al., 2007. E3 ubiquitin ligase Cblb regulates the acute inflammatory response underlying lung injury. *Nature medicine*, 13(8), pp.920–926.
5) Balkwill, F., 2004. Cancer and the chemokine network. *Nature reviews. Cancer*, 4(7), pp.540–550.
6) Barnea, G et al., 2004. Odorant receptors on axon termini in the brain. *Science (New York, N.Y.)*, *304*(5676), 1468.
7) Behrens, B.C. et al., 1987. Characterization of a cis–Diammine dichloroplatinum (II) -resistant Human Ovarian Cancer Cell Line and Its Use in Evaluation of Platinum Analogues. , (Ii), pp.414–418.
8) Bergin, D.A. et al., 2008. Activation of the epidermal growth factor receptor (EGFR) by a novel metalloprotease pathway. *Journal of Biological Chemistry*, 283(46), pp.31736–31744.
9) Bhaumik, D. et al., 2008. Expression of microRNA-146 suppresses NF-κB activity with reduction of metastatic potential in breast cancer cells. *Oncogene*, 27(42), pp.5643–5647.
10) Busser, B. et al., 2011. The multiple roles of amphiregulin in human cancer. *Biochimica et Biophysica Acta - Reviews on Cancer*, 1816(2), pp.119–131. Available at: http://dx.doi.org/10.1016/j.bbcan.2011.05.003.
11) Byrd-Leifer, C. a et al., 2001. The role of MyD88 and TLR4 in the LPS-mimetic activity of Taxol. *European journal of immunology*, 31(8), pp.2448–57. Available at: http://www.ncbi.nlm.nih.gov/pubmed/11500829.
12) Chattopadhyay, S. et al., 2015. EGFR kinase activity is required for TLR4 signaling and the septic shock response. *EMBO Journal*.
13) Cheng, J.Q. et al., 2002. Role of X-linked inhibitor of apoptosis protein in chemoresistance in ovarian cancer: possible involvement of the phosphoinositide-3 kinase/Akt pathway. *Drug resistance updates : reviews and commentaries in antimicrobial and anticancer chemotherapy*, 5(3-4), pp.131–46. Available at: http://www.ncbi.nlm.nih.gov/pub med/ 12237081.
14) Citri, A. & Yarden, Y., 2006. EGF-ERBB signalling: towards the systems level. *Nature reviews. Molecular cell biology*, 7(7), pp.505–516.
15) Craveiro, V. et al., 2013. Phenotypic modifications in ovarian cancer stem cells following Paclitaxel treatment. *Cancer Medicine*, *2*(6), 751–62. doi:10.1002/cam4.115.
16) Cuello, M. et al., 2001. Synergistic Induction of Apoptosis by the Combination of TRAIL and Chemotherapy in Chemoresistant Ovarian Cancer Cells. , 390, pp.380–390.
17) d'Adhemar, C.J. et al., 2014. The MyD88+ Phenotype Is an Adverse Prognostic Factor in Epithelial Ovarian Cancer. *PloS one*, 9(6), p.e100816. Available at: http://www.ncbi.nlm.nih.gov/pubmed/2497 7712 [Accessed July 2, 2014].

18) David, J. et al., 2014. Gene expression profiling and putative biomarkers of calves 3 months after infection with Mycobacterium avium subspecies paratuberculosis. *Veterinary Immunology and Immunopathology*, 160(1-2), pp.107–117. Available at: http://dx.doi.org/10.1016/j.vetimm..2014. 04. 006.
19) DeMaria, S. & Ngai, J., 2010. The cell biology of smell. *Journal of Cell Biology*, 191(3), pp.443–452.
20) De, S. et al., 2015. Erlotinib protects against LPS-induced Endotoxicity because TLR4 needs EGFR to signal. *Proceedings of the National Academy of Sciences of the United States of America*, 112(31), pp.9680–9685.
21) Dong, X.Y. & Tang, S.Q., 2010. Insulin-induced gene: A new regulator in lipid metabolism. *Peptides*, 31(11), pp.2145–2150. Available at: http://dx.doi.org/10.1016/j.peptides.2010.07.020.
22) Echevarría-Vargas, I.M., et al., 2014. Upregulation of miR-21 in cisplatin resistant ovarian cancer via JNK-1/c-Jun pathway. *PLoS ONE*, 9(5).
23) Egunsola, A.T. et al., 2012. Growth, metastasis, and expression of CCL2 and CCL5 by murine mammary carcinomas are dependent upon Myd88. *Cellular immunology*, 272(2), pp.220–9. Available at: http://www.ncbi. nlm.nih.gov/pubmed/22088941 [Accessed October 29, 2012].
24) Fitzpatrick, F.. & Wheeler, R., 2003. The immunopharmacology of paclitaxel (Taxol®), docetaxel (Taxotere®), and related agents. *International Immunopharmacology*, 3(13-14), pp.1699–1714. Available at: http://linkinghub.elsevier.com/retrieve/pii/S1567576903002078 [Acc essed January 28, 2013].
25) Furlong, F. et al., 2012. Low MAD2 expression levels associate with reduced progression-free survival in patients with high-grade serous epithelial ovarian cancer. *The Journal of pathology*, 226(5), pp.746–55. Available at: http://www.ncbi.nlm.nih.gov/pubmed/22069160 [Accessed February 23, 2013].
26) Guo, Y. et al., (2012). Interleukin-6 signaling pathway in targeted therapy for cancer. *Cancer Treatment Reviews*, *38*(7), 904–10. doi:10.1016/j.ctrv.2012.04.007
27) Hackam, D.J. et al., 2013. Innate immune signaling in the pathogenesis of necrotizing enterocolitis. *Clinical and Developmental Immunology*, 2013.
28) Holcik, M. et al., 2001. XIAP: apoptic brake and promising therapeutic target. *Apoptosis*, 6(613), pp.253–261.
29) Hsu, D. et al., 2010. Toll-like receptor 4 differentially regulates epidermal growth factor-related growth factors in response to intestinal mucosal injury. *Laboratory investigation; a journal of technical methods and pathology*, 90(9), pp.1295–1305. Available at: http://dx.doi. org/10.1038/ labinvest.2010.100.
30) Huang, J.-M. et al., 2014. Atractylenolide-I sensitizes human ovarian cancer cells to paclitaxel by blocking activation of TLR4/MyD88-dependent pathway. *Scientific reports*, 4, p.3840. Available at: http://www.pubmedcentral.nih.gov/articlerender.fcgi?artid=3899591&tool=pmcentrez&rendertype=abstract [Accessed June 1, 2014].
31) Hung, P.-S. et al., 2012. Association between the rs2910164 polymorphism in pre-mir-146a and oral carcinoma progression. *Oral oncology*, 48(5), pp.404–8. Available at: http://www.ncbi. nlm.nih. gov/ pubmed/22182931 [Accessed October 29, 2012].
32) Hurst, D.R. et al., 2009. Breast cancer metastasis suppressor 1 up-regulates miR-146, Which suppresses breast cancer metastasis. *Cancer Research*, 69(4), pp.1279–1283.
33) Iqbal, N. & Iqbal, N., 2014. Human Epidermal Growth Factor Receptor 2 (HER2) in Cancers: Overexpression and Therapeutic Implications.

Molecular Biology International, 2014, pp.1–9. Available at: http://www.hindawi.com/journals/mbi/2014/852748/.

34) Jiang, G. et al., 2005. Prevention of obesity in mice by antisense oligonucleotide inhibitors of stearoyl-CoA desaturase -1. *The Journal of clinical investigation*, 115(4), pp.1030–1038.
35) Kalluri, R. & Weinberg, R.A., 2009. Review series The basics of epithelial-mesenchymal transition. , 119(6).
36) Kaupp, U. B. (2010). Olfactory signalling in vertebrates and insects: differences and commonalities. *Nature Reviews. Neuroscience*, *11*(3), 188–200. doi:10.1038/nrn2789.
37) Kelly, M.G. et al., 2006. TLR-4 signaling promotes tumor growth and paclitaxel chemoresistance in ovarian cancer. *Cancer research*, 66(7), pp.3859–68. Available at: http://www.ncbi.nlm.nih.gov/pubmed/16585214 [Accessed October 22, 2012].
38) Kfoury, A. et al., 2013. MyD88 in DNA repair and cancer cell resistance to genotoxic drugs. *Journal of the National Cancer Institute*, 105(13), pp.937–46. Available at: http://www.ncbi.nlm.nih.gov/pubmed/23766530 [Accessed February 20, 2014].
39) Killeen, S.D. et al., 2006. Exploitation of the Toll-like receptor system in cancer: a doubled-edged sword? *British journal of cancer*, 95(3), pp.247–52. Available at: http://www.pubmedcentral.nih.gov/article render. fcgi? artid=2360630&tool=pmcentrez&rendertype=abstract [Accessed Feb-ruary 3, 2013].
40) Kim, K.H. & Yoon, M.S., 2010. MyD88 expression and anti-apoptotic signals of paclitaxel in epithelial ovarian cancer cells. , 53(4), pp.330–338.
41) Kong, Y.W. et al., 2012. microRNAs in cancer management. *The lancet oncology*, 13(6), pp.e249–58. Available at: http://www.ncbi.nlm.nih.gov /pubmed/22652233 [Accessed October 31, 2012].
42) Krapivner, S. et al., 2007. Human evidence for the involvement of insulin-induced gene 1 in the regulation of plasma glucose concentration. *Diabetologia*, 50(1), pp.94–102.
43) Labbaye, C. & Testa, U., 2012. The emerging role of MIR-146A in the control of hematopoiesis, immune function and cancer. *Journal of Hematology & Oncology*, 5(1), p.13.
44) Laird, M.H.W. et al., 2009. TLR4/MyD88/PI3K interactions regulate TLR4 signaling. *Journal of leukocyte biology*, 85(6), pp.966–77. Available at: http://www.pubmedcentral.nih.gov/articlerender. fcgi?artid =2698589&tool =pmcentrez&rendertype=abstract [Accessed March 18, 2013].
45) Landi, M.T. et al., 2008. Gene expression signature of cigarette smoking and its role in lung adenocarcinoma development and survival. *PloS one*, 3(2), p.e1651. Available at: http://www.pubmedcentral.nih.gov/article render.fcgi?artid=2249927&tool=pmcentrez&rendertype=abstract.
46) Li, F. (2013). Taste perception: From the tongue to the testis. *Molecular Human Reproduction*, *19*(6), 349–360. doi:10.1093/molehr/gat009
47) Li, Y. et al., 2010. miR-146a suppresses invasion of pancreatic cancer cells. *Cancer Research*, 70(4), pp.1486–1495.
48) Liang, B. et al., 2013. Myeloid differentiation factor 88 promotes growth and metastasis of human hepatocellular carcinoma. *Clinical cancer research : an official journal of the American Association for Cancer Research*, 19(11), pp.2905–16. Available at: http://www.ncbi.nlm.nih.gov/ pubmed /23549880 [Accessed February 20, 2014].
49) Liu, G. et al., 2014. Myeloid Differentiation Factor 88 Promotes Cisplatin Chemoresistance in Ovarian Cancer. *Cell biochemistry and biophysics*. Available at: http://www.ncbi.nlm.nih.gov /pubmed/25308861 [Accessed December 2, 2014].

50) Lukaszewicz, M. et al.,. (2007). [Clinical significance of interleukin-6 (IL-6) as a prognostic factor of cancer disease]. *Pol Arch Med Wewn*, *117*(5-6), 247–251. Retrieved from http://www.ncbi.nlm.nih.gov/ entrez/query. fcgi?cmd=Retrieve&db=PubMed&dopt=Citation&list_uids=18030875
51) Ma, J. *et al*., 1998. Abrogated energy-dependent uptake of cisplatin in a cisplatin-resistant subline of the human ovarian cancer cell line IGROV-1. *Cancer Chemotherapy and Pharmacology*, 41(3), pp.186–192.
52) Minning, C. et al., 2014. Exploring breast carcinogenesis through integrative genomics and epigenomics analyses. *International Journal of Oncology*, 45, pp.1959–1968. Available at: http://www.spandidos-publications.com/10.3892/ijo.2014.2625.
53) Pasquinelli, A.E., 2012. MicroRNAs and their targets: recognition, regulation and an emerging reciprocal relationship. *Nature Reviews Genetics*, 13(4), pp.271–282. Available at: http://dx.doi.org/10.1038/nrg 3162.
54) Niu, G., & Chen, X. (2010). Vascular endothelial growth factor as an anti-angiogenic target for cancer therapy. *Current Drug Targets*, *11*(8), 1000–1017. doi:10.2174/138945010791591395
55) Park, E.M. et al., 2014. Farnesyl-diphosphate farnesyltransferase 1 regulates hepatitis C virus propagation. *FEBS Letters*, 588(9), pp.1813–1820. Available at: http://dx.doi.org/10.1016/j.febslet.2014.03.043.
56) Prencipe, M. et al., 2009. Cellular senescence induced by aberrant MAD2 levels impacts on paclitaxel responsiveness in vitro. *British journal of cancer*, 102(11), pp.1900–8. Available at: http://www.pubmedcentral. nih.gov/articlerender.fcgi?artid=2788249&tool=pmcentrez&rendertype=abst ract [Accessed November 10, 2012].
57) Rabinovich, A et al., 2007. Regulation of ovarian carcinoma SKOV-3 cell proliferation and secretion of MMPs by autocrine IL-6. *Anticancer Research*, *27*(1A), 267–72. Retrieved from http://www.ncbi.nlm.nih.gov/ pubmed/17352242
58) Quinn, S.R. & O'Neill, L. a., 2011. A trio of microRNAs that control Toll-like receptor signalling. *International Immunology*, 23(7), pp.421–425.
59) Rajput, S. et al., 2013. TLR4 is a novel determinant of the response to paclitaxel in breast cancer. *Molecular Cancer Therapeutics*, 12(8), pp.1676–87. Available at: http://www.pub medcentral.nih.gov/articlerender.fcgi?artid=3742631&tool=pmcentrez&rend ertype=abstract.
60) Roongta, U. V et al., 2011. Cancer cell dependence on unsaturated fatty acids implicates stearoyl-CoA desaturase as a target for cancer therapy. *Molecular cancer research : MCR*, 9(11), pp.1551–61. Available at: http://www.ncbi.nlm.nih.gov/pubmed/21954435.
61) Sabe, A.A. et al., 2015. Preoperative gene expression may be associated with neurocognitive decline after cardiopulmonary bypass. *Journal of Thoracic and Cardiovascular Surgery*, 149(2), pp.613–623.
62) Santos, C.R. & Schulze, A., 2012. Lipid metabolism in cancer. *The FEBS journal*, 279, pp.2610–2623. Available at: http://dx.doi.org/10.1016/j.bb alip. 2013. 08.001.
63) Schmittgen, T.D. & Livak, K.J., 2008. Analyzing real-time PCR data by the comparative C(T) method. *Nature protocols*, 3(6), pp.1101–1108.
64) Shen, J. et al., 2008. A functional polymorphism in the miR-146a gene and age of familial breast/ovarian cancer diagnosis. *Carcinogenesis*, 29(10), pp.1963–1966.
65) Sheyhidin, I. et al., 2011. Overexpression of TLR3, TLR4, TLR7 and TLR9 in esophageal squamous cell carcinoma. *World journal of gastroenterology : WJG*, 17(32), pp.3745–51. Available at: http://www.

pubmedcentral.nih.gov/articlerender.fcgi?artid=3181461&tool=pmcentrez&rendertype=abstract [Accessed February 3, 2013].
66) Silasi, D.-A. et al., 2006. MyD88 predicts chemoresistance to paclitaxel in epithelial ovarian cancer. *The Yale journal of biology and medicine*, 79(3-4), pp.153–63. Available at: http://www.pubmedcentral.nih. gov/articlerender.fcgi?artid=1994803&tool=pmcentrez&rendertype=abstract.
67) Soares, R. et al., 2000. Expression of TGF-alpha and EGFR in Breast Cancer and its Relation to Angiogenesis. *The breast journal*, 6(3), pp.171–177. Available at: http://www.ncbi.nlm.nih.gov/pubmed/11348360.
68) Stordal, B. *et al*., 2012. Resistance to paclitaxel in a cisplatin-resistant ovarian cancer cell line is mediated by P-glycoprotein. *PLoS ONE*, 7(7).
69) Szajnik, M. et al., 2009. TLR4 signaling induced by lipopolysacharide or paclitaxel regulates tumor survival and chemoresistance in ovarian cancer. *Oncogene*, 28(49), pp.4353–4363. Available at: http://www.pubmedcentral.nih.gov/articlerender.fcgi?artid=2794996&tool=pmcentrez&rendertype=abstract.
70) Szlosarek, P. W. et al., 2006. Expression and regulation of tumor necrosis factor alpha in normal and malignant ovarian epithelium. *Molecular Cancer Therapeutics*, *5*(2), 382–390. doi:10.1158/1535-7163.MCT-05-0303
71) Vathipadiekal, V. et al., 2015. Creation of a Human Secretome: A Novel Composite Library of Human Secreted Proteins: Validation Using Ovarian Cancer Gene Expression Data and a Virtual Secretome Array. *Clinical Cancer Research*, (5), pp.1–11. Available at: http://clincancerres.aacrjournals.org/cgi/doi/
72) 10.1158/1078-0432.CCR-14-3173.
73) Vencken, S.F. et al., 2014. An integrated analysis of the SOX2 microRNA response program in human pluripotent and nullipotent stem cell lines. *BMC Genomics*, 15(1), p.711. Available at: http://www.biomedcentral.com/1471-2164/15/711.
74) Volchenboum, S.L. et al., 2010. HHS Public Access. *Ethnicity & Disease*, 20(1 Supplement), pp.1–26.
75) Volinia, S. et al., 2006. A microRNA expression signature of human solid tumors defines cancer gene targets. *Proceedings of the National Academy of Sciences of the United States of America*, 103(7), pp.2257–2261.
76) Wang, A.C. et al., 2009. Role of TLR4 for paclitaxel chemotherapy in human epithelial ovarian cancer cells. *European journal of clinical investigation*, 39(2), pp.157–64. Available at: http://www.ncbi.nlm.nih. gov/pubmed/19200169 [Accessed January 30, 2013].
77) Wang, A.C. et al., 2014. TLR4 induces tumor growth and inhibits paclitaxel activity in MyD88-positive human ovarian carcinoma in vitro. *Oncology Letters*, 7(3), pp.871–877.
78) Wang, L. et al., 2015. A molecular signature for the prediction of recurrence in colorectal cancer. *Molecular Cancer*, 14(1), pp.1–10. Available at: http://www.molecular-cancer.com/content/14/1/22.
79) Wang, Y et al., 2011. Autocrine production of interleukin-8 confers cisplatin and paclitaxel resistance in ovarian cancer cells. *Cytokine*, *56*(2), 365–375.
80) Weiner-Gorzel, K. et al., 2015. Overexpression of the microRNA miR-433 promotes resistance to paclitaxel through the induction of cellular senescence in ovarian cancer cells. *Cancer Medicine*, p.n/a–n/a. Available at: http://doi.wiley.com/10.1002/cam4.409.
81) Weng, D. et al., 2009. Implication of the Akt2/survivin pathway as a critical target in paclitaxel treatment in human ovarian cancer cells. *Cancer Letters*, *273*(2), 257–65. doi:10.1016/j.canlet.2008.08.027
82) www.phe-culturecollections.org.uk/, 2013. General Cell Collection: SK-OV-3.

83) Umekita, Y. et al., 2000. Co-expression of epidermal growth factor receptor and transforming growth factor-alpha predicts worse prognosis in breast-cancer patients. *International journal of cancer. Journal international du cancer*, 89(6), pp.484–7. Available at: http://www.ncbi. nlm. nih. gov/pubmed/11102891.
84) Xiang, F. et al., 2014. Myd88 expression is associated with paclitaxel resistance in lung cancer A549 cells. *Oncology Reports*, 32(5), pp.1837–1844.
85) Xie, Z., Cao, L. & Zhang, J., 2013. miR-21 modulates paclitaxel sensitivity and hypoxia-inducible factor-1?? expression in human ovarian cancer cells. *Oncology Letters*, 6(3), pp.795–800.
86) Yao, Q. et al., 2013. MicroRNA-146a acts as a metastasis suppressor in gastric cancer by targeting WASF2. *Cancer Letters*, 335(1), pp.219–224. Available at: http://dx.doi.org/10.1016/j.canlet.2013.02.031.
87) Yip, K. W., & Reed, J. C. (2008). Bcl-2 family proteins and cancer, 6398–6406. doi:10.1038/onc.2008.307
88) Yue, C. et al., 2011. Polymorphism of the pre-miR-146a is associated with risk of cervical cancer in a Chinese population. *Gynecologic oncology*, 122(1), pp.33–7. Available at: http://www.ncbi.nlm.nih.gov/pubmed/21529907 [Accessed October 29, 2012].
89) Zeng, Y. et al., 2010. Correlation between pre-miR-146a C/G polymorphism and gastric cancer risk in Chinese population. *World Journal of Gastroenterology*, 16(28), pp.3578–3583.
90) Zhang, J., Lu, Y., & Pienta, K. J. (2010). Multiple roles of chemokine (C-C Motif) ligand 2 in promoting prostate cancer growth. *Journal of the National Cancer Institute*, *102*(8), 522–528. doi:10.1093/jnci/djq044
91) Zhan, Y. et al., 2015. MiRNA-149 modulates chemosensitivity of ovarian cancer A2780 cells to paclitaxel by targeting MyD88. *Journal of Ovarian Research*, 8(1), p.48. Available at: http://www. ovarian research.com/content/8/1/48.
92) Zhang, X. et al., 2014. MicroRNA-146a targets PRKCE to modulate papillary thyroid tumor development. *International Journal of Cancer*, 134(2), pp.257–267.
93) Zhu, Y. et al., 2012. Prognostic significance of MyD88 expression by human epithelial ovarian carcinoma cells. *Journal of translational medicine*, 10(1), p.77. Available at: http://www.pubmedcentral.nih.gov/articlerender.fcgi?artid=3438113&tool=pmcentrez&rendertype=abstract [Accessed October 29, 2012].

Chapter 4

The effect of overexpression of MyD88 in A2780 cells on MAD2

Trinity College Dublin

The University of Dublin

Chapter 4

Overexpression of MyD88 in A2780 cells has no impact on MAD2 expression levels

4.1 Overview

This chapter describes the effect of overexpression of MyD88 in A2780 cells on chemoresponsiveness to paclitaxel, MAD2 and TLR4 gene and protein expression and the expression of the regulatory microRNAs miR-21, miR-146a and miR-433.

4.2 Introduction

In parallel with work performed with SKOV-3 cells in chapter 3, a protocol was established for the introduction of MyD88 gene expression in A2780 cells, using a commercially available MyD88 overexpression plasmid vector. A2780 cells are a chemosensitive cell line derived from a primary ovarian tumour (Behrens *et al.* 1987; Cuello *et al*. 2001) and are defined as MyD88 null (Kelly *et al*. 2006; Szajnik *et al*. 2009). Therefore, it was thought, that by exogenously introducing MyD88 expression in these cells it might restore an active TLR4-MyD88 signalling pathway. By doing this, it was thought that it may render these cells chemoresistant to paclitaxel therapy as had previously been shown by (Kelly *et al*. 2006). Subsequently A2780 cells were transfected with the MyD88 overexpression plasmid, with the aim of examining the effect of increased MyD88 expression on (a) chemoresponsiveness to paclitaxel and also the effect this had on (b) MAD2 expression (c) regulatory microRNA expression. The level of expression of MyD88 in ovarian cancer cell lines had previously been shown to influence their response to paclitaxel, with MyD88 negative cell lines such as the A2780s being more sensitive to paclitaxel therapy than their MyD88 positive counterparts (Kelly *et al*. 2006). Cell lines which express MyD88 appear to have an active TLR4-MyD88 pathway and constitutively express the transcription factor nuclear factor kappa-light-chain-enhancer of activated B cells (NF-κB) and secrete a number of inflammatory chemokines and cytokines. NF-κB activity and cytokine secretion is then

increased upon ligation of TLR4 (Kelly *et al*. 2006; Szajnik *et al*. 2009; Kim & Yoon 2010; Alvero *et al*. 2011; Wang *et al*. 2014). A2780 cells in contrast, do not secrete inflammatory chemokines or cytokines, even upon TLR4 ligation. Previously our group demonstrated that high MyD88 immunohistochemical (IHC) staining intensity was associated with reduced progression free survival (PFS) (p=0.02) and reduced overall survival (OS) (p=0.029) in a high grade serous ovarian cancer cohort (d'Adhemar *et al*. 2014). Furthermore MyD88 was also shown to be a marker of a paclitaxel resistant population of ovarian cancer stem cells (CSCs) (Kelly *et al*. 2006; Alvero *et al*. 2011; Craveiro *et al*. 2013). This population of MyD88 positive CSCs has an active TLR4-MyD88 signalling pathway and are resistant to paclitaxel chemotherapy.

In this current study, it was expected that A2780 cells might become paclitaxel resistant following overexpression of MyD88. Therefore, it was important to ascertain what effect any potential alteration of MyD88 expression and paclitaxel chemoresponiveness may also have on MAD2 and regulatory microRNA expression. Upon initiation of this project, no known relationship was thought to exist between MAD2 and MyD88, both of which had been linked to patient prognosis by our group separately in independent immunohistochemical studies (Furlong *et al*. 2012; d'Adhemar *et al*. 2014). *In-silico* analysis also predicted that there was no direct interaction between MyD88 and MAD2 and no pathway linkages (Chapter 3). Therefore it was expected that overexpression of MyD88 would have no effect on MAD2 expression. Despite this, it was important to definitively establish whether there was any potential relationship between these markers in ovarian cancer. This was important to demonstrate in order to determine whether they act as dependent or independent markers in ovarian cancer.

miR-146a and miR-21 are known to negatively regulate the TLR4-MyD88 pathway (Section 1.7.3) and were examined in A2780 cells following overexpression of MyD88. This was performed in order to determine if they played an important regulatory role in this cell model and perhaps a role in paclitaxel resistance. If chemoresistance could be induced in these cells by overexpression of MyD88, it was thought that miR-146a and miR-21 expression patterns may become altered. miR-146a and miR-21 had previously been shown to be upregulated in a subset of MyD88 negative EOC's and Variable expression of these two regulatory miRNAs was seen between each cell model and their chemoresistant counterparts (Section 1.6). miR-433 was also examined as firstly it is known to target and downregulate MAD2 (Furlong *et al*. 2012). Therefore by analysing its expression, it was thought that it may give insight into any potential *in-vitro* relationship between MAD2 and the TLR4-MyD88 pathway. Secondly

mir-433 was also shown to induce paclitaxel resistance in A2780 cells through the induction of senescence (Furlong *et al*. 2012; Weiner-Gorzel *et al*. 2015). Therefore it was important to determine if its expression was altered during MyD88 mediated paclitaxel resistance, to further evaluate any potential link between the TLR4-MyD88 and MAD2 mediated paclitaxel resistance mechanisms.

4.2.1 Hypothesis

Overexpression of MyD88 may render A2780 cells paclitaxel resistant and impact on the expression levels of MAD2 and the expression of the regulatory microRNAs miR-21, miR-146a and miR-433.

4.2.2 Aims

1) To assess the impact of overexpression of MyD88 on MAD2 expression.
2) To assess the impact of overexpression of MyD88 on paclitaxel sensitivity.
3) To investigate the effect of overexpression of MyD88 on the expression of the regulatory microRNAs miR-146a, miR-21 and miR-433.

.

4.3 Methods

4.3.1 MyD88 transfections

A2780 cells were cultured as described in (Section 2.1). MyD88 transfections were carried out in 24 well plates for RNA extraction and 6 well plate formats for flow cytometry, drug selection experiments and western blot analyses as described in (Section 2.3). A2780 cells were transfected with a MyD88 overexpression plasmid (MyD88 OE), the -TIR negative control plasmid (-TIR) or the empty vector negative control plasmid (eV Control), see (Section 2.3) for details about each plasmid. Cell lines were routinely checked for mycoplasma and were mycoplasma-free (Section 2.2)

4.3.2 RNA extraction and TaqMan RT-PCR

Total RNA was isolated using the mirVana™ miRNA Isolation Kit and TaqMan RT-PCR was performed as described (Section 2.5) using commercially available primers and probe sets for miR-146a, miR-21, miR-433, MyD88, TLR4, MAD2, GAPDH (mRNA endogenous control) and miR-16 (microRNA endogenous controls). Gene expression and microRNA expression levels following transfection were calculated using the ΔΔCT method (Schmittgen & Livak 2008), relative to the GAPDH or miR-16 endogenous controls respectively. A significant change in expression was considered to be present if at least a 2-fold change (above 200% expression or below 50% expression) in mRNA or microRNA expression was observed, with a p value of <0.05 compared to untreated cells and/or negative control cells.

4.3.3 Western blot analysis

Protein was isolated following overexpression of MyD88 in A2780 cells as described in (Section 2.6). Western blot analysis was then performed with antibodies directed against MyD88 (1:1000, D80F5, Cell Signalling), TLR4 (1:100, Ab47093, Abcam), MAD2 (1: 1000, 610679, BD Biosciences) and GAPDH (1:10,000, Ab9485, Abcam). Chemiluminescence images were developed using a Fujifilm LAS-4000 luminescent image analyser and densitometry was then carried out using Quantity One software (Biorad) as described (Section 2.6).

4.3.4 Drug treatment and assessment of cell viability using the CCK-8 Assay

A2780 cells were transfected for 48 hours and then were either left untreated, treated with 0.003% DMSO (vehicle control) or with 0.5μM or 1μM of paclitaxel for a further 48 hours. Cell viability was then assessed using the cell cycle kit 8 (CCK-8) assay 48 hours post treatment with paclitaxel. Absorbance values were read at 450nm using the

Sunrise™ microplate reader (Tecan Trading AG, Switzerland). Cell viability for each condition/drug treatment was calculated as a % of non-transfected cells which were left untreated.

4.3.5 Statistical analysis

A student's t-test was performed on RT-PCR results and cell viability data to assess statistical significance of gene silencing experiments and differences in cell viability between drug treated versus untreated and vehicle control groups. A statistically significant difference was considered to be present at $p \leq 0.05$. Statistical analysis was performed using Microsoft excel 2010.

4.3.6 FITC-Annexin V apoptosis assay

The FITC-Annexin V Apoptosis detection kit 1 (Sigma Aldrich) was used to assess any potential toxic effects of the transfection procedures on A2780 cells **(Figure 4.1)**. For this flow cytometry assay, cells were first resuspended in the supplied cell binding buffer and then incubated with a FITC fluorophore conjugated to Annexin V (a phosphatidylserine binding protein) and then incubated with the DNA intercalating dye PI (Propidium Iodide). Following incubation with each of these dyes, the cells were passed through a 0.2µm filter to exclude doublets and analysed using the CyAn™ ADP Analyser (Beckman Coulter). Flow cytometry data was analysed by Summit 4.2 software (Dako Colorado, Inc., Fort Collins, CO, USA).

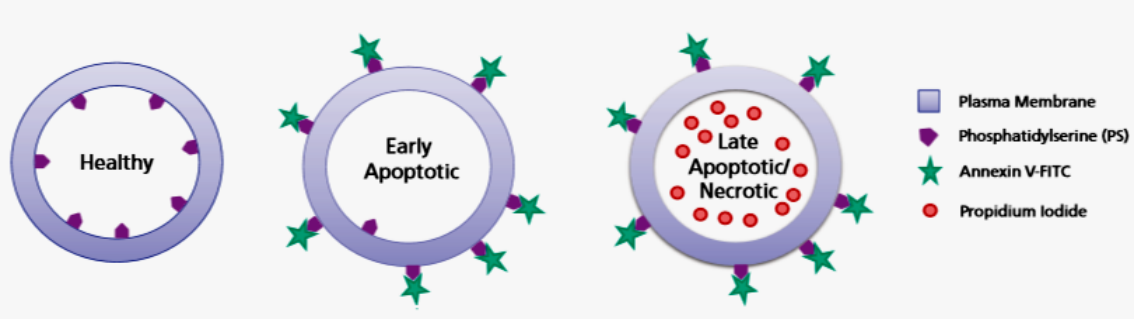

Figure 4.1 An overview of the principle utilised in the FITC Annexin V apoptosis kit. The FITC Annexin V apoptosis kits uses Annexin V, a phospholipid binding protein conjugated with a FITC fluorophore to detect the presence of cells in early apoptosis in combination with propidium iodide (PI) a cell viability dye to detect cells in late apoptosis/necrosis. Cells in late apoptosis which do not have an intact cell membrane will not be able to exclude propidium iodide, however healthy cells will. In summary viable cells will exclude both dyes, early apoptotic cells will stain with Annexin V-FITC and late apoptotic/necrotic cells will stain with both Annexin V-FITC and PI.

4.4 Results

4.4.1 Optimisation of A2780 MyD88 transfection protocol

Initially MyD88 transfections were performed as per the manufacturer's instructions. However use of this protocol resulted in visual signs of toxicity to A2780 cells, despite having been used successfully previously (Furlong *et al*. 2012). The transfection protocol was subsequently shown to induce high levels of apoptosis in A2780 cells following transfection using a flow cytometry assay the FITC Annexin V Apoptosis Detection Kit I (BD Bioscience) **(Figure 4.2)**. A2780 cells were transfected with lipofectamine 2000, the MyD88 overexpression plasmid and the -TIR negative control plasmid, see (Section 2.3) for details about each plasmid. Apoptosis rates were measured using the FITC Annexin V Apoptosis Detection Kit I (BD Bioscience) at both 24 and 48 hours following transfection on the CyAn™ ADP Analyzer (Beckman Coulter). Depending on whether cells stained with FITC annexin and/or PI cells were classified as being viable ($FITC^{neg}$, PI^{neg}), in early apoptosis ($FITC^{pos}$, PI^{neg}), in late apoptosis/necrosis ($FITC^{pos}$, PI^{pos}), or dead ($FITC^{neg}$, PI^{pos}). At 24 hours, cells transfected with lipofectamine 2000 and either the -TIR negative control plasmid or the MyD88 overexpression plasmid displayed a reduction in cell viability of 23.4% and 30.5% respectively, with 11.8% and 13.9% of cells in early apoptosis, 9.1% and 14.4% of cells in late apoptosis and 2.5% and 2.2% were dead respectively. At 48 hours, cells transfected with the -TIR negative control or MyD88 overexpression plasmid exhibited a reduction in cell viability of 46.3% and 31.1% respectively, with 9.1% and 4.1% of cells in early apoptosis and 31.3% and 21.2% of cells in late apoptosis and 5.9% and 5.8% were dead respectively. The results demonstrate the effect this transfection protocol had on cell viability, therefore future experiments focused on optimising the transfection protocol and reducing the toxic effect.

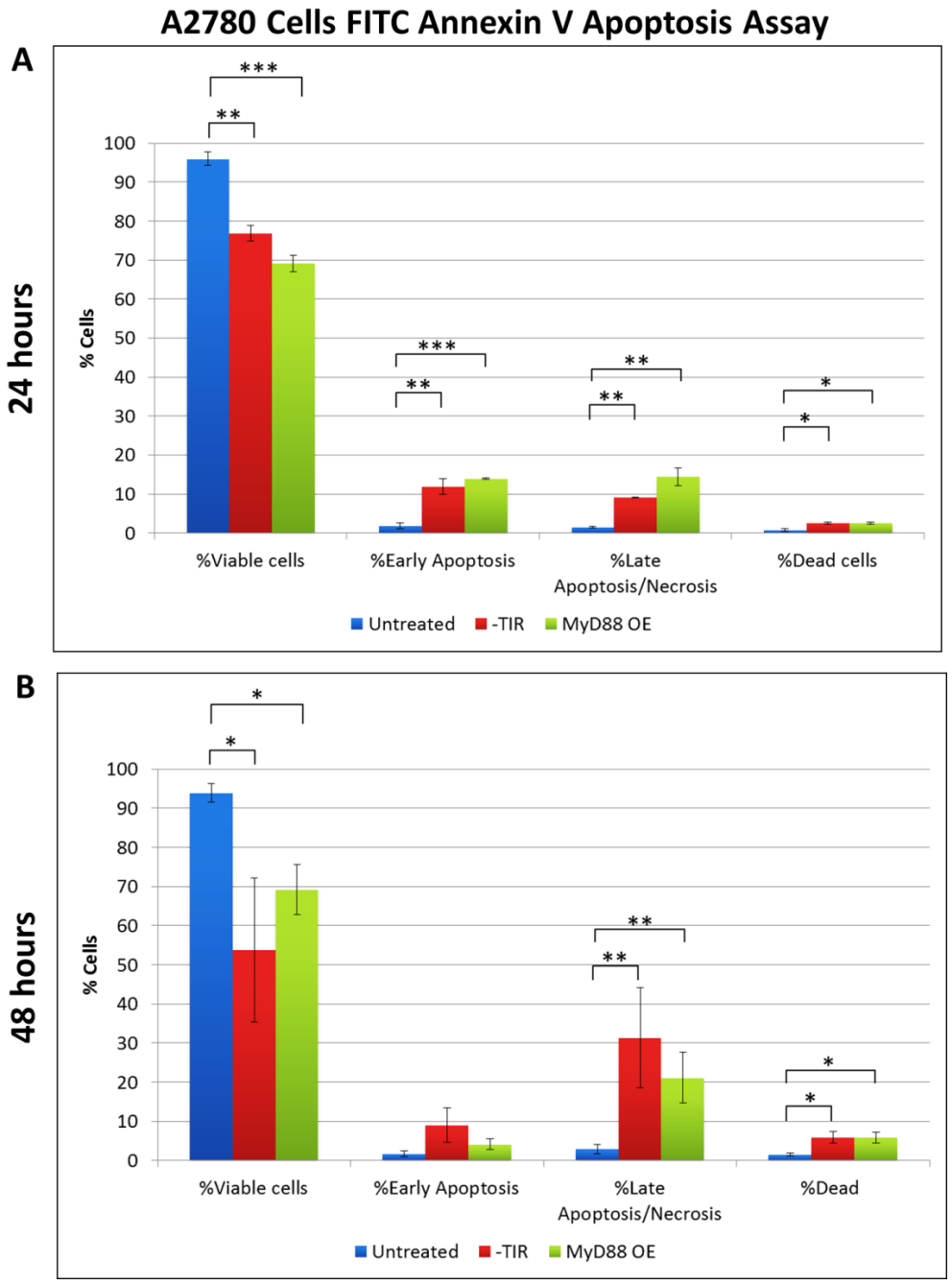

Figure 4.2 Apoptosis rates in A2780 cells at 24 hours (A) and 48 hours (B) as determined using the FITC Annexin V Apoptosis Detection Kit I. A2780 cells were transfected with lipofectamine 2000 and either the MyD88 overexpression plasmid (MyD88 OE) or a mutated negative control plasmid (-TIR) or were left untreated for 24 or 48 hours. After 24 and 48 hours, apoptosis rates were assessed by flow cytometry using the FITC Annexin V Apoptosis Detection Kit I (BD Bioscience) on the CyAn™ ADP Analyzer (Beckman Coulter). Depending on whether cells stained with FITC annexin and/or PI, cells were classified as being viable ($FITC^{neg}$, PI^{neg}), in early apoptosis ($FITC^{pos}$, PI^{neg}), in late apoptosis/necrosis ($FITC^{pos}$, PI^{pos}), or dead ($FITC^{neg}$, PI^{pos}). The percentage of cells under each transfection condition at each stage of cell death is represented on the y axis. The results demonstrate that the transfection protocol was severely toxic to A2780 cells. Results are expressed as mean +/-SD, n=3; *p<0.05, **p<0.01, ***p<0.001 (Student's t-test).

Cell toxicity as a result of the transfection protocol was resolved by switching to an alternative transfection reagent lipofectamine RNAiMAX, where previously lipofectamine 2000 had been used. A new commercially available, empty vector negative control plasmid pDEST 26, became available and was purchased from Invitrogen and used in subsequent experiments. This new negative control plasmid was assessed in parallel with the –TIR negative control and found to visually result in less toxicity using the same protocol. Therefore, the new empty vector negative control plasmid was taken forward as a negative control for future experiments, while the –TIR negative control plasmid was discarded. Lipofectamine RNAiMAX initially, similar to lipofectamine 2000 also resulted in a visual reduction in cell viability, but not as substantially as lipofectamine 2000 using the recommended protocol from the manufacturer. Therefore, the amount of lipofectamine and the amount of plasmid DNA used was optimised. A2780 cells were transfected with two concentrations of lipofectamine RNAiMAX (0.5µl, 1µl) and a range of concentrations of plasmid DNA (10-600ng) in order to determine a suitable transfection protocol which had no toxic effect on cells and gave significant overexpression of MyD88 gene expression **(Figure 4.3)**. When 1µl of lipofectamine RNAiMAX was used in each well of a 24 well plate, a small reduction in cell viability was observed, while all concentrations of plasmid DNA gave significant overexpression of MyD88 as determined by RT-PCR **(Figure 4.3)**. From the optimisation experiment, 0.5µl of lipofectamine RNAiMAX and 600ng of plasmid DNA were selected for future 24 well transfection experiments. This combination was selected as the concentration of lipofectamine used seemed to impact on cell viability rather than the amount of plasmid DNA used. Therefore it was decided to use the same amount of plasmid DNA that had been recommended by the manufacturer.

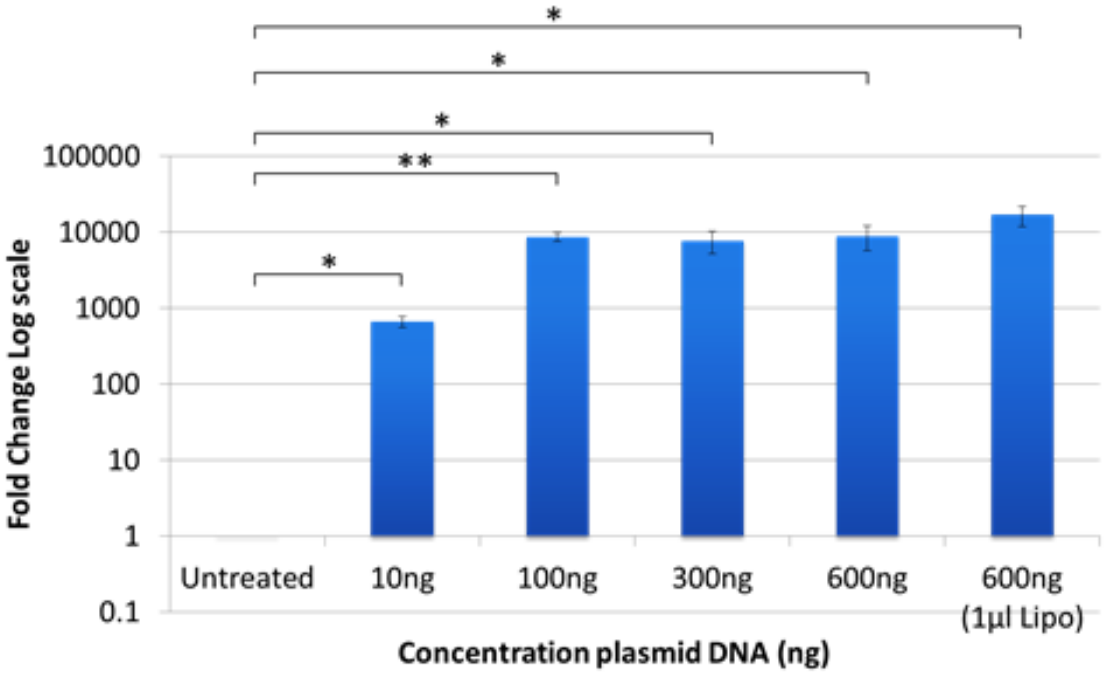

Figure 4.3 Assessment of A2780 MyD88 gene expression following transfection with different concentration of plasmid DNA and lipofectamine RNAiMAX. A2780 cells were transfected for 24 hours in a 24 well plate with various concentrations of the MyD88 overexpression plasmid (10ng, 100ng, 300ng, 600ng). All were transfected with 0.5µl of lipofectamine RNAiMAX apart from the sample labelled 600ng (1µl Lipo), which was transfected with 1µl of lipofectamine RNAiMAX. Following transfection RNA was isolated using the mirVana™ miRNA Isolation Kit and MyD88 expression levels were measured using TaqMan RT-PCR. MyD88 expression levels were normalised to the endogenous control GAPDH, and calibrated to that of untreated cells to establish the relative change in gene expression. Results are expressed in fold change as mean +/-SD, n=3; *p<0.05, **p<0.01 (Student's t-test).

Once this new protocol was established, its effect on cell viability was assessed using the CCK-8 assay. A2780 cells were transfected with the MyD88 overexpression plasmid, the empty vector negative control plasmid or were left untreated for 24 hours. Cells were transfected in 24 well plates with 0.5µl of lipofectamine RNAiMAX and 600ng of plasmid DNA. A2780 cells were transfected for 24 hours and then cell viability was assessed using the CCK-8 assay. When A2780 cells were transfected for 24 hours in a 24 well plate with 0.5µl of lipofectamine RNAiMAX and 600ng of plasmid DNA, no loss in cell viability was observed using the CCK-8 assay **(Figure 4.4)**, where previously even visually at 24 hours a reduction in cell viability would have been observed.

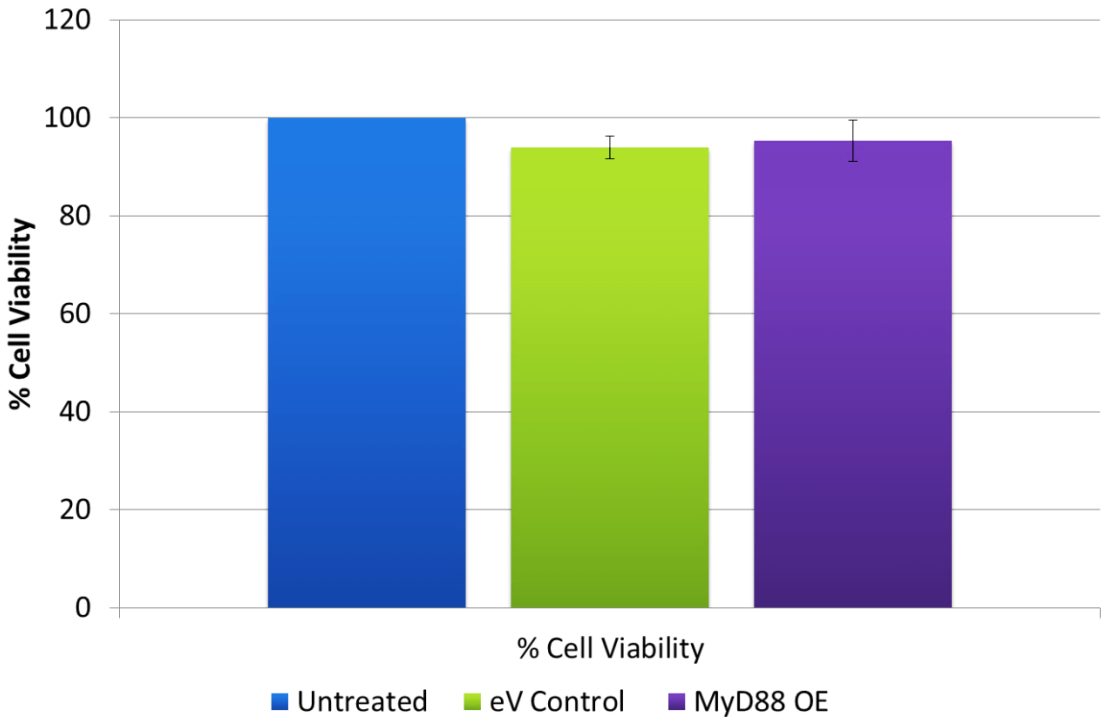

Figure 4.4 A2780 cell viability as assessed by the CCK-8 Assay at 24 hours with new optimised transfection protocols. The CCK-8 assay was used to assess cell viability in A2780 cells following transfection for 24 hours with new optimised transfection protocols. Absorbance at 450nm was then measured using the using the Sunrise™ microplate reader (Tecan Trading AG, Switzerland). The results demonstrate that overexpression of MyD88 using optimised transfection protocols has no impact on A2780 cell viability. Cell viability for each condition was calculated as a % of the untreated A2780 cells. Results are expressed as mean +/-SD, n=3.

4.4.2 Overexpression of MyD88 has no impact on MAD2 expression or its regulatory microRNA miR-433

Following optimisation of the A2780 transfection protocol, A2780 cells were transfected with the MyD88 overexpression plasmid, the empty vector negative control plasmid, or were left untreated, for 24, 48, 72 and 144 hours. Following transfection RNA was isolated using the mirVana™ miRNA Isolation Kit and MyD88, TLR4 and MAD2 expression levels were measured using TaqMan RT-PCR. MyD88 expression levels were normalised to the endogenous control GAPDH, and calibrated to that of untreated cells to establish the relative change in gene expression **(Figure 4.5)**. The MyD88 overexpression was assessed at multiple timepoints to determine whether MyD88 would continue to be overexpressed over the timecourse of future drug experiments and to determine if overexpression at any time point might have an impact on MAD2 expression levels. The level of overexpression varied at each timepoint depended on the transfection efficiency and was substantially lower but still overexpressed at 144 hours, suggesting that the MyD88 overexpression is beginning to diminish at this point. At 72 hours, the negative control plasmid exhibited significant upregulation of MyD88 compared to untreated cells however this phenomenon was not consistently observed throughout all timepoints and is likely due to the low expression levels of MyD88 in A2780 cells which are detected at low cycle thresholds (Cts), ~35Cts. This does not represent a true change in MyD88 expression; see 72 hour western blot **(Figure 4.6C)**. In summary successful overexpression was confirmed at all timepoints and this had no effect on MAD2 or TLR4 expression levels.

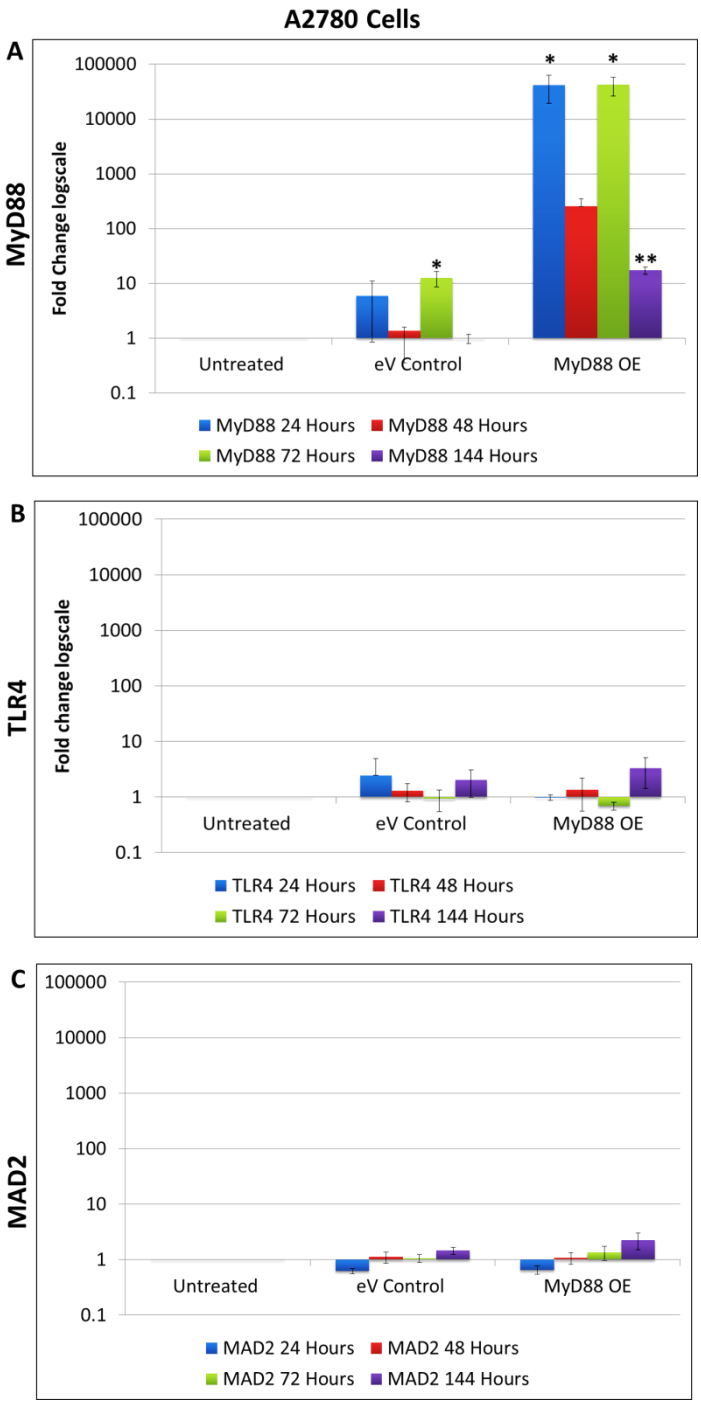

Figure 4.5 Analysis of A2780 MyD88, TLR4 and MAD2 gene expression following overexpression of MyD88 for 24, 48, 72 and 144 hours. A2780 cells were transfected with a MyD88 overexpression plasmid (MyD88 OE), a negative control empty vector plasmid (eV Control) or were left untreated for 24, 48, 72 and 144 hours. Following overexpression MyD88 (A) TLR4 (B) and MAD2 (C) gene expression was assessed using TaqMan RT-PCR. MyD88, TLR4 and MAD2 gene expression levels were normalised to the endogenous control GAPDH and calibrated to that of untreated cells. The results demonstrate that overexpression of MyD88 has no impact on MAD2 gene expression. Results are expressed in fold change as mean +/-SD, n=3; *p<0.05 (Student's t-test).

Following confirmation of MyD88 overexpression and evaluation of its effect on MAD2 and TLR4 at the gene level, overexpression of MyD88 and its effect on MAD2 and TLR4 protein expression was examined. Following overexpression of MyD88 for 24, 48, 72 and 96 hours, protein was harvested and then western blot analysis was performed. Western blot analysis was performed for MyD88 and GAPDH at 24 hours **(Figure 4.6A)** and for MyD88, TLR4, MAD2 and GAPDH at 48, 72 and 96 hours **(Figure 4.6B-D)**. Following western blot analysis, differences in band sizes were quantified using densitometry. At all timepoints 24-96 hours, MyD88 was found to be successfully overexpressed in all samples transfected with the MyD88 overexpression plasmid. Overexpression of MyD88 did not affect MAD2 or TLR4 protein expression at any of the timepoints analysed. This demonstrated the specificity of the overexpression of MyD88 as did not impact on TLR4 expression levels. It also demonstrates that MyD88 does not influence the expression of MAD2.

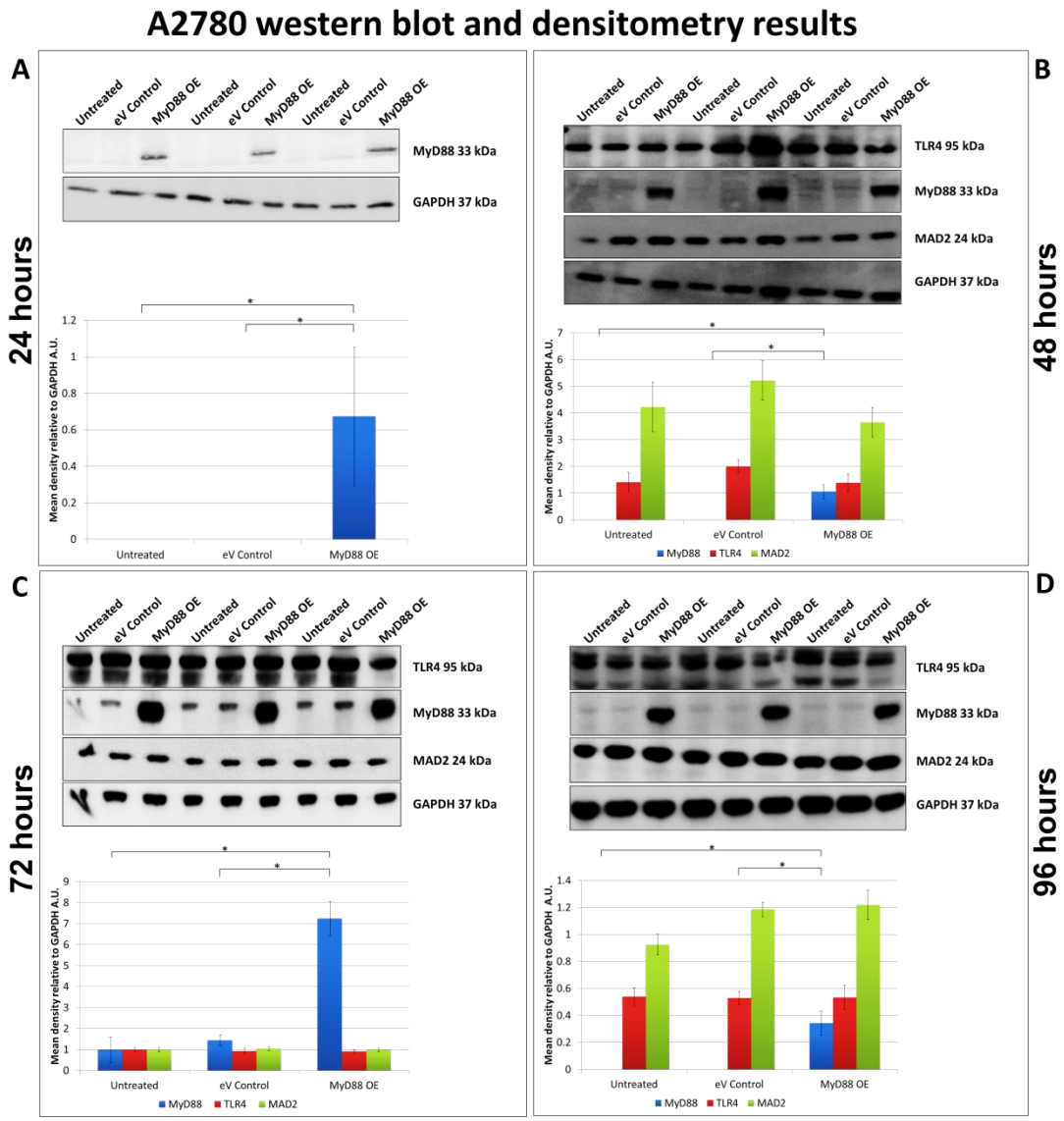

Figure 4.6 A2780 western blot and densitometry results 24 48, 72 and 96 hours following transfection with a MyD88 overexpression plasmid. A2780 cells were transfected with a MyD88 overexpression plasmid (MyD88 OE), a negative control empty vector plasmid (eV Control) or were left untreated for 24(A), 48 (B), 72 (C), and 96 hours (D). After 24, 48, 72 and 96 hours, protein was harvested using RIPA lysis buffer and western blot analysis at 24 hours for MyD88 and GAPDH and at 48, 72 and 96 hours western blot analysis was performed for MAD2, MyD88, TLR4 and GAPDH. Chemiluminescence images were developed using a Fujifilm LAS-4000 luminescent image analyser and densitometry was then carried out using Quantity One software (Biorad) (A-D). Protein expression is represented as the mean density ratio normalised to GAPDH in arbitrary units (A.U.) for each condition. The results demonstrate that overexpression of MyD88 has no impact on MAD2 protein expression. Results are expressed as mean +/-SD, n=3; *p<0.05, **p<0.01 (Student's t-test).

miR-433 directly targets and downregulates MAD2 (Furlong *et al*. 2012). Overexpression of miR-433 has been shown to induce paclitaxel resistance in A2780 cells. Therefore it was hypothesised that if overexpression of MyD88 in A2780 could induce chemoresistance and impacted upon the expression levels of miR-433 it could represent a partial overlap in their paclitaxel resistance mechanisms and demonstrate a link between MAD2 and MyD88. miR-433 expression was analysed in A2780 cells following overexpression of MyD88 at 24, 48 and 72 hours. Due to low expression levels of miR-433, which was detected between 35-43 Cts, miR-433 expression levels are represented by the Delta Ct values for each condition **(Figure 4.7)**. The Delta Ct values for miR-433 were calculated by normalising to the endogenous control miR-16. No differences in miR-433 expression were observed at 24, 48 or 72 hours following overexpression of MyD88. This again gives further evidence to suggest that there is no *in-vitro* relationship between MyD88 and MAD2.

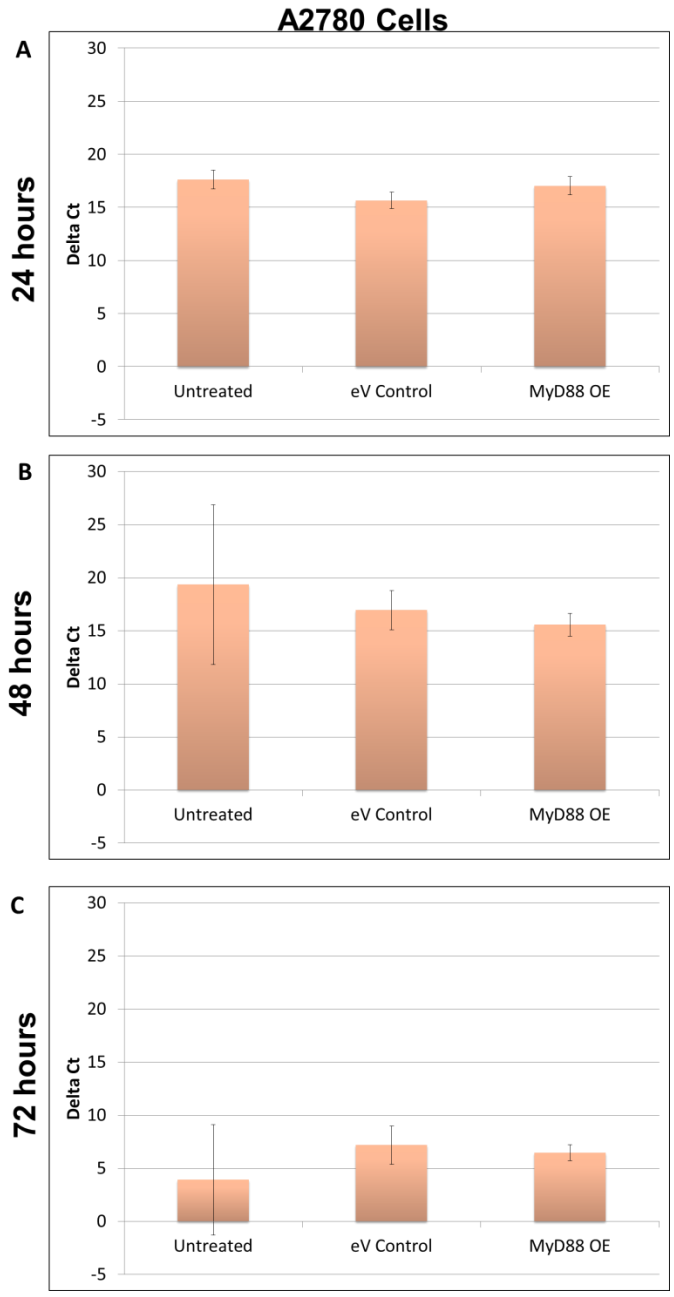

Figure 4.7 A2780 miR-433 expression 24, 48 and 72 hours after transfection with a MyD88 overexpression plasmid. Following over-expression of MyD88 at 24 (A), 48 (B) and 72 hours (C) in A2780 cells, miR-433 expression levels were measured using TaqMan RT-PCR. The Delta Ct values under each condition are displayed on the y axis of each graph n=3, +/-SD. No significant change in the levels of miR-433 was observed at any of the timepoints analysed.

4.4.3 Overexpression of MyD88 has no impact on the expression of the TLR4-MyD88 pathway regulatory microRNAs miR-146a and miR-21

miR-21 and miR-146a are known to target various downstream components of the TLR4-MyD88 pathway and are also capable of directly targeting TLR4 and MyD88 (Quinn & O'Neill 2011; Yang *et al*. 2011; Zhao *et al*. 2012; Lario *et al*. 2012; Chen *et al*. 2013). Therefore miR-21 and miR-146a were examined following overexpression of MyD88 as it was hypothesised that overexpression of MyD88 may impact on their expression levels. This in turn may also suggest a potential role for these microRNAs in paclitaxel chemoresistance. Therefore miR-21 and miR-146a expression was analysed in A2780 cells following overexpression of MyD88 at 24, 48 and 72 hours **(Figure 4.8)**. No differences in the expression levels of miR-21 and miR-146 were observed at any of the three timepoints. These results therefore suggest that MyD88 expression does not influence the expression of these two regulatory microRNAs in the A2780 model.

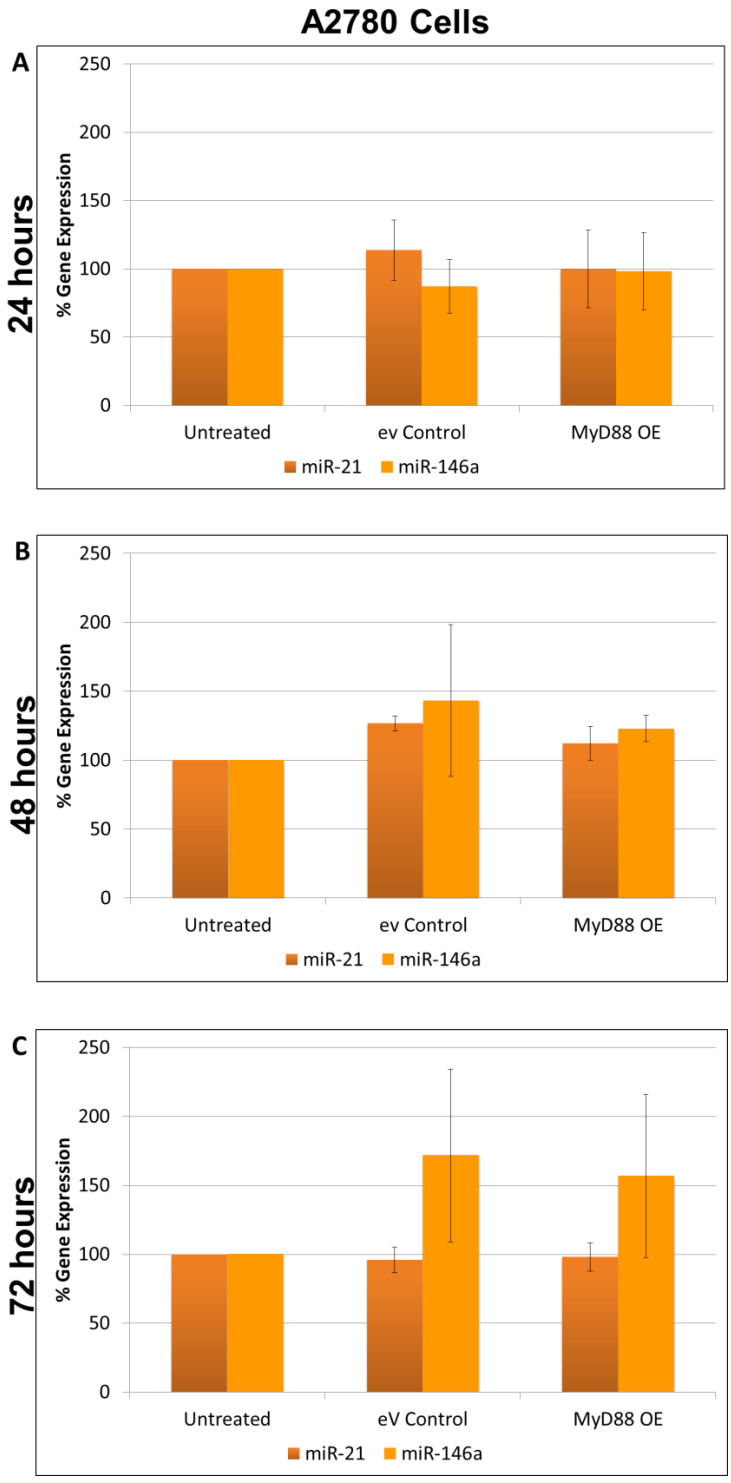

Figure 4.8 A2780 miR-146a and miR-21 expression 24, 48 and 72 hours after transfection with a MyD88 overexpression plasmid. Following over-expression of MyD88 at 24 (A), 48 (B) and 72 hours (C) in A2780 cells, miR-146a and miR-21 expression was assessed using TaqMan RT-PCR. miR-146a and miR-21 expression levels were normalised to the endogenous control miR-16 and calibrated to that of untreated cells (% Gene Expression). No significant change in the levels of miR-146a and miR-21 was observed at any of the timepoints analysed.

4.4.4 Assessment of A2780 chemoresponse to paclitaxel

Following optimisation of the MyD88 transfection protocol and confirmation of successful MyD88 overexpression at the gene and protein level, the chemoresponsiveness of untransfected A2780 cells to paclitaxel was assessed prior to drug treatment experiments with transfected cells. Fifteen thousand A2780 cells were seeded into each well of a 96 well plate in quintuplicate (n=5) and allowed to adhere overnight. After 24 hours, cells were treated with various concentrations of paclitaxel ranging from 4nM-4μM **(Figure 4.9)**. When A2780 cells were treated with, 0.004μM, 0.01μM, 0.05μM, 0.1μM, 0.2μM, 0.5μM, 1μM, 2μM, 3μM or 4μM, a 4.1%,6%, 2.3%, 4.9%, 5.2%, 20.8%, 55.8%, 63.2%, 62.4% and 63% reduction in cell viability was observed respectively. As a significant amount of cell loss was observed using 0.5μM or above, it was decided to treat cells with 0.5μM or 1μM paclitaxel in future drug treatment experiments.

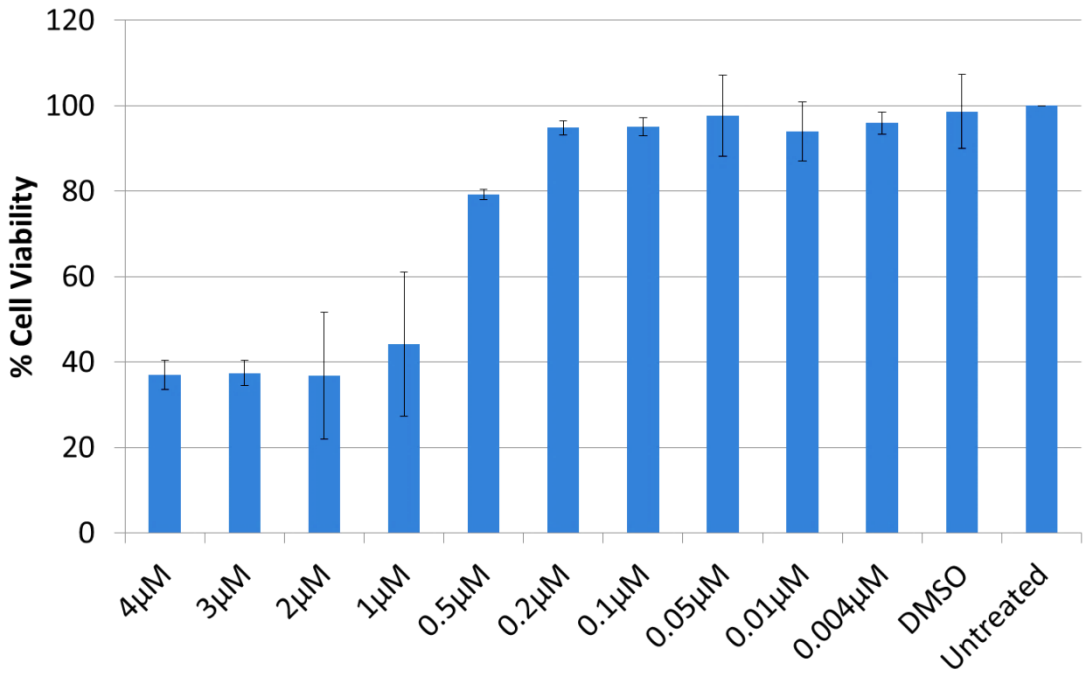

Figure 4.9 Assessment of A2780 paclitaxel chemoresponsiveness using the CCK-8 assay. A2780 cells were seeded into multiple wells of a 96 well plate. After 24 hours cells were either left untreated, incubated with DMSO or treated with various concentration of paclitaxel (0.004μM -4μM) and incubated for a further 48 hours. After the 48 hour incubation, cell viability was measured using the CCK-8 assay. % cell viability for each condition was then calculated as % of the untreated A2780 cells. Results are expressed as mean +/-SD, n=5.

Following assessment of paclitaxel chemoresponsiveness in untransfected A2780 cells, their response to paclitaxel treatment following overexpression of MyD88 was assessed. A2780 cells were transfected with the MyD88 overexpression vector or were left untreated for 24 hours. After 24 hours, cells were removed from 6 well plates and 15,000 A2780 cells which were left untreated, transfected with negative empty vector control plasmid or transfected with the MyD88 overexpression vector were then seeded into multiple wells of 96 well plates. Cells were allowed to adhere for 24 hours and then were either left untreated, treated with the DMSO control or treated with 0.5µM or 1µM paclitaxel and then cell viability was assessed using the CCK-8 assay **(Figure 4.10)**. Untransfected A2780 cells which were left untreated had a 21.3% and 21.6% reduction in cell viability compared to cells transfected the eV control (eV control) or the MyD88 overexpression plasmid (MyD88 OE) which were left untreated respectively, this was significant but was due to the presence of a single outlier. The eV control should be considered the true comparator and no significant difference in cell viability was observed between cells transfected with the eV control and the MyD88 overexpression plasmid vectors. No significant difference was observed between untreated cells, cells transfected with the eV control (eV control) or the MyD88 overexpression plasmid (MyD88 OE) which were treated with DMSO. Following treatment with 0.5µM paclitaxel a 38%, 42.8% and 39.1% reduction in cell viability was observed in untreated A2780 cells, cells transfected with the eV control and cells transfected with the MyD88 overexpression plasmid respectively. Following treatment with 1µM paclitaxel a 36.3%, 40.2% and 39.4% reduction in cell viability was observed in untreated A2780 cells, cells transfected with the eV control and cells transfected with the MyD88 overexpression plasmid respectively. Overall the results demonstrated no significant difference in cell viability between cells treated the MyD88 overexpression plasmid, cells transfected with the empty vector control or untreated cells when treated with paclitaxel demonstrating that overexpression of MyD88 did not induce chemoresistance in A2780 cells.

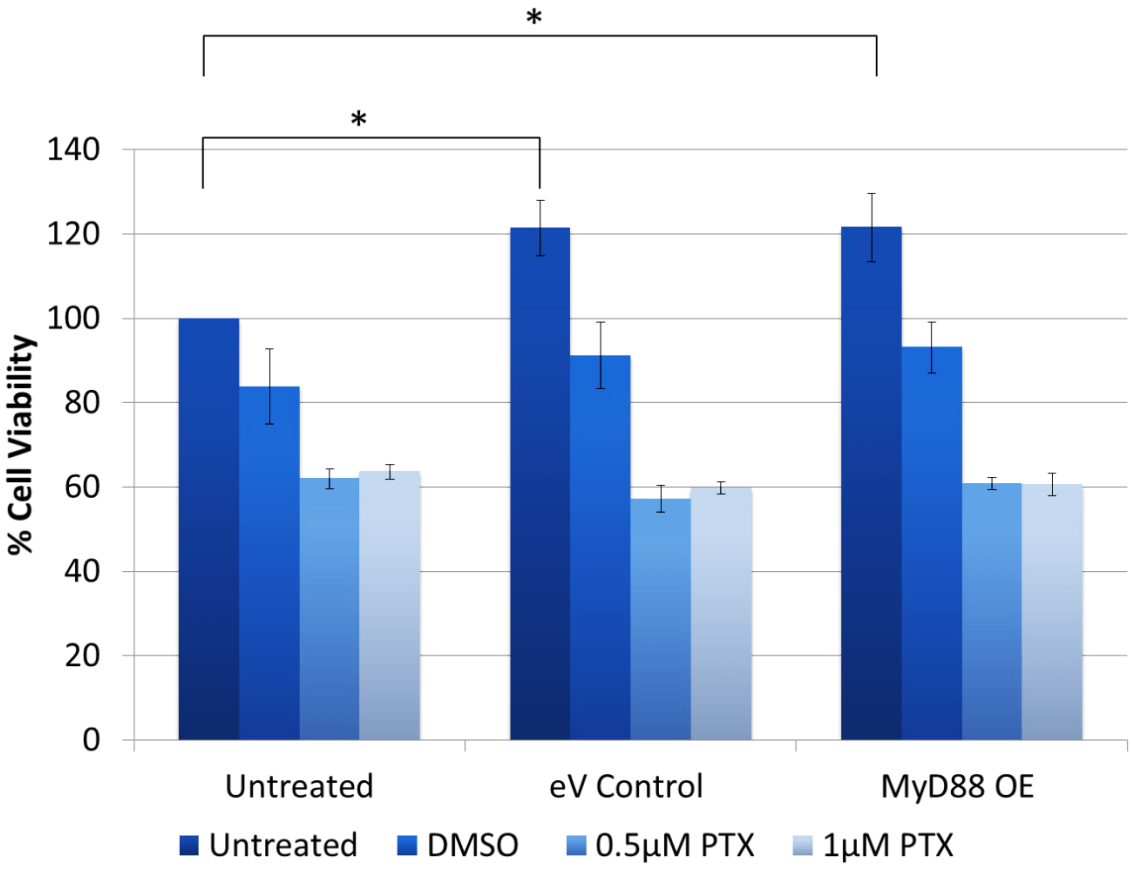

Figure 4.10 Assessment of A2780 chemoresponsiveness to paclitaxel following overexpression of MyD88. A2780 cells were transfected into 6 well plates with a MyD88 overexpression plasmid (MyD88 OE), a negative control empty vector plasmid (eV Control) or were left untreated. After 24 hours, 15,000 cells were reseeded into new wells of a 96 well plate and cells were incubated for a further 24 hours. At 48 hours, cells were either left untreated, incubated with DMSO or treated with either 0.5µM or 1µM of paclitaxel (PTX) and incubated for a further 48 hours. At 96 hours, cell viability was assessed using the CCK-8 assay. % cell viability for each condition was then calculated as % of the non-transfected A2780 cells which were left untreated. The results demonstrate that overexpression of MyD88 does not render A2780 cells resistant to paclitaxel therapy. Results are expressed as mean +/-SD, n=3.

4.5 Discussion

MyD88 is an adaptor protein involved in toll-like receptor signalling and high IHC staining intensity of this marker has previously been associated with reduced progression free survival (PFS) and reduced overall survival (OS) in high grade serous ovarian cancer by our group (d'Adhemar *et al*. 2014) and others (Silasi *et al*. 2006; Kim *et al*. 2012; Zhu *et al*. 2012) MyD88 has also been shown to be a marker for a population of paclitaxel resistant ovarian CSCs (Alvero *et al*. 2011). Furthermore these MyD88 positive CSCs and cancer cell lines which express MyD88 appear to have an active TLR4-MyD88 signalling pathway and produce various inflammatory chemokines and cytokines which render them resistant to paclitaxel based chemotherapy (Alvero *et al*. 2011). Therefore, it was thought that if, a functioning TLR4-MyD88 pathway could be induced in the A2780 cells, it may render them resistant to paclitaxel therapy.

In this study, successful overexpression of MyD88 in the A2780 cells was achieved. However, overexpression of MyD88 did not render A2780 cells chemoresistance to paclitaxel. Upon initiation of this project, it was expected that by overexpressing MyD88 in A2780 cells would render these cells chemoresistant as was shown previously by (Kelly *et al*. 2006). This would have definitively demonstrated the role of the TLR4-MyD88 pathway in chemoresistance. It was expected that by demonstrating this, it would have allowed further exploration of both the TLR4-MyD88 and MAD2 mediated paclitaxel resistance mechanisms in a single cell model. Knockdown of MAD2 had previously been shown to induce paclitaxel resistance in the A2780 cells (Furlong *et al*. 2012). In this study in contrast to what was observed in a study by (Kelly *et al* 2006), overexpression of MyD88 did not induce chemoresistance. However, there are a number of possible reasons why chemoresistance was not achieved in this study and was demonstrated by (Kelly *et al* 2006). Even when same experiments are performed between labs, different outcomes may arise due to intrinsic properties and differences between the same cell lines. Studies of the same cell lines by different laboratories are common in the literature and often show different results with the same methodology. Assay outcomes are easily influenced by many factors including changes in functionality, morphology, doubling time of cells, passage numbers, microbial contamination, and misidentification of cells (Reid 2011).

There were also a number of differences between the experimental protocol used in this study and the study by (Kelly *et al* 2006). In the Kelly *et al* (2006) study a higher dose of paclitaxel, was used compared to this study, 2µM and cells which were 50% confluent were used. Although a high level of MyD88 expression was achieved using

the MyD88 overexpression plasmid, transfection efficiency was never examined in this study. Perhaps the percentage uptake by cells of the MyD88 overexpression plasmid may have impacted on their response to paclitaxel therapy. The use of antibiotic selection to ensure 100% uptake by cells may provide similar results to those observed by (Kelly *et al* 2006). Also the A2780 cells in our study were first plated in 6 well plates and transfected for 24 hours before 15,000 cells were reseeded into 96 well plates for drug selection, therefore transfection efficiency of these 15,000 cells may have had a major influence on the results that were obtained. Furthermore, an entirely different MyD88 overexpression plasmid vector was used to induce high levels of MyD88 expression in these cells. The protocol for use with this MyD88 overexpression plasmid was initially toxic to cells. Although toxicity issues were resolved following protocol optimisation, perhaps the transfection itself still induces a small amount of stress on the cells. This effect may then be amplified by the addition of paclitaxel, masking the true results of the experiment. Therefore using a different MyD88 overexpression plasmid or another method of overexpressing MyD88 such as a lentiviral approach may yield similar results to the (Kelly *et al* 2006) study.

Another potential explanation for the differences observed between the (Kelly *et al* 2006) study and the results demonstrated in this study is the success of the MyD88 transfections themselves, specifically the degree to which MyD88 is overexpressed. Both this study and the (Kelly *et al* 2006) study used a 48 hour transfection. It appears after comparing the western blot from this study to the western blot in the (Kelly *et al* 2006) study that the level of MyD88 expression was much higher in this study **(Figure 4.11)**. This difference in the expression levels of MyD88 could reflect the differences in paclitaxel chemoresponsiveness that was observed between the two studies. In another study involving the A2780 cell model by (Zhan *et al*. 2015) miR-149 downregulation was shown to increase paclitaxel sensitivity of A2780 cells by upregulating expression of MyD88. (Zhan *et al*. 2015) also found that this in turn lead to enhanced expression of Bcl-2 and inhibition of BAX expression. Furthermore the level of increase in MyD88 expression in the Zhan *et al*. (2015) study was much lower than the level of overexpression that was achieved in this study. The downregulation of this microRNA also may have had different effects on the A2780 cells as perhaps MyD88 is not its only target, as microRNAs have multiple mRNA targets. However different expression levels of MyD88 may exert different effects on cells.

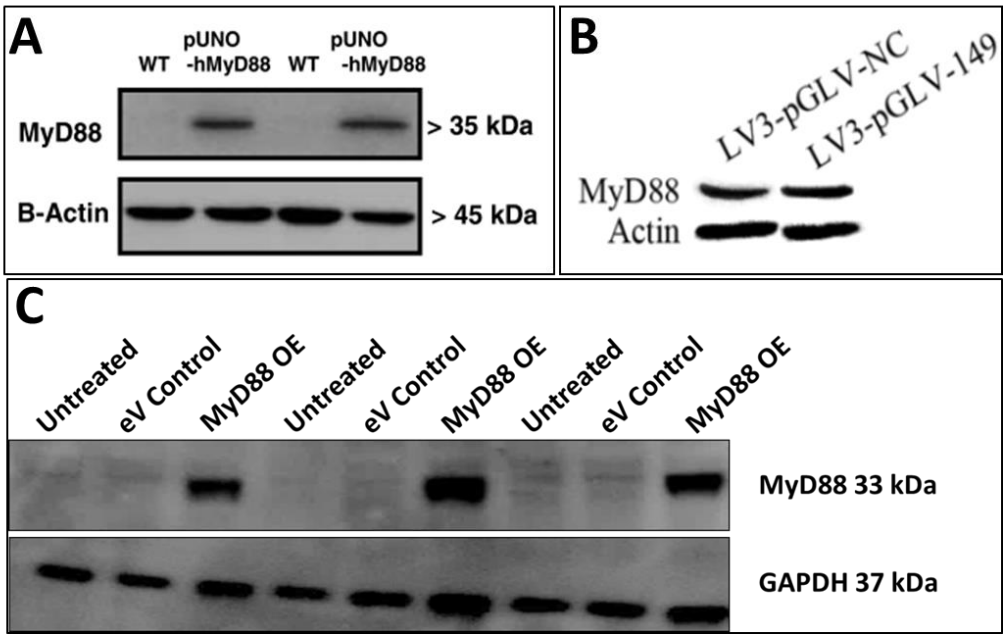

Figure 4.11 A comparison of MyD88 protein expression in three different studies. A comparison of MyD88 protein overexpression observed in a study by (Kelly *et al*. 2006) in which, CP70 cells were transfected with a MyD88 overexpression plasmid (pUNO-hMyD88) (A), a study by(Zhan *et al*. 2015) in which MyD88 was upregulated in A2780 using lentiviral knockdown miR-149 (LV3-pGLV-149) (B), and the level of MyD88 protein expression achieved in this study using an MyD88 overexpression plasmid (MyD88 OE) (C).

Many of the cytokines released by NFκB signalling have both pro-tumourigenic and anti-tumourigenic effects (Killeen *et al*. 2006). Depending on the expression of MyD88, the balance of the overall effect of these cytokines may perhaps shift in favour of either a pro-tumourigenic response or an anti-tumourigenic response. Various other studies examining MyD88 in other cancer models have highlighted the importance of cytokines and survival proteins. Egunsola *et al*. (2012) observed that the use of a MyD88 peptide inhibitor reduced the growth of MDA-MB-231 breast cancer cells in response to LPS. They attributed this to a decrease in the expression of the cytokines CCL2 and CCL5. In another study by Xiang *et al*. (2014), lentiviral transfection of the MyD88 gene was shown to increase the resistance of A549 lung cells to paclitaxel. This was attributed to an increase of IL-8 secretion and an increase in the expression of BCL-2 and downregulation of BAX expression. While it was also found that knockdown of MyD88 in A549 using a shRNA increased the sensitivity of these cells to paclitaxel, with the authors concluding that MyD88 modulates paclitaxel resistance in these cells. (Liang *et al*. 2013) showed similar results, with knockdown or overexpression of MyD88 using a lentiviral vector increasing or decreasing responsiveness to paclitaxel in hepatocellular carcinoma cells. Interestingly a MyD88 mutation exists known as the L265P mutation,

which is implicated in various types of leukaemia and lymphoma (Ngo *et al*. 2011; Puente *et al*. 2011; Gonzalez-Aguilar *et al*. 2012; Treon *et al*. 2012; Choi *et al*. 2013; Ansell *et al*. 2014).This mutation leads to hyper-activation of NFKB and JAK-STAT signalling and secretion of inflammatory cytokines and chemokines including IL-6, IL-8 and TGF-β. In a study by (Liu *et al*. 2014), MyD88 has also shown to play a role in cisplatin resistance. Specifically, knockdown of MyD88 in the cisplatin adapted SKOV-3 DPP cell line increased the chemosensitivity of these cells to cisplatin therapy. (Kfoury *et al*. 2013) inhibited MyD88 in a number of colon cancer lines with mutations in the RAS oncogene and a functional P53. They demonstrated that MyD88 inhibition lead to defective ERCC1 dependent DNA repair and the accumulation of DNA damage. These inhibitions lead to cancer cell death in cells with an intact P53. ERCC1 is involved in NER pathway, which is responsible for repairing DNA damage induced by genotoxic agents such as cisplatin. They found that MyD88 inhibition in cell lines acted, synergistically with both cisplatin and oxaliplatin, but not paclitaxel to enhance their genotoxic activity. The genotoxicity of cisplatin was also enhanced in a mouse model transfected with shRNA for MyD88. Interestingly in the study by (Kelly *et al*. 2006) MyD88 overexpression restored chemosensitvity to paclitaxel but not carboplatin. These results suggest that MyD88 is capable of modulating chemoresponsiveness to different therapeutic agents. Also that it appears to modulate chemoresponsiveness differently in different cell lines.

All these studies also highlight the importance of downstream signalling pathways and specifically the release of cytokines and activation of apoptosis and survival proteins such as BAX, BCL-2, XIAP, rather than a specific role for MyD88 in chemoresistance. MyD88 may simply serve to highlight activation of molecular processes which lead to paclitaxel resistance, rather than MyD88 having any sort of effector role in paclitaxel resistance. Interestingly Rabinovich *et al*. (2007) showed that autocrine IL-6 signalling in SKOV-3 cells regulated their proliferation and blockage of IL-6 using an IL-6 antibody significantly reduced SKOV-3 proliferation rates. Similarly blockage of autocrine production of IL-8 in SKOV-3 ovarian cancer cells or exogenous treatment of A2780 cells was shown to modulate chemosensitivity of these cell lines to both cisplatin and paclitaxel. So the difference in paclitaxel sensitivity observed in this study may reflect the impact on cytokine expression that was achieved through alteration of MyD88 status.

Another possible explanation is the effect or lack thereof that this overexpression may have had on the ovarian cancer stem cell population which exist within the A2780 cell model. MyD88 suppression or overexpression may be suppressing or enriching for a populations of CSCs within tumour cell lines. Interestingly in a study by Han *et al*. (2013), when comparing A2780 cells with a paclitaxel resistant counterpart A2780/PTX, showed enrichment of a population of ALDH1 positive cancer stem cells. Our group has found that MyD88 is important in the differentiation of embryonal carcinoma stem cells and therefore may be important in the maintenance of ovarian cancer stem cells. Furthermore, Alvero *et al*. (2011) found that MyD88 is a marker for a specific population of ovarian cancer stem cells which secrete various cytokines at high levels and are resistant to paclitaxel induced apoptosis. It is possible therefore that MyD88 is an essential protein involved in the maintenance of this population of cancer stem cells. MyD88 inhibition or knockdown may therefore target and eliminate this population of stem cells and overexpression depending on the level of expression may enrich for these cells (Sharma & Settleman 2007; Greaves & Maley 2012). This reprograming of non-cancer stem cells into cancer stem cells has previously been demonstrated (Scaffidi & Misteli 2011). Interestingly Dimicoli *et al*. (2013) examined the impact of MyD88 expression in myelodysplastic syndrome. They found that blockade of MyD88 in CD34+ cells using a MyD88 inhibitor resulted in a decrease in erythroid colony formation and upregulated a number of markers involved in differentiation. MyD88 blockade was found to negatively regulate IL-8 secretion. Subsequent treatment of MDS CD34+ cells with an IL-8 antibody was then shown to increase the formation of erythroid colonies. This suggests that blockage of MyD88 signalling may force differentiate cancer stem cells alleviating their tumourigenic potentially and also suggest a role for cytokines such as IL-8 is cancer stem cell maintenance.

Overexpression of MyD88 in A2780 cells was also carried out to determine whether it would impact on expression levels of MAD2 and demonstrate whether there was any sort of *in-vitro* relationship between MyD88 and MAD2. Secondly it was carried out in order to determine whether MyD88 and MAD2 contribute to chemoresistance through separate independent mechanisms, or whether they share a common paclitaxel resistance mechanism, or synergistically feed one another. Overexpression of MyD88 in A2780 cells was shown not to have any impact on MAD2 expression levels. No significant change in MAD2 expression was shown at any of the timepoints analysed. This indicates that MAD2 acts independently of MyD88 and supporting results from *in-silico* analysis which predicted no direct interaction or pathway linkage between MyD88 and MAD2. However although MAD2 appears to act independently of MyD88, MAD2

may still be capable of regulating MyD88 expression. Furthermore as paclitaxel resistance was not induced by overexpression of MyD88 in this study, it is unclear whether or not the paclitaxel resistance mechanisms intersect at some point.

Furthermore MyD88 overexpression in A2780 cells was carried out to examine any potential effect on regulatory microRNA expression. The effect of MyD88 overexpression was assessed at multiple timepoints (24-72 hours). This was found to have no impact on miR-21, miR-14a and miR-433 expression. miR-21 and miR-146a are known to negatively theTLR4-MyD88 pathway and supress the expression and secretion of inflammatory cytokines and chemokines. If cytokine secretion was restored in these cells it might be expected that the expression levels of these microRNAs might be altered in response to this. However these two microRNAs do not specifically target MyD88, therefore this may explain why their expression patterns remained unaltered. However our group had previously demonstrated that miR-21, miR-146a were upregulated in a subset of MyD88 negative serous ovarian tumour samples compared to MyD88 positive and Variable expression of these two regulatory miRNAs was seen between each cell model and their chemoresistant counterparts (Section 1.6). These microRNAs may still play an important regulator role in ovarian cancer. Interestingly in a study by (Zhan *et al*. 2015), inhibition of miR-149 which directly targets and negatively regulates MyD88 expression, using a lentiviral inhibitor of miR-149 was able to induce paclitaxel resistance in A2780 cells. Perhaps by adopting a similar approach and inhibiting or overexpressing either miR-146a or miR-21 it may give definitive evidence to their role in the regulation of MyD88 expression and any potential role in paclitaxel resistance in this cell model. Both miR-146a and miR-21 have been shown to act as tumour suppressors in numerous other cancers (Bhaumik *et al*. 2008; Hurst *et al*. 2009; Kulda *et al*. 2010; Ren *et al*. 2010; Li *et al*. 2010; Mei *et al*. 2011; Kida *et al*. 2011; Zhao *et al*. 2011; Gao *et al*. 2012; Li *et al*. 2012; Yao *et al*. 2013; Gao *et al*. 2013; X. Wang *et al*. 2013; N. Wang *et al*. 2013; Zhang *et al*. 2014; Ali *et al*. 2014; Mao *et al*. 2014). Aberrant expression of these of microRNAs may therefore lead to tumourigenesis. Interestingly a number of studies have identified mutations in pre-miR-146a as contributing to cancer (Zeng *et al*. 2010; Yue *et al*. 2011; Hung *et al*. 2012; Forloni *et al*. 2014) including one in patients with familial breast/ovarian cancer (Shen *et al*. 2008). Inhibition of miR-21 was also shown to sensitise ovarian cancer cells to cisplatin therapy in a study by (Chan *et al*. 2014). All of these studies demonstrate the important regulatory roles of miR-21 and miR-146a in cancer.

miR-433 expression was also unaffected by overexpression of MyD88. It was thought that perhaps if an *in-vitro* link between MyD88 and MAD2 existed or if paclitaxel chemoresistance could be induced, miR-433 expression levels might be affected as miR-433 is known to negatively regulate MAD2 and has been shown to induce paclitaxel resistance in the A2780 model previously (Furlong *et al*. 2012). Furthermore high miR-433 expression is associated with reduced PFS in patient samples. However in this instance, paclitaxel chemoresistance was not restored and no *in-vitro* relationship between MAD2 and MyD88 was demonstrated. But similarly overexpression of miR-433 and then examination of its effect on MyD88 expression may give further evidence as to whether or not any potential relationship exists between this microRNA, MyD88 and MAD2.

4.6 Conclusion

Despite optimisation of the MyD88 overexpression protocol in A2780 cells and successful overexpression of MyD88 in these cells, which was confirmed at both the gene and protein level, overexpression of MyD88 in these cells did not alter their sensitivity to paclitaxel. Overexpression of MyD88 did not have any impact on the expression of miR-21, miR-146a or miR-433. MAD2 expression was unaffected by the overexpression of MyD88, suggesting that MAD2 acts independently of MyD88 and functions through a separate mechanism in ovarian cancer *in-vitro*.

4.7 References

1) Ali, S. *et al*., 2014. Deregulation of miR-146a expression in a mouse model of pancreatic cancer affecting EGFR signaling. *Cancer Letters*, 351(1), pp.134–142. Available at: http://dx.doi.org/10.1016/j.canlet.2014.05.013.
2) Alvero, A.B. *et al*., 2011. Molecular phenotyping of human ovarian cancer stem cells unravel the mechanisms for repair and chemo-resistance. *Cell Cycle*, 8(1), pp.158–166.
3) Ansell, S.M. *et al*., 2014. Activation of TAK1 by MYD88 L265P drives malignant B-cell Growth in non-Hodgkin lymphoma. *Blood cancer journal*, 4(November 2013), p.e183. Available at: http://www.pubmed central.nih.gov/articlerender.fcgi ?artid=3944662&tool=pmcentrez&r endertype=abstract [Accessed December 30, 2014].
4) Behrens, B.C. *et al*., 1987. Characterization of a cis-Diamminedichloroplatinum (II) -resistant Human Ovarian Cancer Cell Line and Its Use in Evaluation of Platinum Analogues. , (Ii), pp.414–418.
5) Bhaumik, D. *et al*., 2008. Expression of microRNA-146 suppresses NF-κB activity with reduction of metastatic potential in breast cancer cells. *Oncogene*, 27(42), pp.5643–5647.
6) Chan, J.K. *et al*., 2014. The inhibition of miR-21 promotes apoptosis and chemosensitivity in ovarian cancer. *Gynecologic Oncology*, 132(3), pp.739–744.
7) Choi, J.-W. *et al*., 2013. MYD88 expression and L265P mutation in diffuse large B-cell lymphoma. *Human pathology*, 44(7), pp.1375–81. Available at: http://www.ncbi.nlm.nih.gov/pubmed/23380077 [Accessed February 20, 2014].
8) Craveiro, V. *et al*., 2013. Phenotypic modifications in ovarian cancer stem cells following Paclitaxel treatment. *Cancer medicine*, 2(6), pp.751–62. Available at: http://www.pubmedcentral.nih.gov/articlerender.fcgi?artid=38 92380&tool=pmcentrez&rendertype=abstract [Accessed April 30, 2014].
9) Cuello, M. *et al*., 2001. Synergistic Induction of Apoptosis by the Combination of TRAIL and Chemotherapy in Chemoresistant Ovarian Cancer Cells. , 390, pp.380–390.
10) d'Adhemar, C.J. *et al*., 2014. The MyD88+ Phenotype Is an Adverse Prognostic Factor in Epithelial Ovarian Cancer. *PloS one*, 9(6), p.e100816. Available at: http://www.ncbi.nlm.nih.gov/pubmed/24977712 [Accessed July 2, 2014].
11) Dimicoli, S. *et al*., 2013. Overexpression of the toll-like receptor (TLR) signaling adaptor MYD88, but lack of genetic mutation, in myelodysplastic syndromes. *PloS one*, 8(8), p.e71120. Available at: http://www.pubmed central.nih.gov/articl e render.fcgi?artid=3744562&tool= pmcentrez& render type=abstract [Accessed January 13, 2014].
12) Egunsola, A.T. *et al*., 2012. Growth, metastasis, and expression of CCL2 and CCL5 by murine mammary carcinomas are dependent upon Myd88. *Cellular immunology*, 272(2), pp.220–9. Available at: http://www.ncbi.nlm.nih.gov/ pub med/22088941 [Accessed October 29, 2012].
13) Forloni, M. *et al*., 2014. miR-146a promotes the initiation and progression of melanoma by activating Notch signaling. *eLife*, 2014(3), pp.1–20.
14) Furlong, F. *et al*., 2012. Low MAD2 expression levels associate with reduced progression-free survival in patients with high-grade serous epithelial ovarian cancer. *The Journal of pathology*, 226(5), pp.746–55.

Available at: http://www.ncbi.nlm.nih.gov/pubmed/22069160 [Accessed February 23, 2013].
15) Gao, J. *et al*., 2013. Clinical significance of serum miR-21 in breast cancer compared with CA153 and CEA. *Chinese journal of cancer research = Chung-kuo yen cheng yen chiu*, 25(6), pp.743–8. Available at: http:// www. pubmed central.nih.gov/articlerender.fcgi? artid=3872537 &tool =pmcentrez &rendertype=abstract.
16) Gao, W. *et al*., 2012. A systematic-analysis of predicted miR-21 targets identifies a signature for lung cancer. *Biomedicine & pharmacotherapy = Biomédecine & pharmacothérapie*, 66(1), pp.21–8. Available at: http://www. ncbi.nlm.nih.gov/pubmed/22244963 [Accessed October 29, 2012].
17) Gonzalez-Aguilar, A. *et al*., 2012. Recurrent mutations of MYD88 and TBL1XR1 in primary central nervous system lymphomas. *Clinical cancer research : an official journal of the American Association for Cancer Research*, 18(19), pp.5203–11. Available at: http://www.ncbi.nlm. nih.gov/ pubmed/22837180 [Accessed February 20, 2014].
18) Greaves, M. & Maley, C.C., 2012. Clonal Evolution in Cancer. , 481(7381), pp.306–313.
19) Han, X. *et al*., 2013. A2780 human ovarian cancer cells with acquired paclitaxel resistance display cancer stem cell properties. *Oncology Letters*, 6(5), pp.1295–1298.
20) Hung, P.-S. *et al*., 2012. Association between the rs2910164 polymorphism in pre-mir-146a and oral carcinoma progression. *Oral oncology*, 48(5), pp.404–8. Available at: http://www.ncbi.nlm.nih.gov /pubmed/22182931 [Accessed October 29, 2012].
21) Hurst, D.R. *et al*., 2009. Breast cancer metastasis suppressor 1 up-regulates miR-146, Which suppresses breast cancer metastasis. *Cancer Research*, 69(4), pp.1279–1283.
22) Kelly, M.G. *et al*., 2006. TLR-4 signaling promotes tumor growth and paclitaxel chemoresistance in ovarian cancer. *Cancer research*, 66(7), pp.3859–68. Available at: http://www.ncbi.nlm.nih.gov/pubmed/16585214 [Accessed October 22, 2012].
23) Kfoury, A. *et al*., 2013. MyD88 in DNA repair and cancer cell resistance to genotoxic drugs. *Journal of the National Cancer Institute*, 105(13), pp.937–46. Available at: http://www.ncbi.nlm.nih.gov/pubmed/23766530 [Accessed Feb ruary 20, 2014].
24) Kida, K. *et al*., 2011. PPAR?? is regulated by miR-21 and miR-27b in human liver. *Pharmaceutical Research*, 28(10), pp.2467–2476.
25) Killeen, S.D. *et al*., 2006. Exploitation of the Toll-like receptor system in cancer: a doubled-edged sword? *British journal of cancer*, 95(3), pp.247–52. Available at: http://www.pubmedcentral.nih.gov/articlerender.fcgi? artid=236 0630&tool =pm centrez&rendertype=abstract [Accessed February 3, 2013].
26) Kim, K.H. *et al*., 2012. Expression and significance of the TLR4/MyD88 signaling pathway in ovarian epithelial cancers. *World journal of surgical oncology*, 10(1), p.193. Available at: http://www.pubmedcentral.nih.gov/ article render.fcgi ?artid=3539930&tool=pmcentrez&rendertype=abstract [Accessed March 12, 2014].
27) Kim, K.H. & Yoon, M.S., 2010. MyD88 expression and anti-apoptotic signals of paclitaxel in epithelial ovarian cancer cells. , 53(4), pp.330–338.
28) Kulda, V. *et al*., 2010. Relevance of miR-21 and miR-143 expression in tissue samples of colorectal carcinoma and its liver metastases. *Cancer Genetics and Cytogenetics*, 200(2), pp.154–160. Available at: http://www. ncbi.nlm.nih.gov /pubmed/20620599.

29) Li, B. sheng *et al*., 2012. Plasma microRNAs, miR-223, miR-21 and miR-218, as novel potential biomarkers for gastric cancer detection. *PLoS ONE*, 7(7).
30) Li, Y. *et al*., 2010. miR-146a suppresses invasion of pancreatic cancer cells. *Cancer Research*, 70(4), pp.1486–1495.
31) Liang, B. *et al*., 2013. Myeloid differentiation factor 88 promotes growth and metastasis of human hepatocellular carcinoma. *Clinical cancer research : an official journal of the American Association for Cancer Research*, 19(11), pp.2905–16. Available at: http://www.ncbi.nlm.nih. gov/pubmed/23549880 [Accessed February 20, 2014].
32) Liu, G., Du, P. & Zhang, Z., 2014. Myeloid Differentiation Factor 88 Promotes Cisplatin Chemoresistance in Ovarian Cancer. *Cell biochemistry and biophysics*. Available at: http://www.ncbi.nlm.nih.gov/ pubmed/25308861 [Accessed December 2, 2014].
33) Mao, X., Sun, Y. & Tang, J., 2014. Serum miR-21 is a diagnostic and prognostic marker of primary central nervous system lymphoma. *Neurological Sciences*, 35(2), pp.233–238.
34) Mei, J., Bachoo, R. & Zhang, C.-L., 2011. MicroRNA-146a Inhibits Glioma Development by Targeting Notch1. *Molecular and cellular biology*, 31(17), pp.3584–3592.
35) Ngo, V.N. *et al*., 2011. Oncogenically active MYD88 mutations in human lymphoma. *Nature*, 470(7332), pp.115–9. Available at: http://www.ncbi. nlm. nih.gov/pubmed/21179087 [Accessed February 20, 2014].
36) Puente, X.S. *et al*., 2011. Whole-genome sequencing identifies recurrent mutations in chronic lymphocytic leukaemia. *Nature*, 475(7354), pp.101–5. Available at: http://www.pubmedcentral.nih.gov/articlerender. fcgi?artid =33 22590&tool=pmcentrez&rendertype=abstract [Accessed February 20, 2014].
37) Rabinovich, A. *et al*., 2007. Regulation of ovarian carcinoma SKOV-3 cell proliferation and secretion of MMPs by autocrine IL-6. *Anticancer research*, 27(1A), pp.267–72. Available at: http://www.ncbi.nlm.nih.gov/ pubmed /17352 242.
38) Reid, Y.A., 2011. Characterization and authentication of cancer cell lines: An overview. *Methods in Molecular Biology*, 731, pp.35–43.
39) Ren, Y. *et al*., 2010. MicroRNA-21 inhibitor sensitizes human glioblastoma cells U251 (PTEN-mutant) and LN229 (PTEN-wild type) to taxol. *BMC Cancer*, 10(1), p.27. Available at: http://www.pubmed central.nih.gov/articlerender.fcgi?artid=2824710&tool=pmcentrez& render type=abstract.
40) Scaffidi, P. & Misteli, T., 2011. In vitro generation of human cells with cancer stem cell properties. *Nature cell biology*, 13(9), pp.1051–1061.
41) Schmittgen, T.D. & Livak, K.J., 2008. Analyzing real-time PCR data by the comparative C(T) method. *Nature protocols*, 3(6), pp.1101–1108.
42) Sharma, S. V & Settleman, J., 2007. Oncogene addiction: setting the stage for molecularly targeted cancer therapy. *Genes & development*, 21(24), pp.3214–3231.
43) Shen, J. *et al*., 2008. A functional polymorphism in the miR-146a gene and age of familial breast/ovarian cancer diagnosis. *Carcinogenesis*, 29(10), pp.1963–1966.
44) Silasi, D.-A. *et al*., 2006. MyD88 predicts chemoresistance to paclitaxel in epithelial ovarian cancer. *The Yale journal of biology and medicine*, 79(3-4), pp.153–63. Available at: http://www.pubmedcentral.nih. gov/ articlerender.fcgi?artid=1994803&tool =pmcentrez& rendertype=abs tract.
45) Szajnik, M. *et al*., 2009. TLR4 signaling induced by lipopolysacharide or paclitaxel regulates tumor survival and chemoresistance in ovarian

cancer. *Oncogene*, 28(49), pp.4353–4363. Available at: http://www.pubmedcentral.nih.gov/articlerender.fcgi?artid=2794996&tool=pmcentrez & render type= abstract.
46) Treon, S.P. *et al*., 2012. MYD88 L265P somatic mutation in Waldenström's macroglobulinemia. *The New England journal of medicine*, 367(9), pp.826–33. Available at: http://www.ncbi.nlm.nih.gov/pubmed/22931316 [Accessed February 20, 2014].
47) Wang, A.C. *et al*., 2014. TLR4 induces tumor growth and inhibits paclitaxel activity in MyD88-positive human ovarian carcinoma in vitro. *Oncology Letters*, 7(3), pp.871–877.
48) Wang, N. *et al*., 2013. MiR-21 down-regulation suppresses cell growth, invasion and induces cell apoptosis by targeting FASL, TIMP3, and RECK genes in esophageal carcinoma. *Digestive Diseases and Sciences*, 58(7), pp.1863–1870.
49) Wang, X. *et al*., 2013. Krüppel-like factor 8 promotes tumorigenic mammary stem cell induction by targeting miR-146a. *American journal of cancer research*, 3(4), pp.356–73. Available at: http://www.pubmedcentra .nih.gov /article render .fcgi?artid= 3744016&tool=pmcentrez &rendertyp e=abstract.
50) Weiner-Gorzel, K. *et al*., 2015. Overexpression of the microRNA miR-433 promotes resistance to paclitaxel through the induction of cellular senescence in ovarian cancer cells. *Cancer Medicine*, p.n/a–n/a. Available at: http://doi.wiley.com/10.1002/cam4.409.
51) Xiang, F. *et al*., 2014. Myd88 expression is associated with paclitaxel resistance in lung cancer A549 cells. *Oncology Reports*, 32(5), pp.1837–1844.
52) Yao, Q. *et al*., 2013. MicroRNA-146a acts as a metastasis suppressor in gastric cancer by targeting WASF2. *Cancer Letters*, 335(1), pp.219–224. Available at: http://dx.doi.org/10.1016/j.canlet.2013.02.031.
53) Yue, C. *et al*., 2011. Polymorphism of the pre-miR-146a is associated with risk of cervical cancer in a Chinese population. *Gynecologic oncology*, 122(1), pp.33–7. Available at: http://www.ncbi.nlm.nih.gov/pubmed/2152 9907 [Access ed October 29, 2012].
54) Zeng, Y. *et al*., 2010. Correlation between pre-miR-146a C/G polymorphism and gastric cancer risk in Chinese population. *World Journal of Gastroenterology*, 16(28), pp.3578–3583.
55) Zhan, Y. *et al*., 2015. MiRNA-149 modulates chemosensitivity of ovarian cancer A2780 cells to paclitaxel by targeting MyD88. *Journal of Ovarian Research*, 8(1), p.48. Available at: http://www.ovarian research.com/content /8/1/48.
56) Zhang, X. *et al*., 2014. MicroRNA-146a targets PRKCE to modulate papillary thyroid tumor development. *International Journal of Cancer*, 134(2), pp.257–267.
57) Zhao, J.L. *et al*., 2011. NF-kappaB dysregulation in microRNA-146a-deficient mice drives the development of myeloid malignancies. *Proceedings of the National Academy of Sciences of the United States of America*, 108(22), pp.9184–9. Available at: http://www.pubmedcentral.nih.gov/articlerender.fcgi?artid=3107319&tool=pmcentrez&rendertype= abstract [Accessed March 5, 20 14].
58) Zhu, Y. *et al*., 2012. Prognostic significance of MyD88 expression by human epithelial ovarian carcinoma cells. *Journal of translational medicine*, 10(1), p.77. Available at: http://www.pubmedcentral.nih.gov/articlerender.fcgi? artid =343811 & tool=pmcentrez&rendertype=abstract [Accessed October 29, 2012].

Chapter 5

The effect of siRNA knockdown of MAD2 on TLR4 and MyD88 expression levels in A2780 and SKOV-3 cells

Trinity College Dublin

The University of Dublin

Chapter 5

The effect of siRNA knockdown of MAD2 on TLR4 and MyD88 expression levels in A2780 and SKOV-3 cells

5.1 Overview

This chapter describes the effect of siRNA knockdown of MAD2 in A2780 and SKOV-3 cells on chemoresponsiveness to paclitaxel, MyD88 and TLR4 expression patterns and the expression of the regulatory microRNAs miR-21, miR-146a and miR-433.

5.2 Introduction

It was previously shown that knockdown of MAD2 in A2780 cells or MCF-7 breast cancer cells could induce paclitaxel resistance (Prencipe *et al*. 2009; Furlong *et al*. 2012). This acquired paclitaxel resistance was attributed to a weakened spindle assembly checkpoint and the induction of senescence. The previous two chapters explored the role of TLR4 and MyD88 in paclitaxel chemoresistance and the relationship between MAD2, TLR4 and MyD88. In chapter 3 siRNA knockdown of no change in MAD2 expression was shown when TLR4 or MyD88 was knocked down in SKOV-3 cells or when MyD88 was overexpressed in A2780 cells, demonstrating that MAD2 expression is not influenced by the expression of TLR4 and MyD88. Furthermore, *in-silico* analysis did not predict any direct interactions or pathway linkages between these markers (Chapter 3). Therefore it was hypothesised that knockdown of MAD2 would have no effect on MyD88 or TLR4 expression. A major aim of this chapter was to investigate this and determine whether the paclitaxel resistance mechanisms in which MAD2 and TLR4 are involved in intersect. It was thought upon commencement of this work that MAD2 and MyD88/TLR4 were independent biomarkers in ovarian cancer and contributed to paclitaxel resistance through separate mechanisms. Downregulation of MAD2 was thought to contribute to paclitaxel

resistance through the induction of senescence (Prencipe *et al*. 2009). The TLR4-MyD88 pathway was thought to contribute to paclitaxel resistance by inducing the secretion of various chemokines/cytokines and upregulating the expression of anti-apoptotic/pro-survival proteins (Kelly *et al*. 2006; Wang *et al*. 2009; Szajnik *et al*. 2009; Huang *et al*. 2014). Therefore, to assess this, TLR4 and MyD88 expression was analysed in A2780 and SKOV-3 cells following knockdown of MAD2. Furthermore as knockdown of MAD2 had previously been shown to induce paclitaxel resistance in A2780 cells and other cancer cell models (Sudo 2004; Prencipe *et al*. 2009; Hao *et al*. 2010; Furlong *et al*. 2012), it was decided to assess the effect of MAD2 knockdown on chemoresponsiveness to paclitaxel in SKOV-3 cells only. Another aim as with previous chapters was to examine the effect on regulatory microRNA expression and further discern any potential role in paclitaxel resistance and in the regulation of MAD2, TLR4 or MyD88 expression within our cell models. miR-433 had previously been shown to directly target MAD2 and induce paclitaxel resistance, therefore it was hypothesised that perhaps it may be affected following knockdown of MAD2.

5.2.1 Hypothesis

siRNA knockdown of MAD2 in A2780 and SKOV-3 ovarian cancer cells may impact on MyD88 or TLR4 expression, render SKOV-3 cells chemoresistant to paclitaxel therapy and alter the expression of the regulatory microRNAs miR-146a, miR-21 and miR-433.

5.2.2 Aims

1) To assess the impact of knockdown of MAD2 on SKOV-3 sensitivity to paclitaxel.
2) To assess the impact of knockdown of MAD2 on MyD88 and TLR4 expression levels.
3) To investigate the effect of knockdown of MAD2 on the expression of the regulatory microRNAs miR-146a, miR-21 and miR-433.
4) Following knockdown of MAD2 in SKOV-3 cells, carry out microarray analysis and compare to parent cells to identify deregulated genes and pathways.

5.3 Methods

5.3.1 Small-interfering RNA transfection

SKOV-3 cells and A2780 cells were cultured as described in (Section 2.2). siRNA knockdown of MAD2 was carried out in both 24 well and 6 well plates as described in (Section 2.5) using lipofectamine RNAiMAX, siRNA targeting MAD2 or a scrambled non targeting negative control siRNA at final concentration of 1nM for SKOV-3 cells and a final concentration of 30nM for A2780 cells (See Section 5.4 for MAD2 knockdown protocol optimisation). Cell lines were routinely checked for mycoplasma and were mycoplasma-free (Section 2.2).

5.3.2 RNA extraction and TaqMan RT-PCR

RNA was isolated and TaqMan RT-PCR was performed as described in Section 2.5 using commercially available primers and probe sets for miR-146a, miR-21, miR-433, MyD88, TLR4, MAD2, GAPDH (mRNA endogenous control) and miR-16 (microRNA endogenous control). mRNA expression and microRNA expression levels following transfection were calculated using the ΔΔCT method (Schmittgen & Livak 2008), relative to GAPDH or miR-16 endogenous controls respectively. A significant change in expression was considered to be present if at least a 2-fold change (above 200% expression or below 50% expression) in mRNA or microRNA expression was observed, with a p value of <0.05 compared to untreated cells and/or negative control cells.

5.3.3 Western blot analysis

Protein was isolated and western blot analysis was performed as described in (Section 2.6). Blots were probed with antibodies directed against MyD88 (1:1000, D80F5 Cell Signalling), TLR4 (1:100, Ab47093, Abcam), MAD2 (1: 1000, 610679, BD Biosciences) and GAPDH (1:10,000, Ab9485, Abcam). Chemiluminescence images were developed using a Fujifilm LAS-4000 luminescent image analyser and densitometry was then carried out using Quantity One software (Biorad) as described previously (Section 2.6).

5.3.4 Microarray analysis

RNA samples were converted into cDNA using the GeneChip® WT PLUS Reagent Kit and hybridised to Affymetrix GeneChip® Human Gene 2.0 ST Arrays (as per section 2.10).

5.3.5 Drug treatment and assessment of cell viability using the CCK-8 assay

Following transfection for 72 hours, SKOV-3 cells were either left untreated, treated with DMSO or treated with an appropriate concentration of paclitaxel for 48 hours. 48 hours post treatment, cell viability was assessed by means of the CCK-8 assay. % cell viability for each condition was calculated as % of non-transfected cells which were left untreated.

5.3.6 Senescence β-galactosidase staining kit

The induction of senescence in cells is usually accompanied by an increase in β-Galactosidase activity (Dimri *et al*. 1995). In order to demonstrate this, cells were stained with the senescence β-Galactosidase staining kit (Cell Signalling) following transfection. SKOV-3 cells were transfected with siRNA targeting MAD2, a scrambled non-targeting negative control siRNA or were left untreated for 72 hours and 120 hours. 72 hours and 120 hours following transfection, cells were stained for β-Galactosidase. Images were then taken at 10X magnification using an Olympus CKX41 microscope and an Olympus E600 camera. The percentage of β-galactosidase positive cells within each image was then calculated for each condition for (n=3) technical and (n=3) biological replicates.

5.3.7 Statistical analysis

A student's t-test was performed on RT-PCR results and cell viability data to assess statistical significance of gene silencing experiments and differences in cell viability between drug treated versus untreated and vehicle control groups. A statistically significant difference was considered to be present at $p \leq 0.05$. Statistical analysis was performed using Microsoft excel 2010.

5.4 Results

5.4.1 Optimisation of MAD2 knockdown protocol in A2780 and SKOV-3 cells

SKOV-3 and A2780 cells were transfected with different concentrations of the non-targeting scrambled negative control siRNA or siRNA targeting MAD2. This was performed in order to determine the optimum concentration of siRNA needed in order to achieve successful knockdown of MAD2 **(Figure 5.1).** A2780 cells or SKOV-3 cells were transfected with 1nM, 10nM or 30nM of the scrambled negative control non-targeting siRNA or siRNA targeting MAD2 (siMAD2) or were left untreated for 72 hours. After 72 hours, RNA was harvested and RT-PCR was performed to determine the effect on MAD2 gene expression. In A2780 cells a MAD2 knockdown of 12.9%, 47.2% and 85.3% was achieved using 1nM, 10nM and 30nM of siRNA respectively. In SKOV-3 cells, a MAD2 knockdown of 91.9%, 91.8% and 91.3% were achieved using 1nM, 10nM and 30nM respectively. The results demonstrate that MAD2 was successfully knocked down in A2780 cells following transfection with 30nM of MAD2 siRNA only and efficient knockdown was not achieved with 1nM or 10nM of siRNA. In SKOV-3 cells, MAD2 was successfully knocked down using all three doses of siRNA 1nM, 10nM and 30nM. Therefore, the 1nM concentration of MAD2 siRNA and 30nM of siRNA for A2780 and SKOV-3 cells respectively were chosen for future experiments. Following confirmed knockdown of MAD2 at the mRNA level, it was necessary to confirm knockdown of MAD2 at the protein level. A2780 and SKOV-3 cells were transfected with siRNA targeting MAD2 for 72 hours. After 72 hours, total protein was harvested and western blot analysis was performed for MAD2 and GAPDH in A2780 and SKOV-3 cells **(Figure 5.2).** Successful knockdown of MAD2 at the protein level was confirmed in both cell lines.

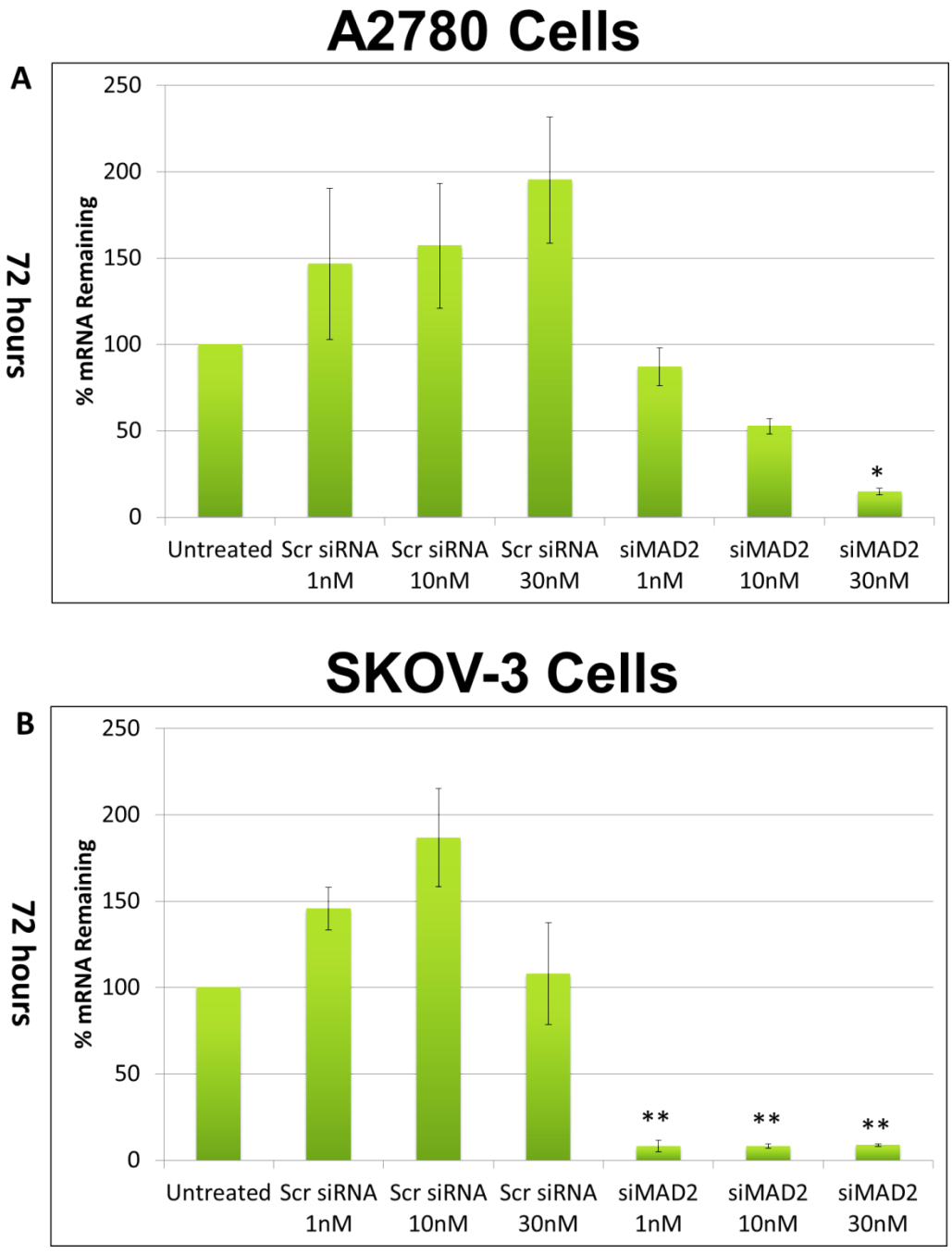

Figure 5.1 Optimisation of A2780 and SKOV-3 MAD2 knockdown protocol. A2780 (A) and SKOV-3 cells (B) were transfected with 1nM, 10nM and 30nM of siRNA targeting MAD2 (siMAD2), a non-targeting scrambled negative control siRNA (Scr siRNA) or were left untreated for 72 hours. After 72 hours, RNA was harvested and then MAD2 mRNA expression levels were analysed using TaqMan RT-PCR. MAD2 mRNA expression levels were normalised to the endogenous control GAPDH and calibrated to that of untreated cells to establish the relative change in mRNA expression (% mRNA remaining). Results are expressed as mean +/-SD, n=3; *p<0.05, **p<0.01 (Student's t-test).

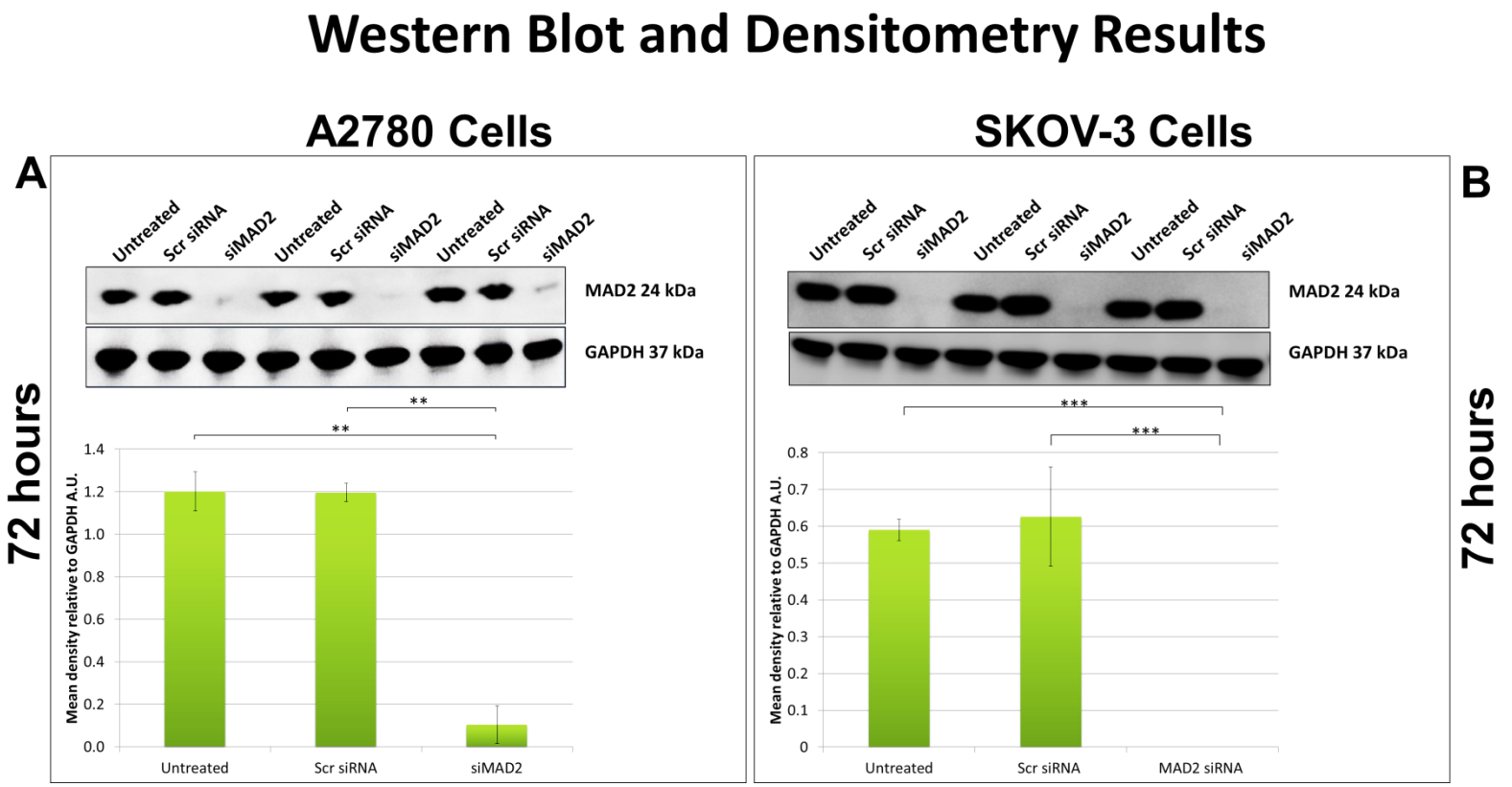

Figure 5.2 Analysis of A2780 and SKOV-3 MAD2 protein expression 72 hours following transfection with siRNA targeting MAD2. A2780 (A) and SKOV-3 cells (B) were transfected with siRNA targeting MAD2 (siMAD2), a scrambled negative control siRNA (Scr siRNA) or were left untreated for 72 hours. After 72 hours, protein was harvested using RIPA lysis buffer and then western blot analysis was performed for MAD2 and GAPDH in SKOV-3 cells. Chemiluminescence images were developed using a Fujifilm LAS-4000 luminescent image analyser. Densitometry was then carried out using Quantity One software (Biorad). Protein expression is represented as the mean density normalised to GAPDH in arbitrary units (A.U.) for each condition. The results demonstrate that MAD2 was successfully knocked down at protein level in both A2780 and SKOV-3 cells. Results are expressed as mean +/-SD, n=3. *p<0.05, **p<0.01, ***p<0.001 (Student's t-test).

5.4.2 Loss of MAD2 in SKOV-3 cells induces senescence and paclitaxel resistance

As the response to paclitaxel had been already thoroughly investigated in the A2780 cells following knockdown of MAD2, it was decided to only assess the chemoresponsiveness of SKOV-3 cells to paclitaxel following knockdown of MAD2. First the chemoresponsiveness of untreated SKOV-3 cells to paclitaxel (PTX) was assessed using concentrations of paclitaxel determined from dose response curves generated using graph pad prism software (Section 3.8). 1pM (No cell death), 3.5nM (IC_{25}), 7nM (IC_{50}), and 1µM (Maximum cell death) concentrations of paclitaxel were chosen to assess SKOV-3 chemoresponsiveness. Untreated SKOV-3 cells were seeded into 24 well plates for 72 hours, cells were then treated with 1pM PTX, 3.5nM PTX, 7nM PTX (IC_{50}), and 1µM PTX, with DMSO treated cells and untreated cells serving as controls. Cells were incubated for a further 48 hours and then cell viability was assessed by the CCK-8 assay **(Figure 5.3)**. When SKOV-3 cells were treated with 1pM, 3.5nM, 7nM and 1µM of paclitaxel, 0.5%, 9.9%, 24.7% and 59.2% reductions in cell viability were detected respectively. Therefore, in future experiments to assess the effect of knockdown of MAD2 in SKOV-3 on chemoresponsiveness to paclitaxel, 7nM and 21nM doses of paclitaxel were selected. Following assessment of SKOV-3 chemoresponsiveness, SKOV-3 cells were transfected with siRNA targeting MAD2 for 72 hours. After 72 hours cells were treated with 7nM or 21nM paclitaxel, DMSO or were left untreated to assess their chemoresponsiveness following knockdown of MAD2. Interestingly knockdown of MAD2 in SKOV-3 cells resulted in a complete change in morphology including an increase in cell size, cell shape and an increase nuclear size and also resulted in a reduction in cell proliferation **(Figure 5.4)**. Furthermore, when untreated or scrambled control cells were treated with 7nM or 21nM paclitaxel a large amount of rounded apoptotic cells were observed, whereas no visual signs of apoptosis were observed in cells which were transfected with siRNA targeting MAD2 which were treated with 7nM or 21nM paclitaxel.

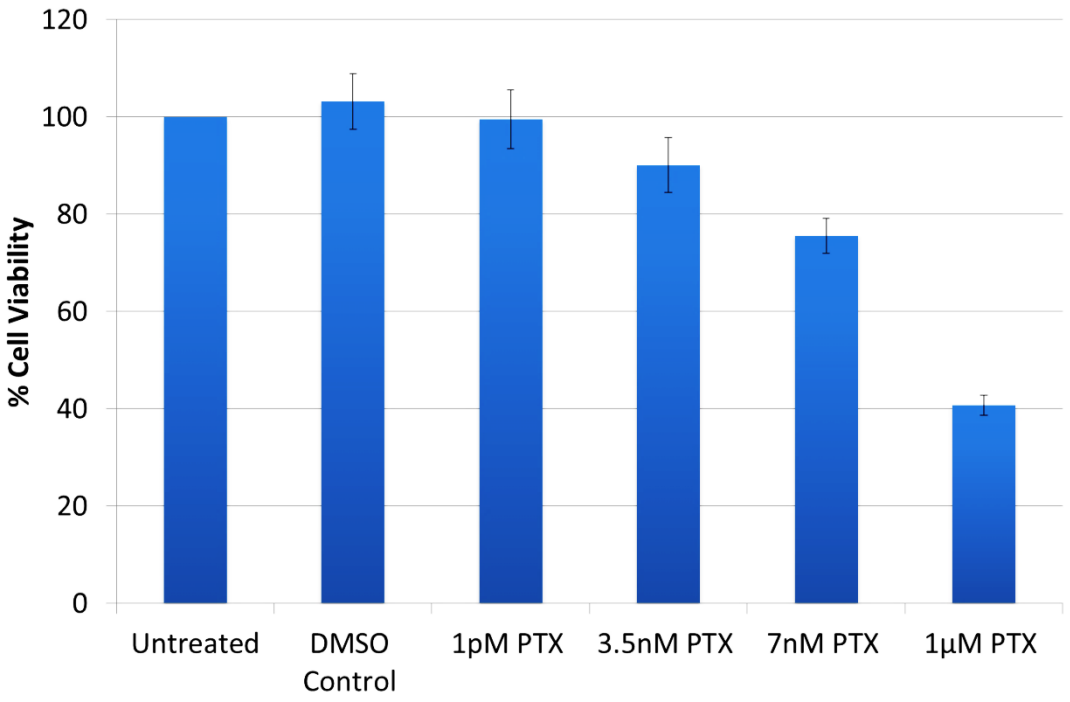

Figure 5.3 Assessment of SKOV-3 paclitaxel chemoresponsiveness using the CCK-8 assay. SKOV-3 cells were seeded into 24 well plates for 72hours and then were treated for a further 48 hours, with 1pM, 3.5nM, 7nM and 1µM paclitaxel (PTX) with untreated and DMSO treated cells serving as additional controls. After the 48 hours cell viability was assessed using the CCK-8 assay. % cell viability for each condition was then calculated as % of untreated SKOV-3 cells. Results are expressed as mean +/-SD, n=3.

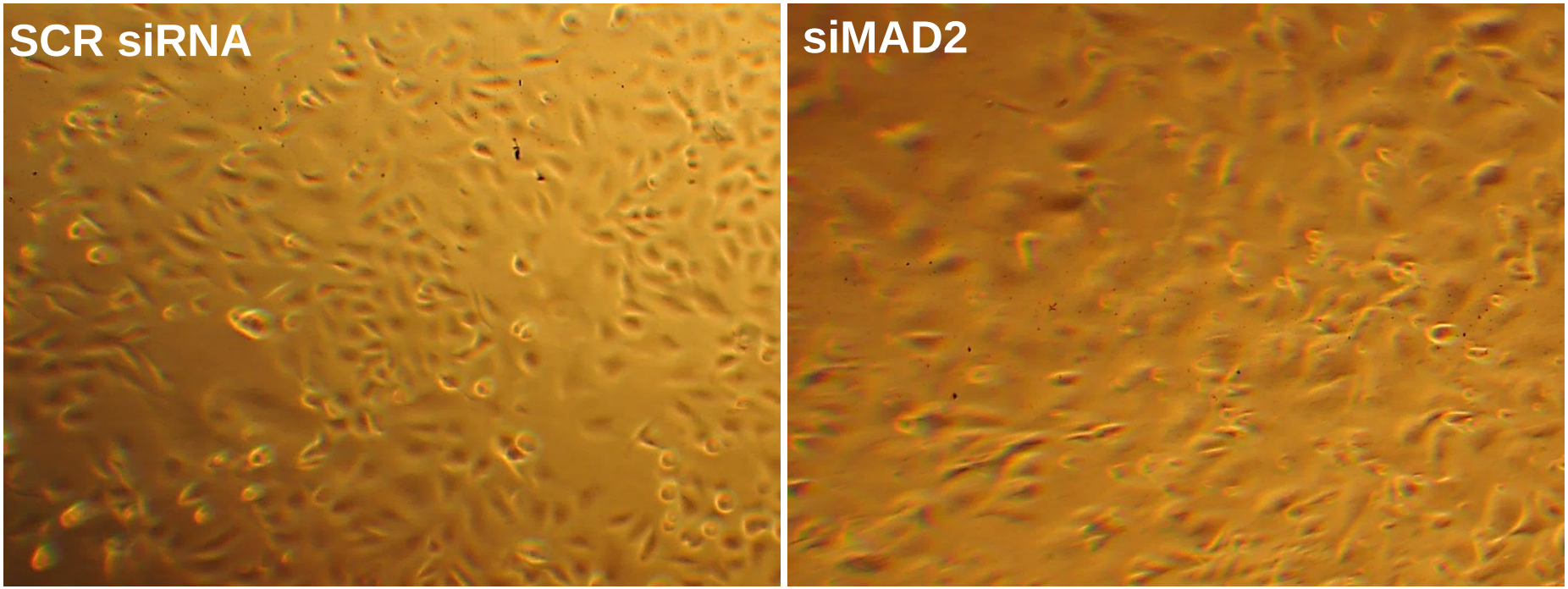

Figure 5.4 SKOV-3 cells 120 hours following knockdown of MAD2. SKOV-3 cells were transfected for 120 hours with a non-targeting scrambled negative control siRNA or siRNA targeting MAD2. Images were taken at 4X magnification using an axiovert 35 inverted microscope (Zeiss, Germany) and a Canon Powershot A620 digital camera. The results demonstrate that knockdown of MAD2 in SKOV-3 cells leads to an alteration in cell morphology included, cell size, cell shape and the size of the nucleus.

When untreated SKOV-3 cells and cells transfected with the scrambled non targeting negative control siRNA or with siRNA targeting MAD2 were assessed with the CCK-8 assay **(Figure 5.5)** following treatment with 7nM PTX a 5.3%, 44.4% and 53% reduction in cell viability was observed respectively. When untreated SKOV-3 cells and cells transfected with the scrambled non targeting negative control siRNA or with siRNA targeting MAD2 were treated with 21nM PTX, a 19%, 59.6% and 52.7% reduction in cell viability was observed respectively. A significant increase in cell viability was observed when SKOV-3 cells were transfected with siRNA targeting MAD2 and treated with 21nM PTX compared to scrambled control cells treated with the same dose of PTX. Following knockdown of MAD2, SKOV-3 cells displayed a 6.9% increase in cell viability. No difference in cell viability was also observed between SKOV-3 cells transfected with siRNA targeting MAD2 which were left untreated, treated with DMSO or treated with 7nM or 21nM PTX. In this experiment, treatment with 7nM PTX following knockdown of MAD2 in SKOV-3 did not show an increase in chemoresponsiveness, however an increase in cell viability was observed compared to scrambled control treated cells following treatment with 21nM PTX.

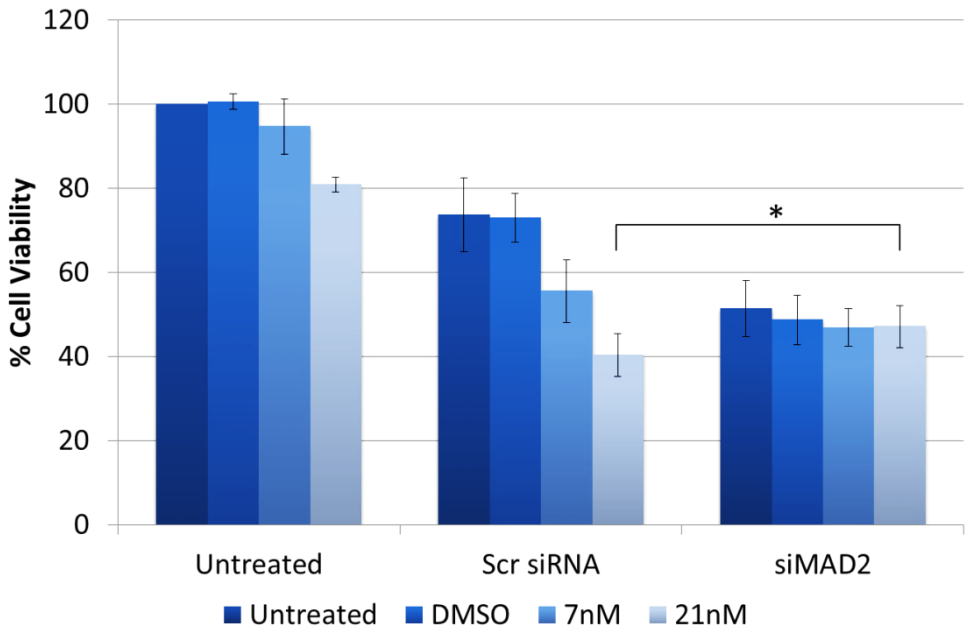

Figure 5.5 SKOV-3 cells following 72 hour knockdown of MAD2 and drug treatment with 7nM and 21nM paclitaxel. SKOV-3 cells were transfected with siRNA targeting MAD2, a non-targeting scrambled negative control siRNA or were left untreated for 72 hours. 72 hours following transfection cells were either left untreated, treated with DMSO or treated with 7nM or 21nM paclitaxel for a further 48 hours. Following the 48 hour drug treatment, cell viability was assessed using the CCK-8 assay. % cell viability for each condition was then calculated as % of non-transfected SKOV-3 cells which were left untreated. Results are expressed as mean +/-SD, n=3; *p<0.05, Student's t-test).

From these results, it was decided that an earlier time point for transfection would be more suitable to demonstrate that SKOV-3 cells were becoming chemoresistant following knockdown of MAD2. It was visually apparent following paclitaxel treatment that SKOV-3 transfected with siRNA targeting MAD2 were chemoresistant. However the CCK-8 results did not reflect this as by 120 hours, proliferation rates in SKOV-3 cells transfected with siRNA targeting MAD2 had slowed considerably. This made the impact of paclitaxel treatment in respect to untreated and scrambled cells less apparent. A 24 hour transfection and 48 hour drug treatment was then selected for future experiments. SKOV-3 cells were also treated with 21nM and 1µM of paclitaxel as 7nM of paclitaxel did not appear to induce a consistent decrease in cell viability even in untransfected SKOV-3 cells. Therefore SKOV-3 cells were transfected with a scrambled negative control siRNA, siRNA targeting MAD2 or left untreated for 24 hours. 24 hours following transfection cells were left untreated, treated with DMSO or treated with 21nM or 1µM paclitaxel for a further 48 hours **(Figure 5.6)**. SKOV-3 cells which were left untreated or transfected with a scrambled non-targeting negative control siRNA displayed a 55.4% and 56.3% reduction in cell viability when treated with

21nM paclitaxel. When treated with 1µM paclitaxel a 66.2% and 66.4%% reduction in cell viability, was observed. However in SKOV-3 cells transfected with siRNA targeting MAD2 displayed a 36.2% reduction in cell viability when treated with 21nM paclitaxel and a 36.1% reduction in cell viability when treated with 1µM paclitaxel. SKOV-3 transfected with siRNA targeting MAD2 displayed a significant increase of 19.1% and 20.1% in cell viability when treated with 21nM and a significant increase of 30.1% and 30.3% in cell viability when treated with 1µM paclitaxel compared to untreated SKOV-3 cells and SKOV-3 cells treated with the scrambled non targeting negative control siRNA. These cells visually displayed no signs of apoptosis, while in SKOV-3 cells transfected with the non-targeting scrambled negative control siRNA, although visually a reduction in cell growth rates was observed. Furthermore, this reduction in growth rates was also observed in SKOV-3 cells transfected with siRNA targeting MAD2, which were left untreated or treated with DMSO which exhibited a 19.3% and 23% reduction in cell viability compared with untreated cells which were not treated with paclitaxel. Again demonstrating that cell proliferation rates are reduced in response to knockdown of MAD2. Furthermore no significant difference in cell viability was observed between SKOV-3 cells which were transfected with siRNA targeting MAD2 which were left untreated, treated with DMSO or were treated with 21nM or 1µM paclitaxel. These results demonstrate that knockdown of MAD2 is rendering SKOV-3 cells highly resistant to paclitaxel.

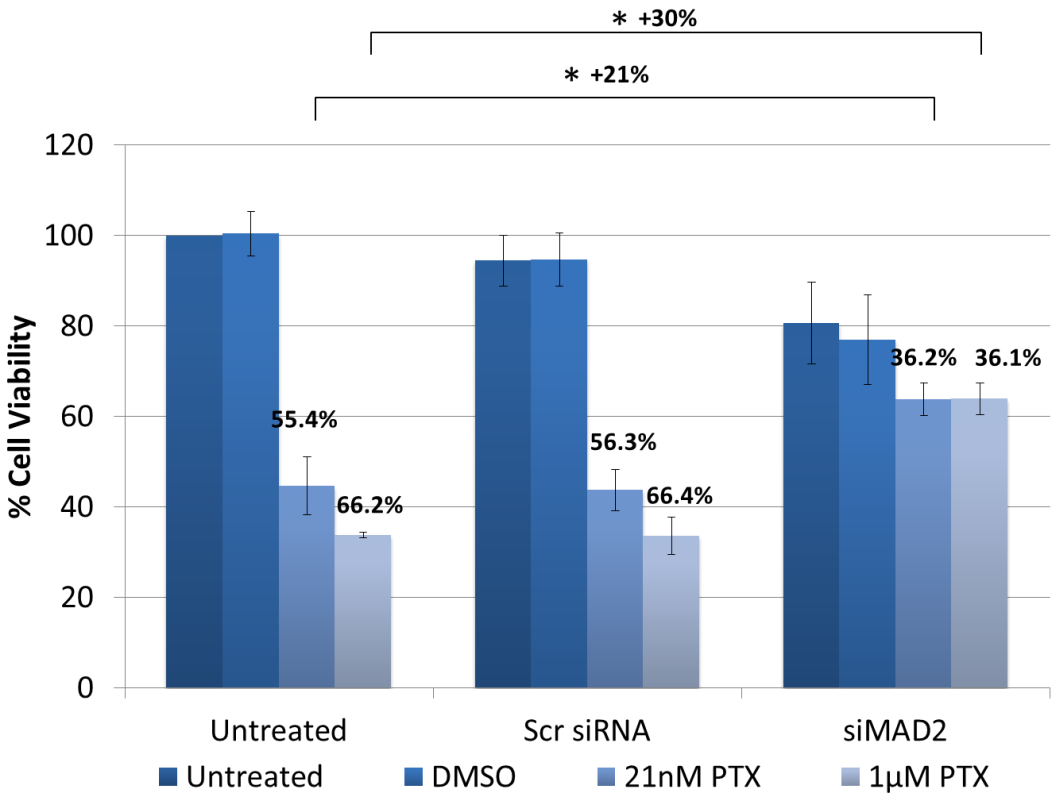

Figure 5.6 SKOV-3 cells following 24 hour knockdown of MAD2 and a 48 hour drug treatment with 21nM and 1µM paclitaxel. SKOV-3 cells were transfected with siRNA targeting MAD2, a non-targeting scrambled negative control siRNA or were left untreated for 72 hours. 72 hours following transfection cells were either left untreated, treated with DMSO or treated with 21nM or 1µM paclitaxel for a further 48 hours. Following the 48 hour drug treatment, cell viability was assessed using the CCK-8 assay. % cell viability for each condition was then calculated as % of non-transfected SKOV-3 cells which were left untreated. The results demonstrate that knockdown of MAD2 renders SKOV-3 cells resistant to paclitaxel. Results are expressed as mean +/- SD, n=3. Results are expressed as mean +/-SD, n=3; *p<0.05, Student's t-test).

As knockdown of MAD2 had previously been shown to induce senescence and paclitaxel resistance in A2780 cells and MCF-7 breast cancer cells (Prencipe *et al*. 2009; Furlong *et al.* 2012) it was decided to assess whether SKOV-3 cells were undergoing senescence. In order to assess whether SKOV-3 cells were undergoing senescence, β-galactosidase activity was assessed following transfection. β-galactosidase is the most frequently used biomarker used to detect *in-vitro* senescence (Sharpless & Sherr 2015). SKOV-3 cells were transfected with siRNA targeting MAD2 for 72 hours and 120 hours. After 72 hours and 120 hours, cells were stained using the β-Galactosidase staining kit. Cells were then counted and the percentage of cells staining positive for β-Galactosidase was calculated for each condition for (n=3) technical and (n=3) biological replicates. At both 72 hours and 120 hours, an increase in β-Galactosidase staining was observed in SKOV-3 cells transfected with siRNA targeting MAD2, compared to untreated an negative control cells **(Figure 5.7)**. At 72 and 120 hours following transfection with siRNA targeting MAD2, 24% and 26% of cells stained β-galactosidase positive compared to 7% and 10% of cells which stained β-galactosidase positive in untreated cells and 3% and 7% of cells stained β-galactosidase positive in cells transfected with the scrambled non targeting negative control siRNA **(Figure 5.8)**. The results demonstrate that knockdown of MAD2 induced upregulation of β-Galactosidase and that these cells are likely senescent.

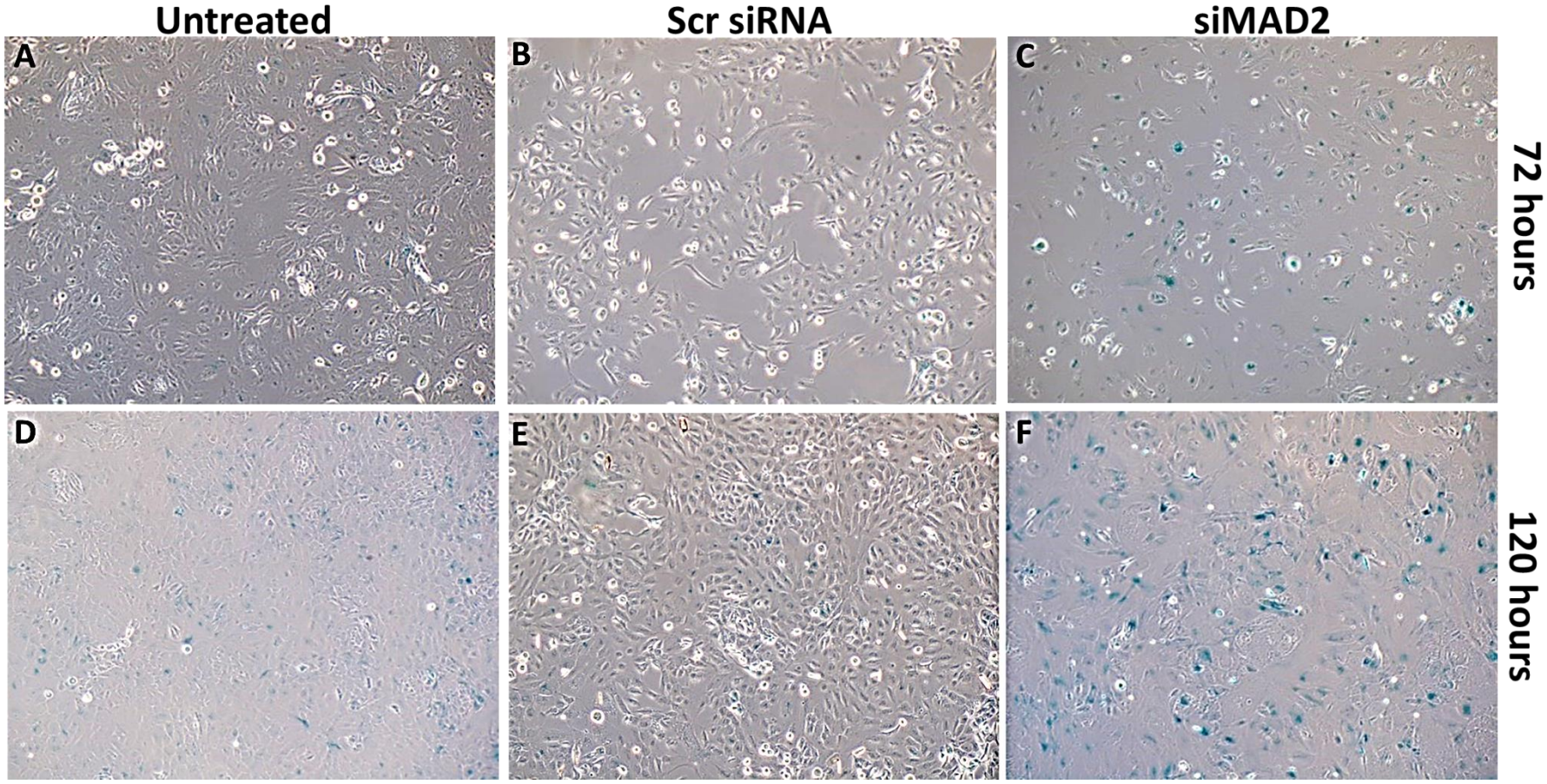

Figure 5.7 β-galactosidase staining in SKOV-3 cells following knockdown of MAD2. SKOV-3 cells were transfected with siRNA targeting MAD2 (siMAD2), a scrambled non-targeting negative control siRNA (Scr siRNA) or were left untreated for 72(A-C) hours or 120 hours (D-F). After 72 hours or 120 hours, cells were stained using the β-Galactosidase staining kit (Cell Signalling). Images were then taken at 10X magnification using an Olympus CKX41microscope and an Olympus E600 camera.

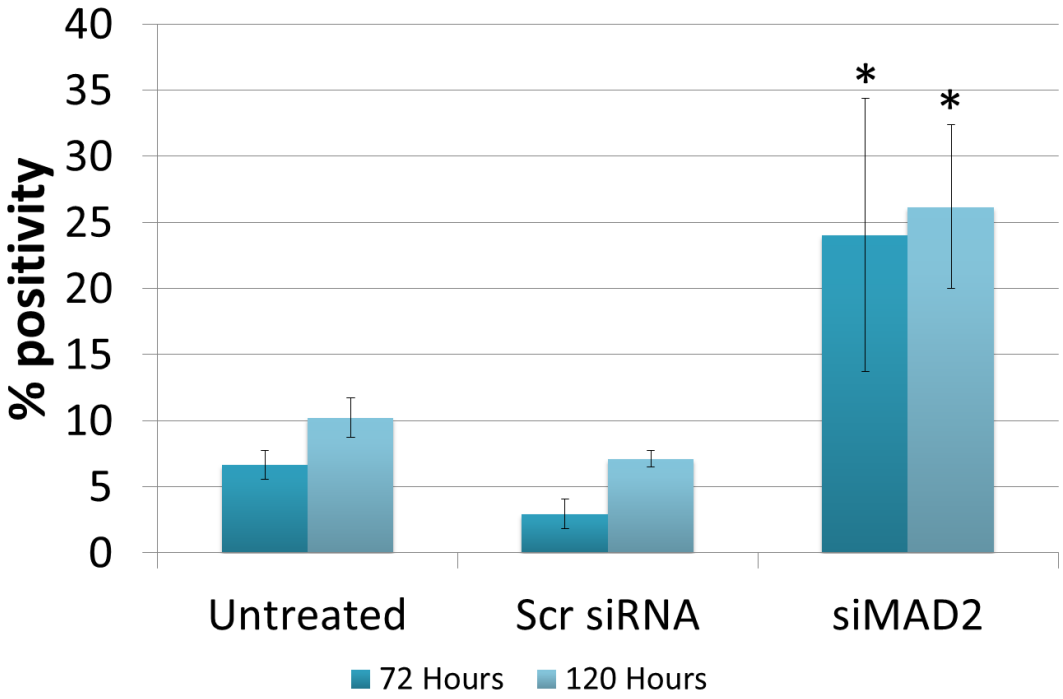

Figure 5.8 β-Galactosidase staining in SKOV-3 cells following knockdown of MAD2. SKOV-3 cells were transfected with siRNA targeting MAD2 (siMAD2), a scrambled non-targeting negative control siRNA (Scr siRNA) or were left untreated for 72 hours or 120 hours. After 72 hours or 120 hours, cells were stained using the β-Galactosidase staining kit (Cell Signalling). Images were then taken at 10X magnification using an Olympus CKX41microscope and an Olympus E600 camera (A). The percentage of β-galactosidase positive cells was then calculated for each condition for (n=3) technical and (n=3) biological replicates. Results are expressed as mean +/-SD, n=3; *p<0.05, **p<0.01 Student's t-test).

5.4.3 Knockdown of MAD2 in SKOV-3 and A2780 cells increases the expression of TLR4 but not MyD88

Following optimisation of the MAD2 knockdown protocol in both A2780 and SKOV-3 cells, TLR4 and MyD88 expression was also analysed in these samples in order to assess any potential relationship between MAD2 and TLR4 or MyD88 **(Figure 5.9)**. In both cell lines knockdown of MAD2 induced a 3 fold upregulation of TLR4 mRNA expression but had no impact on MyD88 expression. These results demonstrate that siRNA knockdown of MAD2 is capable of increasing the expression levels of TLR4, demonstrating a previously never before shown link between these genes. Following confirmed knockdown of MAD2 at the gene level, knockdown of MAD2 at protein level and its impact on TLR4 and MyD88 protein expression was investigated. Therefore SKOV-3 cells were transfected with siRNA targeting MAD2 for 72 hours. After 72 hours, protein was harvested and western blot analysis was performed for TLR4, MyD88 and GAPDH in SKOV-3 cells only **(Figure 5.10).** In SKOV-3 cells knockdown of MAD2 did not seem to have any impact on TLR4 or MyD88 protein expression.

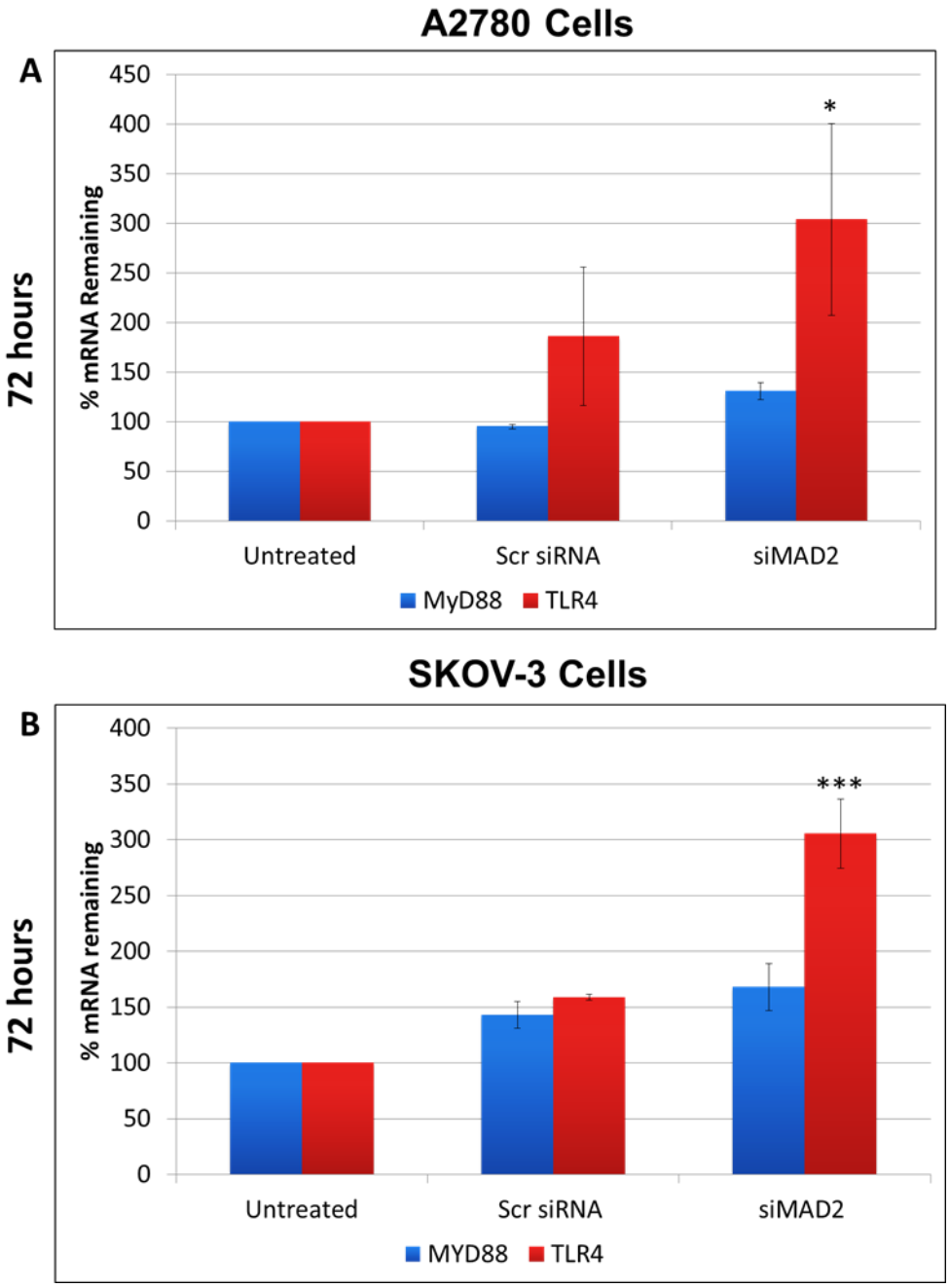

Figure 5.9 A2780 and SKOV-3 TLR4 and MyD88 mRNA expression 72 hours after transfection with siRNA targeting MAD2. A2780 (A) and SKOV-3 cells (B) were transfected with with siRNA targeting MAD2 (siMAD2), a scrambled negative control siRNA (Scr siRNA) or were left untreated for 72 hours. After 72 hours, RNA was harvested and then mRNA expression levels were analysed using TaqMan RT-PCR. TLR4 and MyD88 mRNA expression levels were normalised to the endogenous control GAPDH and calibrated to that of untreated cells to establish the relative change in mRNA expression (% mRNA remaining). Knockdown of MAD2 in both SKOV-3 and A2780 cells resulted in a 3 fold increase in TLR4 expression, but had no impact on MyD88 expression. Results are expressed as mean +/-SD, n=3; *p<0.05, **p<0.01, ***p<0.001 (Student's t-test).

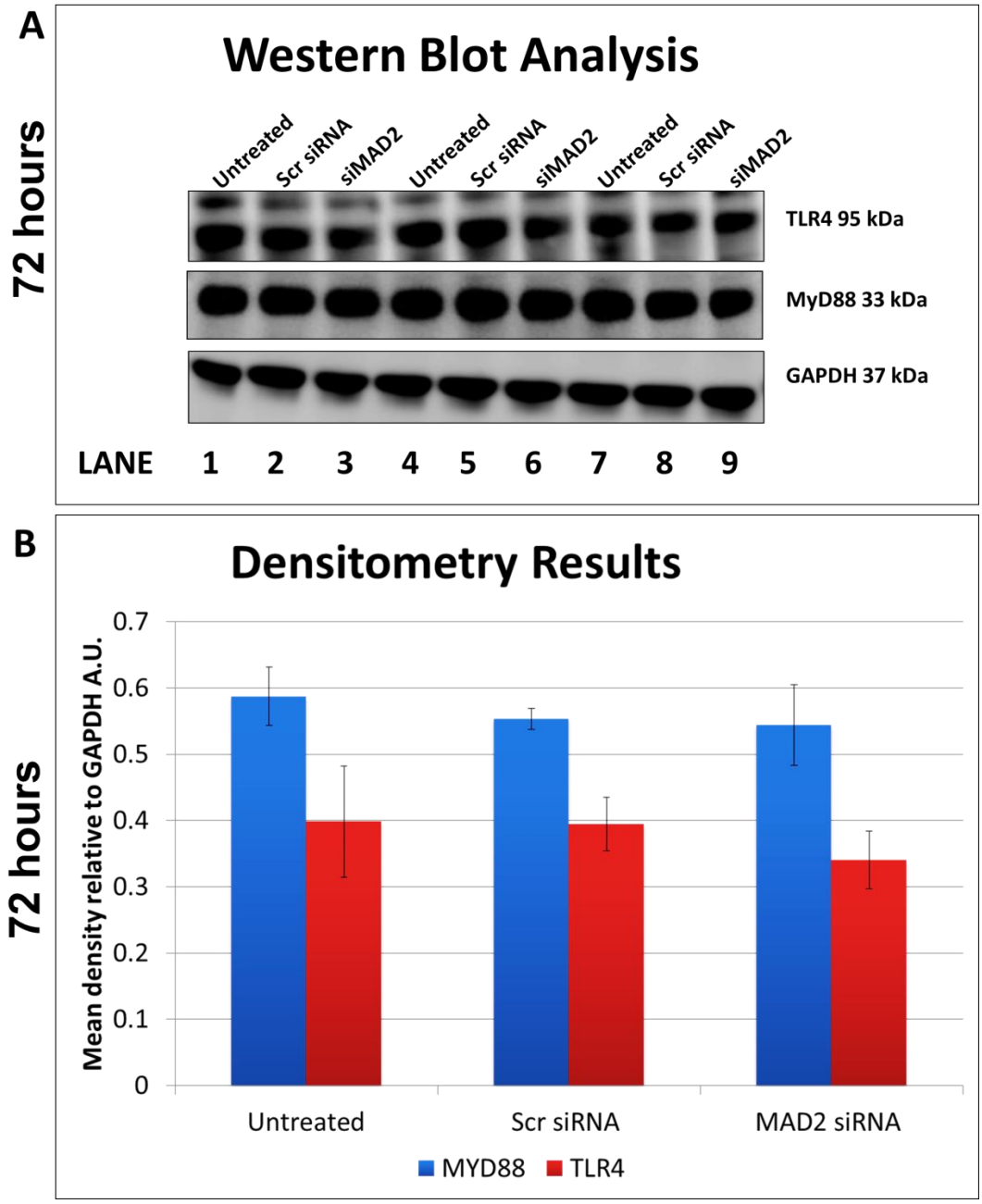

Figure 5.10 SKOV-3 TLR4 and MyD88 protein expression 72 hours following knockdown of MAD2. SKOV-3 cells were transfected with siRNA targeting MAD2 (siMAD2) a negative control siRNA (Scr siRNA) or were left untreated for 72 hours. After 72 hours, protein was harvested using RIPA lysis buffer and then western blot analysis was performed for MyD88, TLR4 and GAPDH in SKOV-3 cells. Chemiluminescence images were developed using a Fujifilm LAS-4000 luminescent image analyser. Densitometry was then carried out using Quantity One software (Biorad). Protein expression is represented as the mean density normalised to GAPDH in arbitrary units (A.U.) for each condition. The results demonstate that knockdown of MAD2 did no impact on MyD88 or TLR4 protein expression levels in SKOV-3 cells. Results are expressed as mean +/-SD, n=3.

5.4.4 Loss of MAD2 expression does not impact on the expression of its regulatory microRNA miR-433 or the expression of the TLR4-MyD88 pathway microRNAs miR-146a and miR-21

As knockdown of MAD2 in both A2780 and SKOV-3 cells had been shown by our group to induce paclitaxel resistance and increase the expression of TLR4 mRNA, it was decided to assess what impact this was having on regulatory microRNA expression. Therefore, the expression levels of the MAD2 regulatory microRNA miR-433 and the TLR4-MyD88 pathway regulatory microRNAs miR-146a and miR-21 were analysed following knockdown of MAD2 for 72 hours in both cell models **(Figure 5.11 & Figure 5.12)**. It was hypothesised that examining the expression of these microRNA post knockdown might give further insight into the relationship between TLR4 and MAD2 and their roles in paclitaxel resistance. Due to low expression levels of miR-433, which was detected between 35-43 Cts, the expression levels of miR-433 are represented by Delta Ct values for each condition **(Figure 5.12)**. No changes in miR-21, miR-146a or miR-433 were detected in either cell model following knockdown of MAD2.

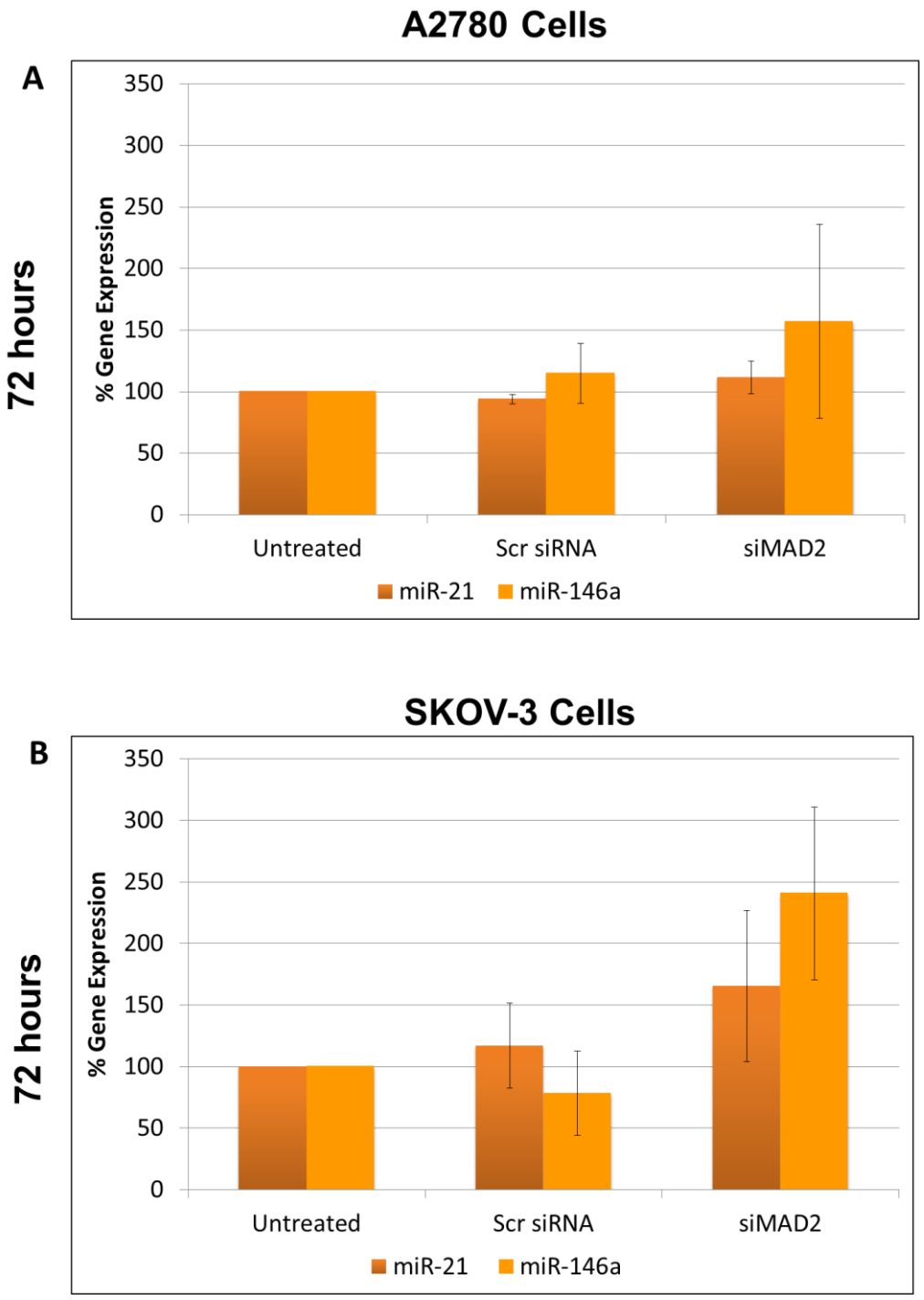

Figure 5.11 A2780 and SKOV-3 miR-146a and miR-21 expression 72 hours after transfection with siRNA targeting MAD2. Following knockdown of MAD2 at 72 hours miR-146a and miR-21 expression levels were measured in A2780 (A) and SKOV-3 cells (B) transfected with siRNA targeting MAD2 (siMAD2), a non-targeting scrambled negative control siRNA (Scr siRNA) or untreated cells. Following confirmed knockdown of MAD2 in each cell line, miR-146a and miR-21 expression levels were measured using TaqMan RT-PCR. miR-146a and miR-21 expression levels were normalised to the endogenous control miR-16 and calibrated to that of untreated cells (% Gene Expression). Following knockdown of MAD2, no significant change in the levels of miR-146a and miR-21 was observed. Results are expressed as mean +/-SD, n=3.

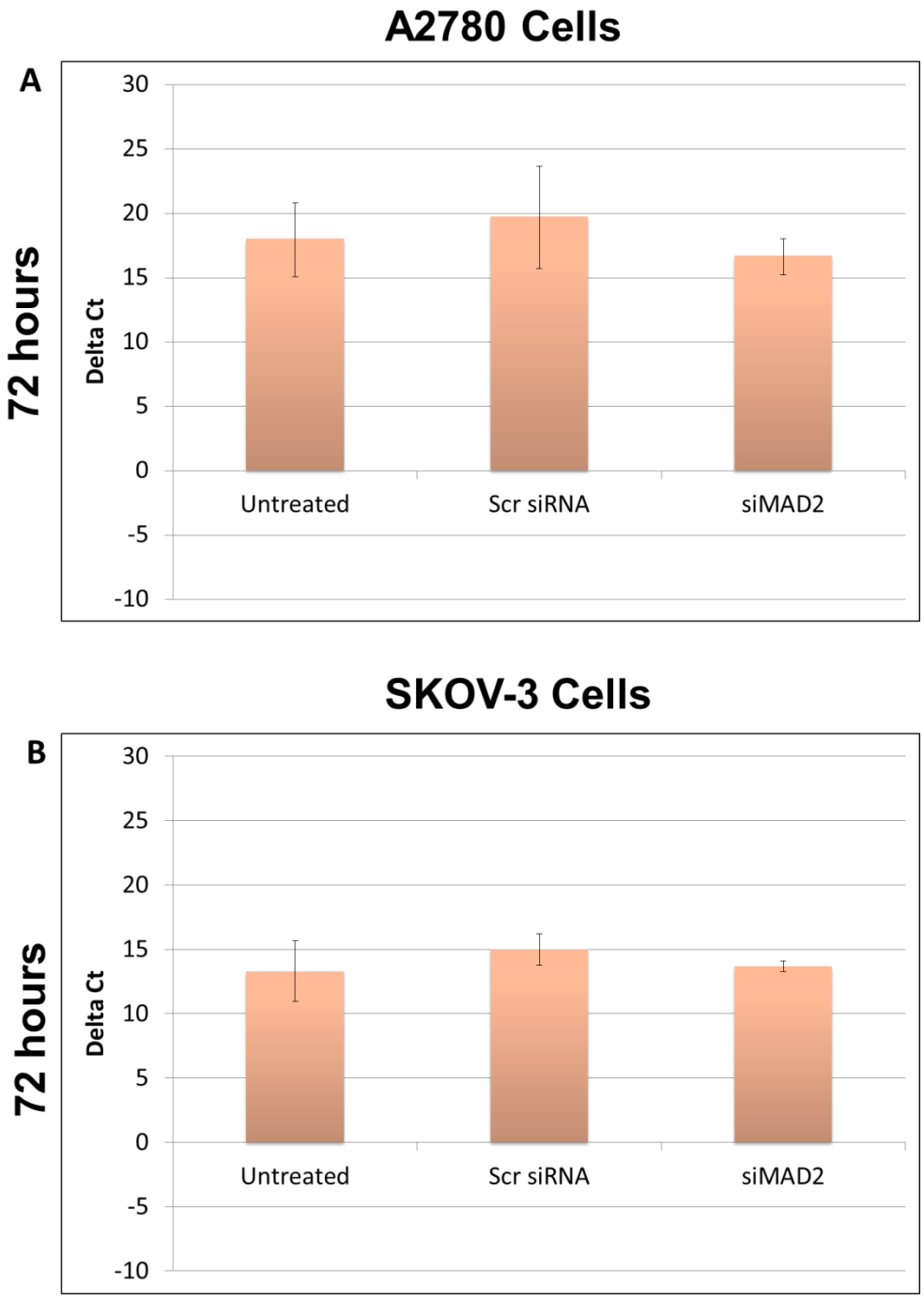

Figure 5.12 A2780 and SKOV-3 miR-433 expression 72 hours after transfection with siRNA targeting MAD2. Following knockdown of MAD2 at 72 hours miR-433 expression levels were measured in A2780 (A) and SKOV-3 cells (B) transfected with siRNA targeting MAD2 (siMAD2), a non-targeting scrambled negative control siRNA (Scr siRNA) or untreated cells. Following confirmed knockdown of MAD2 in each cell line, miR-433 expression levels were measured using TaqMan RT-PCR. No significant change in miR-433 was detected in either cell line following knockdown of MAD2.The Delta Ct values for miR-433 under each condition are displayed on the y axis of each graph n=3, +/-SD.

5.4.5 Microarray analysis following knockdown of MAD2 in SKOV-3 cells

Following assessment of the MAD2 knockdown in SKOV-3 on paclitaxel sensitivity and discovery of its effect on TLR4 mRNA expression, microarray analysis was performed. This was done in order to identify key molecular pathways involved in this acquired paclitaxel resistance and further discern a link between the TLR4-MyD88 pathway and MAD2. It was decided to also cross-compare microarray analysis performed following knockdown of TLR4 (Chapter 3). This was performed in order to identify any differentially expressed genes affected in both data sets that might give further insight into the cross-talk that occurs between the two pathways. A 1.5 fold change in gene expression and a p value of ≤0.05 was set as the threshold for a significantly upregulated/downregulated gene identified from microarray analysis. When MAD2 was knocked down in the SKOV-3 cell model 124 protein coding genes were found to be upregulated and 111 protein coding genes were found to be downregulated. The top 20 upregulated and top 20 downregulated genes identified following knockdown of MAD2 are displayed in **(Table 5.1)** and **(Table 5.2)** respectively.

Table 5.1 Top 20 upregulated genes following knockdown of MAD2 for 72 hours in SKOV-3 cells.

Ensemble Gene ID	Description	Fold Change
ENSG00000035664	Death-associated protein kinase 2	2.1
ENSG00000184831	Apolipoprotein O	2.1
ENSG00000100292	Heme oxygenase (decycling) 1	2.1
ENSG00000186529	Cytochrome P450, family 4, subfamily F, polypeptide 3	2.0
ENSG00000164008	Chromosome 1 open reading frame 50	2.0
ENSG00000169067	Actin, beta-like 2	2.0
ENSG00000187689	Amelotin	2.0
ENSG00000149591	Transgelin	1.9
ENSG00000130305	NOP2/Sun domain family, member 5	1.9
ENSG00000197557	Tetratricopeptide repeat domain 30A	1.9
ENSG00000155265	Golgin A7 family, member B	1.9
ENSG00000188056	Triggering receptor expressed on myeloid cells-like 4	1.9
ENSG00000172548	NIPA-like domain containing 4	1.8
ENSG00000137673	Matrix metallopeptidase 7 (matrilysin, uterine)	1.8
ENSG00000164683	HES-related family bHLH transcription factor with YRPW motif 1	1.8
ENSG00000266996	Transcription elongation factor B polypeptide 3C-like 2	1.8
ENSG00000112541	Phosphodiesterase 10A	1.8
ENSG00000161921	Chemokine (C-X-C motif) ligand 16	1.8
ENSG00000075043	Potassium voltage-gated channel, KQT-like subfamily, member 2	1.7
ENSG00000100031	Gamma-glutamyltransferase 1	1.7

Ensemble Gene ID - Unique gene ID, **Description** - Gene name, **P-value** - the significance value of the expression change observed. **Fold change** - indicates the degree of expression change. The fold change indicates the degree of expression change. A 1.5 fold change in gene expression and a p value of ≤0.05 was set as the threshold for a significant alteration in gene expression.

Table 5.2 Top 20 downregulated genes following knockdown of MAD2 for 72 hours in SKOV-3 cells.

Ensemble Gene ID	Description	Fold Change
ENSG00000164109	MAD2 mitotic arrest deficient-like 1 (yeast)	3.2
ENSG00000124900	Tripartite motif-containing 51	2.2
ENSG00000154229	Protein kinase C, alpha	2.2
ENSG00000255012	Olfactory receptor, family 5, subfamily M, member 1	2.1
ENSG00000221955	Solute carrier family 12, member 8	2.1
ENSG00000173406	Dab, reelin signal transducer, homolog 1 (Drosophila)	2.1
ENSG00000244624	Keratin associated protein 20-1	2.1
ENSG00000186458	Defensin, beta 132	2.0
ENSG00000177688	Small ubiquitin-like modifier 4	2.0
ENSG00000204700	Olfactory receptor, family 2, subfamily J, member 2	1.9
ENSG00000222031	HCG1817310; Uncharacterized protein	1.9
ENSG00000240542	Keratin associated protein 9-1	1.9
ENSG00000272514	UPF0704 protein C6orf165	1.9
ENSG00000213366	Glutathione S-transferase mu 2 (muscle)	1.9
ENSG00000111670	N-acetylglucosamine-1-phosphate transferase, alpha and beta subunits	1.9
ENSG00000212725	Keratin associated protein 2-1	1.8
ENSG00000242265	Paternally expressed 10	1.8
ENSG00000140368	Proline-serine-threonine phosphatase interacting protein 1	1.8
ENSG00000124693	Histone cluster 1, H3b	1.8
ENSG00000165621	Oxoglutarate (alpha-ketoglutarate) receptor 1	1.8

Ensemble Gene ID-Unique gene ID, **Description**- Gene name, **P-value** -the significance value of the expression change observed. **Fold change** -indicates the degree of expression change. The fold change indicates the degree of expression change. A 1.5 fold change in gene expression and a p value of ≤0.05 was set as the threshold for a significant alteration in gene expression.

5.4.5.1 Cross-comparison of differentially expressed genes following knockdown of TLR4 and MAD2

Microarray analyses exploring the effect of knockdown of TLR4 in SKOV-3 cells (Chapter 3) and the effect of knockdown of MAD2 in SKOV-3 cells (Chapter 5) were cross compared in order to identify any further potential links between MAD2 and TLR4 and the paclitaxel resistance mechanisms in which they are involved. When microarray data sets were compared following knockdown of TLR4 and MAD2, 12 genes were found to be significantly deregulated in both data sets **(Table 5.3)**. Cbp/p300-interacting transactivator, with Glu/Asp-rich carboxy-terminal domain 4 (CITED 4) was upregulated in both data sets. Family with sequence similarity 153, member B (FAM153B), olfactory receptor family 5 subfamily I member 1 (OR5L1), paternally expressed 10 (PEG10) and serglycin (SRGN) were downregulated in both data sets. Two genes CDC2B protein kinase regulatory subunit 2 (CKS2) and collagen and calcium binding EGF domain 1 (CCBE1) were downregulated by knockdown of MAD2 and upregulated following knockdown of TLR4. Five proteins actin beta like 2 (ACTBL2), amelotin (AMTN), lysozyme like 1 (LYZL1), matrix metallopeptidase 12 (MMP12) and plexin domain containing 2 (PLXDC2) were upregulated by knockdown of MAD2 and downregulated by knockdown of TLR4.

Table 5.3 Cross-comparison of genes differentially expressed following knockdown of TLR4 and MAD2.

Description
Upregulated by knockdown of MAD2 and TLR4
Cbp/p300-interacting transactivator, with Glu/Asp-rich carboxy-terminal domain, 4
Downregulated by knockdown of MAD2 and upregulated by knockdown of TLR4
CDC28 protein kinase regulatory subunit 2
Collagen and calcium binding EGF domains 1
Upregulated by knockdown of MAD2 and downregulated by knockdown of TLR4
Actin, beta-like 2
Amelotin
Lysozyme-like 1
Matrix metallopeptidase 13 (collagenase 3)
Plexin domain containing 2
Downregulated by knockdown of MAD2 and TLR4
Family with sequence similarity 153, member B
Olfactory receptor, family 5, subfamily I, member 1
Paternally expressed 10
Serglycin

5.4.5.2 Gene ontology analysis

Gene lists of the differentially expressed genes identified following knockdown of MAD2 were analysed using the online gene ontology database DAVID in order to identify over-represented pathways, cellular components, molecular functions and biological processes. Significantly over-represented pathways identified by the DAVID & KEGG databases following knockdown of MAD2 including pathways involved in systemic lupus erythematosus, sphingolipid metabolism, olfactory transduction, smooth muscle contraction, vascular smooth muscle contraction and Arachidonic acid metabolism **(Table 5.4)**. Molecular functions highlighted by DAVID included olfactory receptor activity, insulin-like growth factor binding activity, phospholipase activity, lipase activity and transcription coactivator activity **(Table 5.5)**. Cellular components over-represented following knockdown of MAD2 including components of the extracellular matrix, extracellular space, Protein-DNA complexes, genes associated with the nucleosome, chromatin and chromosomes, and the insulin-like growth factor binding protein complex **(Table 5.6)**.

Table 5.4 Significantly over-represented pathways identified by the DAVID & KEGG databases following a 72 hour knockdown of MAD2 in SKOV-3 cells.

Pathways	Count	%	P-Value
Systemic lupus erythematosus	7	3.3	0.0032
Sphingolipid metabolism	4	1.9	0.019
Olfactory transduction	12	5.7	0.022
Vascular smooth muscle contraction	6	2.8	0.024
Arachidonic acid metabolism	4	1.9	0.049

Pathways – The different pathways over-represented following knockdown of MAD2 are represented in column 1. **P-value** – the significance value of the expression change observed, a p value of ≤0.05 was set as the threshold for a significant alteration in pathway expression. **Count** – The number of genes involved in a particular pathway which was found to be over-represented following knockdown of MAD2. **%** – Percentage of genes affected out of the total number of genes altered following knockdown of MAD2.

Table 5.5 Significantly over-represented molecular functions identified by the DAVID database following a 72 hour knockdown of MAD2 in SKOV-3 cells.

Molecular Functions	Count	%	P-Value
Olfactory receptor activity	12	5.7	0.0081
Insulin-like growth factor binding	3	1.4	0.031
Phospholipase activity	4	1.9	0.064
Insulin-like growth factor I binding	2	0.9	0.064
Transcription coactivator activity	6	2.8	0.088
Lipase activity	4	1.9	0.098

Molecular Functions – The different molecular functions over-represented following knockdown of MAD2 are represented in column 1. **P-value** – the significance value of the expression change observed, a p value of ≤0.05 was set as the threshold for a significant alteration in molecular function. **Count** – The number of genes involved in a particular pathway which was found to be over-represented. **%** – Percentage of genes affected out of the total number of genes altered following knockdown of MAD2.

Table 5.6 Significantly over-represented cellular components identified by the DAVID database following a 72 hour knockdown of MAD2 in SKOV-3 cells.

Cellular Components	Count	%	P-Value
Extracellular space	24	11.4	0.0000023
Extracellular region part	28	13.3	0.0000079
Protein-DNA complex	8	3.8	0.000051
Nucleosome	7	3.3	0.000074
Extracellular region	37	17.5	0.0025
Chromatin	8	3.8	0.0075
Proteinaceous extracellular matrix	10	4.7	0.01
Extracellular matrix part	6	2.8	0.01
Extracellular matrix	10	4.7	0.016
Chromosomal part	10	4.7	0.031
Chromosome	11	5.2	0.035
Insulin-like growth factor binding protein complex	2	0.9	0.044

Cellular Components – The different cellular components over-represented following knockdown of MAD2 are represented in column 1. **P-value** – the significance value of the expression change observed, a p value of ≤0.05 was set as the threshold for a significant alteration in a particular cellular component. **Count** – The number of genes involved in a particular cellular component which was found to be over-represented. **%** – Percentage of genes affected out of the total number of genes altered following knockdown of MAD2.

Forty-four biological processes were significantly over-represented following knockdown of MAD2. The top 30 biological processes identified by the DAVID database following knockdown of MAD2 **(Table 5.7)**. Of the biological processes over-represented were processes involved in chromatin rearrangement, DNA packaging, regulation of cell migration and locomotion, ossification and bone development, response to various organic substances and ion transmembrane transport among others. For interpretation of these results **(See Section 5.5)**.

Table 5.7 The top 30 significantly over-represented biological processes identified by the DAVID database following a 72 hour knockdown of MAD2 in SKOV-3 cells.

Biological Process	Count	%	P-Value
Nucleosome assembly	7	3.3	0.00035
Chromatin assembly	7	3.3	0.00042
Protein-DNA complex assembly	7	3.3	0.00053
Chromatin assembly or disassembly	8	3.8	0.00055
Nucleosome organization	7	3.3	0.0006
DNA packaging	7	3.3	0.002
Sensory perception of smell	13	6.2	0.0032
Response to endogenous stimulus	12	5.7	0.0057
Sensory perception of chemical stimulus	13	6.2	0.0073
Biomineral formation	4	1.9	0.008
Ossification	6	2.8	0.0093
Response to organic cyclic substance	6	2.8	0.011
Bone development	6	2.8	0.012
Response to organic substance	16	7.6	0.015
Response to tropane	3	1.4	0.019
Response to cocaine	3	1.4	0.019
Collagen catabolic process	3	1.4	0.021
Regulation of locomotion	7	3.3	0.021
Response to steroid hormone stimulus	7	3.3	0.021
Response to hormone stimulus	10	4.7	0.022
Response to alkaloid	4	1.9	0.022
Cognition	18	8.5	0.025
Regulation of blood pressure	5	2.4	0.026
Negative regulation of cell migration	4	1.9	0.026
Regulation of ion transmembrane transporter activity	3	1.4	0.029
Response to estrogen stimulus	5	2.4	0.03
Negative regulation of locomotion	4	1.9	0.031
Regulation of foam cell differentiation	3	1.4	0.031
Regulation of ion transmembrane transport	3	1.4	0.031
Negative regulation of cell motion	4	1.9	0.033

Biological Process – The different biological processes over-represented following knockdown of MAD2 are represented in column 1. **P-value** – the significance value of the expression change observed, a p value of ≤0.05 was set as the threshold for a significant alteration in a biological process. **Count** – The number of genes involved in a particular biological process which was found to be over-represented. **%** – Percentage of genes affected out of the total number of genes altered following knockdown of MAD2.

5.5 Discussion

Low MAD2, high MyD88 and high TLR4 expression levels have previously been linked to poor patient prognosis (Silasi et al. 2006; Kim & Yoon 2010; Kim et al. 2012; Zhu et al. 2012; Furlong et al. 2012; Park et al. 2013; McGrogan et al. 2014; d'Adhemar et al. 2014). Furthermore all three biomarkers have been shown to play a role in paclitaxel resistance *in-vitro* (Kelly *et al*. 2006; Szajnik *et al*. 2009; Prencipe *et al*. 2009; Furlong *et al*. 2012; d'Adhemar *et al*. 2014; Wang *et al*. 2014). Downregulation of MAD2 has been shown occur in hypoxic tumour regions (Prencipe *et al*. 2010) and is linked to aberrant spindle assembly and the induction of senescence. While high TLR4 and MyD88 expression in patient tumours is linked to cytokine expression and the induction of pro-survival genes and may also potentially highlight a subpopulation of ovarian cancer stem cells (Alvero *et al*. 2011).

Previously it had been shown that knockdown of MAD2 in MCF-7 and A2780 cells induced paclitaxel chemoresistance and the induction of cellular senescence (Prencipe *et al*. 2009; Furlong *et al*. 2012). In this study, knockdown of MAD2 in SKOV-3 cells similarly, rendered these cells highly resistant to paclitaxel. SKOV-3 cells were shown to be resistant to 1µM paclitaxel a dose nearly 200X the IC_{50} for these cells (7nM) and this was attributed to the induction of cellular senescence. We believe these cells are senescent as they demonstrate an increase in β-galactosidase activity and visually display cell enlargement and reduced proliferation rates. In a study by Hao *et al*. (2010), it was reported that overexpression of MAD2 in SKOV-3 cells rendered these cells more chemosensitive to paclitaxel therapy, suggesting that MAD2 plays a role in modulating paclitaxel sensitvity in this cell model. The effect on paclitaxel chemoresponsiveness in SKOV-3 cells following kncokdown of MAD2 demonstrated in this chapter is an interesting result, as it could have very important clinical implications, as those with a MAD2 low phenotype are highly unlikely to respond to paclitaxel chemotherapy.

In-silico analysis predicted no interaction or pathway linkage between TLR4, MyD88 and MAD2 (Chapter 3). Furthermore the previous two chapters showed no changes in MAD2 expression following knockdown of TLR4 or MyD88 in SKOV-3 cells or overexpression of MyD88 in A2780 cells. Therefore it was anticipated that knockdown of MAD2 would have no impact on TLR4 or MyD88 expression patterns. However, interestingly in this chapter it was demonstrated that knockdown of MAD2 in both A2780 and SKOV-3 cells led to a 3-fold upregulation of TLR4 mRNA. This is an interesting link between TLR4 and MAD2 that has never been shown before. This has

important implications for ovarian cancer and paclitaxel therapy, as patients may not only be chemoresistant as a result of the downregulation of MAD2 but also due to a concomitant upregulation of TLR4. However this was only demonstrated at the mRNA level and not at the protein level, therefore closer examination of this relationship between MAD2 and TLR4 will need to be explored. TLR4 protein expression post knockdown of MAD2 was also only analysed in a single cell model at a single timepoint. Examination of TLR4 protein in additional cell models post knockdown of MAD2 at additional timepoints may reveal an effect on TLR4 protein expression. The fact that TLR4 protein expression was not upregulated here may be due to a delay in TLR4 mRNA translation or perhaps due to some posttranslational modification such as ubiquitination as result of the induction of senescence.

An important characteristic of senescence is the development of what is known as a senescence associated secretory phenotype (SASP). Following the induction of senescence, senescent cells begin to secrete a variety of factors including various cytokines and chemokines. Previously our group demonstrated that following the induction of senescence in the ovarian cancer cell lines PEO1 and PEO4 results in an increase in the secretion of both IL-6 and IL-8 (Weiner-Gorzel *et al*. 2015). We hypothesise that knockdown of MAD2 in the SKOV-3 cell results in the development of a SASP phenotype and the production of various chemokines such as IL-6. IL-6 and possibly other cytokines potentially then induce an upregulation in TLR4 gene expression (**Figure 5.13)**. IL-6 has previously been shown to upregulate TLR4 cell surface expression and increased the ability to activate NFκB and activator protein 1 (AP-1) after LPS stimulation in human monocytes (Tamandl *et al*. 2003). IL-6 has also been shown to transmodulate TLR4 signalling through STAT6 in *in-vivo* mouse models (Greenhill *et al*. 2010). Other cytokines such as TNF-α (Greenhill *et al*. 2010) IL-18 (Dias-melicio *et al*. 2015) and IL-27 (Guzzo *et al*. 2011) similarly are capable of regulating the expression of TLR4 expression and various other cytokines produced by the induction of a SASP phenotype may also have an impact upon TLR4 expression. IL-6 and other cytokines though both autocrine and paracrine signalling drive up the expression of TLR4 further promoting paclitaxel chemoresistance. The end product of this is the potential establishment of a lethal phenotype which survives chemotherapy and drives the development chemoresistance and recurrent disease.

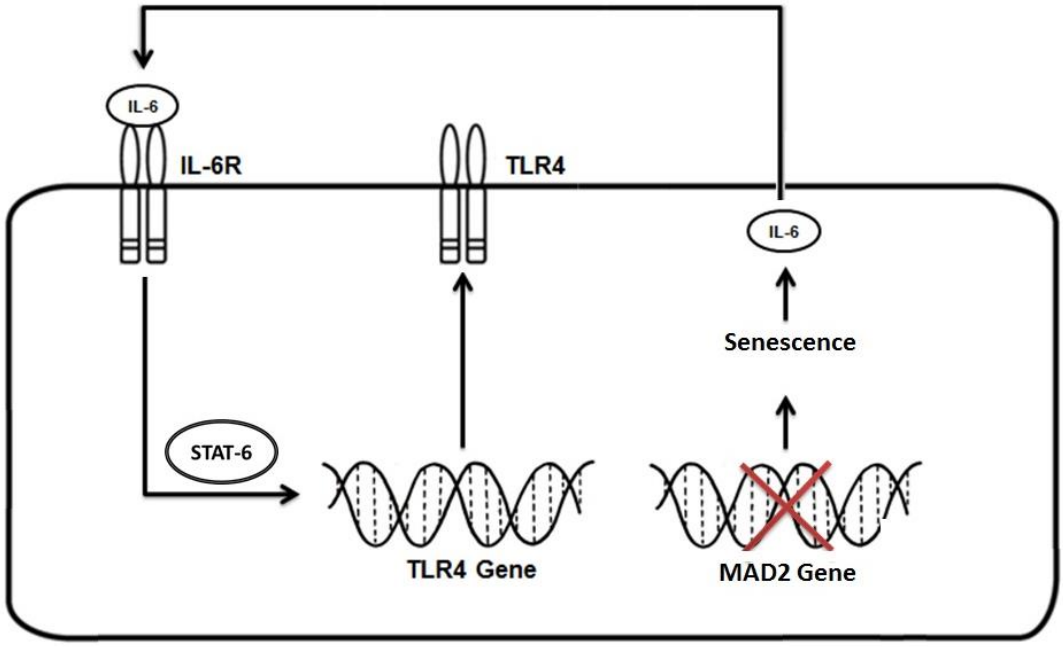

Figure 5.13 Proposed model for regulation of TLR4 signalling by IL-6. Downregulation of MAD2 induces the production of various cytokines including IL-6 as part of a SASP phenotype. IL-6 then activates the transcription factor STAT-6 which in turn causes the upregulation of TLR4 gene expression. Adapted from (Greenhill *et al*. 2010).

Similar to previous chapters microRNA expression levels remained unchanged despite highly significant knockdown of MAD2 in both A2780 and SKOV-3 cells. However despite this it is clear from the work performed with miR-433 by Furlong *et al* (2012) and Weiner-Gorzel *et al* (2015) that microRNAs play an important role to play in paclitaxel resistance in ovarian cancer. Overexpressing the regulatory microRNAs miR-146a and miR-21 may give further insight into their role in ovarian cancer and the regulation of TLR4 and MyD88 gene expression.

Microarray analysis following knockdown of MAD2 was performed to identify global changes in gene expression and identify molecular pathways involved in paclitaxel resistance. It was also performed in order to identify molecular links between the TLR4-MyD88 pathway and MAD2. Upon cross comparison of the microarray analyses performed following knockdown of TLR4 and MAD2 a small number of protein coding genes were found to be differentially expressed in both data sets. Gene ontology analysis highlighted a number of different processes being affected following knockdown of MAD2 in the SKOV-3 cells. Among these were perception of smell and olfactory receptor activity, insulin like growth factor binding activity. Some of the main cellular components affected were the extracellular matrix and the

nucleus/chromosomes. Other processes highlighted were the response to a number of different chemical stimuli, cell motility, collagen and bone catabolism and ion transporter activity.

Insulin growth factor binding activity was significantly over-represented following knockdown down of MAD2. Various members of this family and their receptors are known to be upregulated following the induction of a SASP phenotype. These include IGFBP2, IGFBP3, IGFBP4, IGFBP5, IGFBP6, IGFBPRP1 and IGFBPRP2 (Martin *et al*. 1997; Wang *et al*. 1996; Kim, Seu, *et al*. 2007; Severino *et al*. 2013). As IGFs play an important role in regulation of cell growth, differentiation and apoptosis, it is possible that the upregulation of IGFBPs likely occurs in an attempt to counteract these effects during senescence. Interestingly upregulation of IGFBP3 and IGFBP5, both of which were upregulated in this study, has been shown to accelerate cellular senescence (Kim, Kim, *et al*. 2007; Chen *et al*. 2008).

Ion transporter activity was significantly over-represented by gene ontology analysis. Ion transporters encompass a huge class of proteins which regulate the entry of various molecules into the cytosol. Ion channels have been shown to contribute to tumourigenesis, through their various roles in cell proliferation, cell invasiveness, chemoresistance, angiogenesis, cell cycle regulation and apoptosis (Arcangeli & Becchetti 2010; Litan & Langhans 2015). Alteration in ion transporter activity may be as result of the increase in cell size that was observed following knockdown of MAD2 in these cells. As with the increasing size, a greater degree of ion channel activity may be needed to maintain homeostasis within the cell. Certain ion channels are reported to be associated with the induction of senescence in both cancerous and non-cancerous cells including calcium and potassium channels (Wohlrab *et al*. 1988; Elble & Pauli 2001; Yee, Brown, *et al*. 2012; Tanikawa *et al*. 2012; Yee, Zhoud, *et al*. 2012; Lansu & Gentile 2013; Wiel *et al*. 2014).

Gene ontology highlighted genes involved in negative regulation of cell migration as significantly over-represented. Three of the four genes involved, dopamine receptor D2, heme oxygenase decycling 1 and Insulin-like growth factor binding protein 3 were upregulated. As these cells are likely in a senescent state they no longer require the use of motility associated genes. One of the roles of senescence is to serve as an anti-neoplastic response, therefore limiting motility in these cells is essential, to prevent invasion and metastasis.

Microscopically following knockdown of MAD2, an increase in nuclear size was observed. A known feature of senescent cells is that they exhibit an unusual pattern of

heterochromatin, that is present in discrete nuclear subdomains, known as senescence-associated heterochromatic foci (SAHFs)(Sharpless & Sherr 2015). This may explain why changes in the nucleus, nucleolus, chromosomes and DNA packaging were highlighted by gene ontology analysis. Among the genes affected following knockdown of MAD2 were members of the histone family, all of which were downregulated. These genes play a key role in DNA packaging, their downregulation suggests that DNA is less tightly packed and would explain the change in nuclear size that was observed. Besides the nucleus, the extracellular matrix was the main cellular component found to be altered by microarray analysis. This likely reflects the huge increase in cell size that was observed following knockdown of MAD2. Following the induction of a SASP phenotype various proteases known to be involved in ECM remodelling are known to be expressed including members of the MMP family (Zeng & Millis 1996; West *et al*. 1989; Millis *et al*. 1992; McQuibban *et al*. 2002; Blasi & Carmeliet 2002). In this study MMPs 2,7,13 were all found to be upregulated following knockdown of MAD2.

Following knockdown of MAD2, SKOV-3 cells were shown to be senescent and highly resistant to paclitaxel. Cellular senescence occurs as result of loss of key tumour suppressor genes and through cellular stress from genotoxic stimuli (Pérez-Mancera *et al*. 2014). The induction of senescence may therefore induce the downregulation of various genes involved in the response to various toxic stimuli, which under normal circumstances may perhaps have induced cell death. Among the over-represented biological pathways highlighted in this study were the response to various stimuli including; organic cyclic substances, organic substances, endogenous stimuli, cocaine, tropane, alkaloids, steroid hormones and hormones. Ten out of seventeen genes involved in these processes were downregulated following knockdown of TLR4. These processes may have contributed to the increased resistance of these cells to paclitaxel.

Lipase activity was found to be over-represented by DAVID analysis following knockdown of MAD2. Mobilisation and breakdown of lipids may be an intrinsic feature of senescence. As although senescent cells are non-dividing, maintaining a senescent state is arguable permanent, maintaining this state likely requires a continual source of energy. Lipase and phospholipase activity may also reflect the change in cell size that occurred as a result of knockdown of MAD2. As lipids, phospholipids and cholesterol are huge components of cell membranes, they likely needed to be mobilised in order to help facilitate this massive increase in cell size and the accompanying increase in the size of the cell membrane. Arachidonic acid metabolism was also over-represented by

gene ontology analysis. This is a polyunsaturated fatty acid present in many membrane phospholipids. Increased arachidonic acid release has been shown to be a common feature of senescence (Lorenzini *et al*. 2001).

Interestingly similar to results found in chapter 3, a large number of members of the olfactory receptor family were downregulated following knockdown of MAD2. Our group has also found that olfactory receptors are downregulation during differentiation in the embryonal carcinoma 2102Ep model (Sulaiman 2015). Therefore downregulation of olfactory receptors may be and important event which occurs during both differentiation and senescence. A list of the various members of olfactory receptors which were differentially expressed following knockdown of MAD2 is displayed in **(Table S5)**. Among the olfactory receptors affected were members of the olfactory receptor families 1, 2, 3, 4, 5, 6, 52 and 56.

Cross-comparison of microarray data sets from chapter 3 and chapter 5 identified 12 common genes deregulated following knockdown of MAD2 or TLR4 **(Figure 5.14)**. Interestingly a number of these genes have been shown to contribute to tumourigenesis in different types of cancer including ovarian cancer (Kerkelä *et al*. 2000; Kerkelä *et al*. 2002; Okabe *et al*. 2003; Fox *et al*. 2004; Jie *et al*. 2007; Kainz *et al*. 2007; Barton *et al*. 2010; Shen *et al*. 2010; Menghi *et al*. 2011; Solár & Sytkowski 2011; Tanaka *et al*. 2011; Chen *et al*. 2011; Chang *et al*. 2011; Grasso *et al*. 2012; Martin *et al*. 2013; Del Rincón *et al*. 2014; Liu *et al*. 2014). Further analysis of these genes may help to further define the relationship between TLR4 and MAD2.

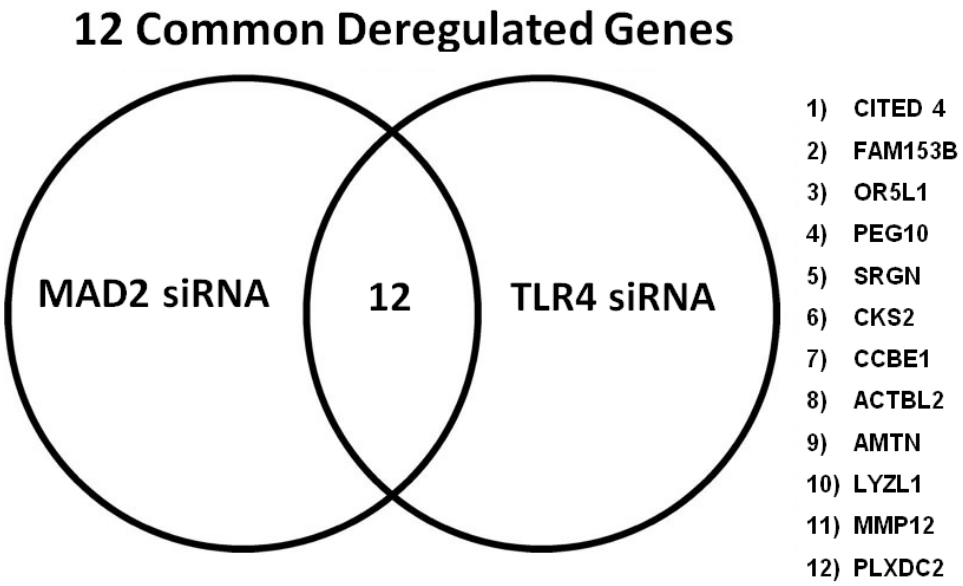

Figure 5.14 Twelve common deregulated genes. The 12 common genes deregulated following knockdown of TLR4 or MAD2 for 72 hours in SKOV-3 cells.

5.6 Conclusion

Knockdown of MAD2 in the SKOV-3 cell model, as has been shown with both A2780 cells and MCF-7 cells by our group previously, induced paclitaxel resistance. This paclitaxel resistance, as with the A2780 cells and MCF-7 cells, was attributed to the induction of senescence. These cells exhibited increased β-galactosidase activity and displayed an enlarged phenotype, which are known features of senescence. Microarray analysis following knockdown of MAD2 in SKOV-3 cells, identified a number of genes known to be upregulated during senescence that were affected. Knockdown of MAD2 in both the SKOV-3 and A2780 cells led to a 3 fold increase in TLR4 expression highlighting a never before shown molecular link between MAD2 and TLR4. Cross-comparison of microarray data sets also identified a number of genes differentially expressed in both data sets that may help further define the relationship between MAD2 and TLR4 that was highlighted in this study.

5.7 References

1) Alvero, A.B. et al., 2011. Molecular phenotyping of human ovarian cancer stem cells unravel the mechanisms for repair and chemo-resistance. *Cell Cycle*, 8(1), pp.158–166.
2) Arcangeli, A. & Becchetti, A., 2010. New trends in cancer therapy: Targeting ion channels and transporters. *Pharmaceuticals*, 3(4), pp.1202–1224.
3) Barton, C. a et al., 2010. Collagen and calcium-binding EGF domains 1 is frequently inactivated in ovarian cancer by aberrant promoter hypermethylation and modulates cell migration and survival. *British journal of cancer*, 102(1), pp.87–96.
4) Beauséjour, C.M. et al., 2003. Reversal of human cellular senescence: Roles of the p53 and p16 pathways. *EMBO Journal*, 22(16), pp.4212–4222.
5) Blasi, F. & Carmeliet, P., 2002. uPAR: a versatile signalling orchestrator. *Nature reviews. Molecular cell biology*, 3(12), pp.932–943.
6) Chang, K.W. et al., 2011. Overexpression of κ-actin alters growth properties of hepatoma cells and predicts poor postoperative prognosis. *Anticancer Research*, 31(6), pp.2037–2044.
7) Chen, D. et al., 2008. Multiple pathways differentially regulate global oxidative stress responses in fission yeast. *Molecular biology of the cell*, 19(1), pp.308–317.
8) Chen, R., Feng, C. & Xu, Y., 2011. Cyclin-dependent kinase-associated protein Cks2 is associated with bladder cancer progression. *The Journal of international medical research*, 39(2), pp.533–540.
9) d'Adhemar, C.J. et al., 2014. The MyD88+ Phenotype Is an Adverse Prognostic Factor in Epithelial Ovarian Cancer. *PloS one*, 9(6), p.e100816. Available at: http://www.ncbi.nlm.nih.gov/pubmed/24977712 [Accessed July 2, 2014].
10) Davalos, A.R. et al., 2010. Senescent cells as a source of inflammatory factors for tumor progression. *Cancer and Metastasis Reviews*, 29(2), pp.273–283.
11) Debacq-Chainiaux, F. et al., 2009. Protocols to detect senescence-associated beta-galactosidase (SA-betagal) activity, a biomarker of senescent cells in culture and in vivo. *Nature protocols*, 4(12), pp.1798–1806. Available at: http://dx.doi.org/10.1038/nprot.2009.191.
12) Dias-melicio, L.A. et al., 2015. Interleukin-18 Increases TLR4 and Mannose Receptor Expression and Modulates Cytokine Production in Human Monocytes. , 2015.
13) Dimri, G.P. et al., 1995. A biomarker that identifies senescent human cells in culture and in aging skin in vivo. , 92(September), pp.9363–9367.
14) Elble, R.C. & Pauli, B.U., 2001. Tumor suppression by a proapoptotic calcium-activated chloride channel in mammary epithelium. *The Journal of biological chemistry*, 276(44), pp.40510–40517.
15) Ffrench, B. et al., 2014. Developing ovarian cancer stem cell models: laying the pipeline from discovery to clinical intervention. *Molecular Cancer*, 13(1), p.262. Available at: http://www.molecular-cancer.com/content/13/1/262.
16) Finkel, T. & Holbrook, N.J., 2000. Oxidants, oxidative stress and the biology of ageing. *Nature*, 408(6809), pp.239–247.
17) Flint, D.J. et al., 2005. Insulin-like growth factor binding proteins initiate cell death and extracellular matrix remodeling in the mammary gland. In *Domestic Animal Endocrinology*. pp. 274–282.
18) Forloni, M. et al., 2014. miR-146a promotes the initiation and progression of melanoma by activating Notch signaling. *eLife*, 2014(3), pp.1–20.
19) Fox, S.B., Bragança, J. & Turley, H., 2004. CITED4 Inhibits Hypoxia-Activated Transcription in Cancer Cells , and Its Cytoplasmic Location in Breast Cancer Is Associated with Elevated Expression of Tumor Cell Hypoxia-Inducible Factor 1 α

CITED4 Inhibits Hypoxia-Activated Transcription in Cancer Cel. , (13), pp.6075–6081.
20) Furlong, F. et al., 2012. Low MAD2 expression levels associate with reduced progression-free survival in patients with high-grade serous epithelial ovarian cancer. *The Journal of pathology*, 226(5), pp.746–55. Available at: http://www.ncbi.nlm.nih.gov/pubmed/22069160 [Accessed February 23, 2013].
21) Gilkes, D.M., Semenza, G.L. & Wirtz, D., 2014. Hypoxia and the extracellular matrix: drivers of tumour metastasis. *Nature reviews. Cancer*, 14(6), pp.430–9. Available at: http://www.ncbi.nlm.nih.gov/pubmed/24827 502.
22) Giordano, C.R. & Terlecky, S.R., 2012. Peroxisomes, cell senescence, and rates of aging. *Biochimica et Biophysica Acta - Molecular Basis of Disease*, 1822(9), pp.1358–1362. Available at: http://dx.doi.org/10.1016/j.bbadis. 2012.03.013.
23) Gotanda, K. et al., 2013. MicroRNA-433 negatively regulates the expression of thymidylate synthase (TYMS) responsible for 5-fluorouracil sensitivity in HeLa cells. *BMC cancer*, 13(1), p.369. Available at: http://www.pubmedcentral. nih.gov/articlerender.fcgi?artid=3750578&tool=pmcentrez&rendertype=abstract.
24) Grasso, C.S. et al., 2012. The mutational landscape of lethal castration-resistant prostate cancer. *Nature*, 487(7406), pp.239–243.
25) Greenhill, C.J. et al., 2010. IL-6 Trans-Signaling Modulates TLR4-Dependent Inflammatory Responses via STAT3. *The Journal of Immunology*, 186(2), pp.1199–1208. Available at: http://www.jimmunol.org/cgi/doi/10.4049/jimmunol. 1002971.
26) Guzzo, C. et al., 2011. IL-27 Enhances LPS-Induced Proinflammatory Cytokine Production via Upregulation of TLR4 Expression and Signaling in Human Monocytes. *The Journal of Immunology*, 188(2), pp.864–873. Available at: http://www.jimmunol.org/cgi/doi/10.4049/jimmunol.1101912.
27) Hao, X. et al., 2010. Effect of Mad2 on paclitaxel-induced cell death in ovarian cancer cells. *Journal of Huazhong University of Science and Technology. Medical sciences = Hua zhong ke ji da xue xue bao. Yi xue Ying De wen ban = Huazhong keji daxue xuebao. Yixue Yingdewen ban*, 30(5), pp.620–5. Available at: http://www.ncbi.nlm.nih.gov/pubmed/2106 3845 [Accessed March 12, 2014].
28) Haussecker, D. & Kay, M. a, 2010. miR-122 continues to blaze the trail for microRNA therapeutics. *Molecular therapy : the journal of the American Society of Gene Therapy*, 18(2), pp.240–242. Available at: http://dx.doi.org/10.1038/ mt.2009.313.
29) Hsu, R.Y.C. et al., 2011. LPS-induced TLR4 signaling in human colorectal cancer cells increases B1 integrin mediated cell adhesion and liver metastasis. *Cancer Research*, 71(5), pp.1989–1998.
30) Huang, J.-M. et al., 2014. Atractylenolide-I sensitizes human ovarian cancer cells to paclitaxel by blocking activation of TLR4/MyD88-dependent pathway. *Scientific reports*, 4, p.3840. Available at: http://www.pubmedcentral.nih.gov/article render.fcgi? artid=3899591&tool=pmcentrez&rendertype=abstract [Accessed June 1, 2014].
31) Jie, X. et al., 2007. Androgen activates PEG10 to promote carcinogenesis in hepatic cancer cells. *Oncogene*, 26(39), pp.5741–5751.
32) Kainz, B. et al., 2007. Overexpression of the paternally expressed gene 10 (PEG10) from the imprinted locus on chromosome 7q21 in high-risk B-cell chronic lymphocytic leukemia. *International Journal of Cancer*, 121(9), pp.1984–1993.
33) Kelly, M.G. et al., 2006. TLR-4 signaling promotes tumor growth and paclitaxel chemoresistance in ovarian cancer. *Cancer research*, 66(7), pp.3859–68. Available at: http://www.ncbi.nlm.nih.gov/pubmed/16585214 [Accessed October 22, 2012].
34) Kerkelä, E. et al., 2000. Expression of human macrophage metalloelastase (MMP-12) by tumor cells in skin cancer. *The Journal of investigative dermatology*, 114(6), pp.1113–1119.

35) Kerkelä, E. et al., 2002. Metalloelastase (MMP-12) expression by tumour cells in squamous cell carcinoma of the vulva correlates with invasiveness, while that by macrophages predicts better outcome. *Journal of Pathology*, 198(2), pp.258–269.
36) Kim, K.H. et al., 2012. Expression and significance of the TLR4/MyD88 signaling pathway in ovarian epithelial cancers. *World journal of surgical oncology*, 10(1), p.193. Available at: http://www.pubmedcentral.nih.gov/ articlerender.fcgi?artid =3539930&tool=pmcentrez&rendertype=abstract [Accessed March 12, 2014].
37) Kim, K.H. & Yoon, M.S., 2010. MyD88 expression and anti-apoptotic signals of paclitaxel in epithelial ovarian cancer cells. , 53(4), pp.330–338.
38) Kim, K.S., Seu, Y.B., et al., 2007. Induction of cellular senescence by insulin-like growth factor binding protein-5 through a p53-dependent mechanism. *Molecular biology of the cell*, 18(11), pp.4543–4552.
39) Kim, K.S., Kim, M.-S., et al., 2007. Regulation of replicative senescence by insulin-like growth factor-binding protein 3 in human umbilical vein endothelial cells. *Aging cell*, 6(4), pp.535–545.
40) Kuilman, T. et al., 2008. Oncogene-induced senescence relayed by an interleukin-dependent inflammatory network. *Cell*, 133(6), pp.1019–31. Available at: http://www.ncbi.nlm.nih.gov/pubmed/18555778 [Accessed April 30, 2014].
41) Kuilman, T. & Peeper, D.S., 2009. Senescence-messaging secretome: SMS-ing cellular stress. *Nature reviews. Cancer*, 9(2), pp.81–94.
42) Lansu, K. & Gentile, S., 2013. Potassium channel activation inhibits proliferation of breast cancer cells by activating a senescence program. *Cell death & disease*, 4(6), p.e652. Available at: http://www.pubmedcentral.nih.gov/articlerender.fcgi?artid=3698542&tool=pmcentrez&rendertype=abstract.
43) Lee, A.C. et al., 1999. Ras proteins induce senescence by altering the intracellular levels of reactive oxygen species. *Journal of Biological Chemistry*, 274(12), pp.7936–7940.
44) Litan, A. & Langhans, S. a., 2015. Cancer as a channelopathy: ion channels and pumps in tumor development and progression. *Frontiers in Cellular Neuroscience*, 9(March), pp.1–11. Available at: http://journal.frontiersin.org/Article/10.3389/fncel.2015.00086/abstract.
45) Liu, W.-T. et al., 2015. Toll like receptor 4 facilitates invasion and migration as a cancer stem cell marker in hepatocellular carcinoma. *Cancer Letters*, 358(2), pp.136–143. Available at: http://linkinghub.elsevier.com/retrieve/pii/S0304383514007629.
46) Liu, Z. et al., 2014. TSG101 and PEG10 are prognostic markers in squamous cell/adenosquamous carcinomas and adenocarcinoma of the gallbladder. *Oncology Letters*, 7(4), pp.1128–1138.
47) Van der Loo, B. et al., 2000. Enhanced peroxynitrite formation is associated with vascular aging. *The Journal of experimental medicine*, 192(12), pp.1731–1744.
48) López-Otín, C. & Matrisian, L.M., 2007. Emerging roles of proteases in tumour suppression. *Nature reviews. Cancer*, 7(10), pp.800–808.
49) Lorenzini, a et al., 2001. Is increased arachidonic acid release a cause or a consequence of replicative senescence? *Exp Gerontol*, 36(1), pp.65–78. Available at: http://www.ncbi.nlm.nih.gov/htbin-post/Entrez/query?db=m&form=6&dopt=r&uid =11162912.
50) Luo, H. et al., 2009. Down-regulated miR-9 and miR-433 in human gastric carcinoma. *Journal of experimental & clinical cancer research : CR*, 28, p.82. Available at: http://www.pubmedcentral.nih.gov/articlerender.fcgi?artid=2739520&tool=pmcentrez&rendertype=abstract [Accessed October 29, 2012].
51) Macip, S. et al., 2002. Inhibition of p21-mediated ROS accumulation can rescue p21-induced senescence. *EMBO Journal*, 21(9), pp.2180–2188.
52) Martin, J.A., Ellerbroek, S.M. & Buckwalter, J.A., 1997. Age-related decline in chondrocyte response to insulin-like growth factor-I: the role of growth factor

binding proteins. *Journal of orthopaedic research : official publication of the Orthopaedic Research Society*, 15(4), pp.491–498.
53) Martin, T.J., Peer, C.J. & Figg, W.D., 2013. Uncovering the genetic landscape driving castration-resistant prostate cancer. *Cancer Biology and Therapy*, 14(5), pp.399–400.
54) Mcgrogan, B. et al., 2014. Spindle assembly checkpoint protein expression correlates with cellular proliferation and shorter time to recurrence in ovarian cancer, *Human Pathology*, 45(7), pp.1509–1519. Available at: http://dx.doi.org/10.1016/j.humpath.2014.03.004.
55) McQuibban, G.A. et al., 2002. Matrix metalloproteinase processing of monocyte chemoattractant proteins generates CC chemokine receptor antagonists with anti-inflammatory properties in vivo. *Blood*, 100(4), pp.1160–1167.
56) Menghi, F. et al., 2011. DNA Microarray Analysis Identifies CKS2 and LEPR as Potential Markers of Meningioma Recurrence. *The Oncologist*, 16(10), pp.1440–1450.
57) Millis, A.J. et al., 1992. Differential expression of metalloproteinase and tissue inhibitor of metalloproteinase genes in aged human fibroblasts. *Experimental cell research*, 201(2), pp.373–379.
58) Mirzayans, R. et al., 2012. Role of p16INK4A in Replicative Senescence and DNA Damage-Induced Premature Senescence in p53-Deficient Human Cells. *Biochemistry Research International*, 2012, pp.1–8.
59) Noppe, G. et al., 2009. Rapid flow cytometric method for measuring senescence associated β-galactosidase activity in human fibroblasts. *Cytometry Part A*, 75(11), pp.910–916.
60) Okabe, H. et al., 2003. Involvement of PEG10 in human hepatocellular carcinogenesis through interaction with SIAH1. *Cancer Research*, 63(12), pp.3043–3048.
61) Park, P.E. et al., 2013. MAD2 expression in ovarian carcinoma: Different expression patterns and levels among various types of ovarian carcinoma and its prognostic significance in high-grade serous carcinoma. *Korean Journal of Pathology*, 47(5), pp.418–425.
62) Pérez-Mancera, P. a., Young, A.R.J. & Narita, M., 2014. Inside and out: the activities of senescence in cancer. *Nature Reviews Cancer*, 14(8), pp.547–558. Available at: http://www.nature.com/nrc/journal/v14/n8/full/nrc3773. html?WT.ec_id=NRC201408\nhttp://www.nature.com/nrc/journal/v14/n8 /pdf/nrc3773.pdf.
63) Prencipe, M. et al., 2009. Cellular senescence induced by aberrant MAD2 levels impacts on paclitaxel responsiveness in vitro. *British journal of cancer*, 102(11), pp.1900–8. Available at: http://www.pubmedcentral.nih.gov/articlerender.fcgi?artid=2788249&tool=pmcentrez&rendertype=abstract [Accessed November 10, 2012].
64) Prencipe, M. et al., 2010. MAD2 downregulation in hypoxia is independent of promoter hypermethylation. *Cell Cycle*, 9(14), pp.2856–2865. Available at: http://www.landesbioscience.com/journals/cc/article/12362/ [Accessed October 29, 2012].
65) Del Rincón, S. V et al., 2014. Cks overexpression enhances chemotherapeutic efficacy by overriding DNA damage checkpoints. *Oncogene*, (October 2013), pp.1–7. Available at: http://www.ncbi.nlm.nih. gov/pubmed/24858038.
66) Rogers, S.C. et al., 2013. Exposure to high or low glucose levels accelerates the appearance of markers of endothelial cell senescence and induces dysregulation of nitric oxide synthase. *Journals of Gerontology - Series A Biological Sciences and Medical Sciences*, 68(12 A), pp.1469–1481.
67) Salzman, D.W. & Weidhaas, J.B., 2012. SNPing cancer in the bud: MicroRNA and microRNA-target site polymorphisms as diagnostic and prognostic biomarkers in cancer. *Pharmacology & therapeutics*. Available at: http://www.ncbi.nlm.nih.gov/pubmed/ 22964086 [Accessed November 7, 2012].

68) Sano, T. et al., 1998. Expression status of p16 protein is associated with human papillomavirus oncogenic potential in cervical and genital lesions. *The American journal of pathology*, 153(6), pp.1741–1748.
69) Sato, I. et al., 1993. Reduction of nitric oxide producing activity associated with in vitro aging in cultured human umbilical vein endothelial cell. *Biochem Biophys Res Commun*, 195(2), pp.1070–1076. Available at: http://www.ncbi.nlm.nih.gov/entrez/query.fcgi?cmd=Retrieve&db=PubMed&dopt=Citation&list_uids=7690550.
70) Schmittgen, T.D. & Livak, K.J., 2008. Analyzing real-time PCR data by the comparative C(T) method. *Nature protocols*, 3(6), pp.1101–1108.
71) Severino, V. et al., 2013. Insulin-like growth factor binding proteins 4 and 7 released by senescent cells promote premature senescence in mesenchymal stem cells. *Cell death & disease*, 4(11), p.e911. Available at: http://www.pubmedcentral.nih.gov/articlerender.fcgi?artid=3847322&tool=pmcentrez&rendertype=abstract.
72) Sharpless, N.E. & Sherr, C.J., 2015. Forging a signature of in vivo senescence. *Nature Reviews Cancer*, 15(7), pp.397–408. Available at: http://www.nature.com/doifinder/10.1038/nrc3960.
73) Shen, D.Y. et al., 2010. Clinical significance and expression of cyclin kinase subunits 1 and 2 in hepatocellular carcinoma. *Liver International*, 30(1), pp.119–125.
74) Shen, J. et al., 2008. A functional polymorphism in the miR-146a gene and age of familial breast/ovarian cancer diagnosis. *Carcinogenesis*, 29(10), pp.1963–1966.
75) Silasi, D.-A. et al., 2006. MyD88 predicts chemoresistance to paclitaxel in epithelial ovarian cancer. *The Yale journal of biology and medicine*, 79(3-4), pp.153–63. Available at: http://www.pubmedcentral.nih.gov/ article render.cgi?artid=1994803&tool=pmcentrez&rendertype=abstract.
76) Simon, D. et al., 2010. A mutation in the 3′-UTR of the HDAC6 gene abolishing the post-transcriptional regulation mediated by hsa-miR-433 is linked to a new form of dominant X-linked chondrodysplasia. *Human Molecular Genetics*, 19(10), pp.2015–2027.
77) Snyder, C.M. et al., 2013. MEF2A regulates the Gtl2-Dio3 microRNA mega-cluster to modulate WNT signaling in skeletal muscle regeneration. *Development (Cambridge, England)*, 140(1), pp.31–42. Available at: http://www.pubmedcentral.nih.gov/articlerender.fcgi?artid=3513991&tool=pmcentrez&rendertype=abstract.
78) Solár, P. & Sytkowski, A.J., 2011. Differentially expressed genes associated with cisplatin resistance in human ovarian adenocarcinoma cell line A2780. *Cancer letters*, 309(1), pp.11–8. Available at: http://www.ncbi.nlm.nih.gov/pubmed/21676537 [Accessed December 11, 2012].
79) Sudo, T., 2004. Dependence of Paclitaxel Sensitivity on a Functional Spindle Assembly Checkpoint. *Cancer Research*, 64(7), pp.2502–2508. Available at: http://cancerres.aacrjournals.org/cgi/doi/10.1158/0008-5472.CAN-03-2013 [Accessed November 10, 2012].
80) Sulaiman, G., 2015. The Role Of MyD88 in Embryonal Carcinoma Stem Cells. *Unpublished Thesis*.
81) Szajnik, M. et al., 2009. TLR4 signaling induced by lipopolysaccharide or paclitaxel regulates tumor survival and chemoresistance in ovarian cancer. *Oncogene*, 28(49), pp.4353–4363. Available at: http://www.pubmedcentral.nih.gov/articlerender.fcgi?artid=2794996&tool=pmcentrez&rendertype=abstract.
82) Tamandl, D. et al., 2003. Modulation of Toll-Like Receptor4 Expression On Human Monocytes by Tumor Necrosis Factor and Interleukin-6:Tumor Necrosis Factor Evokes Lipopolysaccharide Hyporesponsiveness,whereas Interleukin-6 Enhances Lipopolysaccharide activity. *Shock*, 20(3), pp.224–229. Available at: http://www.ncbi.nlm.nih.gov/pubmed/12923490.

83) Tanaka, F. et al., 2011. Clinicopathological and biological significance of CDC28 protein kinase regulatory subunit 2 overexpression in human gastric cancer. *International Journal of Oncology*, 39(2), pp.361–372.
84) Tanikawa, C. et al., 2012. CLCA2 as a p53-inducible senescence mediator. *Neoplasia*, 14(2), pp.141–149. Available at: http://www.ncbi.nlm.nih.gov/pubmed/22431922.
85) Del Vescovo, V. et al., 2013. A cross-platform comparison of Affymetrix and Agilent microarrays reveals discordant miRNA expression in lung tumors of c-Raf transgenic mice. *PLoS ONE*, 8(11).
86) Wang, A.C. et al., 2009. Role of TLR4 for paclitaxel chemotherapy in human epithelial ovarian cancer cells. *European journal of clinical investigation*, 39(2), pp.157–64. Available at: http://www.ncbi.nlm.nih. gov/pubmed/19200169 [Access ed January 30, 2013].
87) Wang, A.C. et al., 2014. TLR4 induces tumor growth and inhibits paclitaxel activity in MyD88-positive human ovarian carcinoma in vitro. *Oncology Letters*, 7(3), pp.871–877.
88) Wang, S. et al., 1996. Characterization of IGFBP-3, PAI-1 and SPARC mRNA expression in senescent fibroblasts. *Mechanisms of Ageing and Development*, 92(2-3), pp.121–132.
89) Weiner-Gorzel, K. et al., 2015. Overexpression of the microRNA miR-433 promotes resistance to paclitaxel through the induction of cellular senescence in ovarian cancer cells. *Cancer Medicine*, p.n/a–n/a. Available at: http://doi.wiley.com/10.1002/cam4.409.
90) West, M.D., Pereira-Smith, O.M. & Smith, J.R., 1989. Replicative senescence of human skin fibroblasts correlates with a loss of regulation and overexpression of collagenase activity. *Experimental cell research*, 184(1), pp.138–147.
91) Wiel, C. et al., 2014. Endoplasmic reticulum calcium release through ITPR2 channels leads to mitochondrial calcium accumulation and senescence. *Nature communications*, 5(May), pp.3792–3793. Available at: http://www.nature.com.gate2.inist.fr/ncomms/2014/140506/ncomms4792/full/ncomms4792.html.
92) Wohlrab, H. et al., 1988. Towards a biomarker of mammalian senescence: carbonic anhydrase III. *Biochemical and biophysical research communications*, 154(3), pp.1130–1136.
93) Xin, M.G. et al., 2003. Senescence-enhanced oxidative stress is associated with deficiency of mitochondrial cytochrome c oxidase in vascular endothelial cells. *Mech Ageing Dev*, 124(8-9), pp.911–919. Available at: http://www.ncbi.nlm.nih.gov/pubmed/14499496.
94) Yang, Z. et al., 2013. MicroRNA-433 inhibits liver cancer cell migration by repressing the protein expression and function of cAMP response element-binding protein. *The Journal of biological chemistry*, 288(40), pp.28893–9. Available at: http://www.ncbi.nlm.nih.gov/pubmed/23979134.
95) Yee, N.S., Zhoud, W., et al., 2012. Targeted silencing of TRPM7 ion channel induces replicative senescence and produces enhanced cytotoxicity with gemcitabine in pancreatic adenocarcinoma. *Cancer letters*, 318(1), pp.99–105.
96) Yee, N.S., Brown, R.D., et al., 2012. TRPM8 ion channel is aberrantly expressed and required for preventing replicative senescence in pancreatic adenocarcinoma: Potential role of TRPM8 as a biomarker and target. *Cancer Biology and Therapy*, 13(8), pp.592–599.
97) Yue, C. et al., 2011. Polymorphism of the pre-miR-146a is associated with risk of cervical cancer in a Chinese population. *Gynecologic oncology*, 122(1), pp.33–7. Available at: http://www.ncbi.nlm.nih.gov/pubmed/2152 9907 [Accessed October 29, 2012].
98) Zeng, G. & Millis, A.J., 1996. Differential regulation of collagenase and stromelysin mRNA in late passage cultures of human fibroblasts. *Experimental cell research*, 222(1), pp.150–156.

99) Zeng, Y. et al., 2010. Correlation between pre-miR-146a C/G polymorphism and gastric cancer risk in Chinese population. *World Journal of Gastroenterology*, 16(28), pp.3578–3583.
100) Zhu, Y. et al., 2012. Prognostic significance of MyD88 expression by human epithelial ovarian carcinoma cells. *Journal of translational medicine*, 10(1), p.77. Available at: http://www.pubmedcentral.nih.gov/articlerender.fcgi?artid=343 8113 &tool=pmcentrez&rendertype=abstract [Accessed Octob- er 29, 2012].

Chapter 6

Immunohistochemical evaluation of MAD2, TLR4 and MyD88 expression in a high grade serous ovarian cancer cohort

Trinity College Dublin

The University of Dublin

Chapter 6

Immunohistochemical evaluation of MAD2, TLR4 and MyD88 expression in a high grade serous ovarian cancer cohort

6.1 Overview

In this chapter, the use of MAD2, TLR4 and MyD88 as immunohistochemial biomarkers was evaluated in a cohort of patients with high grade serous ovarian cancer. The ability of these markers to predict patient prognosis, when used individually or in combination was assessed in a tissue microarray and in full face paraffin embedded (FFPE) tissue sections.

6.2 Introduction

Ovarian cancer is the most lethal of the gynaecological malignancies and the 4th leading cause of cancer death in women in Ireland. Current therapy for advanced ovarian cancer includes cytoreductive surgery followed by taxol/carboplatin based chemotherapy. However despite the use of these frontline anticancer drugs, little has been done to improve upon the poor prognosis rates in ovarian cancer with mortality rates remaining almost unchanged for the past number of decades (National Cancer Registry 2012b). Although initial response rates may be as high as 80%, most patients will develop chemoresistant, recurrent disease and eventually succumb to the disease within 5 years. The molecular mechanisms which underlie the development of recurrent disease and chemoresistance need to be elucidated. Furthermore, new diagnostic, prognostic and theranostic biomarkers need to be identified in order to direct patient chemotherapy and improve patient prognosis rates. Currently no reliable prognostic markers, which can guide patient therapy, are in use for ovarian cancer. Ovarian cancer for decades has been recognised as a heterogeneous disease

composed of multiple types, subtypes and molecular subtypes. However it is still being treated as a singular disease and current chemotherapy regimens do not recognise this fact (Schorge *et al*. 2010; Domcke *et al*. 2013). High grade serous cancer is the most common and lethal phenotype of ovarian cancer and therefore was the focus of this study (Bell 2005). Much research and many clinical trials focus on dose alterations and drug combinations for already available therapeutic agents, for the treatment of recurrent disease and overcoming platinum resistant cancers. Many of these clinical trials, boast minimal increases in progression free survival (PFS) and have little or no measureable impact on overall survival (OS) and have poor endpoint criteria such as the RECIST criteria (Ledermann & Raja 2011). As of August 2015, there were 120 active clinical trials for treatment of recurrent ovarian cancer alone (www.clinicaltrials.gov). The use of such resources may be more beneficial, if used to better understand why patients develop recurrent disease and chemoresistance initially. More focus is required on identifying patients who will not respond well initially to chemotherapy. These patients could be directed towards clinical trials and given alternative therapies such as targeted therapy. This may enhance their survival and prevent the development of recurrent and chemoresistant ovarian from the offset (Joo *et al*. 2013).

Prognostic markers need to be used to understand chemoresistance and recurrence and direct patient therapy as they highlight a molecular mechanism which underlies these traits. However no single biomarker may be enough to accurately guide the therapy of all patients, and biomarker panels are therefore necessary. This is evident with breast cancer, where great improvements in patient outcomes has been achieved by assessing the expression of HER-2 and a number of other biomarkers which triage patients into different therapy groups (Oakman *et al*. 2009; Olopade *et al*. 2008; Yanagawa *et al*. 2012; National Cancer Registry 2012a). A similar model or approach to treating ovarian cancer needs to be adopted in order to improve patient outcomes.

TLR4, MyD88 and MAD2 were shown individually to be useful indicators of patient prognosis. High TLR4 expression being associated with reduced PFS, high MyD88 expression being associated with reduced PFS and OS and low MAD2 expression being associated with reduced PFS (Furlong *et al*. 2012; d'Adhemar *et al*. 2014). Furthermore alarmingly, paclitaxel is a known ligand for TLR4 (Byrd-Leifer *et al*. 2001). Binding of paclitaxel to TLR4 not only prevents paclitaxel from reaching its intended target microtubules, but activates inflammatory and antiapoptotic signalling supporting tumour growth and preventing tumour cell death (Szajnik *et al*. 2009; Rajput *et al*. 2013b; Wang *et al*. 2014; Huang *et al*. 2014). siRNA knockdown of MAD2 leads to the

development a senescent phenotype which is paclitaxel resistant. Downregulation of MAD2 has been shown to occur in hypoxic tumour regions (Prencipe *et al*. 2010; Furlong *et al*. 2012). From this it is evident that immunohistochemistry results reflect molecular mechanisms which contribute to chemoresistance and recurrent disease. The aim of this chapter was to investigate the combined utility of MAD2, TLR4 and MyD88 in a high grade serous ovarian cancer cohort of predicting patient outcomes and response to chemotherapy. Another aim of this project was to investigate the expression pattern of these three markers in the omentum and during disease recurrence and determine whether expression patterns of each of these three markers differed/changed from the original phenotype of the primary tumour and what impact this had on patient survival outcomes. Interestingly in the previous chapter, a link between the TLR4 mediated and MAD2 mediated paclitaxel resistance mechanisms was demonstrated, therefore it was predicted that those with a MyD88 high TLR4 high and MAD2 low phenotype would have significantly worst outcomes and poor response to chemotherapy.

6.2.1 Hypothesis

TLR4, MyD88 and MAD2 can be used in combination to more accurately predict patient response and triage patients into different at risk groups based on their molecular phenotype and that the expression of these three markers during omental metastasis and recurrence may differ from that of the primary tumour and influence patient survival.

6.2.2 Aims

1) Determine whether TLR4, MyD88 and MAD2 can be used in combination to predict patient prognosis in a TMA cohort.
2) Assess MyD88, TLR4 and MAD2 status in primary disease, metastasis and recurrent disease and its impact on longitudinal patient prognosis.

6.3 Methods

6.3.1 Case selection

Cases were identified from the Discovary bioresource in the Department of Obstetrics and Gynaecology in Trinity College Dublin. All patients gave informed consent and ethical approval was received from St. James's Hospital and Adelaide and Meath hospital, Dublin, incorporating the National Children's Hospital Research Ethics Committee (041213/12904 and ref 2009/29/01).

6.3.2 Cell block generation

Cell blocks were generated from SKOV-3 cells for use as immunostaining controls. Formalin fixed cells were re-suspended and pelleted in molten agar, agar pellets were then processed on the tissue tek vip 5 tissue processor and then embedded in paraffin using the Tissue-Tek® TEC™ 5 Tissue Embedding Console System. 5µM sections were then cut from paraffin embedded cell blocks for use as immunostaining controls; 0.6mm cores were also removed from paraffin cell blocks and inserted into tissue microarrays for use as internal immunostaining controls.

6.3.3 Tissue microarray construction

Two tissue microarrays were constructed using the MTA-1 Manual Tissue Arrayer, (Beecher Instruments, Inc). Tissue cores were selected from representative tumour regions from 46 high grade serous FFPE sections stage I-IV, cell blocks and orientation control tissue blocks **(See supplementary data)**. Representative tumour regions within patient samples were marked by a pathologist based on haematoxylin and eosin stained slides. Three 0.6mm cores per patient sample were extracted and inserted into recipient blocks in a precise and ordered array fashion.

6.3.4 Primary-metastatic-recurrent study

A subset of 30 FFPE sections from 10 patient matched primary ovarian, metastatic omental tissue and recurrent tissue blocks were also analysed within this study.

6.3.5 Immunohistochemistry (IHC)

Five µm sections were cut from tissue microarrays or full face sections for the primary-metastatic recurrent study and immunostained with antibodies directed against MAD2 (BD Transduction Laboratories) 1:25, TLR4 1:10 (Santa Cruz) on an automated platform the benchmark LT (Ventana) and MyD88 staining 1:5 (Santa Cruz) was performed on the benchmark ultra (Ventana).

6.3.6 Manual IHC scoring

IHC expression was quantified in the primary-metastatic-recurrent patient cohort 1 (n=30 full-face sections) and in patient cohort 2 (n=46 on two TMA's) by two pathologists, (JOL and DC). The full-face sections and the TMA cores were scored manually for immunointensity, based on the intensity of staining in tumour cells (0, negative; 1+, weak; 2+, moderate; and 3+, strong) and immunopositivity, based on the percentage of tumour stained cells (1+, 0-10%; 2+, 10-40%, and 3+, 40-70%, 4+ 70-100%). The product of the immunopositivity score and the immunointensity score was then used to generate an overall score for each patient with a maximum score of 12. Those with a score of 0-8 were then classified as having low expression and those with a score of 9-12 were classified as high expression for each marker. Images were taken using a Leica DM2500 microscope, Leica DFC290 HD camera and leica application suite V4 software.

6.3.7 Statistical analysis

SPSS statistics version 22 software for Windows (IBM) was used for statistical analysis of survival data. Survival analysis takes the survival times of a group of subjects and generates a survival curve, which shows how many of the members remain alive over time. Survival time is defined as the length of the interval between diagnosis and death. The overall survival (OS) was measured in months from the date of surgery. Progression free survival (PFS) was determined as the survival time (months) from the date of surgery to the time of last follow-up for those with no evidence of disease, or the number of months to time of relapse for those with evidence of progressive disease or a recurrence after surgery and treatment. Disease free interval (DFI) was measured as the survival time in months, from the date of completion of chemotherapy until the date in which the patient had relapsed. Several methods have been developed for calculating OS, PFS and DFI. The most common one is the Kaplan-Meier procedure (Kaplan & Meier 2008) which estimates time-to-event models in the presence of censored cases. Censored cases are cases for which the second event (death /recurrence) is not recorded. Patients that were still alive or had not progressed were censored. Kaplan-Meier analysis was used to estimate DFI, PFS and OS in patients. Patient survival time was compared by log-rank test. All significance testing was two-sided and a p value of ≤ 0.05 was considered statistically significant.

6.4 Results

6.4.1 Characteristics of the tissue microarray cohort

The TMA cohort was composed of 46 patients with high grade serous ovarian cancer. The mean age of the population was 60±12 years. The mean progression free survival (PFS) for these patients was 32±28 months. The mean disease free interval (DFI) for these patients was 28 ± 27 months. The mean overall free survival (OS) for these patients was 45± 31 months. Patient tumours were staged and graded according to the FIGO staging and grading system (Section 1.4). 4/46 (8.7%) patient tumours were classified as stage I, 3/46 (6.5%) were stage II, 35/46 (76.1%) were stage III and 4/46 (8.7%) were stage IV. 4/46 (8.7%) were grade 2, 42/46 (91.3%) were grade 3. Of these 6/46 (13%) patients underwent suboptimal debulking (>1cm residual disease) and 40/46 (87%) patients underwent optimal surgical debulking (<1cm residual disease). As of July 2015, at the time of the analysis, 24/46 (52.2%) were alive and 22/46 (47.8%) were dead. 33/46 (71.7%) had recurred and 13/46 (28.3%) had not recurred. A list of the demographics for each patient is available in **(Table 6.1)**.

6.4.2 Distribution of staining in SKOV-3 cell block controls

Cell blocks were generated from SKOV-3 cells and used as immunostaining controls as they express all three markers, MyD88, TLR4 and MAD2 at high levels. These were included in all immunostaining runs and displayed strong cytoplasmic staining for MyD88, membranous/cytoplasmic staining for TLR4 and strong nuclear staining for MAD2 **(Figure 6.1)**.

Table 6.1 Demographics of the TMA cohort.

TCDOG	Age	Stage	Grade	Debulking Status	DFI	PFS	OS	Recurred	RIP
8	59	3	3	Optimal	10	16	43	Recurred	Dead
15	60	3	3	Sub-optimal	11	17	41	Recurred	Dead
34	74	3	2	Sub-optimal	0	0	1	Recurred	Dead
36	86	3	2	Sub-optimal	2	7	9	Recurred	Dead
38	66	2	3	Optimal	42	45	106+	Recurred	Alive
52	60	3	2	Optimal	89	95	112+	Recurred	Alive
55	68	3	3	Optimal	0	2	4	Recurred	Dead
71	41	4	3	Optimal	0	5	7	Recurred	Dead
74	71	1	3	Optimal	52	59	92	Recurred	Dead
75	54	3	3	Optimal	14	20	47	Recurred	Dead
80	63	2	3	Optimal	39	46	95	Recurred	Dead
87	60	3	3	Optimal	104+	109+	109+	No Recurrence	Alive
89	44	3	3	Optimal	2	7	18	Recurred	Dead
115	61	3	3	Sub-optimal	100+	105+	105+	No Recurrence	Alive
137	51	3	3	Optimal	16	21	73	Recurred	Dead
148	51	3	2	Optimal	1	6	8	Recurred	Dead
159	60	3	3	Sub-optimal	7	12	23	Recurred	Dead
165	50	3	3	Optimal	51	56	103+	Recurred	Alive
172	72	3	3	Optimal	2	7	11	Recurred	Dead
184	57	4	3	Sub-optimal	1	5	9	Recurred	Dead
188	74	3	3	Optimal	30	38	75	Recurred	Dead
189	59	3	2	Optimal	18	22	48	Recurred	Dead
195	44	3	2	Optimal	9	13	30	Recurred	Dead
202	77	3	3	Sub-optimal	0	0	3	Recurred	Dead
223	49	1	3	Optimal	81	85+	85+	No Recurrence	Alive
225	52	3	3	Optimal	8	14	28	Recurred	Dead
228	76	3	3	Optimal	0	0	4	Recurred	Dead
251	70	3	3	Optimal	12	18	36	Recurred	Dead
257	61	1	3	Optimal	57+	61+	61+	No Recurrence	Alive
260	58	3	3	Optimal	19	25	46	Recurred	Dead
268	64	1	3	Optimal	59+	64+	64+	No Recurrence	Alive
277	86	2	3	Optimal	1+	1+	1+	No Recurrence	Alive
282	66	3	3	Optimal	35	41	71+	Recurred	Alive
287	79	3	3	Optimal	54	59	71+	Recurred	Alive
303	58	3	3	Optimal	62+	69+	69+	No Recurrence	Alive
313	70	3	3	Optimal	48	52	65+	Recurred	Alive
358	40	3	3	Optimal	0	22	24	Recurred	Dead
369	65	3	3	Optimal	51+	55+	55+	Recurred	Alive
373	72	3	3	Optimal	15	21	56+	Recurred	Alive
391	59	3	3	Optimal	17	22	41	Recurred	Dead
444	54	3	3	Optimal	42+	48+	48+	No Recurrence	Alive
456	37	3	3	Optimal	16	21	47+	Recurred	Alive
473	52	3	3	Optimal	0	21+	21+	No Recurrence	Alive
481	53	3	3	Optimal	38+	43+	43+	No Recurrence	Alive
507	56	3	3	Optimal	30+	38+	38+	No Recurrence	Alive
515	59	3	3	Optimal	2	7	16	Recurred	Dead
517	66	3	3	Optimal	34+	41+	41+	Recurred	Alive
562	68	1	3	Optimal	26+	30+	30+	No Recurrence	Alive
574	82	3	3	Optimal	0	0	5	Recurred	Dead
649	67	4	3	Sub-optimal	0	0	8	Recurred	Dead
661	57	4	3	Optimal	13	19	26+	Recurred	Alive
717	43	3	3	Optimal	0	10+	10+	No Recurrence	Alive

Abbreviations: **TCDOG**- Unique patient identifier **DFI**- Disease free interval **PFS**- Progression free survival **OS**-Overall survival **RIP**- Dead or Alive. Patient samples staged according Federation International of Gynaecology & Obstetrics (FIGO) system (+)-patient is censored as the even has not occurred yet.

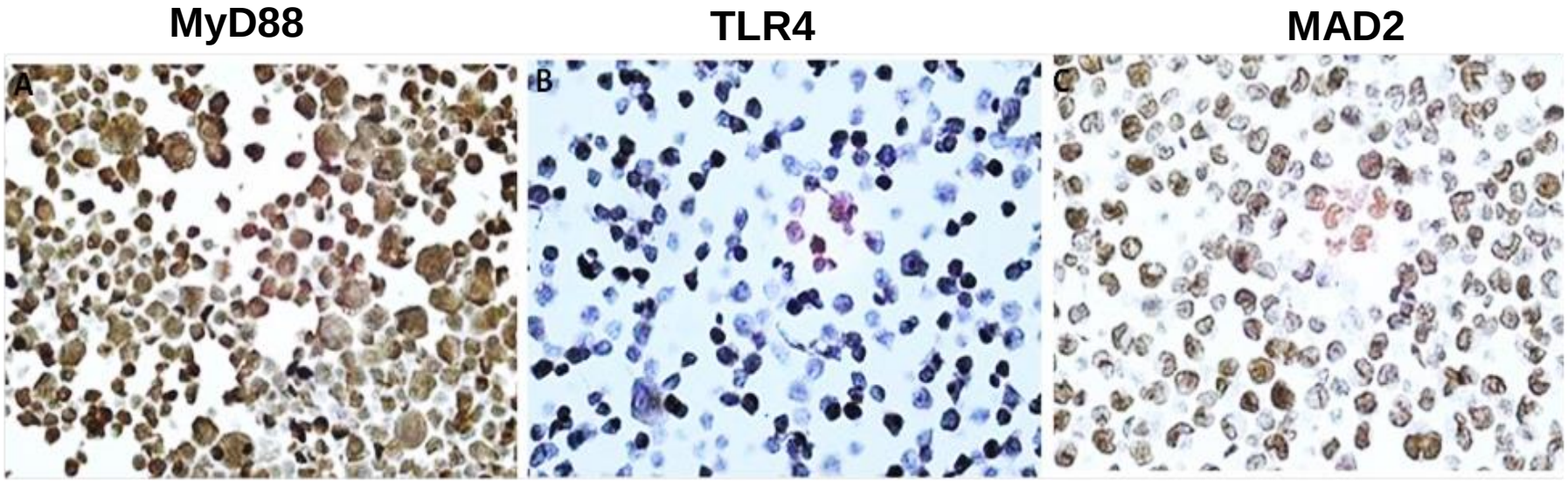

Figure 6.1 An SKOV-3 cell block stained for MyD88, TLR4 and MAD2. An SKOV-3 cell block was stained with antibodies directed against MyD88 (A), TLR4 (B) and MAD2 (C). Images were taken at 20X magnification using a Leica DM2500 microscope, Leica DFC290 HD camera and leica application suite V4 software.

6.4.3 Distribution of staining patterns in the TMA cohort

5µM sections were cut from each TMA and sections were then stained using antibodies directed against MAD2 and TLR4 on the Ventana Benchmark LT and for MyD88 on the Ventana benchmark ultra automated immunostaining modules. Tissue cores were then scored based on immunointensity and immunopositivity for all three stains. Examples of the differing immunointensities observed for each stain are shown in **(Figure 6.2, Figure 6.3 and Figure 6.4**).

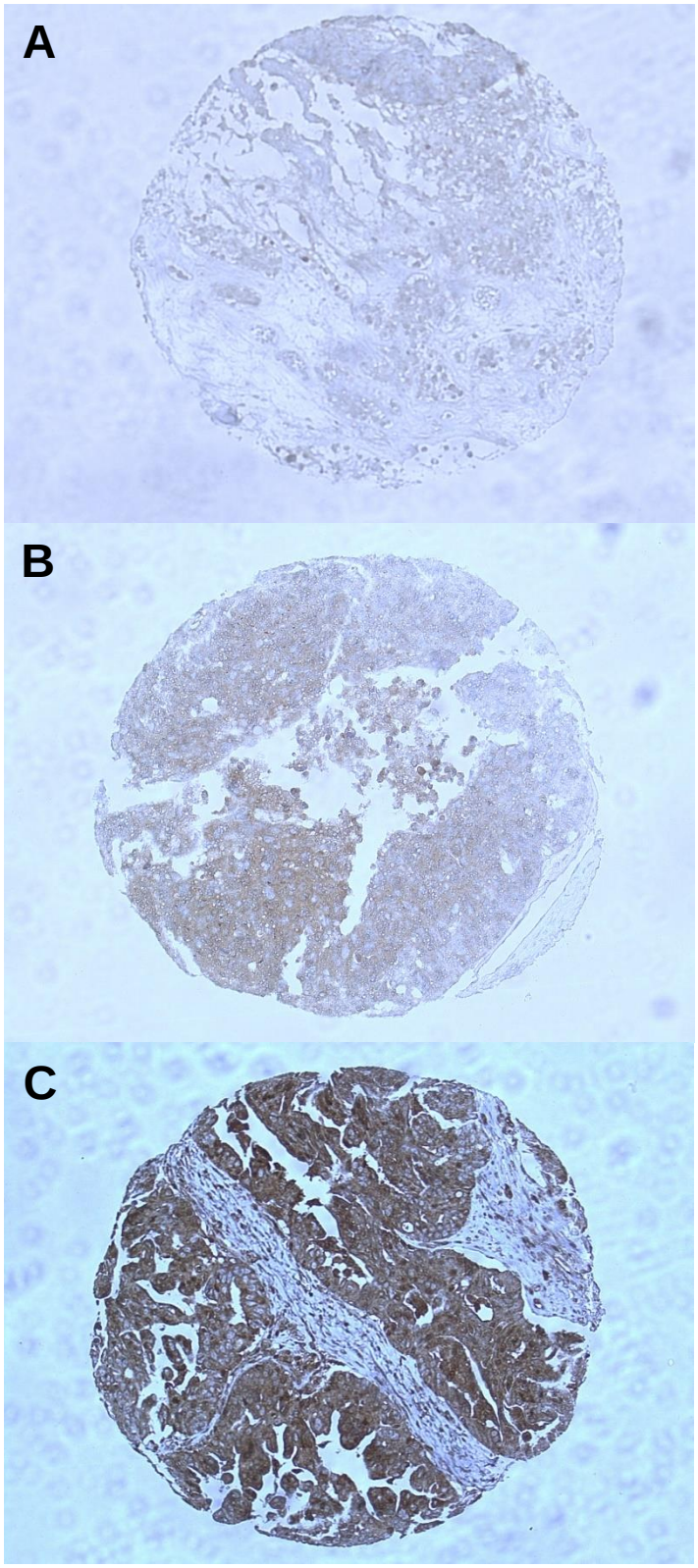

Figure 6.2 Tissue microarray cores which stained weak, moderate and strongly immunopositive for MyD88. TMA sections were stained for MyD88, the Immunointensity of individual cores were then scored as weak (A),moderate (B) or strong (C). Images were taken at 10X magnification using a Leica DM2500 microscope, Leica DFC290 HD camera and leica application suite V4 software.

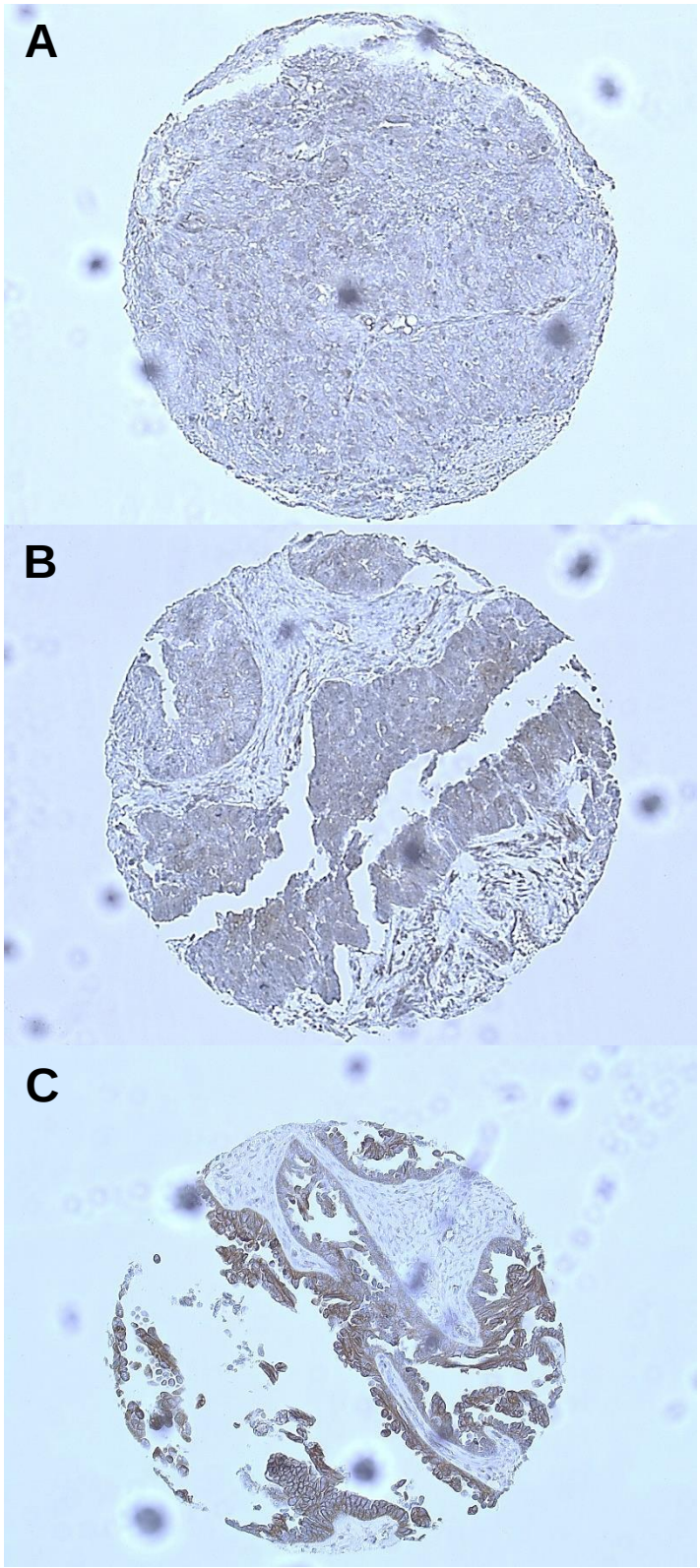

Figure 6.3 Tissue microarray cores which stained weak, moderate and strongly immunopositive for TLR4. TMA sections were stained for TLR4 and the Immunointensity of individual cores were then scored as weak (A), moderate (B) or strong (C). Images were taken at 10X magnification using a Leica DM2500 microscope, Leica DFC290 HD camera and leica application suite V4 software.

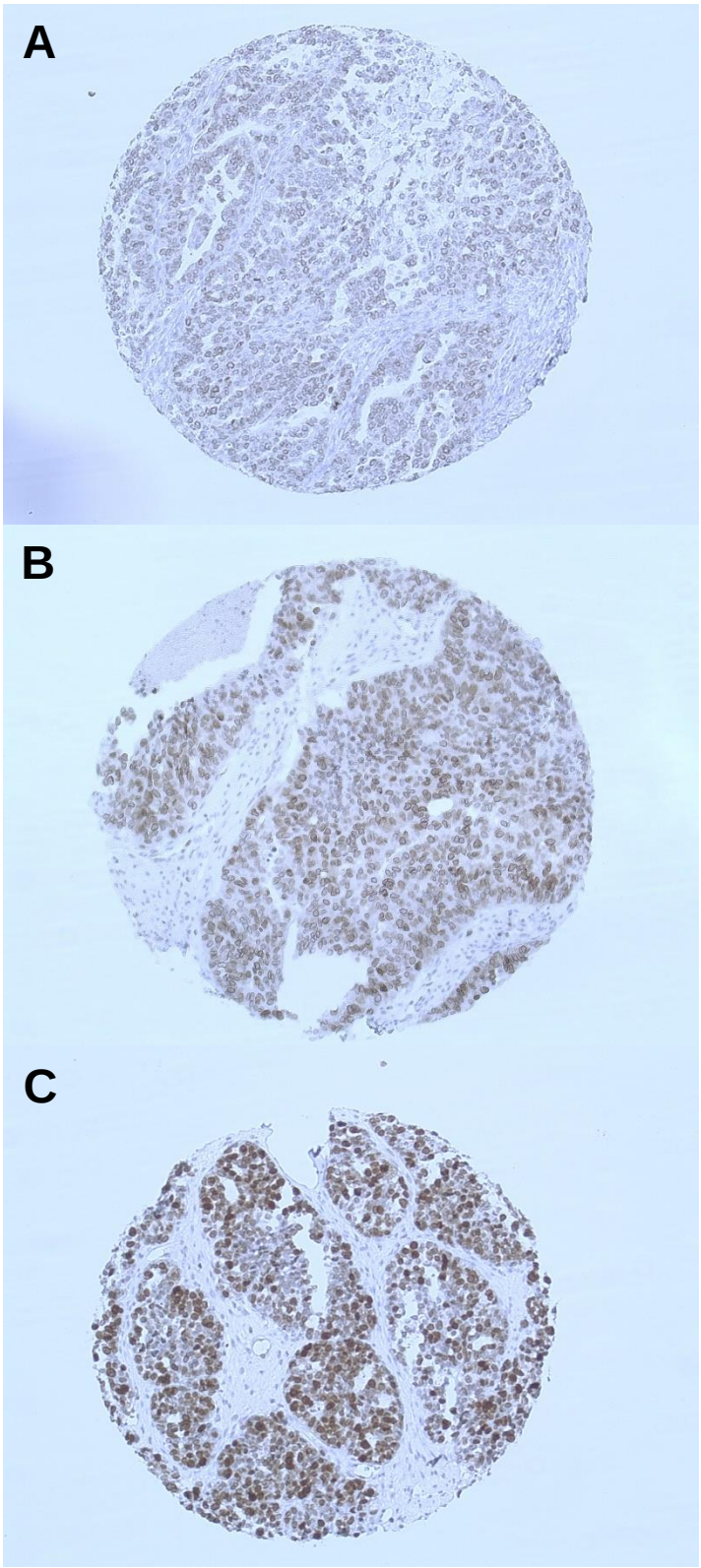

Figure 6.4 Tissue microarray cores which stained weak, moderate and strongly immunopositive for MAD2. TMA sections were stained for MAD2 and the Immunointensity of individual cores were then scored as weak (A),moderate (B) or strong (C). Images were taken at 10X magnification using a Leica DM2500 microscope, Leica DFC290 HD camera and leica application suite V4 software.

The product of the immunointensity and the immunopositivity scores was used to generate an overall score for each core, with a maximum possible score of 12. Based on the average overall immunostaining score of triplicate cores patient samples were classified into high expression and low expression categories for each of the three markers MyD88, TLR4 and MAD2 **(Figure 6.5)**.Those with an average overall score of 0-8 were classified as having low expression and those with an average overall score of 9-12 were classified as having high expression. Of the 46 patients in the TMA cohort, 24/46 (52%) patients stained strongly positive for MyD88, 6/46 (13%) stained strongly positive for TLR4 and 6/46 (13%) stained strongly positive for MAD2.

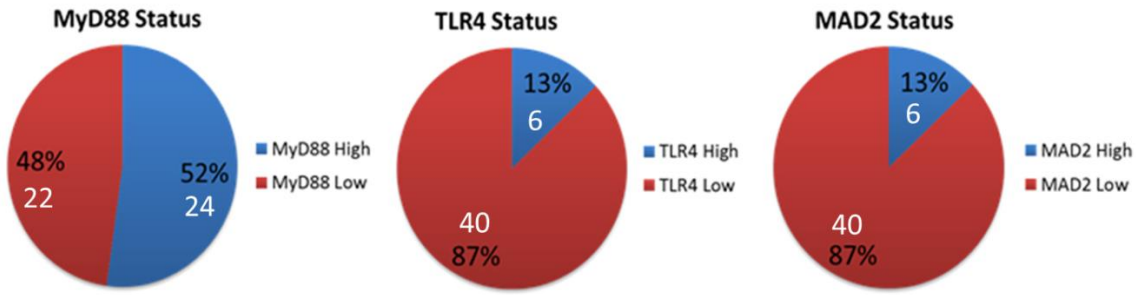

Figure 6.5 The distribution of MyD88, TLR4 and MAD2 staining scores within the TMA cohort. The tissue microarray was stained for MYD88, TLR4 and MAD2 and the average score from triplicate cores was tabulated. Of the 46 patients, 52% stained strongly positive for MyD88, 13% stained strongly positive for TLR4 and 13% stained strongly positive for MAD2.

6.4.4 Evaluation of MAD2, MyD88 and TLR4 as independent biomarkers

Following assessment of MAD2, TLR4 and MyD88 staining patterns in the TMA cohort, Kaplan-Meier analysis was performed in order to determine whether MAD2, TLR4 or MyD88 expression individually influenced patient prognosis within the TMA cohort. To remove bias from the impact of debulking status or early stage disease, then Kaplan-Meier analysis was done excluding these 10 cases.

6.4.4.1 Patients with low MAD2 expression exhibit a small reduction in their DFI

Following immunostaining for MAD2, Kaplan-Meier analysis was performed in order to determine whether MAD2 expression influenced patient prognosis within the TMA cohort. It was predicted that those with a MAD2 low phenotype would have worse outcomes. In this study, compared to patients exhibiting high MAD2 expression, patients who had a low MAD2 immunostaining score exhibited a small reduction in their mean and median DFI, 35 months vs 27 months and 48 months vs 17 months

respectively, although this was not significant. Patients with a low MAD2 score also had a comparable PFS and OS to those with a MAD2 high phenotype.

6.4.4.2 Patients with high MyD88 expression exhibit a reduction in their DFI, PFS and OS

Following immunostaining for MyD88, Kaplan-Meier analysis was performed in order to determine whether high MyD88 expression influenced patient prognosis within the TMA cohort **(Figure 6.6)**. It was predicted that those with a MyD88 high phenotype would have worse outcomes. Compared to patients who had a low MyD88 immunostaining score, patients who had a high MyD88 immunostaining score exhibited a reduction in their mean and median DFI, 34 months vs 21 months and 35 months vs 17 months respectively, although this was not significant. They also exhibited a reduction in their mean and median PFS, 37 months vs 28 months and 41 months vs 22 months respectively, although this was not significant. They also exhibited a reduction in their mean and median OS, 52 months vs 39 months and 46 months vs 28 months respectively, although again this was not significant. A definite trend was observed that indicated that patients with a high MyD88 immunostaining score have worse outcomes than those with a low MyD88 immunostaining score.

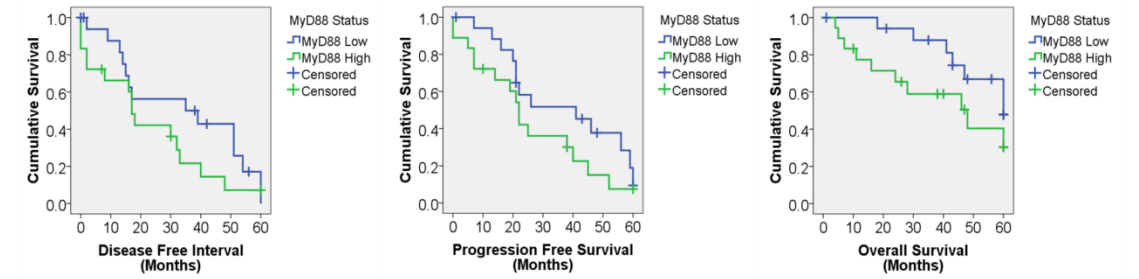

	MyD88 Low	MyD88 High	Significance
No. of Cases	18	18	0.163
No. of cases censored	5	3	
Mean Survival	34	21	
Median Survival	35	17	

	MyD88 Low	MyD88 High	Significance
No. of Cases	18	18	0.146
No. of cases censored	5	3	
Mean Survival	38	26	
Median Survival	41	22	

	MyD88 Low	MyD88 High	Significance
No. of Cases	18	18	0.126
No. of cases censored	11	8	
Mean Survival	52	39	
Median Survival	46	28	

Figure 6.6 MyD88 and patient prognosis. Patient samples within the TMA cohort were stained for MyD88. Patients who had a high MyD88 immunostaining score exhibited a reduction in their Mean and Median DFI, PFS and OS, although this was not significant. The results demonstrate that patients with a MyD88 high score had poorer prognosis than those with a MyD88 low score.

6.4.4.3 Patients with high TLR4 expression exhibit a significant reduction in their DFI, PFS and OS

Following immunostaining for TLR4, Kaplan-Meier analysis was performed in order to determine whether TLR4 expression influenced patient prognosis within the TMA cohort **(Figure 6.7)**. It was predicted that those with a TLR4 high phenotype would have worse outcomes. Compared to those who a low TLR4 immunostaining score, patients who had a high TLR4 immunostaining score exhibited a significant reduction in their mean and median DFI, 31 months vs 10 months and 33 months vs 9 months respectively (p=0.006). They also exhibited a significant reduction in their mean and median PFS, 34 months vs 15 months and 38 months vs 14 months (p=0.007). They also exhibited a significant reduction in their mean and median OS, 49 months vs 32 months and 50 months vs 25 months respectively (p=0.049).

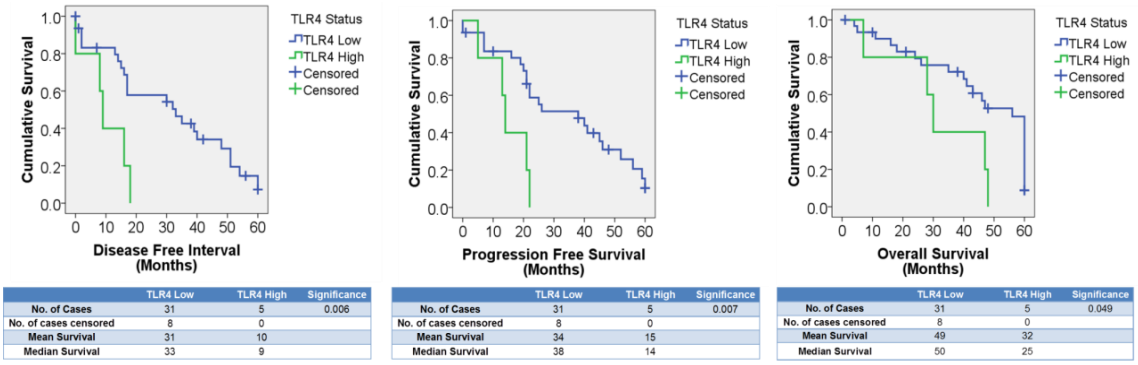

	TLR4 Low	TLR4 High	Significance
No. of Cases	31	5	0.006
No. of cases censored	8	0	
Mean Survival	31	10	
Median Survival	33	9	

	TLR4 Low	TLR4 High	Significance
No. of Cases	31	5	0.007
No. of cases censored	8	0	
Mean Survival	34	15	
Median Survival	38	14	

	TLR4 Low	TLR4 High	Significance
No. of Cases	31	5	0.049
No. of cases censored	8	0	
Mean Survival	49	32	
Median Survival	50	25	

Figure 6.7 TLR4 and patient prognosis. Patient samples within the TMA cohort were stained for TLR4. Patients who had a high TLR4 immunostaining score exhibited a significant reduction in their mean and median DFI, PFS and OS, $p<0.05$, $p<0.01$.

6.4.5 Evaluation of the combined use of MyD88, TLR4 and MAD2 as indicators of prognosis

Following assessment of the impact of MAD2, TLR4 and MyD88 expression individually on patient prognosis in the TMA cohort, Kaplan-Meier analysis was performed in order to determine whether various combinations of MAD2, TLR4 and MyD88 expression influenced patient prognosis within the TMA cohort.

6.4.5.1 TLR4 and MAD2 can be used successfully in combination to accurately predict patient prognosis

This section explores the various phenotypes observed when TLR4 and MAD2 staining patterns were examined within the same patients. Patients were classified into low expression and high expression categories for both TLR4 and MAD2 **(Figure 6.8)**. When combined TLR4 and MAD2 expression patterns were assessed within the TMA cohort, 2/46 (4%) of patients exhibited high expression of both TLR4 and MAD2, 4/46(9%) exhibited high expression of TLR4 and low expression of MAD2, 4/46(9%) exhibited low expression of TLR4 and low expression of MAD2 and 36/46(78%) exhibited low expression of TLR4 and high expression of MAD2.

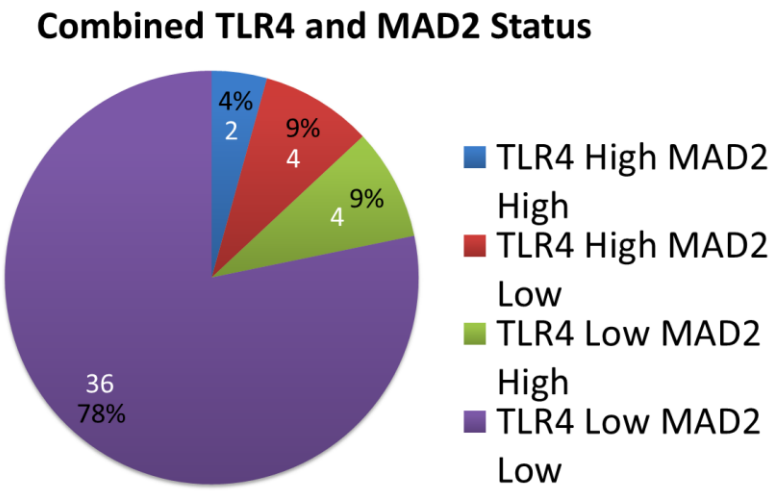

Figure 6.8 Combined TLR4 and MAD2 status within the TMA cohort. When TLR4 and MAD2 expression were assessed within the TMA cohort, 4% of patients exhibited high expression of both TLR4 and MAD2 (TLR4 High MAD2 High), 9% exhibited high expression of TLR4 and low expression of MAD2 (TLR4 High MAD2 Low), 9% exhibited low expression of TLR4 and low expression of MAD2 (TLR4 Low MAD2 Low) and 78% exhibited low expression of TLR4 and high expression of MAD2 (TLR4 Low MAD2 Low).

From this information, Kaplan-Meier analysis was performed to determine whether the combined expression of TLR4 and MAD2 influenced the prognosis of patients within the cohort **(Figure 6.9)**. High TLR4 expression and low MAD2 expression was shown to strongly influence patient prognosis upon individual assessment. Therefore the DFI, PFS and OS of patients with a TLR4 high MAD2 low phenotype was determined and compared against all other patients which did not display this phenotype. Patients with a TLR4 high MAD2 low phenotype exhibited a significant reduction in their mean and median DFI, 31 months vs 8 months and 32 months vs 8 months respectively

(p=0.002). They also exhibited a significant reduction in their mean and median PFS, 34 months vs 13 months and 26 months vs 13 months respectively (p=0.002). They also exhibited a reduction in both their mean and median OS, 47 months vs 28 months and 60 months vs 28 months respectively, however this was just below significance p=0.081. These results demonstrate that those with high TLR4 and low MAD2 expression have poorer outcomes.

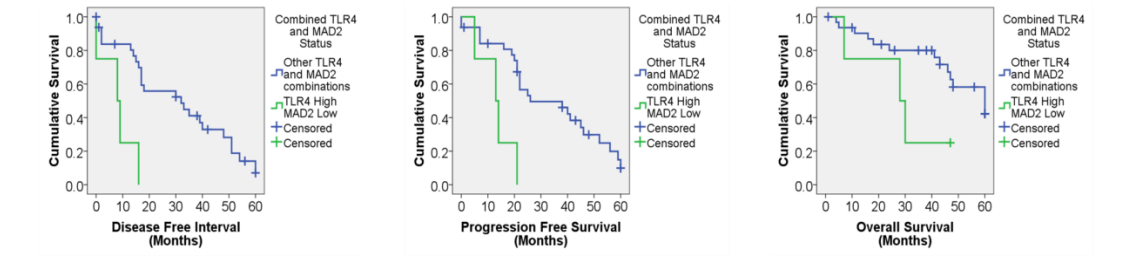

	Other TLR4 MAD2 combinations	TLR4 High MAD2 Low	Significance
No. of Cases	32	4	0.002
No. of cases censored	8	0	
Mean Survival	31	8	
Median Survival	32	8	

	Other TLR4 MAD2 combinations	TLR4 High MAD2 Low	Significance
No. of Cases	32	4	0.002
No. of cases censored	8	0	
Mean Survival	34	13	
Median Survival	26	13	

	Other TLR4 MAD2 combinations	TLR4 High MAD2 Low	Significance
No. of Cases	32	4	0.081
No. of cases censored	18	1	
Mean Survival	47	28	
Median Survival	60	28	

Figure 6.9 TLR4, MAD2 and patient prognosis. Patient samples within the TMA cohort were stained for TLR4 and MAD2. Patients who had a high TLR4 immunostaining and low MAD2 immunostaining score exhibited a reduction in both their mean and median progression free survival times and this was highly significant. Patients who had a high TLR4 immunostaining and Low MAD2 immunostaining score exhibited a significant reduction in both their mean and median DFI and PFS. They also exhibited a reduction in both their mean and median OS however this was just below significance, $p<0.05$, $p<0.01$.

Six patients within the cohort exhibited high TLR4 expression and exhibited significantly reduced survival. Therefore it was also decided to examine the impact of MAD2 expression in the remaining thirty-one patients who exhibited low TLR4 expression to further assess the impact of using MAD2 and TLR4 in combination. Upon analysis of MAD2 expression within this group, it was found that patients with low MAD2 expression exhibited a reduction in their mean and median DFI compared to those with high MAD2 expression in this group, 30 vs 40 months and 32 months vs 48 respectively. This demonstrates that a population of patients within the low TLR4 expression group with low MAD2 have worse outcomes and indicates the clinical utility of using this marker combination. Combined assessment of MAD2 and TLR4 perhaps highlights different subpopulations of patients with different disease outcomes.

6.4.5.2 MyD88 and TLR4 can be used successfully in combination to accurately predict patient prognosis

This section explores the various phenotypes observed when MyD88 and TLR4 staining patterns were examined within the same patients **(Figure 6.10)**. When MyD88 and TLR4 expression was assessed within the TMA cohort, it was found that 4/46 (9%) of patients exhibited high expression of both MyD88 and TLR4 (MyD88 High TLR4 High). 20/46(44%) patients exhibited high expression of MyD88 and low expression of TLR4 (MyD88 High TLR4 Low) and 20/46(44%) exhibited low expression of MyD88 and low expression of TLR4 (MyD88 Low TLR4 Low). 2/46 (4%) patients also exhibited low expression of MyD88 and high expression of TLR4 (MyD88 Low TLR4 High).

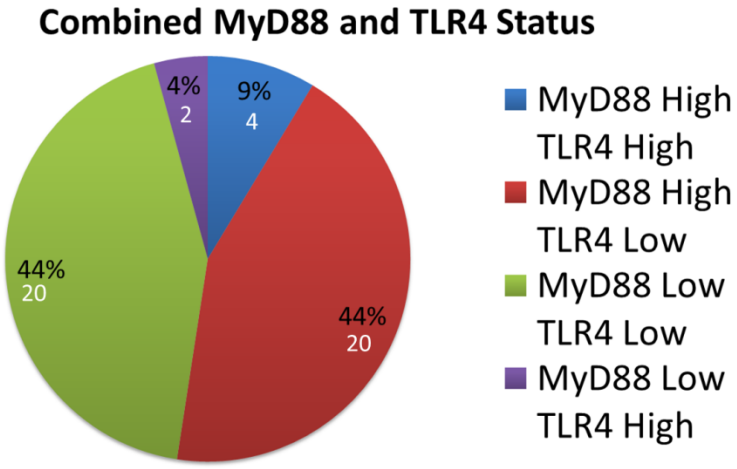

Figure 6.10 Combined MyD88 and TLR4 status within the TMA cohort. When MyD88 and TLR4 expression were assessed within the TMA cohort, 9% of patients exhibited high expression of both MyD88 and TLR4 (MyD88 High TLR4 High), 44% exhibited high expression of MyD88 and low expression of TLR4 (MyD88 High TLR4 Low), 44% exhibited low expression of MyD88 and low expression of TLR4 (MyD88 Low TLR4 Low) and 4% exhibited low expression of MyD88 and high expression of TLR4 (MyD88 Low TLR4 high).

From this information, Kaplan-Meier analysis was performed to determine whether the combined expression of TLR4 and MyD88 influenced the prognosis of patients within the cohort **(Figure 6.11)**. High TLR4 expression and high MyD88 expression was expected to strongly influence patient prognosis. Therefore the DFI, PFS and OS of patients with a TLR4 high MyD88 high phenotype was determined and compared against all other patients which did not display this phenotype. Compared to patients possessing any other phenotype, patients with a TLR4 high MyD88 high phenotype exhibited a significant reduction in both their mean and median DFI (p=0.023), and

PFS (p=0.029), they also exhibited a reduction in both their mean and median overall survival times however this was not significant (p=0.189). These results demonstrate that those with high TLR4 expression and high MyD88 expression have poorer outcomes.

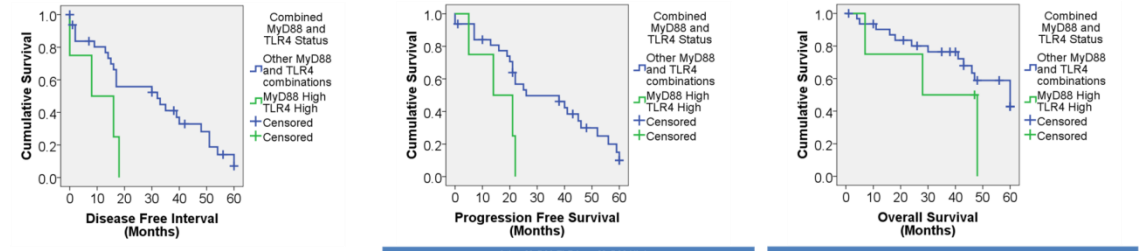

	Other MyD88 TLR4 combinations	MyD88 High TLR4 High	Significance
No. of Cases	32	4	0.023
No. of cases censored	8	0	
Mean Survival	30	11	
Median Survival	32	8	

	Other MyD88 TLR4 combinations	MyD88 High TLR4 High	Significance
No. of Cases	32	4	0.029
No. of cases censored	8	0	
Mean Survival	33	16	
Median Survival	26	14	

	Other MyD88 TLR4 combinations	MyD88 High TLR4 High	Significance
No. of Cases	32	4	0.189
No. of cases censored	18	1	
Mean Survival	47	32	
Median Survival	60	28	

Figure 6.11 MyD88, TLR4, and patient prognosis. Patient samples within the TMA cohort were stained for MyD88 and TLR4. Patients who had a high MyD88 and a high TLR4 immunostaining score exhibited a significant reduction in both their mean and median DFI and PFS. Patients with a high MyD88 and a high TLR4 immunostaining score also exhibited a reduction in both their mean and median OS, however this was not significant, $p<0.05$.

Again as only five patients exhibited high expression of TLR4, it was also decided to assess the impact of MyD88 expression in the remaining thirty one patients with low TLR4 expression to further assess the clinical utility of this marker combination. Patients with a high MyD88 immunostaining score within this group compared to those with a low MyD88 immunostaining score exhibited a reduction in their mean and median DFI 36 vs 26 and 39 vs 30 respectively, although this was not significant. They also exhibited a reduction in their mean and median PFS, 39 vs 29 and 41 vs 25 respectively, although this was not significant. They also exhibited a reduction in their in their mean and median OS, 54 VS 40 and 60 vs 48 respectively, although this was not significant. These results highlight the clinical utility of this marker combination. The expression patterns of each marker may highlight different at risk subpopulations that may benefit from different therapeutic approaches.

6.4.5.3 MyD88 and MAD2 can be used successfully in combination to accurately predict patient prognosis

This section explores the various phenotypes observed when MyD88 and MAD2 staining patterns were examined within the same patients **(Figure 6.12)**. Patients were classified into low expression and high expression categories. When MyD88 and MAD2 expression were assessed within the TMA cohort, 4/46 (9%) of patients exhibited high expression of both MyD88 and MAD2 (MyD88 High MAD2 High), 20/46 (44%) exhibited high expression of MyD88 and low expression of MAD2 (MyD88 High MAD2 Low), 20/46 (44%) exhibited low expression of MyD88 and low expression of MAD2 (MyD88 Low MAD2 Low) and 2/46 (4%) exhibited low expression of MyD88 and high expression of MAD2 (MyD88 Low MAD2 High).

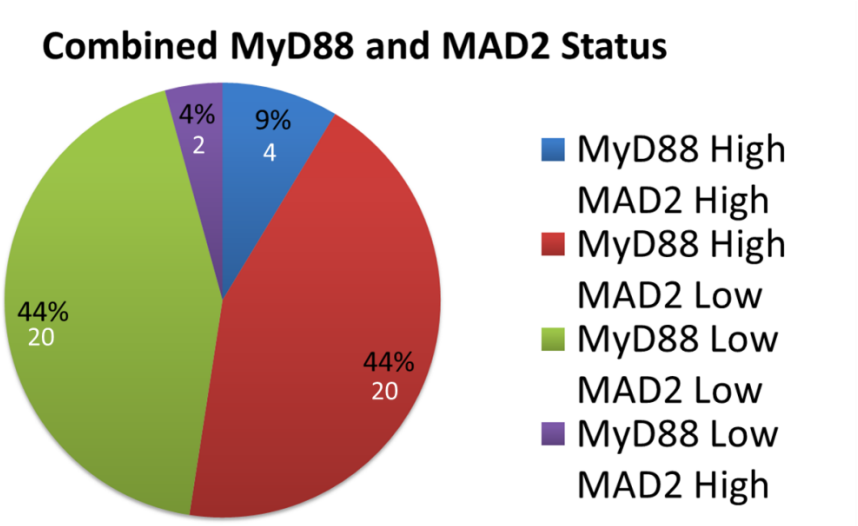

Figure 6.12 MyD88 and MAD2 status within the TMA cohort. When MyD88 and MAD2 expression were assessed within the TMA cohort, 4/46 (9%) of patients exhibited high expression of both MyD88 and MAD2 (MyD88 High MAD2 High), 20/46 (44%) exhibited high expression of MyD88 and low expression of MAD2 (MyD88 High MAD2 Low), 20/46 (44%) exhibited low expression of MyD88 and low expression of MAD2 (MyD88 Low MAD2 Low) and 2/46 (4%) exhibited low expression of MyD88 and high expression of MAD2 (MyD88 Low MAD2 High).

From this information Kaplan-Meier analysis was performed to determine whether the combined expression of MyD88 and MAD2 influenced the prognosis of patients within the cohort **(Figure 6.13)**. Compared to patients with any other phenotype, patients who had a high MyD88 and low MAD2 immunostaining score exhibited a small reduction in both their mean and median DFI, 30 months vs 18 months and 30 months vs 17 months respectively, however this was not significant. They also exhibited a small reduction in both their mean and median PFS 33 months vs 23 months and 25 months vs 22 months respectively, however this was not significant. Moreover they exhibited a small reduction in both their mean and median OS 47 months vs 28 months and 60 months vs 28 months respectively, however this was not significant. These results demonstrate that those with high MyD88 and low MAD2 expression have poorer outcomes.

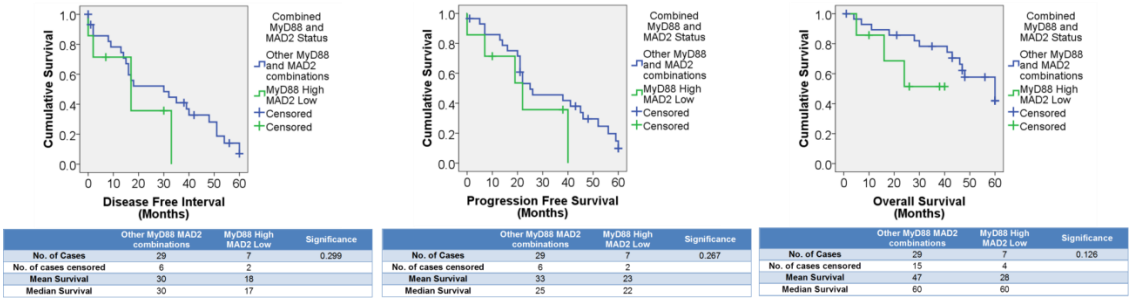

	Other MyD88 MAD2 combinations	MyD88 High MAD2 Low	Significance
No. of Cases	29	7	0.299
No. of cases censored	6	2	
Mean Survival	30	18	
Median Survival	30	17	

	Other MyD88 MAD2 combinations	MyD88 High MAD2 Low	Significance
No. of Cases	29	7	0.267
No. of cases censored	6	2	
Mean Survival	33	23	
Median Survival	25	22	

	Other MyD88 MAD2 combinations	MyD88 High MAD2 Low	Significance
No. of Cases	29	7	0.126
No. of cases censored	15	4	
Mean Survival	47	28	
Median Survival	60	60	

Figure 6.13 MyD88, MAD2 and patient prognosis. Patient samples within the TMA cohort were stained for MyD88 and MAD2. Patients who had a high MyD88, and low MAD2 immunostaining score exhibited a small reduction in both their mean and median disease free intervals however this was not significant. Patients who had a high MyD88, and low MAD2 immunostaining score exhibited a small reduction in both their mean and median DFI, PFS and OS, although this was not significant. These results demonstrate that those with high MyD88 and low MAD2 expression have poorer outcomes.

In this cohort, only a small number of cases expressed high levels of MAD2 (5/46) compared to low expressers (41/46), also there was low expression of MyD88 in only one of the MAD2 high cases. While high MyD88 expression across the low MAD2 expressing cases was quite even 47% vs 39%. Due to this fact it was decided to re-examine the impact of MyD88 expression on prognosis in the low MAD2 expressing group only **(Figure 6.14)**. Within the low MAD2 expressing group patients with high MyD88 expression exhibited a significant reduction in their mean and median DFI (p=0.039) and PFS (p=0.018). They also exhibited a large reduction in their OS, but this was just below significance (p=0.062).

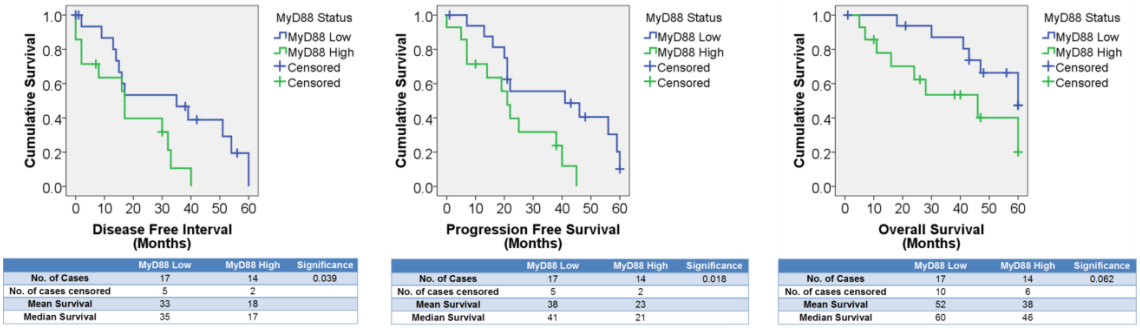

	MyD88 Low	MyD88 High	Significance
No. of Cases	17	14	0.039
No. of cases censored	5	2	
Mean Survival	33	18	
Median Survival	35	17	

	MyD88 Low	MyD88 High	Significance
No. of Cases	17	14	0.018
No. of cases censored	5	2	
Mean Survival	38	23	
Median Survival	41	21	

	MyD88 Low	MyD88 High	Significance
No. of Cases	17	14	0.062
No. of cases censored	10	6	
Mean Survival	52	38	
Median Survival	60	46	

Figure 6.14 MyD88 expression in patients with low MAD2 expression and its effect on patient prognosis. Patients who had a high MyD88 immunostaining score in low MAD2 expression group had a significant reduction in their DFI and PFS, They also exhibited a reduction in their OS, but this was not significant, $p<0.05$.

It was then decided to also remove those with high expression of TLR4, all of whom had significantly worse outcomes from the analysis to further demonstrate the impact of MyD88 expression in the MAD2 low population **(Figure 6.15)**. When MyD88 expression was assessed in this population, compared to those with low MyD88 expression, those with high MyD88 expression exhibited a reduction in both their mean and median DFI, 34 months vs 22 months and 35 months vs 30 months respectively, although this was just below significance p=0.094. They also exhibited a reduction in both their mean and median PFS, 40 months vs 26 months and 46 vs 26 months respectively p=0.062. They also exhibited a significant reduction in both their mean and median OS, 54 months vs 39 months and 60 months vs 46 months respectively, although this was just below significance, p=0.048. All this work has demonstrated that MAD2 and MyD88 can be used very successfully in combination to predict patient prognosis. However further evaluation in a large cohort needs to be performed to assess the impact of MyD88 on patients with high MAD2 expression.

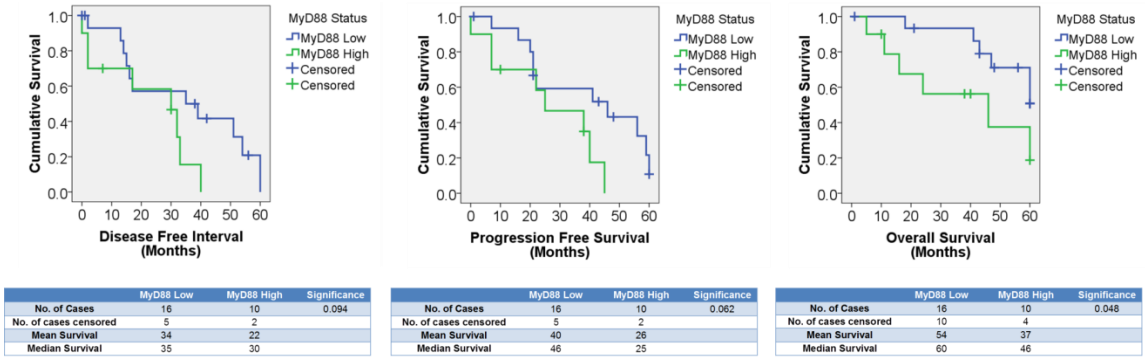

	MyD88 Low	MyD88 High	Significance
No. of Cases	16	10	0.094
No. of cases censored	5	2	
Mean Survival	34	22	
Median Survival	35	30	

	MyD88 Low	MyD88 High	Significance
No. of Cases	16	10	0.062
No. of cases censored	5	2	
Mean Survival	40	26	
Median Survival	46	25	

	MyD88 Low	MyD88 High	Significance
No. of Cases	16	10	0.048
No. of cases censored	10	4	
Mean Survival	54	37	
Median Survival	60	46	

Figure 6.15 MyD88 expression in patients with low MAD2 and low TLR4 expression and its effect on patient prognosis. Patients who had a high MyD88 immunostaining score in the low MAD2 and low TLR4 expression group had a significant reduction in their PFS, They also exhibited a reduction in their DFI, OS, but this was not significant, $p<0.05$.

6.4.5.4 MyD88, TLR4 and MAD2 can be used successfully in combination to accurately predict patient prognosis

This section explores the various phenotypes observed when MyD88, TLR4 and MAD2 staining patterns were examined within the same patients **(Figure 6.16)**. When MyD88, TLR4 and MAD2 expression were assessed within the TMA cohort, 1/46 (2%) of patients exhibited high expression of MyD88, TLR4 and MAD2 (MyD88 High, TLR4 High MAD2 High), 3/46 (7%) of patients exhibited high expression of MyD88 and TLR4 and low expression of MAD2 (MyD88 High, TLR4 High MAD2 Low), 17/46 (37%) of patients exhibited high expression of MyD88 and low expression of TLR4 and MAD2 (MyD88 High, TLR4 Low MAD2 Low), 3/46 (7%) of patients exhibited high expression of MyD88, low expression of TLR4 and high expression of MAD2 (MyD88 High, TLR4 Low MAD2 High), 19/46 (41%) of patients exhibited low expression of MyD88, TLR4 and MAD2 (MyD88 Low, TLR4 Low MAD2 Low), 1/46 (2%) of patients exhibited low expression of MyD88, high expression of TLR4 and low expression of MAD2 (MyD88 Low, TLR4 High MAD2 Low). 2% of patients exhibited low expression of MyD88 and high expression of TLR4 and MAD2 (MyD88 Low, TLR4 High MAD2 High).

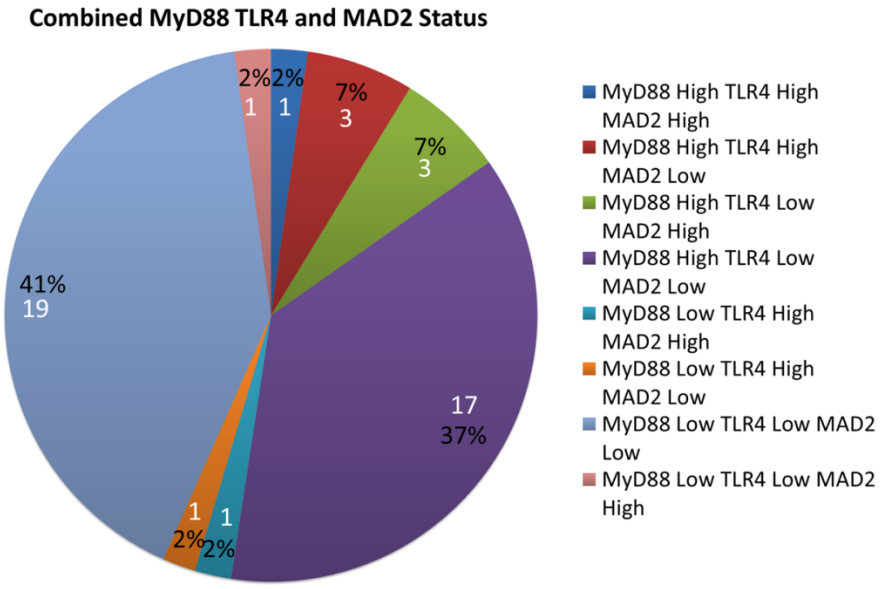

Figure 6.16 Combined MyD88, TLR4 and MAD2 expression in the TMA cohort. When MyD88, TLR4 and MAD2 expression were assessed within the TMA cohort, 2% of patients exhibited high expression of MyD88, TLR4 and MAD2 (MyD88 High, TLR4 High MAD2 High), 7% of patients exhibited high expression of MyD88 and TLR4 and low expression of MAD2 (MyD88 High, TLR4 High MAD2 Low), 37% of patients exhibited high expression of MyD88 and low expression of TLR4 and MAD2 (MyD88 High, TLR4 Low MAD2 Low), 7% of patients exhibited high expression of MyD88, low expression of TLR4 and high expression of MAD2 (MyD88 High, TLR4 Low MAD2 High), 41% of patients exhibited low expression of MyD88, TLR4 and MAD2 (MyD88 Low, TLR4 Low MAD2 Low), 3% of patients exhibited low expression of MyD88, high expression of TLR4 and low expression of MAD2 (MyD88 Low, TLR4 High MAD2 Low). 2% of patients exhibited low expression of MyD88 and high expression of TLR4 and MAD2 (MyD88 Low, TLR4 High MAD2 High).

From this information, Kaplan-Meier analysis was performed to determine whether the combined expression of MyD88, TLR4 and MAD2 influenced the prognosis of patients within the cohort **(Figure 6.17)**. Patients who had a high MyD88, high TLR4 and low MAD2 immunostaining score exhibited a reduction in their mean and median DFI, PFS and OS, although this was not significant. These results demonstrate that those with high MyD88, high TLR4 and low MAD2 expression have poorer outcomes.

6.4.6 The primary metastatic recurrent study

6.4.6.1 Characteristics of the primary metastatic recurrent study cohort

The primary metastatic recurrent (PMR) study cohort was composed of 30 FFPE sections from 10 patients with high grade papillary serous epithelial ovarian cancer. FFPE tissue blocks from each patient were selected from the ovary (primary site), the omentum (metastatic site) and from a site of recurrent disease **(Figure 6.17)**. Sections were then stained for MyD88, TLR4, MyD88 and MAD2 and the staining patterns of the 10 patients at the various sites of disease were then assessed. The mean age of the population was 65 $\pm$ 12 years. The mean progression free survival (PFS) for these patients was 20 $\pm$ 10 months. The mean disease free interval (DFI) for these patients was 12 $\pm$ 8 months. The mean overall survival (OS) for these patients was 45$\pm$ 30 months. All patients had grade 3 and stage 3 tumours, with 1/10 (10%) defined as stage 3A tumour, 2/10 (20%) having a stage 3B tumour and 7/10 (70%) having a stage 3C tumour. 1/10 (10%) of the patients underwent suboptimal debulking and 9/10 (90%) underwent optimal surgical debulking. 1/10 (10%) were alive and 9/10 (90%) were dead . 4/10 (40%) were responders (>12 months), 5/10 (50%) were partial responders (7-12 months) and 1/10 (%) were non responders (0-6 months). A summary of the demographics for each patient is displayed in **(Table 6.2)**.

Table 6.2 Demographics of the PMR study cohort.

Patient No.	Age	Stage	Grade	Debulking Status	DFI	PFS	OS	Recurred	RIP
Patient 1	60	3C	3	SUBOPTIMAL	11	17	41	Recurred	Dead
Patient 2	43	3B	3	OPTIMAL	8	13	30	Recurred	Dead
Patient 3	45	3A	3	OPTIMAL	2	7	32	Recurred	Dead
Patient 4	52	3C	3	OPTIMAL	16	21	73	Recurred	Dead
Patient 5	60	3C	3	OPTIMAL	11	43	60	Recurred	Dead
Patient 6	60	3C	3	OPTIMAL	7	12	23	Recurred	Dead
Patient 7	74	3C	3	OPTIMAL	30	38	75	Recurred	Dead
Patient 8	59	3C	3	OPTIMAL	18	22	48	Recurred	Dead
Patient 9	53	3B	3	OPTIMAL	8	14	28	Recurred	Dead
Patient 10	72	3C	3	OPTIMAL	34	40	60	Recurred	Alive

DFI- Disease free interval **PFS**- Progression free survival **OS**-Overall survival **RIP**- Dead or Alive. Patient samples staged according Federation International of Gynecology & Obstetrics (FIGO) system (+)-patient is censored as the even has not occurred yet.

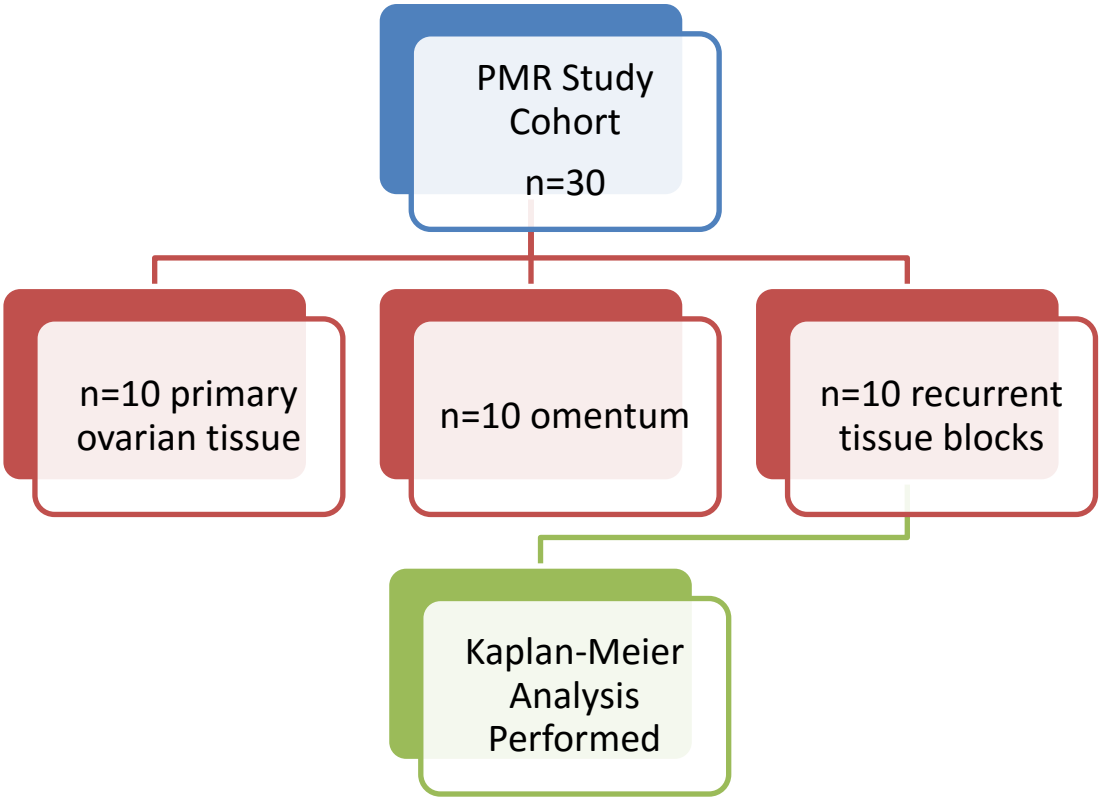

Figure 6.17 An overview of the primary metastatic recurrent (PMR) study cohort. The PMR study cohort consisted of FFPE tissue sections from 10 patients with high grade serous epithelial ovarian cancer. Tissue blocks from each individual were selected from the primary site, metastatic omental disease, and from a site of recurrent disease. Sections were stained for TLR4, MyD88 and MAD2 and the staining patterns of the 10 patient were then correlated with patient survival using Kaplan-Meier analysis.

For the PMR study cohort, the same scoring system was used as with the TMA cohort **(Section 6.3.6)**. This scoring system uses the product of the immunointensity and the immunopositivity scores to generate an overall score for each tissue section with a maximum possible score of 12. Based on the overall immunostaining score, patient samples were classified into high expression (9-12) and low expression categories (0-8) for TLR4, MyD88 and MAD2.

In samples exhibiting high TLR4 expression, strong cytoplasmic and membranous staining was observed **(Figure 6.18)**.

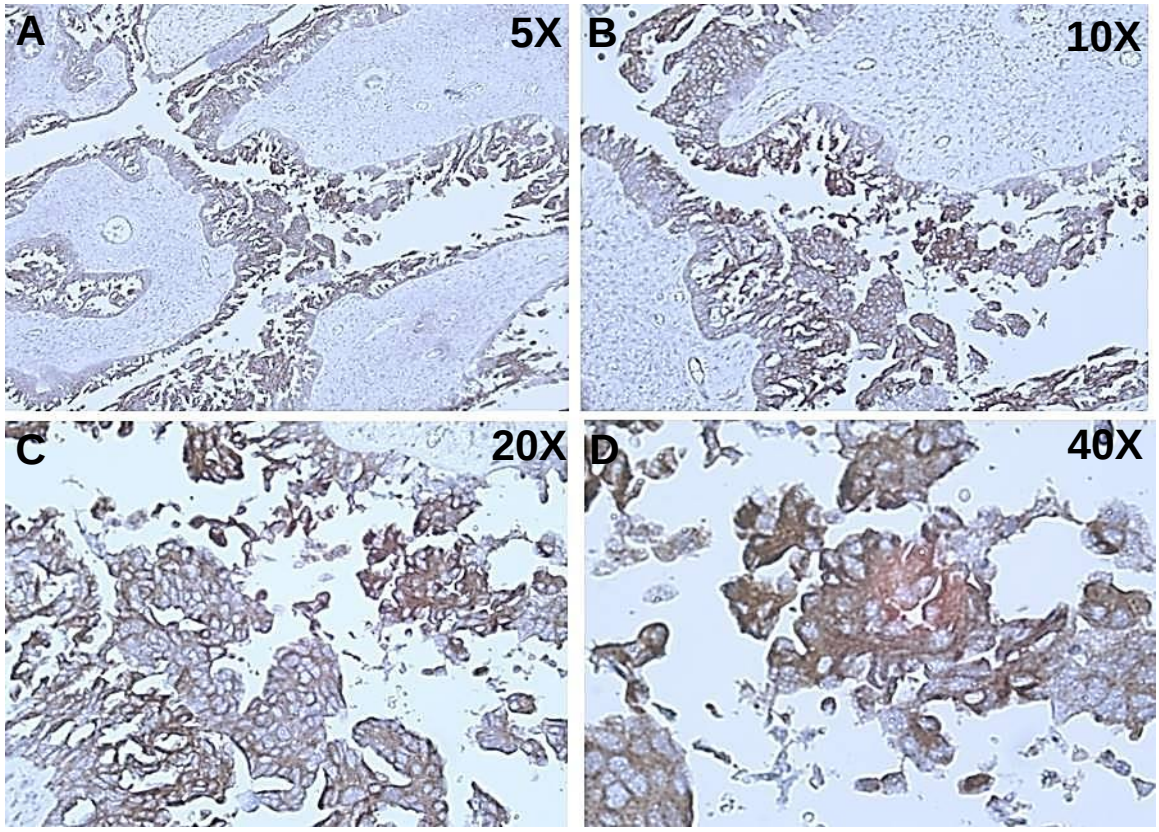

Figure 6.18 A high grade serous ovarian tumour stained for TLR4. Images were taken of a high grade serous tumour which stained strongly for TLR4 at 5X (A), 10X (B), 20X (C) and 40X magnification (D). Images were taken using a Leica DM2500 microscope, Leica DFC290 HD camera and Leica application suite V4 software.

In samples exhibiting high MyD88 expression, strong cytoplasmic staining was observed **(Figure 6.19).**

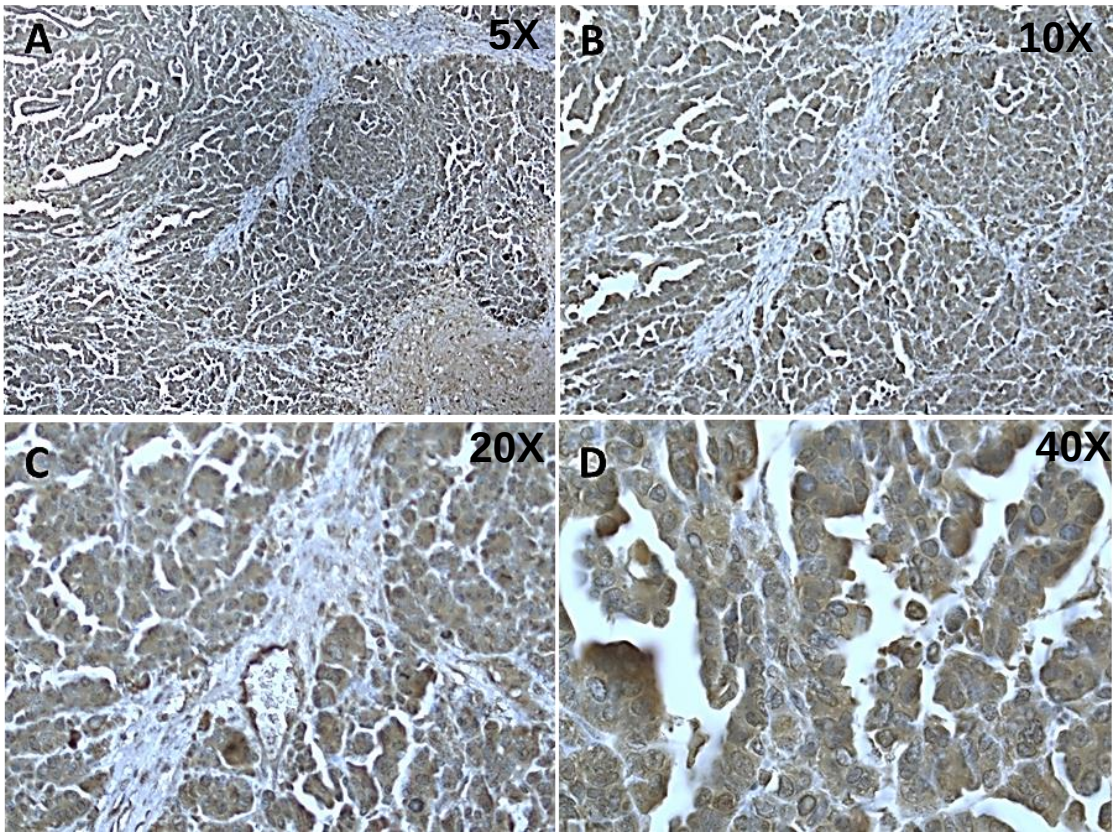

Figure 6.19 A high grade serous ovarian tumour stained for MyD88. Images were taken of a high grade serous tumour which stained strongly for MyD88 at 5X (A), 10X (B), 20X (C) and 40X magnification (D). Images were taken using a Leica DM2500 microscope, Leica DFC290 HD camera and Leica application suite V4 software.

In samples exhibiting high MAD2 expression, strong nuclear staining was observed **(Figure 6.20).**

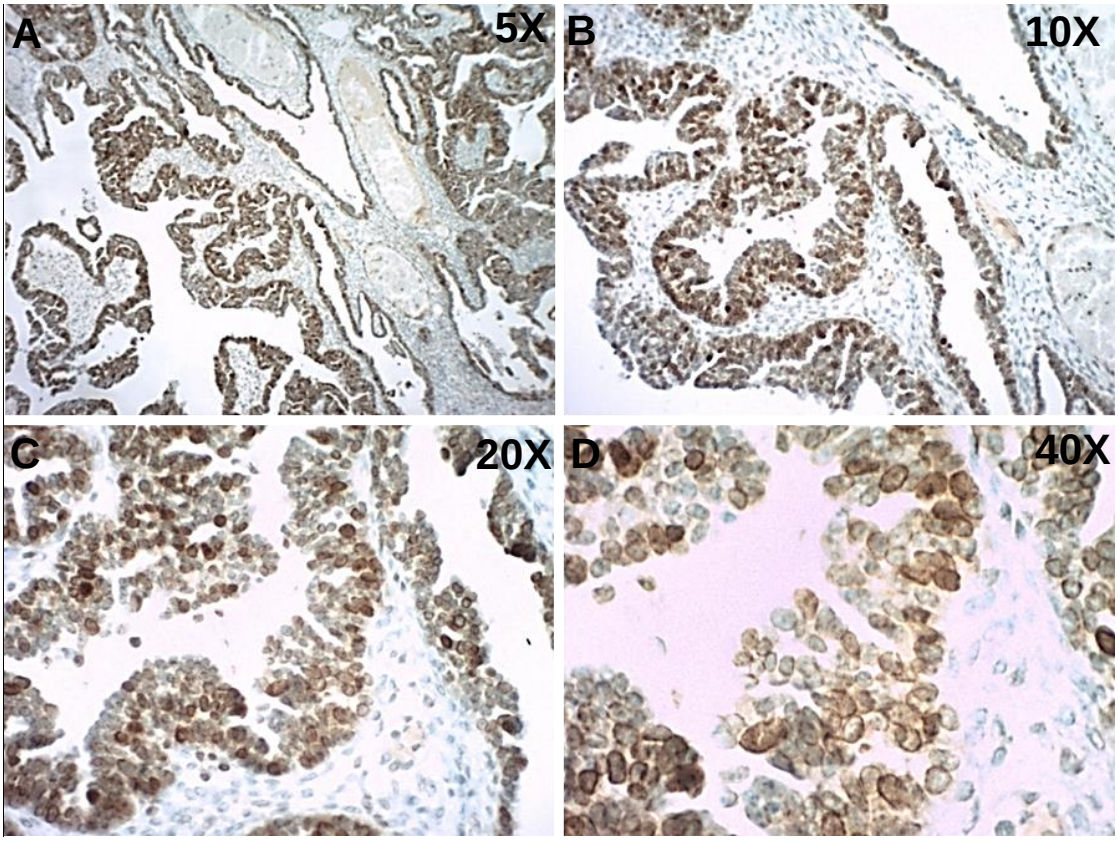

Figure 6.20 A high grade serous ovarian tumour stained for MAD2. Images were taken of a high grade serous tumour which stained strongly for MAD2 at 5X (A), 10X (B), 20X (C) and 40X magnification (D). Images were taken using a Leica DM2500 microscope, Leica DFC290 HD camera and Leica application suite V4 software.

6.4.6.2 Correlation of TLR4, MyD88 and MAD2 immunostaining patterns in the PMR cohort with patient prognosis

Patient samples within the PMR study cohort were stained for MyD88, TLR4 and MAD2 using the Ventana benchmark LT automated immunostaining module. Patient details were obtained from the Discovary bioresource database. The 10 patients were scored from 0-12 for each marker and divided into high (9-12) and low (0-8) immunostaining categories. Details about surgery, chemotherapy, the development of recurrent disease and last correspondence with the patients whether they were deceased or alive were recorded and used to determine the DFI, PFS and OS of each patient. This information, along with immunostaining scores for MAD2, MyD88 and TLR4 were used to assess the impact of these three markers at each stage of disease, primary, omental metastasis and disease recurrence on patient prognosis **(Figure 6.21)**. 1/10 patients stained strongly immunopositive for TLR4 at primary stage of disease. 3/10 patients stained strongly immunopositive for TLR4 once the tumour had spread to the omentum and 4/10 patients stained strongly immunopositive for TLR4 once a recurrent tumour had formed following chemotherapy. 7/10 cases exhibited high expression of MyD88 at primary disease. 8/9 cases exhibited high expression of MyD88 during metastasis, 1 case was void and could not be re-stained over the course of the project. 9/9 cases exhibited high expression of MyD88 disease recurrence, 1 case was void and could not be re-stained over the course of the project. 1/10 patients stained strongly immunopositive for MAD2 at primary stage of disease. 4/10 patients stained strongly immunopositive for MAD2 once the tumour had spread to the omentum and 7/10 patients stained strongly immunopositive for MAD2 once a recurrent tumour had formed following chemotherapy.

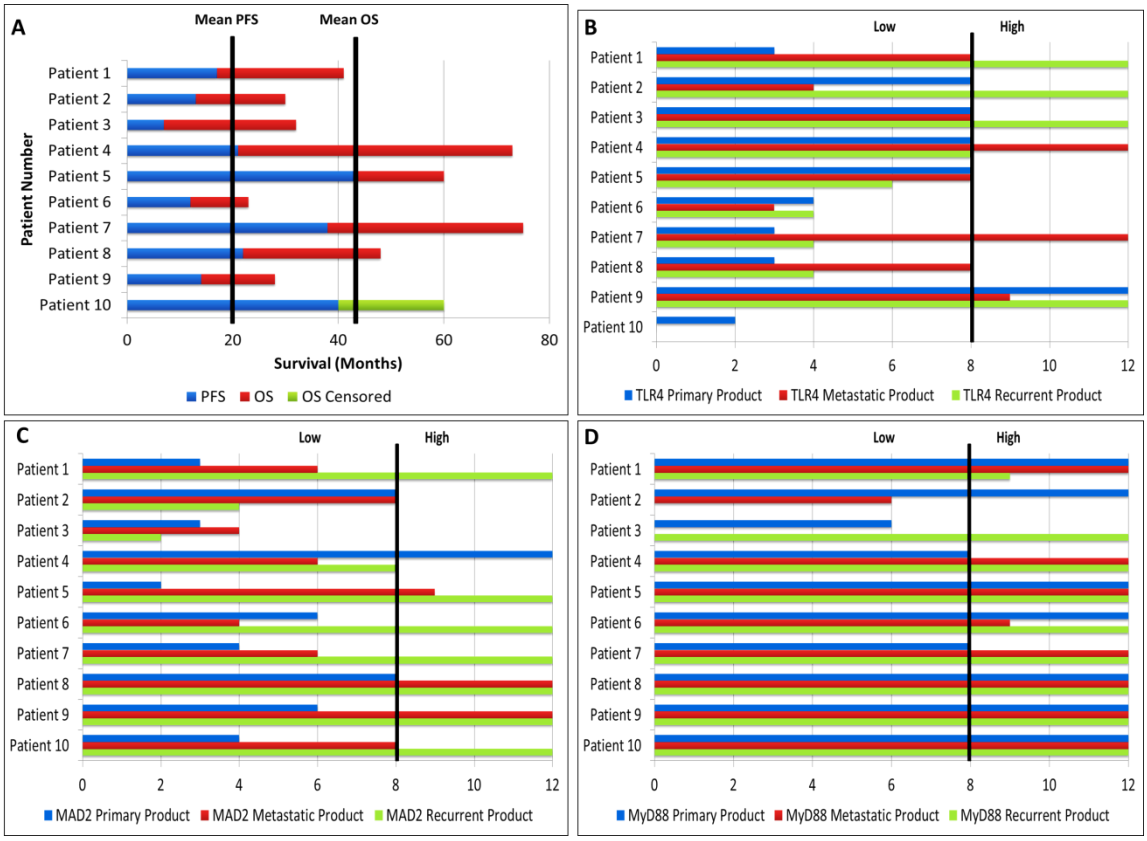

Figure 6.21 Patient timeline, TLR4, MAD2 and MyD88 status during the course of disease. (A) A patient timeline in months (X axis) of each individual patient, which were randomly assigned a number (Patient No.) detailing important events during their disease such as PFS (Blue) and OS (Red) and for one patient whose was still alive during the course of this study their censored overall survival (Green). The first and second black lines in figure A demonstrate the average PFS and OS of the PMR cohort respectively. TLR4 scores (B) MAD2 scores (C) and MyD88 scores (D) at primary disease (Blue), metastatic disease (Red) and during disease recurrence (Green) for each individual patient are also displayed above. Patients were scored from 0-12 and classified as having low expression (0-8) or high expression (9-12) for each marker. Patients 1,2,3,6,9 had the lowest PFS and OS rates among the 10 patients. Interestingly all of these patients apart from patient 6, had high TLR4 expression at recurrent disease. Patients 1, 2 and 3 also had low MAD2 expression at primary disease, omental metastasis and recurrent disease, while patients 6&9 had low MAD2 status at primary disease only. These results therefore suggest that a TLR4 high phenotype during disease recurrence and having low MAD2 status throughout the course of disease, lead to poorer survival outcomes.

Patients 1, 2, 3, 6 and 9 had the lowest PFS and OS rates among the 10 patients. Interestingly all of these patients apart from patient 6, had high TLR4 expression at recurrent disease. Patients 1, 2 and 3 also had low MAD2 expression during primary disease, metastasis and recurrent disease, while patients 6&9 had low MAD2 status at primary disease only. These results therefore suggest that a TLR4 high phenotype during disease recurrence and having low MAD2 status at primary disease and throughout the course of ovarian disease may have led to shorter time to recurrence and death in these patients. Following initial assessment, patient information along with immunostaining scores for each marker, were entered into SPSS and used to generate Kaplan-Meier curves. Kaplan-Meier curves were generated to assess the impact of TLR4 and MAD2 expression patterns at each site of disease. Patient 4 displayed low MyD88 and high MAD2 expression at primary disease. Patient 7 displayed low MyD88 expression and low TLR4 expression at primary disease. These two patients had the best survival outcomes among the 10 patients

6.4.6.3 High TLR4 expression is associated with reduced DFI, PFS and OS during primary disease and disease recurrence and reduced PFS during metastasis

During primary disease patients who had a high TLR4 immunostaining score exhibited a reduction in their mean and median DFI, 15 months vs 8 months and 11 months vs 8 months respectively, although this was not significant as only 1 patient had a high TLR4 score at primary disease. They also exhibited a reduction in their mean and median PFS, 24 months vs 14 months and 21 months vs 14 months, although this was not significant. They also exhibited a reduction in their mean and median OS compared to those with a low TLR4 score, 51 months vs 28 months and 48 months vs 28 months respectively, although this was not significant. During metastasis, in comparison to patients with high TLR4 expression, patients with low TLR4 expression exhibited a reduction in their mean and median OS, 59 vs 42 and 72 vs 41 months respectively, although these differences were not significant. They also exhibited a reduction in their mean and median DFI, 18 months vs 13 months and 18 months vs 11 months respectively, although these differences were not significant. While conversely those with high TLR4 expression exhibited a reduction in their mean and median PFS compared to those with low TLR4 expression, 22 months vs 17 months and 24 months vs 21 months respectively, although these differences were not significant.

During recurrent disease patients who had a high TLR4 immunostaining score exhibited significant reductions in their mean and median DFI (p=0.036), PFS (p=0.017) and OS (p=0.024) compared to those with a low TLR4 immunostaining score **(Figure 6.22)**.

.

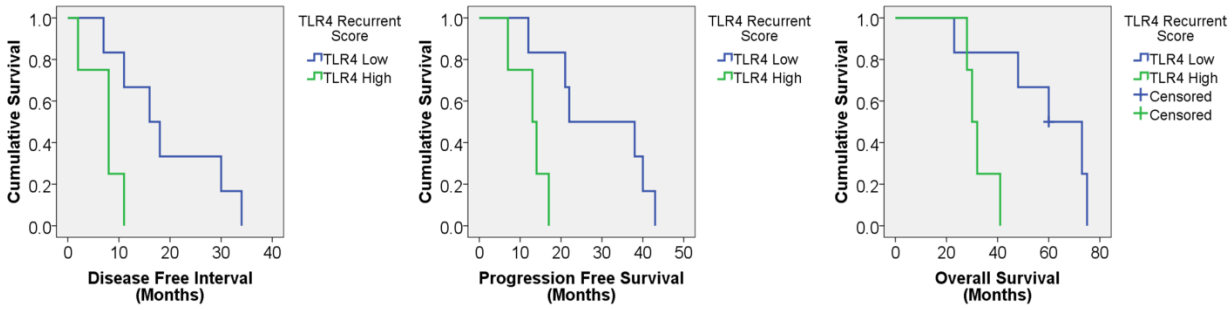

TLR4 Recurrent Score	TLR4 Low	TLR4 High	Significance
No. of Cases	6	4	0.036
No. of cases censored	0	0	
Mean Survival	19	7	
Median Survival	16	8	

TLR4 Recurrent Score	TLR4 Low	TLR4 High	Significance
No. of Cases	6	4	0.017
No. of cases censored	0	0	
Mean Survival	29	13	
Median Survival	22	13	

TLR4 Recurrent Score	TLR4 Low	TLR4 High	Significance
No. of Cases	6	4	0.024
No. of cases censored	1	0	
Mean Survival	59	33	
Median Survival	60	30	

Figure 6.22 TLR4 expression during disease recurrence and patient prognosis. Patient samples within the PMR study cohort were stained for TLR4. TLR4 expression patterns during disease recurrence were then correlated with patient prognosis. In recurrent disease patients who had a high TLR4 immunostaining score exhibited significant reductions in their mean and median DFI, PFS and OS compared to those with high TLR4 score, $p<0.05$.

Overall patients with high TLR4 scores at primary and recurrent sites of disease exhibited reductions in their DFI, PFS and OS indicating that high TLR4 status in tumours at the primary site, or during disease recurrence may impact upon patient prognosis and TLR4 high tumours likely form or re-form quicker following chemotherapy, leading to shorter time to recurrence and shorter overall survival in patients, while low TLR4 expression in the omentum may also have an impact on patient survival.

6.4.6.4 The impact of MyD88 expression during primary disease, metastasis and recurrence

During primary disease patients who had a high MyD88 immunostaining score exhibited a minor reduction in their mean and median DFI compared to those with low MyD88 expression, 14 months vs 16 months respectively and 11 vs 16 months respectively, although this was not significant. They also exhibited a minor reduction in their median PFS compared to those with low MyD88 expression, 17 months vs 21 months respectively, although this was not significant. They also exhibited a large reduction in their mean and median OS compared to those with low MyD88

expression, 41 months vs 60 months and 41 months vs 73 months respectively, although this was not significant.

During metastasis, patients who had a low MyD88 immunostaining score exhibited reductions in their mean and median DFI, PFS and OS, compared to those with a high MyD88 score. Although this was not significant as it was only based on one patient had a low MyD88 score. 7/9 patients exhibited maximum scores for MyD88 during disease metastasis i.e. they exhibited a product score of 12. When survival rates for those patients who exhibited maximum MyD88 score were compared with those patients who didn't achieve maximum scores, significant differences in survival were detected **(Figure 6.23)**. Specifically patients a maximum MyD88 score exhibited a significant reduction in their mean and median DFI, 8 months vs 17 months and 7 months vs 16 months respectively (p=0.011). They also exhibited a significant reduction in their mean and median PFS, 13 months vs 28 months and 12 months vs 21 months respectively (p=0.002). Patients with maximum MyD88 scores also exhibited a significant reduction in their mean and media OS, 27 months vs 53 months and 25 months vs 68 months respectively (p=0.018). As all 9 patients exhibited high MyD88 immunostaining the effect of MyD88 expression during disease recurrence could not be determined. However as all patients exhibited MyD88 expression it suggests that MyD88 is a highly important in recurrent disease.

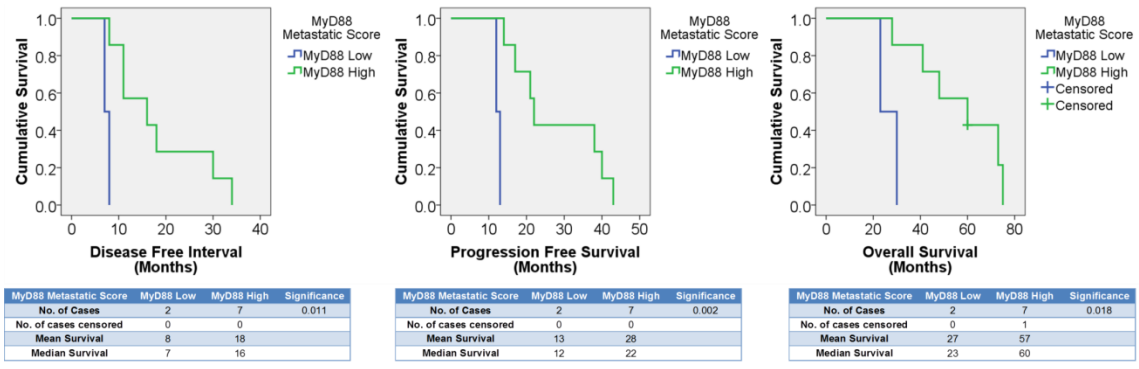

MyD88 Metastatic Score	MyD88 Low	MyD88 High	Significance
No. of Cases	2	7	0.011
No. of cases censored	0	0	
Mean Survival	8	18	
Median Survival	7	16	

MyD88 Metastatic Score	MyD88 Low	MyD88 High	Significance
No. of Cases	2	7	0.002
No. of cases censored	0	0	
Mean Survival	13	28	
Median Survival	12	22	

MyD88 Metastatic Score	MyD88 Low	MyD88 High	Significance
No. of Cases	2	7	0.018
No. of cases censored	0	1	
Mean Survival	27	57	
Median Survival	23	60	

Figure 6.23 MyD88 expression and metastatic disease. Patient samples within the PMR study cohort were stained for MyD88. MyD88 expression patterns during metastatic disease were then correlated with patient prognosis. Patients who had a low MyD88 immunostaining score exhibited reductions in their mean and median DFI, PFS and OS compared to those with a high MyD88 score, $p<0.05$, $p<0.01$.

6.4.6.5 Observations from MyD88 immunostaining within the PMR study

Immunostaning of FFPE sections for MyD88 in the PMR study cohort revealed some interesting staining patterns. In some cases as well as cytoplasmic staining, perinuclear accentuation and nuclear staining for MyD88 was observed. Additionally it was observed that with increasing staining intensity of MyD88 in tumour cells resulted in an increase in MyD88 staining in adjacent stromal tissue **(Figure 6.24)**. This may indicate that MyD88 positive cells are educating stromal tissue, making them express MyD88 and become more "tumour like".

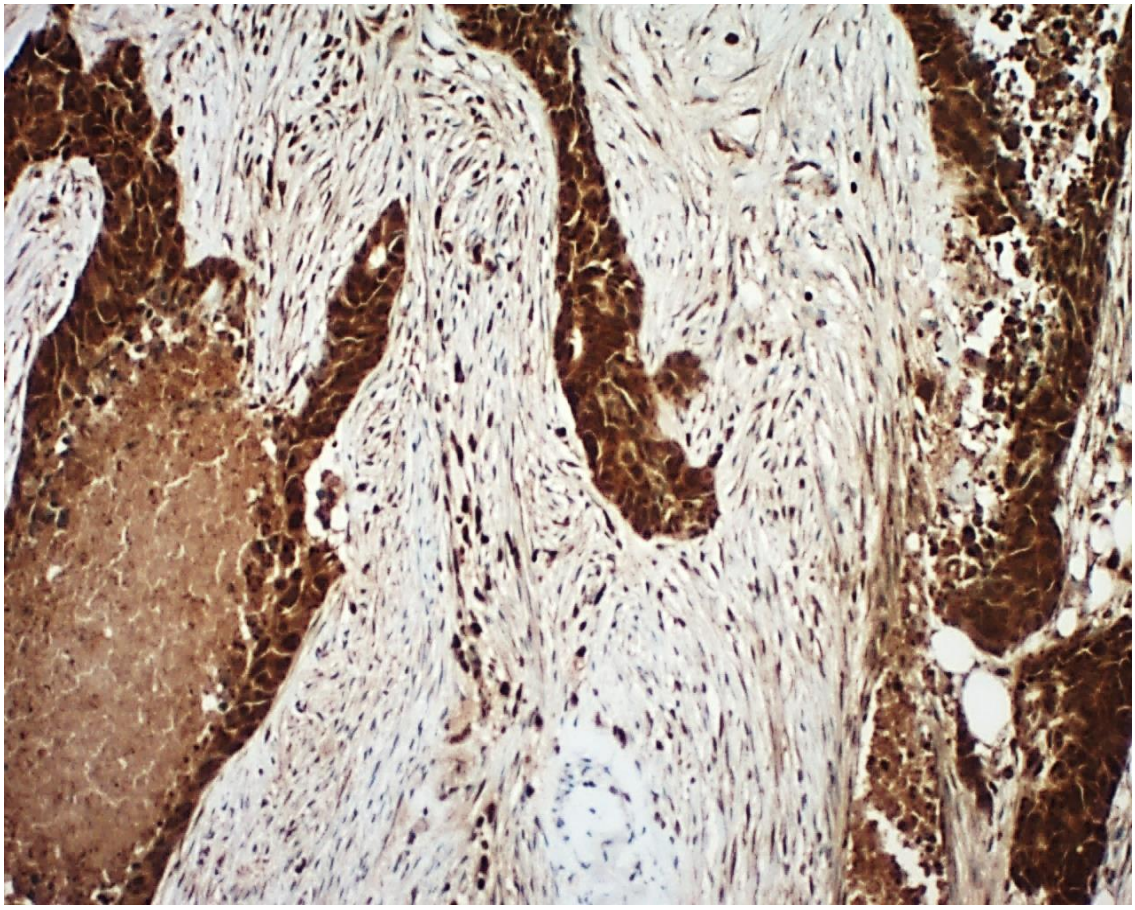

Figure 6.24 Stromal education and nuclear staining of MyD88 by tumour cells. An FFPE section was stained for MyD88. The areas of tumour are staining strongly immunopositive and inducing moderate MyD88 positivity in the surrounding stromal tissue. Images were taken at 40X magnification using a Leica DM2500 microscope, Leica DFC290 HD camera and Leica application suite V4 software.

Areas of necrosis within tumour were also moderately MyD88 immunopositive. These necrotic areas may be influencing MyD88 expression in the surrounding tumour cells **(Figure 6.25)**. Necrotic debris and damage associated molecular patterns (DAMPs) has been shown to activate TLR4 signalling(Sato *et al*. 2009).

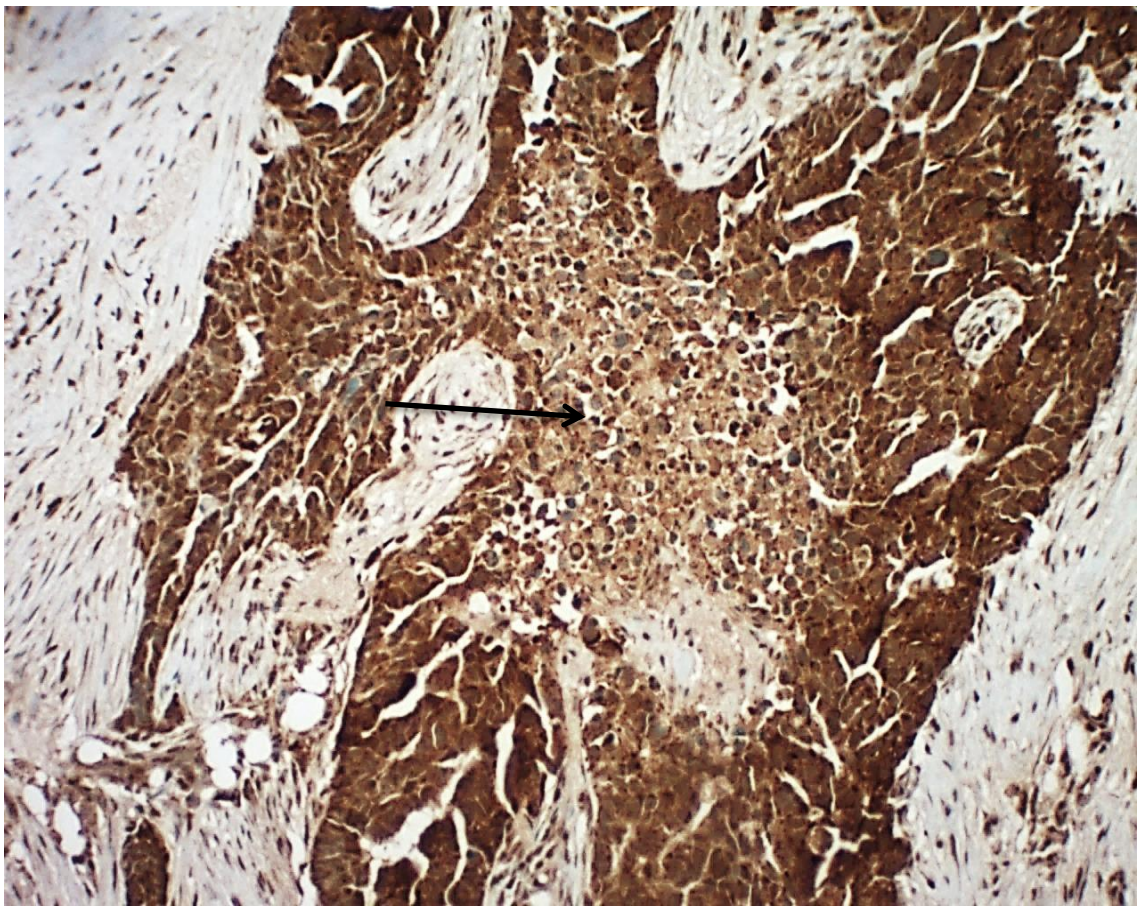

Figure 6.25 MyD88 staining in necrotic cells. An FFPE section was stained for MyD88 and Images were taken at 5X magnification. The arrow indicates the necrotic region which is moderately immunopositive for MyD88, the area surrounded by tumour cells which are strongly immunopositive. Images were taken at 5X magnification using a Leica DM2500 microscope, Leica DFC290 HD camera and Leica application suite V4 software.

MyD88 positive tumour cells adjacent to blood vessels are inducing the expression of MyD88 in endothelial cells, this may be contributing to metastasis in ovarian cancer **(Figure 6.26)**.

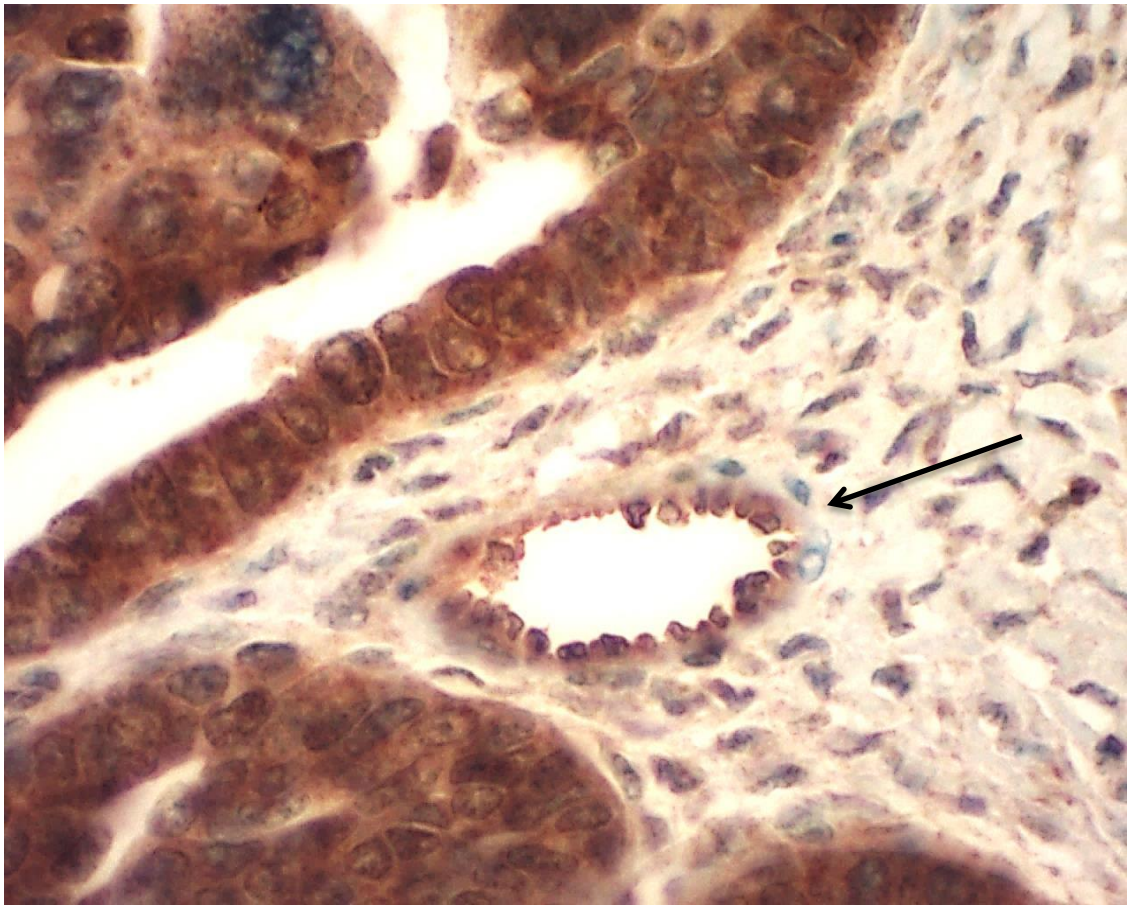

Figure 6.26 Endothelial cells staining MyD88 positive in a primary ovarian tumour. A primary tumour was stained for MyD88. The arrow indicates an artery with MyD88 positive endothelial cells in close proximity to MyD88 positive tumour cells, the surrounding stromal tissue is weakly positive or negative for MyD88 expression. Images were taken at 40X magnification using a Leica DM2500 microscope, Leica DFC290 HD camera and Leica application suite V4 software.

In certain cases MyD88 positive tumour cells appeared quite granular, this may indicate that MyD88 expression may be having an effect on endosomal machinery **(Figure 6.27)**. MyD88 positive tumour cells may therefore be influencing MyD88 expression in surrounding stromal tissue and blood vessels by the secretion of various factors in exosomes.

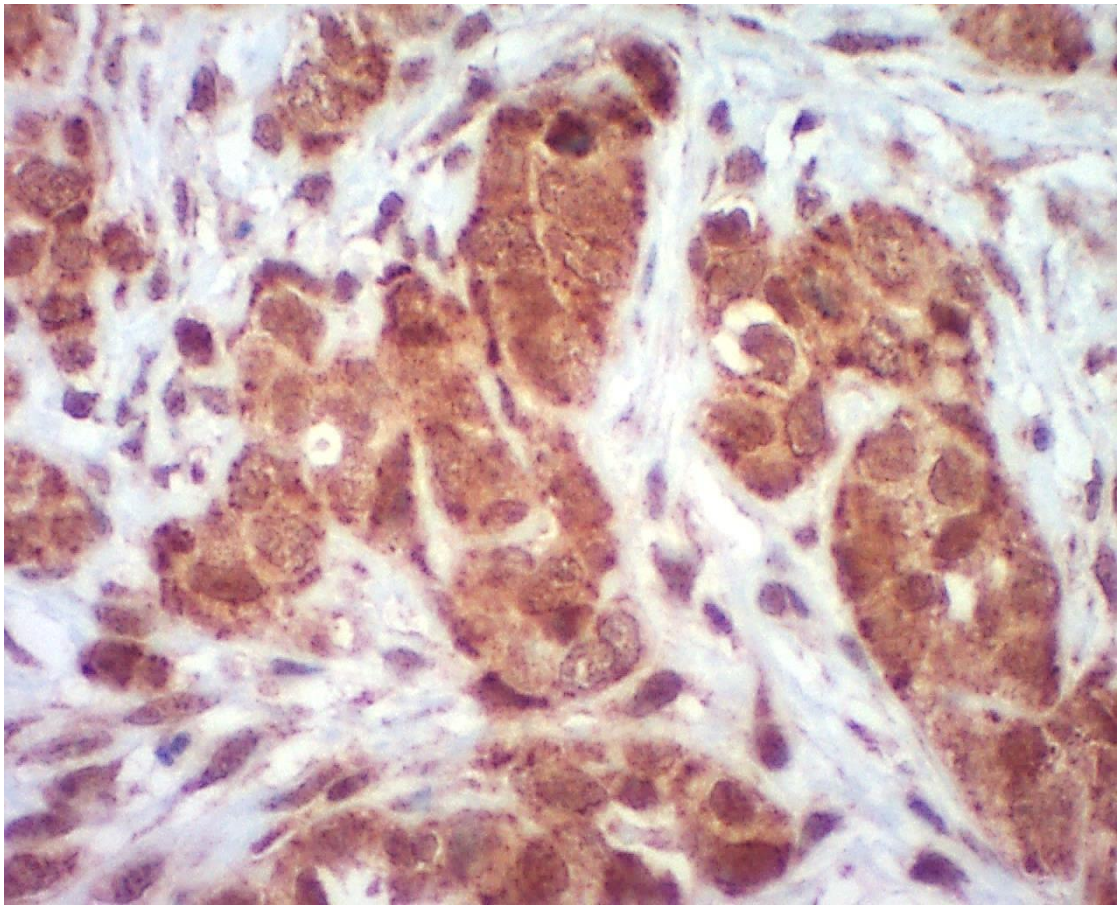

Figure 6.27 Granular MyD88 positive tumour cells. Cells staining strongly positive for MyD88 in certain instances, were highly granular. This may indicate that MyD88 expression is affecting endosomal machinery. Images were taken at 40X magnification using a Leica DM2500 microscope, Leica DFC290 HD camera and Leica application suite V4 software.

In one instance we observed small areas of MyD88 positive cells, within selective pockets of the tumour. We believe that perhaps these are the true MyD88 positive ovarian cancer stem cells, which lead to chemoresistane and recurrence. In this case there was also weak MyD88 positivity in surrounding tumour and stromal cells demonstrating once again that MyD88 positive cells are educating cells within their microenvironment **(Figure 6.28)**.

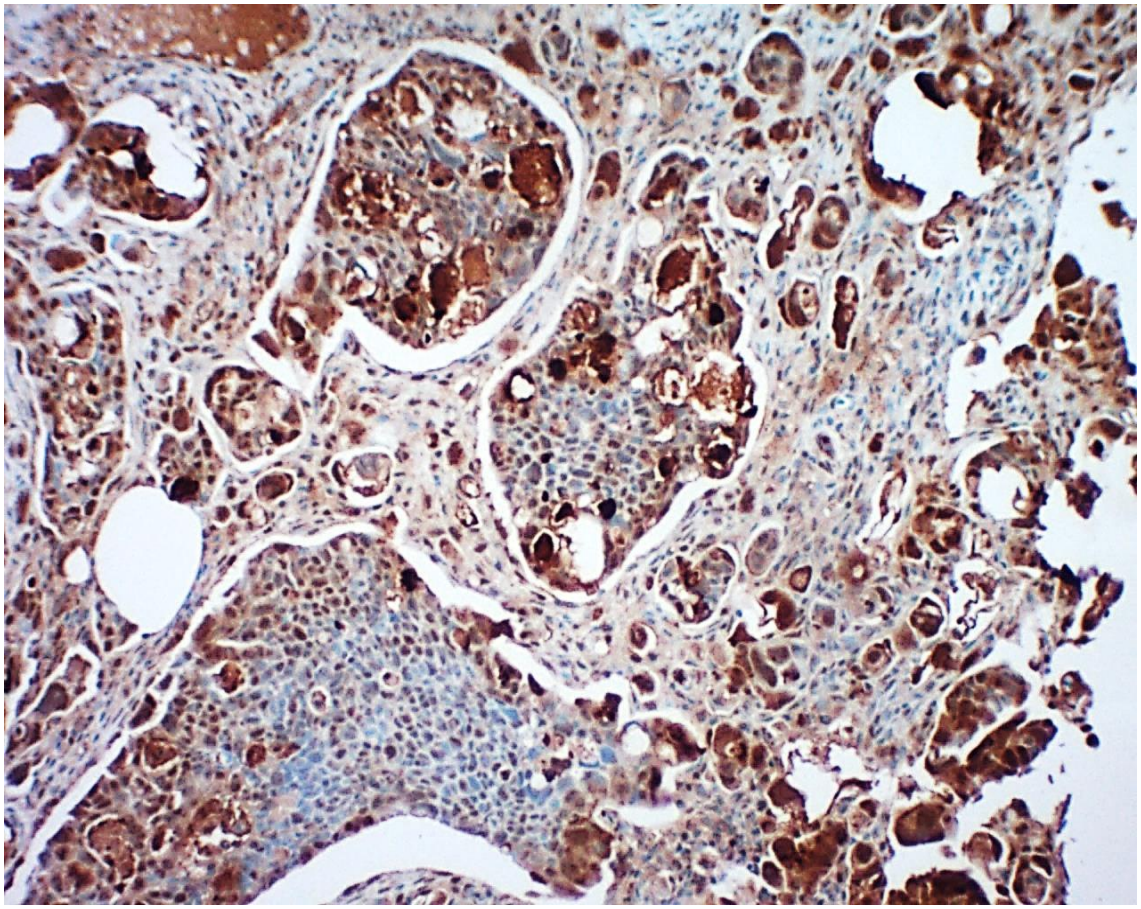

Figure 6.28 MyD88 positivity in cancer stem cell niches. Pockets of cells were staining strongly immunopositive for MyD88. MyD88 staining in this instance may be highlighting MyD88+ ovarian cancer stem cells. Images were taken at 5X magnification using a Leica DM2500 microscope, Leica DFC290 HD camera and Leica application suite V4 software.

6.4.6.6 The impact of MAD2 expression during primary disease, metastasis and recurrence

During primary disease patients who had a low MAD2 immunostaining score exhibited a minor reduction in their mean and median DFI compared to those with high MAD2 expression, 14 months vs 16 months respectively and 11 vs 16 months respectively, although this was not significant as only 1 patient had a MAD2 high score. They also exhibited a minor reduction in their median PFS compared to those with high MAD2 expression, 17 months vs 21 months respectively, although this was not significant. They also exhibited a minor reduction in their mean and median OS compared to those with high MAD2 expression, 46 months vs 73 months and 41 months vs 73 months respectively, although this was not significant. During metastasis, patients who had a low MAD2 immunostaining score had exhibited minor reduction in their median PFS and OS, 17 months vs 22 months and 45 vs 48 months compared to those with high MAD2 score, although this was not significant. During recurrent disease patients who had a low MAD2 immunostaining score exhibited small reductions in their mean and median DFI compared to patients with High MAD2 expression, 9 months vs 17 months and 8 months vs 11 months respectively, although this was not significant. They also exhibited small reductions in their mean and median PFS, 14 vs 22 months and 13 vs 22 months respectively, although this was just below significance (p=0.084). Moreover they exhibited small reductions in their mean and median OS compared to those with high MAD2 score, 45 months vs 50 months and 32 months vs 48 months respectively, although this was not significant. Overall patients with low MAD2 scores at all three sites of disease exhibited minor reductions in their DFI, PFS and OS indicating that low MAD2 status in tumours at the primary site, metastasis or during disease recurrence may impact upon patient prognosis with MAD2 low tumours leading to shorter time to recurrence and shorter overall survival in patients.

6.5 Discussion

There are currently no available prognostic biomarkers which can be used to direct patient therapy in ovarian cancer. Great improvements in prognosis rates in breast cancer have been achieved through the use of a panel of prognostic biomarkers which direct patient therapy (Oakman *et al*. 2009; Olopade *et al*. 2008; Yanagawa *et al*. 2012; National Cancer Registry 2012a), while ovarian cancer prognosis rates have remained almost unchanged for over 30 years (National Cancer Registry 2012b). Previously our group (Furlong *et al*. 2012; d'Adhemar *et al*. 2014; Mcgrogan *et al*. 2014) and others (Kim & Yoon 2010; Zhu *et al*. 2012; Park *et al*. 2013) have demonstrated the ability of MAD2, TLR4 and MyD88 individually to accurately predict patient prognosis in ovarian cancer. MAD2, TLR4 and MyD88 immunostaining patterns likely highlight the key molecular mechanisms in which they are involved in, specifically their molecular roles in the development of paclitaxel resistance (Sudo 2004; Kelly *et al*. 2006; Szajnik *et al*. 2009; Hao *et al*. 2010; Furlong *et al*. 2012; d'Adhemar *et al*. 2014).

A major aim of this study was to assess whether these three markers could be used in combination, to more accurately predict patient prognosis. It was predicted that patients with low MAD2 expression, high TLR4 expression and high MyD88 expression would have the worst prognosis among patients as due to their disease phenotype, these patients are likely to have responded poorly to paclitaxel therapy.

To determine this, the combined expression of MAD2, TLR4 and MyD88 was assessed in a small pilot study composed of a tissue microarray cohort of patients with high grade serous ovarian cancer. All three markers were initially assessed individually for their ability to predict prognosis rates within this cohort. High TLR4 expression, as an independent marker was an indicator of poor prognosis. TLR4 highlighted patients that had the worst prognosis rates among the patients in the TMA cohort, although this was based on a low number of samples with high expression. A definite trend was observed with MyD88, whereby patients exhibiting high MyD88 expression exhibited a large reduction in their DFI, PFS and OS. MAD2 did not appear to strongly influence prognosis in the TMA cohort, although the low number of high MAD2 expressing cases may have led to this result and further evaluation in a larger cohort may reveal significant trends. Following individual assessment, different combinations of markers were examined. In this population a small subgroup of patients with high TLR4 expression exhibited the worst prognosis of any patients in the TMA cohort. These patients also exhibited a low MAD2 score and high MyD88 score confirming the hypothesis that patients with this phenotype have the worst prognosis. However, it

must be admitted that TLR4 expression in this group seems to be a major factor influencing their prognosis and does not therefore demonstrate the true prognostic potential of these markers in combination.

However, examination of all three markers in different combinations in the TMA cohort revealed that there are multiple different groups of patients with different expression patterns of all three markers. Depending on their expression patterns they may have had entirely different disease outcomes. This work demonstrates that the three markers can be used quite successfully in combination and complement each other. For example when MyD88 expression was examined in the MAD2 low group, those with high MyD88 expression had significantly reduced DFI, PFS and a large decrease in OS. This effect was still significant for PFS when the TLR4 high subgroup was eliminated from the analysis, demonstrating that MAD2 and MyD88 are very useful when used in combination. They highlighted an at risk group not identified by TLR4 immunostaining or either by MyD88 or MAD2 alone. The potential clinical benefits of using all three markers in combination are apparent here as individual assessment of each marker may not have identified these various subgroups of patients. Each subgroup may therefore require a different type of targeted therapy and therapeutic strategy. Personalised medicine and targeted therapy have been used quite successfully to treat many types of cancer (Joo *et al*. 2013). They also hold some benefits over conventional chemotherapies which only target actively dividing cells. Patients need to be given targeted therapies against specific markers expressed in their individual tumours. These targeted therapies may potentially be used with or without conventional chemotherapy to boost therapeutic outcomes. This is what is required to prevent recurrent and chemoresistant disease and perhaps to potentially enhance treatment for those patients, who despite our best efforts still develop recurrent and chemoresistant disease.

MyD88, MAD2 and TLR4 seem to successfully highlight different subgroups of patients achieving one of the major aims of this project and confirming our original hypothesis. The next step is to now determine if they are suitable therapeutic targets or if by examining these subgroups closely we may determine new therapeutic targets and additional prognostic biomarkers.

Another major aim of this project was to assess the role of MyD88, TLR4 and MAD2 over the course of disease. Therefore in another small pilot study, FFPE blocks from primary disease, metastasis and a recurrent disease site were obtained from 10 patients and were then stained for MyD88, MAD2 and TLR4. Expression patterns of

MyD88, TLR4 and MAD2 at each disease site were correlated with patient survival. At primary disease and omental disease only minor reductions in the DFI, PFS, OS rates were observed. Interestingly 1/10 patients displayed high MAD2 expression at primary disease compared to 3/10 patients during omental disease and 7/10 patients during disease recurrence. Overexpression of MAD2 is common in many human cancers and is associated with chromosomal instability (CIN) and uncontrolled cellular proliferation (Fung *et al*. 2007; Hisaoka *et al*. 2008; Zhang *et al*. 2008; Schvartzman *et al*. 2011; Kato *et al*. 2011; Nakano *et al*. 2012); therefore high MAD2 status in this study during disease recurrence might indicate an increase in proliferation rates following chemotherapy. However, despite the increase in MAD2 expression during disease recurrence, patients with low MAD2 status during disease recurrence still had worse prognosis rates. This may indicate that MAD2 downregulation or maintenance of a MAD2 low phenotype during both primary and recurrent disease provides a survival advantage to cancerous cells leading to poorer patient outcomes. It is likely that these cells are senescent and were resistant to initial paclitaxel therapy and to additional rounds of chemotherapy that patients may have received. While those who had a MAD2 high phenotype during disease recurrence may have responded better to chemotherapy, as the 2nd line chemotherapeutic agents were able to actively target dividing cells.

At primary disease, 1 patient exhibited high TLR4 expression and had a reduction in their DFI, PFS, OS compared to those with low TLR4 expression. Interestingly 4/10 patients exhibited high TLR4 expression at recurrent disease and this significantly affected their survival outcomes. This may be due to the role of TLR4 in paclitaxel resistance. Our group had previously shown that knockdown of TLR4 *in vitro* renders ovarian cancer cells more sensitive to paclitaxel as detailed in Chapter 3. In addition overexpression of TLR4 in oesophageal cancer (Sheyhidin *et al*. 2011), breast cancer (Rajput *et al*. 2013), colorectal (Doan *et al*. 2009) and hepatocellular cancer (Liu *et al*. 2015) has been shown to render cells more resistant to paclitaxel based chemotherapy. Therefore tumours with a high TLR4 phenotype are likely to survive and re-develop quicker following chemotherapy ultimately reducing the time to recurrence and overall survival of patients. Furthermore there is also a suspected role for TLR4 in the metastasis and the spread of CTCs which may evade conventional chemotherapy and spread to distant target organs and enhance the development of recurrent disease (Hsu *et al*. 2011). TLR4 has also been shown to promote cisplatin resistance in oral squamous cancer cells, through the activation of inflammatory cytokine signalling, an effect that was abolished using siRNA targeting TLR4 (Sun *et*

al. 2012). This suggest that the TLR4 pathway can modulate sensitivity of cancer cells to various chemotherapeutic agents in different in different cell models.

Interestingly, patients with low TLR4 expression in the omentum had reduced although not significant DFI and OS. In a study by Fain (2011), it was previously shown that TLR4 expression negatively correlated with waist circumference and BMI and was downregulated in the omentum of obese patients with diabetes. The authors speculate that perhaps a negative feedback loop exists where TLR4 is downregulated in an effort to restore insulin sensitivity in patients. This may explain the phenomenon observed in this study, and may highlight a link between TLR4, obesity, the metabolome and diabetes which contribute to poor survival rates in ovarian cancer (Bakhru *et al*. 2011; Shah *et al*. 2014; Kumar *et al*. 2014; Horowitz & Wright 2015; Tran *et al*. 2015).

7/10 patients had low MyD88 expression at primary disease and this correlated with DFI, PFS and OS. Interestingly 7/9 patients exhibited maximum scores for MyD88 disease metastasis, those patients who had low MyD88 positivity exhibited significantly reduced survival. This mirrors what occurred with TLR4 in the omentum, again suggesting that perhaps there is crosstalk between the adipose cells in the omentum and tumour cells. All patients exhibited high MyD88 expression during disease recurrence. This highlights the importance of MyD88 throughout ovarian disease and the development of recurrence.

Overall the results demonstrate a strong role for MyD88 TLR4 and MAD2 in ovarian disease and the development of recurrent disease and continued assessment of MyD88, TLR4 and MAD2 expression at different disease sites and during disease recurrence may help guide future patient therapies and give insight into how patients develop recurrent disease and chemoresistance.

6.6 Conclusion

The results demonstrate the clinical utility of TLR4, MAD2 and MyD88 when used individually or in combination to predict patient outcomes. Initial results from this pilot study are promising and could pave the way forward for the introduction of personalised medicine with the ultimate goal of improving upon the poor prognosis rates associated with ovarian cancer. Assessment of MyD88, TLR4 and MAD2 demonstrated that they may play a role in metastasis and recurrent disease and may potentially be useful in directing treatment of patients with recurrent disease.

6.7 References

1) Abraham, J., 2010. OVA1 test for preoperative assessment of ovarian cancer. *Community Oncology*, 7(6), pp.249–250.
2) Anderson, J., Cain, K. & Gelber, R., 1983. Analysis of survival by tumor response. *Journal of Clinical Oncology*, 1(11), pp.710–719. Available at: http://jco.ascopubs.org/content/1/11/710.short.
3) Bakhru, A., Buckanovich, R.J. & Griggs, J.J., 2011. The impact of diabetes on survival in women with ovarian cancer. *Gynecologic Oncology*, 121(1), pp.106–111. Available at: http://dx.doi.org/10.1016/j.ygyno.2010.12.329.
4) Bast, R.C. et al., 1981. Reactivity of a monoclonal antibody with human ovarian carcinoma. *The Journal of clinical investigation*, 68(5), pp.1331–1337.
5) Boivin, M. et al., 2009. CA125 (MUC16) tumor antigen selectively modulates the sensitivity of ovarian cancer cells to genotoxic drug-induced apoptosis. *Gynecologic Oncology*, 115(3), pp.407–413. Available at: http://dx.doi.org/10.10 16/j.ygyno.2009.08.007.
6) Byrd-Leifer, C. a et al., 2001. The role of MyD88 and TLR4 in the LPS-mimetic activity of Taxol. *European journal of immunology*, 31(8), pp.2448–57. Available at: http://www.ncbi.nlm.nih.gov/pubmed/11500829.
7) Cohen, J.G., 2014. In 2014, can we do better than CA125 in the early detection of ovarian cancer? *World Journal of Biological Chemistry*, 5(3), p.286. Available at: http://www.wjgnet.com/1949-8454/full/v5/i3/286.htm.
8) d'Adhemar, C.J. et al., 2014. The MyD88+ Phenotype Is an Adverse Prognostic Factor in Epithelial Ovarian Cancer. *PloS one*, 9(6), p.e100816. Available at: http://www.ncbi.nlm.nih.gov/pubmed/24977712 [Accessed July 2, 2014].
9) Doan, H.Q. et al., 2009. Toll-like receptor 4 activation increases Akt phosphorylation in colon cancer cells. *Anticancer research*, 29(7), pp.2473–2478. Available at: http://ar.iiarjournals.org/content/29/7/2473.short.
10) Domcke, S. et al., 2013. Evaluating cell lines as tumour models by comparison of genomic profiles. *Nature communications*, 4, p.2126. Available at: http://www.pubmedcentral.nih.gov/articlerender.fcgi?artid=3715866&tool=pmcentrez&rendertype=abstract [Accessed January 28, 2014].
11) Fain, J.N., 2011. Correlative studies on the effects of obesity, diabetes and hypertension on gene expression in omental adipose tissue of obese women. *Nutrition and Diabetes*, 1(9), p.e17. Available at: http://dx.doi.org/10.1038/nutd.20 11.14.
12) Felder, M. et al., 2014. MUC16 (CA125): tumor biomarker to cancer therapy, a work in progress. *Molecular cancer*, 13(1), p.129. Available at:http://www.pubmedcentral.nih.gov/articlerender.fcgi?artid=4046138&tool=pmcentrez&rendertype=abstract.
13) Fung, M.K.-L. et al., 2007. MAD2 expression and its significance in mitotic checkpoint control in testicular germ cell tumour. *Biochimica et biophysica acta*, 1773(6), pp.821–32. Available at: http://www.ncbi.nlm.nih.gov/pubmed/17467818 [Accessed October 24, 2012].
14) Furlong, F. et al., 2012. Low MAD2 expression levels associate with reduced progression-free survival in patients with high-grade serous epithelial ovarian cancer. *The Journal of pathology*, 226(5), pp.746–55. Available at: http://www.ncbi.nlm.nih.gov/pubmed/22069160 [Accessed February 23, 2013].
15) Hao, X. et al., 2010. Effect of Mad2 on paclitaxel-induced cell death in ovarian cancer cells. Journal of Huazhong University of Science and Technology. Medical sciences = Hua zhong ke ji da xue xue bao. Yi xue Ying De wen ban = Huazhong keji daxue xuebao. Yixue Yingdewen ban, 30(5), pp.620–5. Available at: http://www.ncbi.nlm.nih.gov/pubmed/21063845 [Accessed March 12, 2014].

16) Hisaoka, M., Matsuyama, A. & Hashimoto, H., 2008. Aberrant MAD2 expression in soft-tissue sarcoma. *Pathology international*, 58(6), pp.329–33. Available at: http://www.ncbi.nlm.nih.gov/pubmed/18477210 [Accessed October 29, 2012].
17) Horowitz, N.S. & Wright, A. a., 2015. Impact of obesity on chemotherapy management and outcomes in women with gynecologic malignancies. *Gynecologic Oncology*, 138(1), pp.201–206. Available at: http://linkinghub. elsevier.com/retrieve/pii/S009082581500791X.
18) Hsu, R.Y.C. et al., 2011. LPS-induced TLR4 signaling in human colorectal cancer cells increases B1 integrin mediated cell adhesion and liver metastasis. *Cancer Research*, 71(5), pp.1989–1998.
19) Huang, J.-M. et al., 2014. Atractylenolide-I sensitizes human ovarian cancer cells to paclitaxel by blocking activation of TLR4/MyD88-dependent pathway. *Scientific reports*, 4, p.3840. Available at: http://www. pubmed central.nih.gov /articlerender.fcgi?artid=3899591&tool=pmcentrez&rendertype=abstract [Accessed June 1, 2014].
20) Joo, W.D., Visintin, I. & Mor, G., 2013. Targeted cancer therapy - Are the days of systemic chemotherapy numbered? *Maturitas*, 76(4), pp.308–314. Available at: http://dx.doi.org/10.1016/j.maturitas.2013.09.008.
21) Kaplan, E.. L.. & Meier, P., 2008. Nonparametric Estimation from Incomplete Observations. , 53(282), pp.457–481.
22) Kato, T. et al., 2011. Overexpression of MAD2 predicts clinical outcome in primary lung cancer patients. *Lung cancer (Amsterdam, Netherlands)*, 74(1), pp.124–31. Available at: http://www.ncbi.nlm.nih.gov/pubmed/21376419 [Accessed October 24, 2012].
23) Kelly, M.G. et al., 2006. TLR-4 signaling promotes tumor growth and paclitaxel chemoresistance in ovarian cancer. *Cancer research*, 66(7), pp.3859–68. Available at: http://www.ncbi.nlm.nih.gov/pubmed/16585214 [Accessed October 22, 2012].
24) Kim, A. et al., 2012. Therapeutic strategies in epithelial ovarian cancer. *Journal of experimental & clinical cancer research : CR*, 31(1), p.14. Available at: http://www.pubmedcentral.nih.gov/articlerender.fcgi?artid=3309949&tool=pmce ntrez&rendertype=abstract [Accessed October 10, 2012].
25) Kim, K.H. & Yoon, M.S., 2010. MyD88 expression and anti-apoptotic signals of paclitaxel in epithelial ovarian cancer cells. , 53(4), pp.330–338.
26) Kumar, A. et al., 2014. Impact of obesity on surgical and oncologic outcomes in ovarian cancer. *Gynecologic Oncology*, 135(1), pp.19–24. Available at: http://dx.doi.org/10.1016/j.ygyno.2014.07.103.
27) Ledermann, J. a & Raja, F. a, 2011. Clinical trials and decision-making strategies for optimal treatment of relapsed ovarian cancer. *European journal of cancer (Oxford, England : 1990)*, 47 Suppl 3, pp.S104–15. Available at: http://www.ncbi.nlm.nih.gov/pubmed/21943964 [Accessed January 2, 2013].
28) Liu, W.-T. et al., 2015. Toll like receptor 4 facilitates invasion and migration as a cancer stem cell marker in hepatocellular carcinoma. *Cancer Letters*, 358(2), pp.136–143. Available at: http://linkinghub.elsevier.com/retrieve/pii/S03043 83514007629.
29) Mcgrogan, B. et al., 2014. Spindle assembly checkpoint protein expression correlates with cellular proliferation and shorter time to recurrence in ovarian cancer, *Human Pathology*, 45(7), pp.1509–1519. Available at: http://dx.doi.org /10.1016/j.humpath.2014.03.004.
30) Nakano, Y. et al., 2012. Mitotic arrest deficiency 2 induces carcinogenesis in mucinous ovarian tumors. *Oncology Letters*, 3(2), pp.281–286.
31) National Cancer Registry, 2012a. Breast Cancer Incidence, Mortality, Treatment and Survival in Ireland : 1994-2009 European Network of Cancer Registries.

32) National Cancer Registry, 2012b. Cancer Trends No 14. Cancers of the ovary.
33) Oakman, C. et al., 2009. Recent advances in systemic therapy: new diagnostics and biological predictors of outcome in early breast cancer. *Breast cancer research : BCR*, 11(2), p.205. Available at: http://www.pubmed central. nih.gov/articlerender.fcgi?artid=2688942&tool=pmcentrez&rendertype=abstract [Accessed January 30, 2013].
34) Olopade, O.I. et al., 2008. Advances in breast cancer: pathways to personalized medicine. *Clinical cancer research : an official journal of the American Association for Cancer Research*, 14(24), pp.7988–99. Available at: http://www.ncbi.nlm.nih.gov/pubmed/19088015 [Accessed March 4, 2013].
35) Park, P.E. et al., 2013. MAD2 expression in ovarian carcinoma: Different expression patterns and levels among various types of ovarian carcinoma and its prognostic significance in high-grade serous carcinoma. *Korean Journal of Pathology*, 47(5), pp.418–425.
36) Prencipe, M. et al., 2010. MAD2 downregulation in hypoxia is independent of promoter hypermethylation. *Cell Cycle*, 9(14), pp.2856–2865. Available at: http://www.landesbioscience.com/journals/cc/article/12362/[Accessed October 29, 2012].
37) Rajput, S., Volk-Draper, L.D. & Ran, S., 2013. TLR4 is a novel determinant of the response to paclitaxel in breast cancer. *Molecular cancer therapeutics*, 12(8), pp.1676–87. Available at: http://www.pubmed central.nih.gov/article render.fcgi? artid=3742631&tool=pmcentrez&rendertype=abstract [Accessed December 2, 2014].
38) Sato, Y. et al., 2009. Cancer Cells Expressing Toll-like Receptors and the Tumor Microenvironment. *Cancer microenvironment : official journal of the International Cancer Microenvironment Society*, 2 Suppl 1, pp.205–14. Available at: http://www.pubmedcentral.nih.gov/articlerender.fcgi?artid=2756339&tool=pmcentrez&rendertype=abstract [Accessed October 17, 2012].
39) Schorge, J.O. et al., 2010. SGO White Paper on ovarian cancer: etiology, screening and surveillance. *Gynecologic oncology*, 119(1), pp.7–17. Available at: http://www.ncbi.nlm.nih.gov/pubmed/20692025 [Accessed November 20, 2012].
40) Schvartzman, J.-M. et al., 2011. Mad2 is a critical mediator of the chromosome instability observed upon Rb and p53 pathway inhibition. *Cancer cell*, 19(6), pp.701–14. Available at: http://www.pubmedcentral.nih.gov/articlerender.fcgi?artid=3120099&tool=pmcentrez&rendertype=abstract [Accessed October 24, 2012].
41) Shah, M.M. et al., 2014. Diabetes mellitus and ovarian cancer: More complex than just increasing risk. *Gynecologic Oncology*, 135(2), pp.273–277. Available at: http://linkinghub.elsevier.com/retrieve/pii/S0090825814013079.
42) Sheyhidin, I. et al., 2011. Overexpression of TLR3, TLR4, TLR7 and TLR9 in esophageal squamous cell carcinoma. *World journal of gastroenterology : WJG*, 17(32), pp.3745–51. Available at: http://www.pubmedcentral.nih.gov/ article render.fcgi?artid=3181461&tool=pmcentrez&rendertype=abstract[Accessed February 3, 2013].
43) Sudo, T., 2004. Dependence of Paclitaxel Sensitivity on a Functional Spindle Assembly Checkpoint. *Cancer Research*, 64(7), pp.2502–2508. Available at: http://cancerres.aacrjournals.org/cgi/doi/10.1158/0008-5472.CAN-03-2013 [Accessed November 10, 2012].
44) Sun, Z. *et al*., 2012. Role of toll-like receptor 4 on the immune escape of human oral squamous cell carcinoma and resistance of cisplatin-induced apoptosis. *Molecular cancer*, 11(1), p.33. Available at: http://www.pubmed central.nih.gov/ articlerender.fcgi?artid=3496658&tool=pmcentrez&rendertype=abstract [Accessed December 4, 2012].

45) Szajnik, M. *et al*., 2009. TLR4 signaling induced by lipopolysacharide or paclitaxel regulates tumor survival and chemoresistance in ovarian cancer. *Oncogene*, 28(49), pp.4353–4363. Available at: http://www.pubmed central .nih.gov/articlerender.fcgi?artid=2794996&tool=pmcentrez&rendertype=abstract
46) Tran, A.-Q., Cohen, J.G. & Li, A.J., 2015. Impact of obesity on secondary cytoreductive surgery and overall survival in women with recurrent ovarian cancer. *Gynecologic Oncology*, 138(2), pp.263–266. Available at: http://linking hub.elsevier.com/retrieve/pii/S0090825815300159.
47) Wang, A.C. *et al*., 2014. TLR4 induces tumor growth and inhibits paclitaxel activity in MyD88-positive human ovarian carcinoma in vitro. *Oncology Letters*, 7(3), pp.871–877.
48) Www.clinicaltrials.gov, No Title.
49) Yanagawa, M. *et al*., 2012. Luminal A and luminal B (HER2 negative) subtypes of breast cancer consist of a mixture of tumors with different genotype. *BMC research notes*, 5(1), p.376. Available at: http://www.pubmedcentral.nih.gov/ articlerender.fcgi?artid=3413599&tool=pmcentrez&rendertype=abstract [Accessed January 30, 2013].
50) Zhang, S.-H. *et al*., 2008. Clinicopathologic significance of mitotic arrest defective protein 2 overexpression in hepatocellular carcinoma. *Human pathology*, 39(12), pp.1827–34. Available at: http://www. ncbi. nlm. nih. gov/ pubmed/18715617 [Accessed October 29, 2012].
51) Zhu, Y. *et al*., 2012. Prognostic significance of MyD88 expression by human epithelial ovarian carcinoma cells. *Journal of translational medicine*, 10(1), p.77. Available at: http://www.pubmedcentral.nih.gov/articlerender.fcgi?artid =3438 113 &tool=pmcentrez&rendertype=abstract [Accessed October 29, 2012].

Chapter 7

General Discussion

Trinity College Dublin

The University of Dublin

Chapter 7

General Discussion

7.1 The role of MyD88, TLR4 and MAD2 in ovarian disease

The hypothesis of this project was that MyD88, TLR4 and MAD2, which individually had been shown to be reliable prognostic markers in ovarian cancer (Furlong *et al*. 2012; d'Adhemar *et al*. 2014) , could be used in combination to more accurately predict patient prognosis. It was hypothesised that patients possessing a MyD88 high, TLR4 high, MAD2 low, phenotype would be least likely to respond to paclitaxel based chemotherapy and most likely to develop chemoresistant recurrent disease. These patients would have the worst survival outcomes. All three markers have been associated with paclitaxel chemoresistance *in-vitro* in ovarian cancer (Kelly *et al*. 2006; Furlong *et al*. 2012; d'Adhemar *et al*. 2014). Another aim of this project was to assess the molecular mechanisms whereby each of these markers contributes to paclitaxel chemoresistance and to investigate whether there was any *in-vitro* relationship between TLR4, MyD88 and MAD2. *In-silico* analysis predicted no direct interactions or pathway linkages between MAD2 and the TLR4-MyD88 pathway. It was thought that MAD2 and TLR4/MyD88 induced paclitaxel resistance through independent mechanisms.

Assessment of each of these markers in a TMA cohort demonstrated that MyD88, MAD2 and TLR4 can accurately predict patient prognosis. The three markers when used in combination identified different "at risk" groups that individually these markers may not have identified. Those with a TLR4 high MyD88 high MAD2 low phenotype had the worst prognosis among patients confirming one of the major hypotheses of this project. Each of these markers highlights different molecular mechanisms occurring within a patient tumour. Depending on the pattern of marker expression, multiple mechanisms may be active within a tumour. Based on their marker expression patients

could potentially be stratified into different at risk groups which should be treated using different therapeutic strategies.

In chapters 3 and 5 the molecular mechanisms by which TLR4 and MAD2 contribute to chemoresistance were characterised. siRNA knockdown of TLR4 was shown to restore chemosensitivity of SKOV-3 cells to paclitaxel. Microarray analysis revealed that these cells are likely pro-apoptotic and/or hypo-proliferative. Those with a TLR4 high phenotype likely elicit a pro-survival and pro-inflammatory cytokine response that drives tumour cell proliferation and prevents apoptosis. Paclitaxel treatment in these patients also likely further drives this TLR4 cytokines and pro-survival gene driven response by acting as a ligand for TLR4. Less paclitaxel may also be reaching its intended target microtubules. Patients with a MAD2 low phenotype likely contain a senescent and highly paclitaxel resistant phenotype. These senescent cells may not only be senescent but are likely secreting various cytokines and chemokines which can promote tumour growth. Following knockdown of MAD2, levels of TLR4 were found to be upregulated 3 fold in both A2780 and SKOV-3 cells demonstrating an important in-vitro link between these biomarkers. This is likely also occurring *in-vivo* and potentially driving up TLR4 expression in adjacent stromal tissue, other non-senescent tumour cells and perhaps even cancer stem cells. This likely further contributes to a highly chemoresistant phenotype.

Interestingly in chapter 6, 1/10 patients at primary disease exhibited high MAD2 expression whereas during disease recurrence 7/10 patients exhibited high MAD2 expression. This may suggest that cells with high MAD2 expression, which are not senescent are largely responsible for recurrent disease. As senescence is considered to be irreversible, senescent cells displaying low MAD2 expression may potentially be promoting the growth of these non-senescent high MAD2 expressing cells leading to recurrent disease.

MyD88 was not shown to contribute to chemoresistance in this study. However other studies have shown that MyD88 contributes to paclitaxel resistance and resistance to other therapeutic agents in various cancer models including ovarian cancer. In chapter 6 assessment of MyD88 status alone accurately predicted patient prognosis including DFI, PFS and OS. Patients with MyD88 high score exhibited a reduction in their median DFI of 18 months, 19 months in their median PFS and 18 months in their median OS. MyD88 likely highlights patients containing a large proportion of a population of ovarian cancer stem cells **(Figure 6.30)**. MyD88 positive cancer stem cells are highly paclitaxel resistant and display active TLR4 signalling, which likely

further enhances the chemoresistant properties of these cells and supports their growth *in-vivo* (Craveiro *et al.* 2013). MyD88 assessment in patients with low MAD2 expression was shown to have significant impact on patient survival.

Combined assessment of these three markers even in this small cohort seemed to be very effective. Further evaluation in a much larger study may further demonstrate the clinical utility of these biomarkers when used in combination. The next step is to now determine if they are suitable therapeutic targets or if by examining these subgroups closely we may determine new therapeutic targets and additional prognostic biomarkers.

As a surface receptor TLR4 is an attractive target for therapeutics, treating patients with a TLR4 inhibitor may increase the efficacy of paclitaxel therapy. A study by Huang *et al*. (2014) demonstrated that the compound Atractylenolide-I sensitises human ovarian cancer cells to paclitaxel by blocking activation of the TLR4/MyD88-dependent pathway. This compound binds to the hydrophobic pocket of MD2, a TLR4 coactivator which helps facilitate binding to LPS, and prevents paclitaxel binding to TLR4. This compound also effectively reduced levels of IL-6, VEGF and survivin, and enhanced early apoptosis and growth inhibition in MyD88 positive EOC cells. Eritoran is another inhibitor of TLR4 which also acts by preventing LPS or paclitaxel from binding to MD2 thus preventing signalling through the MD2-TLR4 complex and the production of inflammatory cytokines. This molecule was tested as a treatment for patients with severe sepsis but a phase III clinical trial found that this molecule failed to improve the mortality rates associated with the disease (Opal *et al*. 2013). Although another study by Shirey *et al*. (2013) did report that administration of Eritoran protected mice against a lethal strain of the influenza virus and was shown to decrease the production of inflammatory cytokines. Eritoran as it has already been used safely in human clinical trials may be suitable therapy to use with ovarian cancer patients.

However, the effects of such an inhibitor must be monitored closely. TLR4 has a very important role in the immune system and patients treated with chemotherapeutic agents such as paclitaxel become severely immunocompromised (Rasmussen & Arvin 1982; Tange *et al*. 2002; Sevko *et al*. 2013). The kind of impact that combined use of a TLR4 inhibitor in combination with conventional paclitaxel/carboplatin based chemotherapy could be detrimental to patient health. A number of other molecules can in fact act as either agonists/antagonists of TLR4 expression. These include high mobility group box 1 protein (HMGB-1), ethanol, members of opioid family such as morphine, oxycodone and methadone, members of benzodiazepine family of

antidepressants and more recently melatonin (Klune *et al*. 2008; Hutchinson *et al*. 2010; Lewis *et al*. 2010; Peri & Piazza 2012; Lewis *et al*. 2013; Chuffa *et al*. 2015). Therefore perhaps modulation of TLR4 expression using compounds such as these may also help improve patient outcomes. However before any work involving the implementation of a TLR4 inhibitor to treat patients, we first need to understand why some patients develop high levels of TLR4 expression. TLR4 mutations have been reported in various human cancers, and may result in aberrant TLR4 expression (Zheng *et al*. 2004; Kutikhin 2011; Eyking *et al*. 2011). Furthermore various negative regulators of TLR4 and downstream signalling molecules exist which also could be influencing TLR4 expression in some patients. These include tollip, RP105, TRIAD3A, ST2L, SIGIRR, SOCS1, IRAK-M, IRAK-2C, MYC88s, TRAF1 and TRAF4, A20, Prat4a, Rab7b, Rab11a and various microRNAs **(Figure 7.1)** (Zhang & Ghosh 2002; Liew *et al*. 2005; Divanovic *et al*. 2005; Wakabayashi *et al*. 2006; Wang *et al*. 2007; Husebye *et al*. 2010; McGettrick & O'Neill 2010; Quinn & O'Neill 2011) Mutation or aberrant expression of any of these key regulators could potentially influence TLR4 expression leading to enhanced tumorigenesis in ovarian cancer.

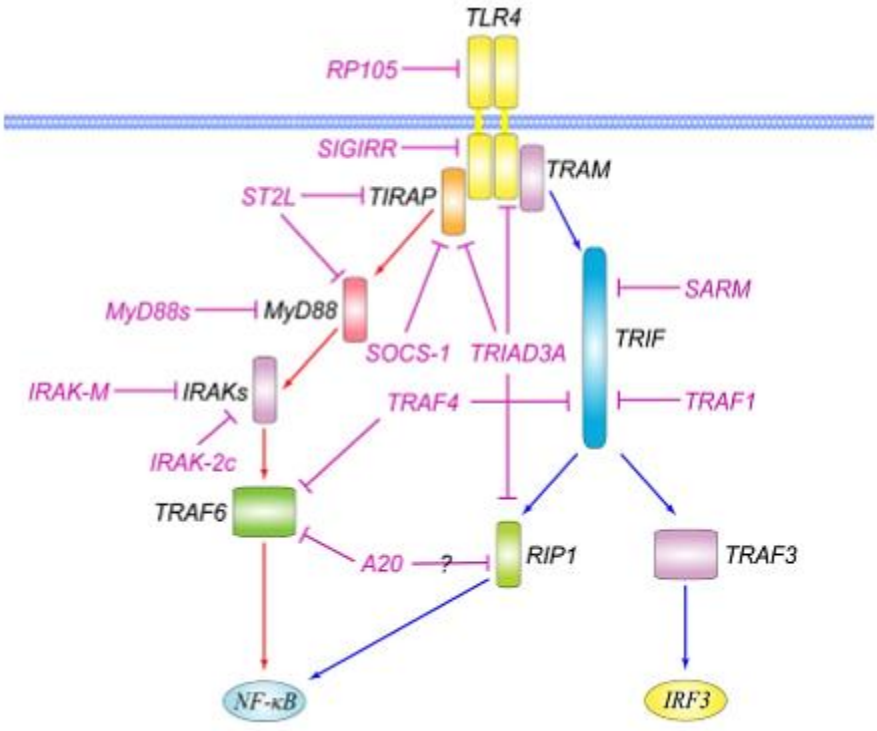

Figure 7.1 Negative regulators involved in TLR4 signaling. Negative regulators target multiple levels of TLR4 signaling. Several molecules, such as RP105 and SIGIRR, inhibit the initiation of this signaling cascade. Other factors target further downstream through different mechanisms (Lu *et al*. 2008).

MAD2 may not be a very suitable target for ovarian cancer therapy, as its downregulation is indicative of poor prognosis, this may make it difficult to target therapeutically. Upregulating MAD2 expression directly may prove difficult and potentially have detrimental effects. Furthermore if MAD2 is indeed inducing senescence, senescence is usually considered to be irreversible and therefore upregulated MAD2 expression artificially may not be able to reverse the development of this highly paclitaxel resistant phenotype. However one approach to potentially reverse MAD2 downregulation may be the inhibition of miR-433 using a microRNA inhibitor. Our group previously reported that miR-433 overexpression could induce MAD2 downregulation, the induction of senescence and paclitaxel resistance in ovarian cancer cell lines (Furlong *et al*. 2012; Weiner-Gorzel *et al*. 2015). Furthermore we also demonstrated that high levels of miR-433 in patient tumour samples is associated with reduced PFS (Furlong *et al*. 2012). miR-433 as it is expressed at high levels in some patients may be a potential therapeutic target and also the initial instigator of MAD2 downregulation in ovarian tumours. Inhibiting miR-433 using a microRNA inhibitor may potentialy reverse MAD2 downregulation in these patients leading to improved disease outcomes. It is important that we also understand why some patients develop a MAD2 low and/or miR-433 high phenotype. High levels of miR-433 may indicate in these particular patients, the presence of a single nucleotide polymorphism (SNP) or mutation in miR-433 or perhaps one of its target genes. A review by Salzman & Weidhaas (2012), highlighted how single nucleotide polymorphisms in microRNAs and microRNA-target sites impact on microRNA biology and associate with cancer risk. Mutations in either the microRNA or a gene target, can lead to aberrant microRNA expression and increased tumourigenesis. Polymorphisms in pre-miR-146a for example have been associated with gastic cancer (Zeng *et al*. 2010), familial breast/ovarian cancer (Shen *et al*. 2008), cervical cancer risk (Yue *et al*. 2011) and progression in malignant melanoma (Forloni *et al*. 2014). It is possible that microRNAs exist at the top of a hierarchy of ovarian cancer biomarkers and mutation and/or aberrant expression of these microRNAs leads to genome wide changes and ovarian cancer progression. The use of microRNA inhibitors may help lead to improved ovarian cancer treatment. An antisense oligo for miR-122 and the treatment of hepatitis is already being tested in clinical trials and results so far have been promising. As a risk factor for hepatocellular carcinoma, this could lead to a preventative treatment for some patients (Haussecker & Kay 2010; Xu *et al*. 2011).

7.2 M Type classification scheme

Based on the different phenotypes that were observed in this study, we propose to divide high grade serous ovarian cancers into three separate categories which we have designated:

1) M Type 1
2) M Type 2
3) M Type 3

M type 1 ovarian cancers express MyD88 and TLR4 at high levels and exhibit low expression of MAD2. These patients will not benefit from paclitaxel based therapy, and in fact paclitaxel therapy in these patients is likely harmful as TLR4 is a known ligand for paclitaxel. From the immunohistochemistry work performed in chapter 6, it has been shown that these patients have very low survival. These patients exhibit differences in survival of not only a few short months, but in fact years compared to those who do not express this phenotype. These patients may perhaps benefit from platinum only therapy, although this needs to be investigated or these patients should perhaps be directed towards clinical trials and given alternative therapies.

M Type 2 ovarian cancers express MyD88 and TLR4 at low levels and MAD2 at high levels. These patients are most likely to respond well to paclitaxel therapy as they likely express low numbers of MyD88+ ovarian cancer stem cells, do not exhibit hyper-activation of TLR4 inflammatory signalling and are likely highly proliferative and not senescent.

M Type 3 ovarian cancers exhibit moderate expression of MyD88, TLR4 and MAD2. These patients represent an intermediate group which will perhaps exhibit a partial response to paclitaxel therapy and who may benefit from other therapeutic options.

7.3 Limitations of the study

The major limitation of this study was the small sample size for the tissue microarray (TMA) cohort and the primary-metastatic-recurrent (PMR) cohort. Originally 51 patient samples were incorporated into the TMA cohort, 10 of these had to be excluded from survival analysis as they were stage 1 and sub-optimally debulked. These perhaps should have been excluded from the outset and not incorporated into the TMA. The remaining 5 were excluded as either all three cores were not present for each stain or they had only partial cores. Therefore perhaps additional cores from each sample should have been included, so that at least three cores could be evaluated. Although even one core which stains positively may perhaps be indicative of the phenotype of a tumour and this perhaps should be examined.

The sample size and the fact that a low number of samples stained strongly positive for TLR4 and MAD2, limits the survival analysis that could be performed. However these were the only samples available for this study. However despite the small sample size significant results were obtained matching in with the biology of the disease as demonstrated in the previous three chapters. Also although the sample size is small these markers have already been validated individually in much larger cohorts. There is great potential to expand on the results represented in chapter 6. Even with the sample size, there is good evidence to support the use of these three markers in combination. The primary-metastatic study similarly had low numbers but showed some interesting results and demonstrated how these markers may play an important role in recurrent disease and resistance to chemotherapy.

There are also a lot of negative results in this study, although these are still results. In retrospect as mentioned throughout the previous chapters an alternative approach to determine the role the three regulatory microRNAs miR-433, miR-146a and miR-21 in the regulation of MAD2, TLR4 and MyD88 and their roles in paclitaxel resistance should have been attempted. A better approach would perhaps have been to purchase overexpression plasmids for each of these microRNAs and to carryout transfections with these in each of our cell lines. Then three sets of experiments would then have definitively established a relationship between these microRNAs and MAD2, TLR4 and MyD88, a role for these microRNAs in paclitaxel resistance and any potential link between their paclitaxel resistance mechanisms.

1) Examine TLR4, MyD88 and MAD2 gene and protein expression following transfection with overexpression plasmids for miR-433, miR-146a and miR-21
2) Perform a luciferase reporter assay to demonstrate whether these microRNAs are capable of directly targeting TLR4, MAD2 and MyD88
3) Treat the cells with paclitaxel following transfection with each plasmid and determine the effect on paclitaxel sensitivity

Chapter 3 and 4 demonstrated no relationship between MAD2 and MyD88 or TLR4. From the start it was expected that perhaps that there would be no relationship between these markers. But this was an important thing to definitively establish given their respective roles in paclitaxel resistance and due to the opposite staining patterns of MAD2 and MyD88/TLR4 ie the fact that low MAD2 expression and high TLR4/MyD88 expression is indicative of poor prognosis. It was important to establish that these markers were truly independent and highlighting different processes, rather than highlighting the same process.

Chapter 3 and 4 also showed that MyD88 did not have a direct role in paclitaxel resistance, instead TLR4 was shown to be the more promising biomarker. However this ties in with what was observed in both the immunostaining results and chapter 4&5. However originally MyD88 from previous immunostaining work seemed to be the more promising and more interesting marker, particularly as it is not expressed in normal ovarian epithelium and therefore this is why it was initially the main focus of the first two chapters.

One of the potential reasons why MyD88 was hypothesised to result in poorer patient prognosis was that it highlights a population of ovarian cancer stem cells (Craveiro *et al*. 2013). However there is no evidence to suggest that MyD88 is a marker of ovarian cancer stem cells in the SKOV-3 or A2780 cell model. It may be interesting to examine the role of cancer stem cells within these cell models and how they may contribute to paclitaxel resistance or to characterise further the MyD88+ CSCs isolated by (Craveiro *et al*. 2013).

In Chapter 4 overexpression of MyD88 did not induce chemoresistance in the A2780 cell model as had previously been shown by (Kelly *et al.* 2006). There may a number of different reasons for this as explained in chapter 4 including the level of overexpression and the methodology used. Given the fact that the protocol was initially toxic to A2780 cells it is not surprising that chemoresistance was not induced. Perhaps

the use of a lentiviral overexpression plasmid, the use anti-biotic selection or altering the dose of plasmid used may yield more favourable results.

In 2013, partway through this project, an article by Domcke *et al*. (2013), questioned the appropriateness of cell models for ovarian cancer research. The article highlighted how many ovarian cancer cell lines based on genome sequencing and mutational analysis may not be truly representative of high grade serous ovarian cancer, the most common phenotype of ovarian cancer. The A2780 and SKOV-3 cells in particular were highlighted among cell lines. Although this research article does highlight a very important issue in ovarian cancer research, it must also be acknowledged that cell models are simply models of disease and are only representative of a single ovarian cancer patient. True prognostic value of any potential biomarker is only realised upon evaluation in patient samples, which this current study utilises aswell as using cell models. The A2780 and SKOV-3 cells models, although perhaps not the most appropriate models for examining high grade serous ovarian cancer, up until that time, these models were the most frequently utilised cell models for ovarian cancer research. The SKOV-3 cell model is among one of the cell models used in the national cancer institute's NCI-60 panel used to test new cytotoxic drugs by the FDA (Lorenzi et al. 2009). The two cell models A2780 and SKOV-3 were also chosen mainly for the fact that they represented positive and negative models of MyD88 respectively, with the A2780 model being MyD88 null and paclitaxel sensitive and the SKOV-3 cells being MyD88 positive and paclitaxel resistant. Both also expressed MAD2 and knockdown of MAD2 in the A2780 cells had been shown to induce paclitaxel resistance (Hao *et al*. 2010; Furlong *et al*. 2012).

A number of limitations restricted some of the outcomes of this project. However despite some of the pitfalls and setback within this project some interesting and significant results are obtained, which support future investigations into the utility of these three biomarkers MyD88, MAD2 and TLR4.

7.4 Future work

The work performed in chapter 6 demonstrated the clinical utility of using these biomarkers in combination to predict patient prognosis. The utility of using these three markers needs to be investigated further in a much larger cohort, but results from this study are promising. The M phenotype classification might be further expanded by incorporating other promising biomarkers. BRCA1/2 mutations occur in 5-10% of germ line and 39% of somatic ovarian cancers (Fasching *et al*. 2009; Hennessy *et al*. 2010). BRCA1 is also a positive regulator of MAD2 expression (Wang *et al*. 2004); therefore it is likely to play significant role in this classification scheme. Folic acid receptor alpha is another promising and targetable biomarker in ovarian cancer research which could be incorporated into the classification scheme (Jelovac & K. Armstrong 2012). This type of molecular taxonomy approach to ovarian cancer will help us to further define the disease and develop more appropriate therapeutic strategies. The women identified by each of these different markers need to be given personalised treatments. Already with the M type classification scheme as it stands patients with the M Type 1 phenotype will likely have no benefit from paclitaxel therapy. In fact paclitaxel treatment may be quite harmful to these patients as it likely promotes the production of pro-inflammatory cytokines and survival proteins. Future work may even focus on potential ways of targeting TLR4, MyD88 and MAD2 or derailing the resistance mechanisms in which they are involved.

Further characterisation of the relationship between TLR4 and MAD2 should be explored. This downregulation of MAD2 may occur *in-vivo* as result of hypoxia or through miR-433 down-regulation, the two processes may even be linked and this also should be investigated. Furthermore in chapter 5, we hypothesised that cytokines released as a result of the induction of SASP phenotype following knockdown of MAD2 drive TLR4 expression. This needs to be effectively demonstrated, it will be interesting to determine whether specific cytokines may be responsible for this. A number of differentially expressed genes identified following both knockdown of TLR4 and MAD2 as discussed in Chapter 5 might help further define the relationship between these markers.

Furthermore knockdown of either TLR4 or MAD2 in the SKOV-3 cell model has only been shown to induce paclitaxel resistance. The impact of knockdown of MAD2 and TLR4 on cisplatin resistance still needs to be investigated and is an important consideration for the M type classification scheme. TLR4 and MAD2 have both been

shown to play a role in cisplatin resistance in different cancers (Fung *et al*. 2006; Sun *et al*. 2012).

A number of different genes and biological pathways were highlighted following microarray analysis of SKOV-3 cells following knockdown of TLR4. One novel pathway highlighted following knockdown of both MAD2 and TLR4, was the perception of smell which involves various members of the olfactory receptor family. A large number of these were downregulated following both knockdown of TLR4 and MAD2. A link between olfactory receptor signalling and TLR signalling has already previously been established (Ward *et al*. 2015). Interestingly our group has also demonstrated that olfactory receptors are downregulated during differentiation in the embryonal carcinoma 2102Ep model (Sulaiman 2015). It may be the case that following knockdown of TLR4 that SKOV-3 cells are becoming less stem like and thus more sensitive to paclitaxel therapy. As following knockdown of MAD2, the SKOV-3 cells are undergoing senescence, downregulation of olfactory receptor signalling may be an event which occurs during both differentiation and senescence.

Other pathways highlighted following knockdown of TLR4 include coagulation and complement cascades, steroid biosynthesis and metabolism, ERBB signalling and cell adhesion. Both the expression of HER2 and one of its binding partners HER3 have been associated with poor survival in ovarian cancer (Berchuck *et al*. 1990; Tanner *et al*. 2006; Bezler *et al*. 2012; Ocana *et al*. 2013). HER3 is highly expressed on both primary tumours and the surface of circulating tumour cells (CTCs) and has been shown to play a role in ovarian metastasis (Sheng *et al*. 2010) In the PMR study in chapter 6, TLR4 was found to be highly expressed in recurrent tumours and significantly affected patient survival rates. Hyper-activation of TLR4 may therefore drive the expression of HER2/3 on CTCs. Future work may focus on characterising the role of TLR4 and HER2/3 in circulating tumour cell biology and how they contribute to metastatic spread, chemoresistance and recurrent disease. HER2/3 may potentially also be incorporated into the M Type classification scheme.

TLR4 is a well-established inflammatory mediator. In chapter 3 microarray analysis revealed that TLR4 also plays a role in regulating energy metabolism and influences the expression of many genes involved in coagulation. In recent years it has become evident that crosstalk between pathways involved in inflammation, coagulation and obesity/metabolic syndrome contribute to the development of ovarian cancer (Zhang & Lawrence 2011). Obese patients exhibit an accumulation of fatty adipose tissue. Adipose tissue is thought to drive chronic inflammation leading to insulin resistance

and hyper-coagulability (Zhang & Lawrence 2011). We have termed this crosstalk between inflammation, coagulation and obesity/metabolic syndrome “the onco-metabolome”. Future work may examine a potential role for TLR4 in the oncometabolome.

7.5 Conclusion

Ovarian cancer is a highly complex disease and multiple cancer associated mechanisms are involved in the pathogenesis of this disease and contribute to its poor prognosis rates. Overcoming and preventing chemoresistant and recurrent disease represents a major challenge in ovarian cancer. The work from this study has highlighted different at risk groups within a high grade serous ovarian cohort who may benefit from different therapeutic approaches. Personalised medicine including the use of targeted therapies and molecular classification of ovarian disease is required in order to enhance patient survival. Future work will include further investigation of the pathway link between TLR4 and MAD2, the role of TLR4 in the oncometabolome in ovarian disease, analysis of mutations in both genes and microRNAs and the further characterisation of primary disease and CTCs. All of this work may help to significantly improve upon the poor prognosis rates associated with ovarian cancer and lead to better patient outcomes.

7.6 References

1) Berchuck, A. et al., 1990. Overexpression of HER-2/neu is Associated with Poor Survival in Advanced Epithelial Ovarian Cancer. *Cancer Research*, 50, pp.4087–4091.
2) Bezler, M., Hengstler, J.G. & Ullrich, A., 2012. Inhibition of doxorubicin-induced HER3-PI3K-AKT signalling enhances apoptosis of ovarian cancer cells. *Molecular Oncology*, 6(5), pp.516–529. Available at:http://dx.doi.org/10.1016/j.molonc.2012.07.001.
3) Chuffa, L.G. a et al., 2015. Melatonin attenuates the TLR4-mediated inflammatory response through MyD88- and TRIF-dependent signaling pathways in an in vivo model of ovarian cancer. *BMC Cancer*, 15(1), pp.1–13. Available at: http://www.biomedcentral.com/1471-2407/15/34.
4) Craveiro, V. et al., 2013. Phenotypic modifications in ovarian cancer stem cells following Paclitaxel treatment. *Cancer medicine*, 2(6), pp.751–62. Available at: http://www.pubmedcentral.nih.gov/articlerender.fcgi?artid=3892380&tool=pmcentrez&rendertype=abstract [Accessed April 30, 2014].
5) Divanovic, S. et al., 2005. Negative Regulation of TLR4 Signalling by RP105. *Nature Biotechnology*, 6(6), pp.571–578.
6) Domcke, S. et al., 2013. Evaluating cell lines as tumour models by comparison of genomic profiles. *Nature communications*, 4, p.2126. Available at: http://www.pubmedcentral.nih.gov/articlerender.fcgi?artid=3715866&tool=pmcentrez&rendertype=abstract [Accessed January 28, 2014].
7) Eyking, A. et al., 2011. Toll-like receptor 4 variant D299G induces features of neoplastic progression in Caco-2 intestinal cells and is associated with advanced human colon cancer. *Gastroenterology*, 141(6), pp.2154–65. Available at: http://www.pubmedcentral.nih.gov/articlerender.fcgi?artid =3268964&tool=pmcentrez&rendertype=abstract [Accessed December 2, 2014].
8) Fasching, P. a et al., 2009. Role of genetic polymorphisms and ovarian cancer susceptibility. *Molecular oncology*, 3(2), pp.171–81. Available at: http://www.ncbi.nlm.nih.gov/pubmed/19383379 [Accessed October 25, 2012].
9) Fausel, C., 2007. Targeted chronic myeloid leukemia therapy: Seeking a cure. In *American Journal of Health-System Pharmacy*.
10) Forloni, M. et al., 2014. miR-146a promotes the initiation and progression of melanoma by activating Notch signaling. *eLife*, 2014(3), pp.1–20.
11) Fung, M.K.L. et al., 2006. Role of MEK/ERK pathway in the MAD2-mediated cisplatin sensitivity in testicular germ cell tumour cells. *British journal of cancer*, 95(4), pp.475–84. Available at: http://www.pubmedcentral.nih.gov/articlerender.fcgi?artid=2360662&tool=pmcentrez&rendertype=abstract [Accessed November 23, 2012].
12) Furlong, F. et al., 2012. Low MAD2 expression levels associate with reduced progression-free survival in patients with high-grade serous epithelial ovarian cancer. *The Journal of pathology*, 226(5), pp.746–55. Available at: http://www.ncbi.nlm.nih.gov/pubmed/22069160 [Accessed February 23, 2013].
13) Greeno, E.W., Bach, R.R. & Moldow, C.F., 1996. Apoptosis is associated with increased cell surface tissue factor procoagulant activity. *Laboratory Investigation*, 75(2), pp.281–289. Available at: http://www.scopus.com /inward/record.url?eid=2-s2.00029767998&partnerID=40&md5=03ceffd0b97bae0b14c878455d71b982.
14) Hao, X. et al., 2010. Effect of Mad2 on paclitaxel-induced cell death in ovarian cancer cells. *Journal of Huazhong University of Science and Technology. Medical sciences = Hua zhong ke ji da xue xue bao. Yi xue Ying De wen ban = Huazhong keji daxue xuebao. Yixue Yingdewen ban*, 30(5), pp.620–5. Available at: http://www.ncbi.nlm.nih.gov/pubmed/21063845 [Accessed March

12, 2014].
15) Haussecker, D. & Kay, M. a, 2010. miR-122 continues to blaze the trail for microRNA therapeutics. *Molecular therapy : the journal of the American Society of Gene Therapy*, 18(2), pp.240–242. Available at: http://dx.doi.org/ 10.1038/ mt.2009.313.
16) Hennessy, B.T.J. et al., 2010. Somatic mutations in BRCA1 and BRCA2 could expand the number of patients that benefit from poly (ADP ribose) polymerase inhibitors in ovarian cancer. *Journal of Clinical Oncology*, 28(22), pp.3570–3576.
17) Hu, C. et al., 2012. Opposite regulation by PI3K/Akt and MAPK/ERK pathways of tissue factor expression, cell-associated procoagulant activity and invasiveness in MDA-MB-231 cells. *Journal of hematology & oncology*, 5, p.16. Available at: http://www.pubmedcentral.nih.gov/articlerender.fcgi? artid= 33942 20&tool=pmcentrez&rendertype=abstract.
18) Huang, J.-M. et al., 2014. Atractylenolide-I sensitizes human ovarian cancer cells to paclitaxel by blocking activation of TLR4/MyD88-dependent pathway. *Scientific reports*, 4, p.3840. Available at: http://www.pubmedcentral.nih.gov/ articlerender.fcgi?artid=3899591&tool=pmcentrez&rendertype=abstract [Accessed June 1, 2014].
19) Husebye, H. et al., 2010. The Rab11a GTPase controls Toll-like receptor 4-induced activation of interferon regulatory factor-3 on phagosomes. *Immunity*, 33(4), pp.583–96. Available at: http://www.ncbi.nlm.nih.gov/pubmed/20933442 [Accessed March 10, 2014].
20) Hutchinson, M.R. et al., 2010. Evidence that opioids may have toll-like receptor 4 and MD-2 effects. *Brain, behavior, and immunity*, 24(1), pp.83–95. Available at: http://www.pubmedcentral.nih.gov/articlerender.fcgi? artid=2788078 &tool =pmcentrez&rendertype=abstract [Accessed May 22, 2014].
21) Jelovac, D. & K. Armstrong, D., 2012. Role of Farletuzumab in Epithelial Ovarian Carcinoma. *Current Pharmaceutical Design*, 18(25), pp.3812–3815.
22) Kelly, M.G. et al., 2006. TLR-4 signaling promotes tumor growth and paclitaxel chemoresistance in ovarian cancer. *Cancer research*, 66(7), pp.3859–68. Available at: http://www.ncbi.nlm.nih.gov/pubmed/16585214 [Accessed October 22, 2012].
23) Klune, J.R. et al., 2008. HMGB1: Endogenous Danger Signaling. *Molecular Medicine*, 14(7-8), pp.476–484.
24) Kutikhin, A.G., 2011. Impact of Toll-like receptor 4 polymorphisms on risk of cancer. *Human Immunology*, 72(2), pp.193–206.
25) Lewis, S.S. et al., 2010. Evidence that intrathecal morphine-3-glucuronide may cause pain enhancement via toll-like receptor 4/MD-2 and interleukin-1β. *Neuroscience*, 165(2), pp.569–583.
26) Lewis, S.S. et al., 2013. Glucuronic acid and the ethanol metabolite ethyl-glucuronide cause toll-like receptor 4 activation and enhanced pain. *Brain, behavior, and immunity*, 30, pp.24–32. Available at: http://www.pubmedcentral. nih.gov/articlerender.fcgi?artid=3641160&tool=pmcentrez&rendertype=abstract [Accessed May 22, 2014].
27) Li, Y.-D. et al., 2009. NF-kappaB transcription factor p50 critically regulates tissue factor in deep vein thrombosis. *The Journal of biological chemistry*, 284(7), pp.4473–83. Available at:http://www.pubmedcentral.nih.gov /article render. fcgi?artid=2640971&tool=pmcentrez&rendertype=abstract.
28) Liew, F.Y. et al., 2005. Negative regulation of toll-like receptor-mediated immune responses. *Nature reviews. Immunology*, 5(6), pp.446–58. Available at: http://www.ncbi.nlm.nih.gov/pubmed/15928677 [Accessed November 7, 2012].
29) Loiarro, M. et al., 2005. Peptide-mediated interference of TIR domain dimerization in MyD88 inhibits interleukin-1-dependent activation of NF-

{kappa}B. *The Journal of biological chemistry*, 280(16), pp.15809–14. Available at: http://www.ncbi.nlm.nih.gov/pubmed/15755740 [Accessed March 20, 2014].
30) Lopez, M. et al., 2014. Fas-induced apoptosis increases hepatocyte tissue factor procoagulant activity in vitro and in vivo. *Toxicological sciences : an official journal of the Society of Toxicology*, 141(2), pp.453–64. Available at: http://www.ncbi.nlm.nih.gov/pubmed/25015658.
31) Lorenzi, P.L. et al., 2009. DNA fingerprinting of the NCI-60 cell line panel. *Molecular cancer therapeutics*, 8(4), pp.713–724.
32) Lu, Y.-C., Yeh, W.-C. & Ohashi, P.S., 2008. LPS/TLR4 signal transduction pathway. *Cytokine*, 42(2), pp.145–151.
33) McGettrick, A.F. & O'Neill, L. a J., 2010. Localisation and trafficking of Toll-like receptors: an important mode of regulation. *Current opinion in immunology*, 22(1), pp.20–7. Available at: http://www.ncbi.nlm.nih.gov/pubmed/20060278 [Accessed April 28, 2014].
34) Ocana, A. et al., 2013. HER3 overexpression and survival in solid tumors: A meta-analysis. *Journal of the National Cancer Institute*, 105(4), pp.266–273.
35) Olopade, O.I. et al., 2008. Advances in breast cancer: pathways to personalized medicine. *Clinical cancer research : an official journal of the American Association for Cancer Research*, 14(24), pp.7988–99. Available at: http://www.ncbi.nlm.nih.gov/pubmed/19088015 [Accessed March 4, 2013].
36) Opal, S.M. et al., 2013. Effect of Eritoran, an Antagonist of MD2-TLR4, on Mortality in Patients With Severe Sepsis.
37) Paschaki, M. et al., 2013. Retinoic acid regulates olfactory progenitor cell fate and differentiation. *Neural development*, 8, p.13. Available at: http://www.pubmedcentral.nih.gov/articlerender.fcgi?artid=3717070&tool=pmcentrez&rendertype=abstract.
38) Peri, F. & Piazza, M., 2012. Therapeutic targeting of innate immunity with Toll-like receptor 4 (TLR4) antagonists. *Biotechnology advances*, 30(1), pp.251–60. Available at: http://www.ncbi.nlm.nih.gov/pubmed/21664961 [Accessed January 28, 2013].
39) Quinn, S.R. & O'Neill, L. a., 2011. A trio of microRNAs that control Toll-like receptor signalling. *International Immunology*, 23(7), pp.421–425.
40) Rasmussen, L. & Arvin, A., 1982. Chemotherapy-induced immunosuppression. *Environmental health perspectives*, 43(February), pp.21–5. Available at: http://www.pubmedcentral.nih.gov/articlerender.fcgi?artid=1568884&tool=pmcentrez&rendertype=abstract.
41) Salzman, D.W. & Weidhaas, J.B., 2012. SNPing cancer in the bud: MicroRNA and microRNA-target site polymorphisms as diagnostic and prognostic biomarkers in cancer. *Pharmacology & therapeutics*. Available at: http://www.ncbi.nlm.nih.gov/pubmed/22964086 [Accessed November 7, 2012].
42) Sawka, A.M. et al., 2004. A systematic review and metaanalysis of the effectiveness of radioactive iodine remnant ablation for well-differentiated thyroid cancer. *Journal of Clinical Endocrinology and Metabolism*, 89(8), pp.3668–3676.
43) Sevko, A. et al., 2013. Antitumor effect of paclitaxel is mediated by inhibition of myeloid-derived suppressor cells and chronic inflammation in the spontaneous melanoma model. *Journal of immunology (Baltimore, Md. : 1950)*, 190(5), pp.2464–71. Available at: http://www.pubmedcentral.nih.gov/articlerender.fcgi?artid=3578135&tool=pmcentrez&rendertype=abstract.
44) Shen, J. et al., 2008. A functional polymorphism in the miR-146a gene and age of familial breast/ovarian cancer diagnosis. *Carcinogenesis*, 29(10), pp.1963–1966.
45) Sheng, Q. et al., 2010. An Activated ErbB3 / NRG1 Autocrine Loop Supports In Vivo Proliferation in Ovarian Cancer Cells. *Cancer Cell*, 17(3), pp.298–310. Available at: http://dx.doi.org/10.1016/j.ccr.2009.12.047.

46) Shirey, K.A. et al., 2013. The TLR4 antagonist Eritoran protects mice from lethal influenza infection. *Nature*, 497(7450), pp.498–502. Available at: http://www.pubmedcentral.nih.gov/articlerender.fcgi?artid=3725830&tool=pmcentrez&rendertype=abstract [Accessed January 31, 2014].
47) Sulaiman, G., 2015. The Role Of MyD88 in Embryonal Carcinoma Stem Cells. *Unpublished Thesis*.
48) Sun, Z. et al., 2012. Role of toll-like receptor 4 on the immune escape of human oral squamous cell carcinoma and resistance of cisplatin-induced apoptosis. *Molecular cancer*, 11(1), p.33. Available at: http://www.pubmed central.nih .gov/articlerender.fcgi?artid=3496658&tool=pmcentrez&rendertype=abstract [Accessed December 4, 2012].
49) Tange, S. et al., 2002. The antineoplastic drug Paclitaxel has immunosuppressive properties that can effectively promote allograft survival in a rat heart transplant model. *Transplantation*, 73(2), pp.216–223.
50) Tanner, B. et al., 2006. ErbB-3 predicts survival in ovarian cancer. *Journal of Clinical Oncology*, 24(26), pp.4317–4323.
51) Wakabayashi, Y. et al., 2006. A protein associated with toll-like receptor 4 (PRAT4A) regulates cell surface expression of TLR4. *Journal of immunology (Baltimore, Md.: 1950)*, 177(3), pp.1772–9. Available at: http://www.ncbi.nlm.nih.gov/pubmed/16849487.
52) Wang, R.-H., Yu, H. & Deng, C.-X., 2004. A requirement for breast-cancer-associated gene 1 (BRCA1) in the spindle checkpoint. *Proceedings of the National Academy of Sciences of the United States of America*, 101(49), pp.17108–13. Available at: http://www.pubmedcentral.nih.gov/articlerender .fcgi ?artid=535394&tool=pmcentrez&rendertype=abstract.
53) Wang, Y. et al., 2007. Lysosome-associated small Rab GTPase Rab7b negatively regulates TLR4 signaling in macrophages by promoting lysosomal degradation of TLR4. *Blood*, 110(3), pp.962–71. Available at: http://www.ncbi.nlm.nih.gov/pubmed/17395780 [Accessed February 19, 2014].
54) Ward, A. et al., 2015. Toll Receptors Instruct Axon and Dendrite Targeting and Participate in Synaptic Partner Matching in a Drosophila Olfactory Circuit. *Neuron*, 85(5), pp.1013–1028. Available at: http://linkinghub.elsevier. com/retrieve/pii/S0896627315000926.
55) Weiner-Gorzel, K. et al., 2015. Overexpression of the microRNA miR-433 promotes resistance to paclitaxel through the induction of cellular senescence in ovarian cancer cells. *Cancer Medicine*, p.n/a–n/a. Available at: http://doi.wiley.com/10.1002/cam4.409.
56) Xu, J. et al., 2011. Circulating MicroRNAs, miR-21, miR-122, and miR-223, in patients with hepatocellular carcinoma or chronic hepatitis. *Molecular Carcinogenesis*, 50(2), pp.136–142.
57) Yue, C. et al., 2011. Polymorphism of the pre-miR-146a is associated with risk of cervical cancer in a Chinese population. *Gynecologic oncology*, 122(1), pp.33–7. Available at: http://www.ncbi.nlm.nih.gov/pubmed/21529907 [Accessed October 29, 2012].
58) Zeng, Y. et al., 2010. Correlation between pre-miR-146a C/G polymorphism and gastric cancer risk in Chinese population. *World Journal of Gastroenterology*, 16(28), pp.3578–3583.
59) Zhang, G. & Ghosh, S., 2002. Negative regulation of toll-like receptor-mediated signaling by Tollip. *The Journal of biological chemistry*, 277(9), pp.7059–65. Available at: http://www.ncbi.nlm.nih.gov/pubmed/11751856 [Accessed March 9, 2014].
60) Zhang, N. & Lawrence, D. a, 2011. Tissue factor and obesity, a two-way street. *Nature Medicine*, 17(11), pp.1343–1344. Available at: http://dx.doi.org/10.1038/nm.2551.

61) Zheng, S.L. et al., 2004. Sequence variants of toll-like receptor 4 are associated with prostate cancer risk: results from the CAncer Prostate in Sweden Study. *Cancer Res*, 64(8), pp.2918–2922. Available at: http:// www.ncbi.nlm.nih.gov/entrez/query.fcgi?cmd=Retrieve&db=PubMed&dopt=Citation&list_uids=15087412\nhttp://cancerres.aacrjournals.org/content/64/8/2918.full.pdf

Appendix

Trinity College Dublin

The University of Dublin

Appendix

Supplementary Tables

Table S1 Olfactory receptor family members differentially expressed following knockdown of TLR4

Ensemble Gene ID	Description	Fold Change
Olfactory Receptors Upregulated		
ENSG00000172774	Olfactory receptor, family 1, subfamily S, member 1	1.5
ENSG00000196944	Olfactory receptor, family 2, subfamily T, member 4	1.9
Olfactory Receptors downregulated		
ENSG00000168131	Olfactory receptor, family 2, subfamily B, member 2	1.5
ENSG00000171133	Olfactory receptor, family 2, subfamily K, member 2	1.6
ENSG00000196936	Olfactory receptor, family 2, subfamily L, member 8	1.8
ENSG00000175143	Olfactory receptor, family 2, subfamily T, member 1	1.5
ENSG00000196240	Olfactory receptor, family 2, subfamily T, member 2	1.6
ENSG00000181935	Olfactory receptor, family 4, subfamily C, member 16	1.6
ENSG00000176695	Olfactory receptor, family 4, subfamily F, member 17	1.7
ENSG00000172365	Olfactory receptor, family 5, subfamily B, member 2	1.8
ENSG00000167825	Olfactory receptor, family 5, subfamily I, member 1	1.6
ENSG00000205497	Olfactory receptor, family 51, subfamily A, member 4	1.6
ENSG00000180934	Olfactory receptor, family 56, subfamily A, member 1	1.5
ENSG00000197532	Olfactory receptor, family 6, subfamily Y, member 1	1.6
ENSG00000237521	Olfactory receptor, family 7, subfamily E, member 24	1.5
ENSG00000197125	Olfactory receptor, family 8, subfamily B, member 8	1.6

Table S2 Genes involved in regulation of apoptosis and cell death affected by knockdown of TLR4.

Ensemble ID	Description
ENSG00000151694	ADAM metallopeptidase domain 17
ENSG00000100290	BCL2-interacting killer (apoptosis-inducing)
ENSG00000026508	CD44 molecule (Indian blood group)
ENSG00000164442	Cbp/p300-interacting transactivator, with Glu/Asp-rich carboxy-terminal domain, 2
ENSG00000188215	DCN1, defective in cullin neddylation 1, domain containing 3 (S. cerevisiae)
ENSG00000175592	FOS-like antigen 1
ENSG00000213619	NADH dehydrogenase (ubiquinone) Fe-S protein 3, 30kDa (NADH-coenzyme Q reductase)
ENSG00000124766	SRY (sex determining region Y)-box 4
ENSG00000125398	SRY (sex determining region Y)-box 9
ENSG00000181092	Adiponectin, C1Q and collagen domain containing
ENSG00000196975	Annexin A4
ENSG00000164305	Caspase 3, apoptosis-related cysteine peptidase
ENSG00000132357	Caspase recruitment domain family, member 6
ENSG00000117525	Coagulation factor III (thromboplastin, tissue factor)
ENSG00000057593	Coagulation factor VII (serum prothrombin conversion accelerator)
ENSG00000153774	Craniofacial development protein 1
ENSG00000108094	Cullin 2
ENSG00000100867	Dehydrogenase/reductase (SDR family) member 2
ENSG00000106211	Heat shock 27kDa protein-like 2 pseudogene; heat shock 27kDa protein 1
ENSG00000163349	Homeodomain interacting protein kinase 1
ENSG00000110422	Homeodomain interacting protein kinase 3
ENSG00000131203	Indoleamine 2,3-dioxygenase 1
ENSG00000117318	Inhibitor of DNA binding 3, dominant negative helix-loop-helix protein
ENSG00000152409	Junction mediating and regulatory protein, p53 cofactor
ENSG00000111057	Keratin 18; keratin 18 pseudogene 26; keratin 18 pseudogene 19
ENSG00000172175	Mucosa associated lymphoid tissue lymphoma translocation gene 1
ENSG00000005381	Myeloperoxidase
ENSG00000108179	Peptidylprolyl isomerase F
ENSG00000166289	Pleckstrin homology domain containing, family F (with FYVE domain) member 1
ENSG00000118495	Pleiomorphic adenoma gene-like 1
ENSG00000124212	Prostaglandin I2 (prostacyclin) synthase
ENSG00000161011	Sequestosome 1
ENSG00000115415	Signal transducer and activator of transcription 1, 91kDa
ENSG00000157404	Similar to Mast/stem cell growth factor receptor precursor
ENSG00000175793	Stratifin
ENSG00000117289	Thioredoxin interacting protein
ENSG00000198959	Transglutaminase 2 (C polypeptide, protein-glutamine-gamma-glutamyltransferase)
ENSG00000121858	Tumor necrosis factor (ligand) superfamily, member 10
ENSG00000049249	Tumor necrosis factor receptor superfamily, member 9
ENSG00000164938	Tumor protein p53 inducible nuclear protein 1
ENSG00000141736	V-erb-b2 erythroblastic leukemia viral oncogene homolog 2

Table S3 Genes involved in steroid metabolism and biosynthesis affected following knockdown of TLR4

Ensemble Gene ID	Description
ENSG00000112972	3-hydroxy-3-methylglutaryl-Coenzyme A synthase 1 (soluble)
ENSG00000130208	Apolipoprotein C-I
ENSG00000133935	Chromosome 14 open reading frame 1
ENSG00000001630	Cytochrome P450, family 51, subfamily A, polypeptide 1
ENSG00000079459	Farnesyl-diphosphate farnesyltransferase 1
ENSG00000186480	Insulin induced gene 1
ENSG00000052802	Sterol-C4-methyl oxidase-like
ENSG00000109929	Sterol-C5-desaturase (ERG3 delta-5-desaturase homolog, S. cerevisiae)-like

Table S4 Cell adhesion associated genes deregulated following knockdown of TLR4

Ensemble Gene ID	Description
ENSG00000062038	Cadherin 3, type 1, P-cadherin (placental)
ENSG00000026508	CD44 molecule (Indian blood group)
ENSG00000162706	Cell adhesion molecule 3
ENSG00000163347	Claudin 1
ENSG00000213937	Claudin 9
ENSG00000108821	Collagen, type I, alpha 1
ENSG00000164692	Collagen, type I, alpha 2
ENSG00000115414	Fibronectin 1
ENSG00000091409	Integrin, alpha 6
ENSG00000196878	Laminin, beta 3
ENSG00000058085	Laminin, gamma 2
ENSG00000204287	Major histocompatibility complex, class II, DR alpha
ENSG00000105976	Met proto-oncogene (hepatocyte growth factor receptor)
ENSG00000101608	Myosin, light chain 12A, regulatory, non-sarcomeric
ENSG00000197822	Occludin pseudogene; occludin
ENSG00000051382	Phosphoinositide-3-kinase, catalytic, beta polypeptide
ENSG00000145675	Phosphoinositide-3-kinase, regulatory subunit 1 (alpha)
ENSG00000197646	Programmed cell death 1 ligand 2
ENSG00000167193	V-crk sarcoma virus CT10 oncogene homolog (avian)
ENSG00000141736	V-erb-b2 erythroblastic leukemia viral oncogene homolog 2

Olfactory Table S5 Olfactory receptor family members differentially expressed following knockdown of MAD2

Ensemble Gene ID	Description	Fold Change
Olfactory Receptors Upregulated		
ENSG00000198601	olfactory receptor, family 2, subfamily M, member 2	1.7
ENSG00000181009	olfactory receptor, family 52, subfamily N, member 5	1.7
ENSG00000178586	olfactory receptor, family 6, subfamily B, member 3	1.5
Olfactory Receptors Downregulated		
ENSG00000197887	olfactory receptor, family 1, subfamily S, member 2	1.6
ENSG00000221933	olfactory receptor, family 2, subfamily A, member 25	1.5
ENSG00000177476	olfactory receptor, family 2, subfamily G, member 3	1.7
ENSG00000204700	olfactory receptor, family 2, subfamily J, member 2	1.9
ENSG00000171180	olfactory receptor, family 2, subfamily M, member 4	1.7
ENSG00000180090	olfactory receptor, family 3, subfamily A, member 1	1.7
ENSG00000182974	olfactory receptor, family 4, subfamily M, member 2	1.5
ENSG00000167825	olfactory receptor, family 5, subfamily I, member 1	1.8
ENSG00000255012	olfactory receptor, family 5, subfamily M, member 1	2.1
ENSG00000184478	olfactory receptor, family 56, subfamily A, member 3	1.8

Tissue Microarray Maps

Tissue Microarray 1

	1	2	3	4	5	6	7	8	9	10	11	12	13	14	15
A	Tonsil	Tonsil	Tonsil	Colon	Colon	Colon	A3	A3	A3	S1	S1	S1	P1	P1	P1
B	Liver	Liver	Liver	Lung	Lung	Lung	A5	A5	A5	S5	S5	S5	P2	P2	P2
C	H05/9418 C8	H05/9418 C8	H05/9418 C8	H05/12122 B2	H05/12122 B2	H05/12122 B2	H06/6133 G7	H06/6133 G7	H06/6133 G7	H07/483 B5	H07/483 B5	H07/483 B5			
D	H05/4811 C13*	H05/4811 C13*	H05/4811 C13*	H05/6210 C2	H05/6210 C2	H05/6210 C2	H06/699 C3	H06/699 C3	H06/699 C3	H07/5081	H07/5081	H07/5081			
E	H05/12562 A2	H05/12562 A2	H05/12562 A2	H05/7364 A5	H05/7364 A5	H05/7364 A5	H06/866 A14	H06/866 A14	H06/866 A14	H08/1523 G4	H08/1523 G4	H08/1523 G4			
F	H05/12606 A18	H05/12606 A18	H05/12606 A18	H05/7480 C11	H05/7480 C11	H05/7480 C11	H06/9984 F3	H06/9984 F3	H06/9984 F3	H08/1970 A10	H08/1970 A10	H08/1970 A10			
G	H05/14076 A3	H05/14076 A3	H05/14076 A3	H05/8918 B4	H05/8918 B4	H05/8918 B4	H07/10545 J2	H07/10545 J2	H07/10545 J2	H08/3414	H08/3414	H08/3414			
H	H05/3015 C1	H05/3015 C1	H05/3015 C1	H06/12760 A3	H06/12760 A3	H06/12760 A3	H07/11712 F8	H07/11712 F8	H07/11712 F8	H09/0162 B3	H09/0162 B3	H09/0162 B3			
I	H05/4288 G17*	H05/4288 G17*	H05/4288 G17*	H06/13561 C4	H06/13561 C4	H06/13561 C4	H07/3270 A3	H07/3270 A3	H07/3270 A3	H09/11994 H3	H09/11994 H3	H09/11994 H3			
J	Kidney	Kidney	Kidney	H06/14633 B2	H06/14633 B2	H06/14633 B2	H07/4289 A5	H07/4289 A5	H07/4289 A5	H09/2707 C14	H09/2707 C14	H09/2707 C14			
K															

Tissue Microarray 2

	1	2	3	4	5	6	7	8	9	10	11	12	13	14	15
A	Tonsil	Tonsil	Tonsil	Colon	Colon	Colon	A3	A3	A3	S1	S1	S1	P1	P1	P1
B	Liver	Liver	Liver	Lung	Lung	Lung	A5	A5	A5	S5	S5	S5	P2	P2	P2
C	H09/3135 A13	H09/3135 A13	H09/3135 A13	H10/9547 B4*	H10/9547 B4*	H10/9547 B4*	H12/6241 A6	H12/6241 A6	H12/6241 A6	Kidney	Kidney	Kidney	Kidney	Kidney	Kidney
D	H09/4184 A7	H09/4184 A7	H09/4184 A7	H11/11223 C4	H11/11223 C4	H11/11223 C4	H12/7211 D22	H12/7211 D22	H12/7211 D22						
E	H09/5041 A19	H09/5041 A19	H09/5041 A19	H11/13117 A7	H11/13117 A7	H11/13117 A7	H13/ 12026 B10	H13/ 12026 B10	H13/ 12026 B10						
F	H09/5870 A10	H09/5870 A10	H09/5870 A10	H11/17539 E11	H11/17539 E11	H11/17539 E11	H13/2660A4	H13/2660A4	H13/2660A4						
G	H09/6445 C5*	H09/6445 C5*	H09/6445 C5*	H11/18895 C6	H11/18895 C6	H11/18895 C6	H13/4674 A4	H13/4674 A4	H13/4674 A4						
H	H09/9230 A2	H09/9230 A2	H09/9230 A2	H11/19281 A5	H11/19281 A5	H11/19281 A5									
I	H10/11400 A2	H10/11400 A2	H10/11400 A2	H11/4307 A3	H11/4307 A3	H11/4307 A3									
J	H10/12427 A17	H10/12427 A17	H10/12427 A17	H11/6464 A7	H11/6464 A7	H11/6464 A7									
K															

Buffers and Reagents: Western Blot

20X MOPS Gel Running Buffer
MOPS 104.6 g
Trizma Base 60.6 g
SDS 10 g
EDTA 3.0 g
Dissolve in 500ml of DH20
Needs to be PH 7.7

1X MOPS Gel Running Buffer
50mls 20X MOPS buffer
Add dH_2O to 1L

25X Tris Glycine Transfer Buffer
18.2g Trizma® base (Sigma-aldrich)
90g of glycine (Sigma-aldrich)
Mix well and Add dH_2O to 1L
The pH of the buffer is 8.3. Do not adjust with acid or base

1X Transfer Buffer
40ml 25X transfer buffer
200mls MeOH
760mls diH_20
Keep cold before use, can reuse.

Ponceau S stain 100ml
0.1g Ponceau S
0.1ml glacial acetic acid
Add dH_2O to 100ml

10X TBS-Tween (TBS-T)
12.11g Trizma base
87.6g NaCl S7653
5mls Tween
Add dH_2O to 1L

1X TBS-Tween (TBS-T)
100mls 10X TBST
Add dH_2O to 1L

Blocking Buffer (5% w/v)
2.5g of milk powder/2.5g BSA
50mls of 1X TBS-T

Coomassie Blue
0.25g of Brilliant Blue
90ml of Methanol:H_2O (Methanol: H_2O = 50mls:40mls)
10ml Glacial acetic acid

Destain solution
900ml Methanol: dH20 (Methanol: H_2O = 50mls:40mls)
100ml Glacial acetic acid

6X loading buffer (Laemeli Buffer)
50 mM Trizma-HCl
0.05% v/v bromophenol blue
10% w/v SDS
30% v/v glycerol
5.5% v/v β-mercaptoethanol

Additional Kaplan-Meir Curves: TMA Cohort

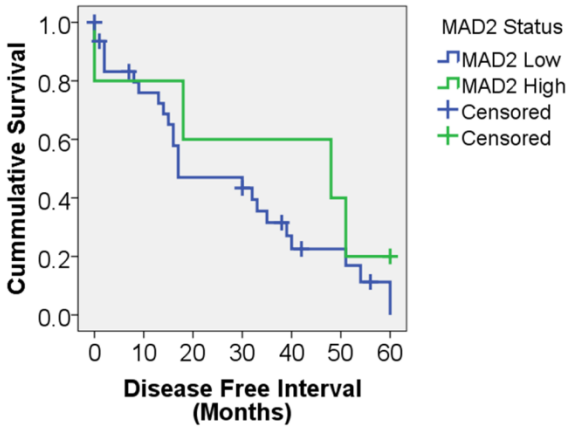

	MAD2 Low	MAD2 High	Significance
No. of Cases	31	5	0.300
No. of cases censored	7	1	
Mean Survival	27	35	
Median Survival	17	48	

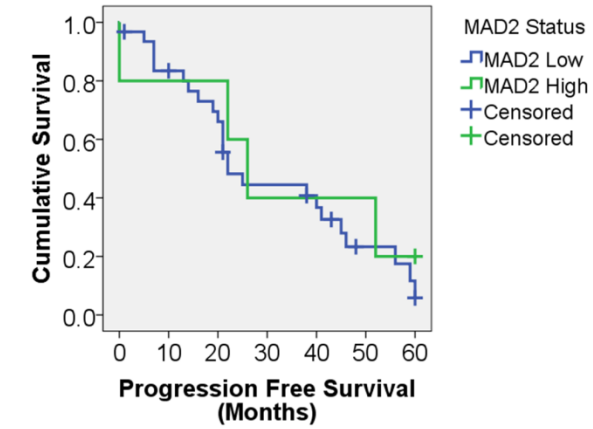

	MAD2 Low	MAD2 High	Significance
No. of Cases	31	5	0.560
No. of cases censored	7	1	
Mean Survival	31	32	
Median Survival	15	17	

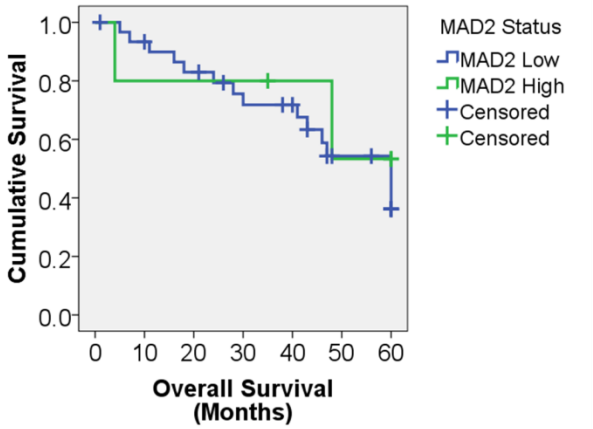

	MAD2 Low	MAD2 High	Significance
No. of Cases	31	5	0.640
No. of cases censored	16	3	
Mean Survival	45	46	
Median Survival	60	60	

MAD2 and patient prognosis. Patient samples within the TMA cohort were stained for MAD2. Patients who had a low MAD2 immunostaining score had a similar PFS and OS, compared to those with a high MAD2 score. Patients who had a low MAD2 immunostaining score also exhibited a reduction in their DFI compared to those with high MAD2 immunostaining score, although this was not significant.

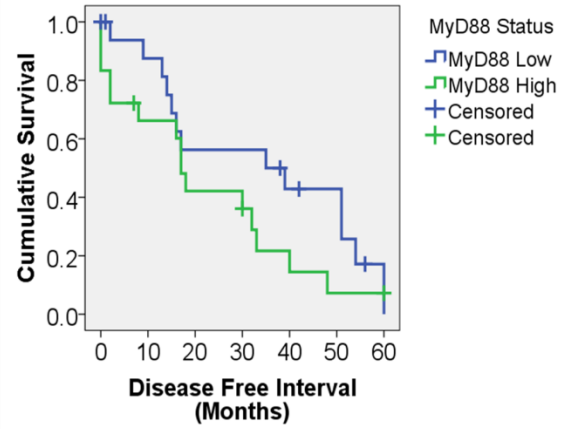

	MyD88 Low	MyD88 High	Significance
No. of Cases	18	18	0.163
No. of cases censored	5	3	
Mean Survival	34	21	
Median Survival	35	17	

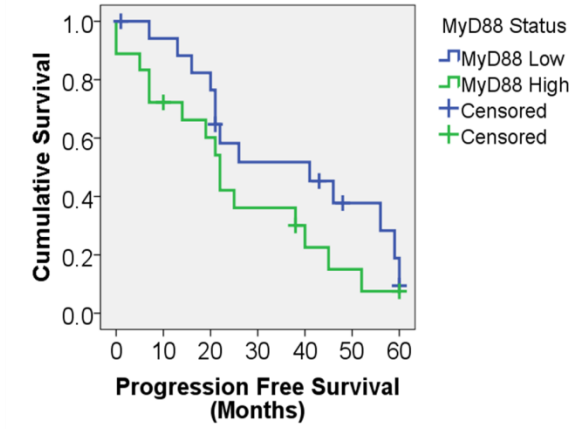

	MyD88 Low	MyD88 High	Significance
No. of Cases	18	18	0.146
No. of cases censored	5	3	
Mean Survival	38	26	
Median Survival	41	22	

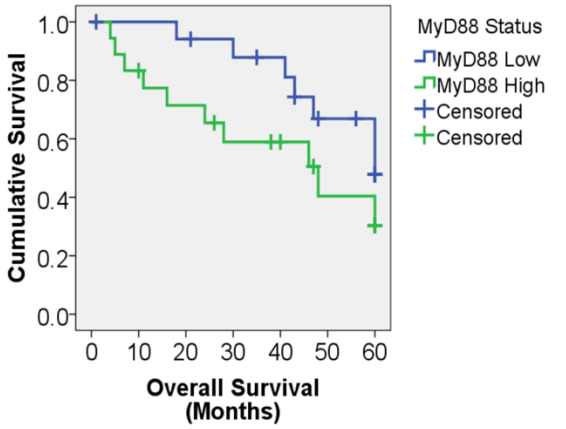

	MyD88 Low	MyD88 High	Significance
No. of Cases	18	18	0.126
No. of cases censored	11	8	
Mean Survival	52	39	
Median Survival	46	28	

MyD88 and patient prognosis. Patient samples within the TMA cohort were stained for MyD88. Patients who had a high MyD88 immunostaining score exhibited a reduction in their Mean and Median DFI, PFS and OS, although this was not significant. The results demonstrate that patients with a MyD88 high score had poorer prognosis than those with a MyD88 low score.

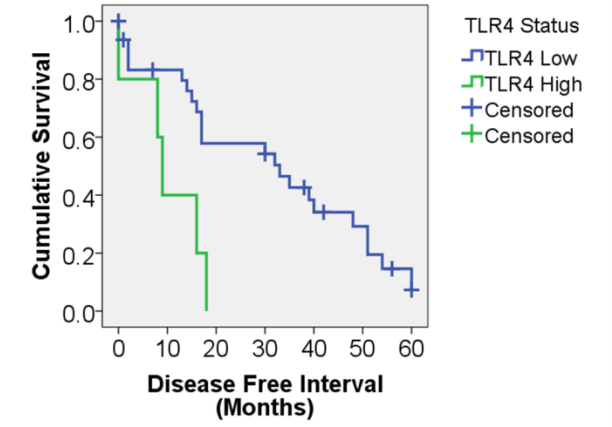

	TLR4 Low	TLR4 High	Significance
No. of Cases	31	5	0.006
No. of cases censored	8	0	
Mean Survival	31	10	
Median Survival	33	9	

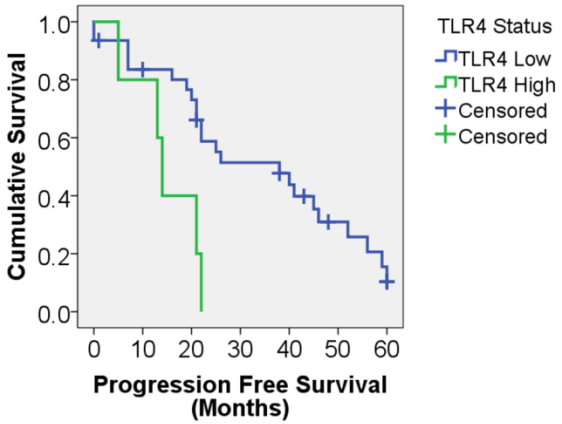

	TLR4 Low	TLR4 High	Significance
No. of Cases	31	5	0.007
No. of cases censored	8	0	
Mean Survival	34	15	
Median Survival	38	14	

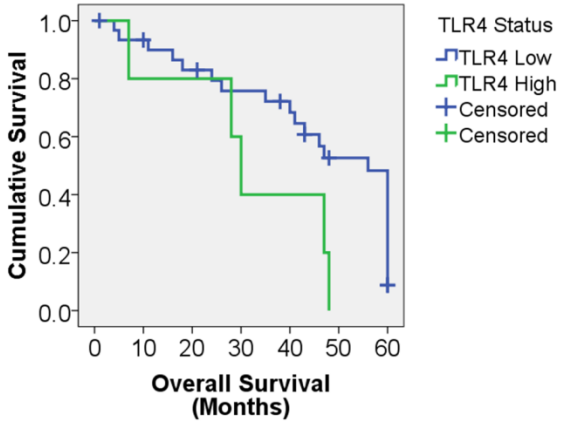

	TLR4 Low	TLR4 High	Significance
No. of Cases	31	5	0.049
No. of cases censored	8	0	
Mean Survival	49	32	
Median Survival	50	25	

TLR4 and patient prognosis. Patient samples within the TMA cohort were stained for TLR4. Patients who had a high TLR4 immunostaining score exhibited a significant reduction in both their mean and median DFI, PFS and OS, *p<0.05, **p<0.01.

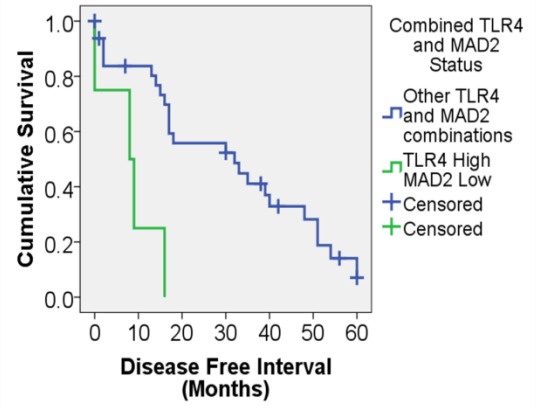

	Other TLR4 MAD2 combinations	TLR4 High MAD2 Low	Significance
No. of Cases	32	4	0.002
No. of cases censored	8	0	
Mean Survival	31	8	
Median Survival	32	8	

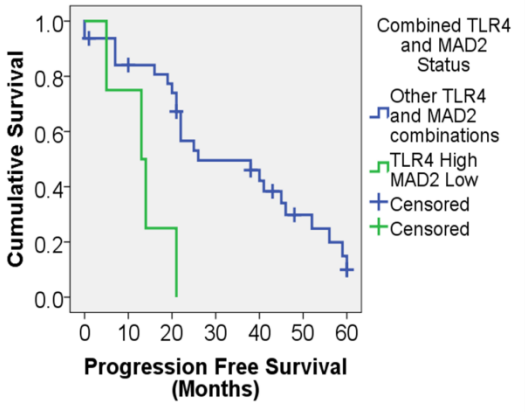

	Other TLR4 MAD2 combinations	TLR4 High MAD2 Low	Significance
No. of Cases	32	4	0.002
No. of cases censored	8	0	
Mean Survival	34	13	
Median Survival	26	13	

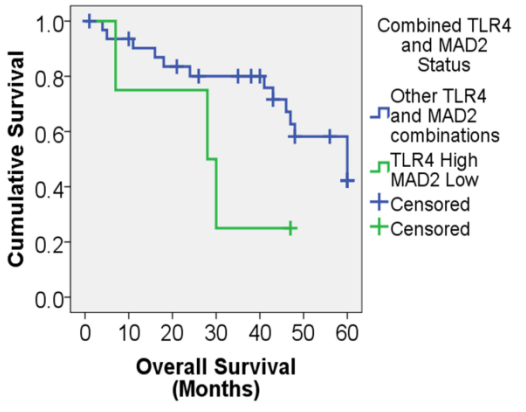

	Other TLR4 MAD2 combinations	TLR4 High MAD2 Low	Significance
No. of Cases	32	4	0.081
No. of cases censored	18	1	
Mean Survival	47	28	
Median Survival	60	28	

TLR4, MAD2 and patient prognosis. Patient samples within the TMA cohort were stained for TLR4 and MAD2. Patients who had a high TLR4 immunostaining and low MAD2 immunostaining score exhibited a reduction in both their mean and median progression free survival times and this was highly significant. Patients who had a high TLR4 immunostaining and Low MAD2 immunostaining score exhibited a significant reduction in both their mean and median DFI and PFS. They also exhibited a reduction in both their mean and median OS however this was just below significance, *p<0.05, **p<0.01.

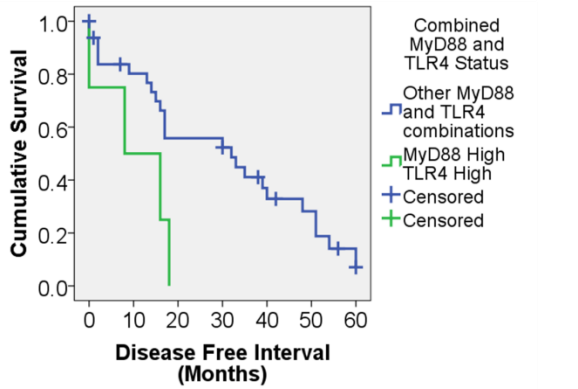

	Other MyD88 TLR4 combinations	MyD88 High TLR4 High	Significance
No. of Cases	32	4	0.023
No. of cases censored	8	0	
Mean Survival	30	11	
Median Survival	32	8	

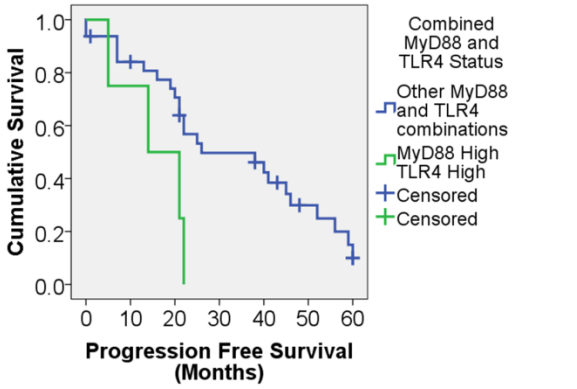

	Other MyD88 TLR4 combinations	MyD88 High TLR4 High	Significance
No. of Cases	32	4	0.029
No. of cases censored	8	0	
Mean Survival	33	16	
Median Survival	26	14	

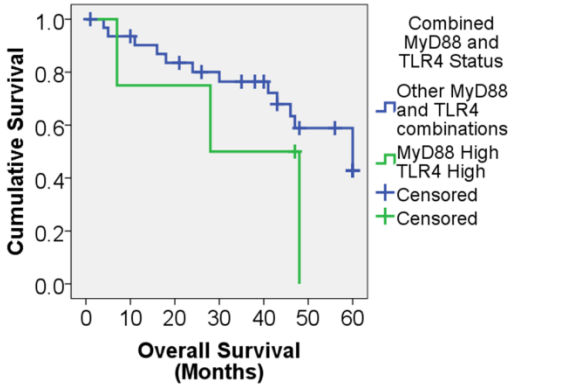

	Other MyD88 TLR4 combinations	MyD88 High TLR4 High	Significance
No. of Cases	32	4	0.189
No. of cases censored	18	1	
Mean Survival	47	32	
Median Survival	60	28	

MyD88, TLR4, and patient prognosis. Patient samples within the TMA cohort were stained for MyD88 and TLR4. Patients who had a high MyD88 and a high TLR4 immunostaining score exhibited a significant reduction in both their mean and median DFI and PFS. Patients with a high MyD88 and a high TLR4 immunostaining score also exhibited a reduction in both their mean and median OS, however this was not significant, *p<0.05.

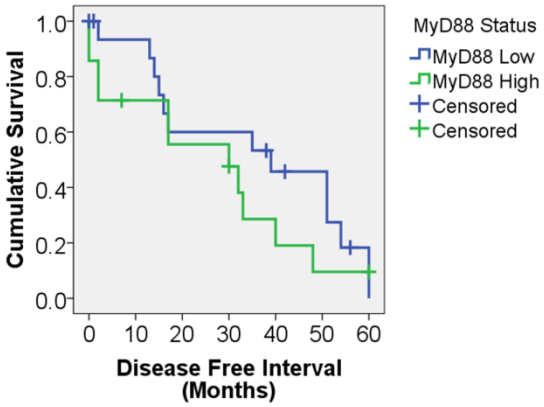

	MyD88 Low	MyD88 High	Significance
No. of Cases	17	14	0.300
No. of cases censored	5	3	
Mean Survival	36	26	
Median Survival	39	30	

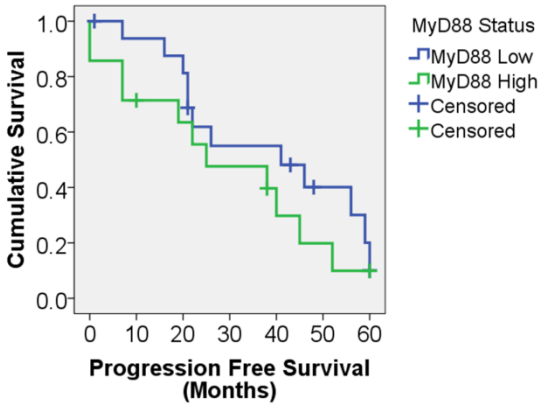

	MyD88 Low	MyD88 High	Significance
No. of Cases	17	14	0.278
No. of cases censored	5	3	
Mean Survival	39	29	
Median Survival	41	25	

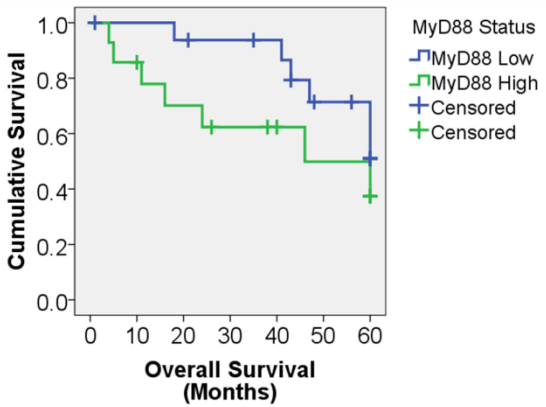

	MyD88 Low	MyD88 High	Significance
No. of Cases	17	14	0.179
No. of cases censored	11	7	
Mean Survival	54	40	
Median Survival	60	46	

MyD88 expression in patients with low TLR4 expression and patient prognosis. Patient samples within the TMA cohort were stained for MyD88 and TLR4. Patients who had a high MyD88 immunostaining score within in low TLR4 expression group exhibited a reduction in both their mean and median DFI, PFS and OS, however this was not significant.

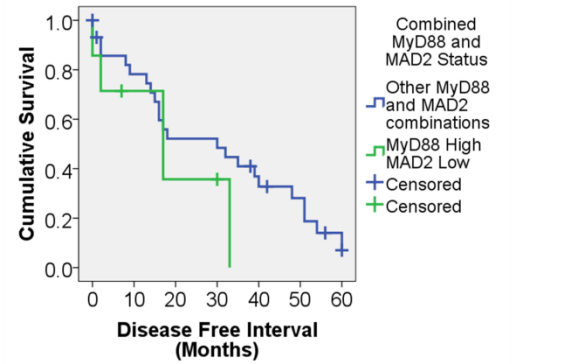

	Other MyD88 MAD2 combinations	MyD88 High MAD2 Low	Significance
No. of Cases	29	7	0.299
No. of cases censored	6	2	
Mean Survival	30	18	
Median Survival	30	17	

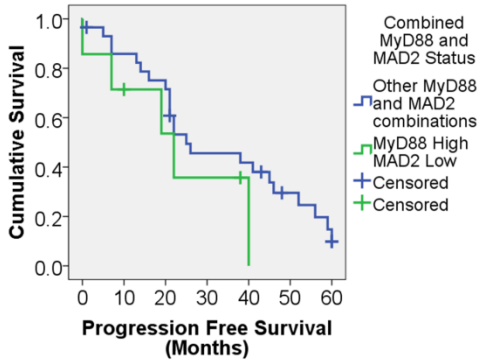

	Other MyD88 MAD2 combinations	MyD88 High MAD2 Low	Significance
No. of Cases	29	7	0.267
No. of cases censored	6	2	
Mean Survival	33	23	
Median Survival	25	22	

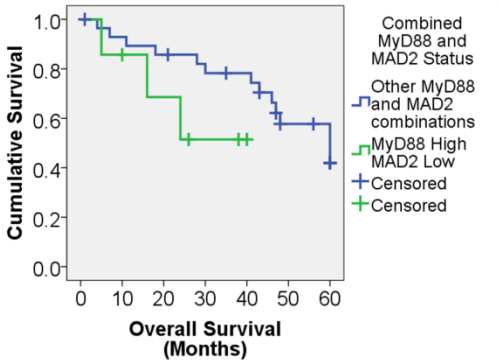

	Other MyD88 MAD2 combinations	MyD88 High MAD2 Low	Significance
No. of Cases	29	7	0.126
No. of cases censored	15	4	
Mean Survival	47	28	
Median Survival	60	60	

MyD88, MAD2, and patient prognosis. Patient samples within the TMA cohort were stained for MyD88 and MAD2. Patients who had a high MyD88, and low MAD2 immunostaining score exhibited a small reduction in both their mean and median disease free intervals however this was not significant. Patients who had a high MyD88, and low MAD2 immunostaining score exhibited a small reduction in both their mean and median DFI, PFS and OS, although this was not significant. These results demonstrate that those with high MyD88 and low MAD2 expression have poorer outcomes.

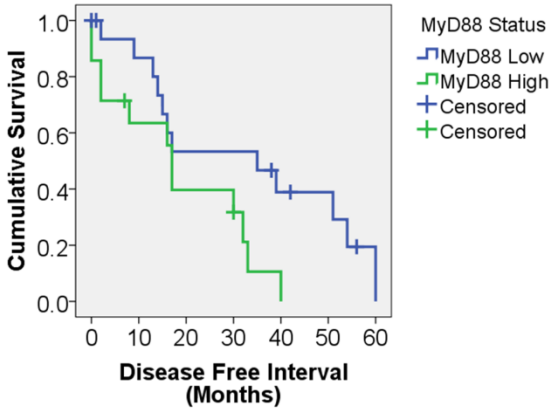

	MyD88 Low	MyD88 High	Significance
No. of Cases	17	14	0.039
No. of cases censored	5	2	
Mean Survival	33	18	
Median Survival	35	17	

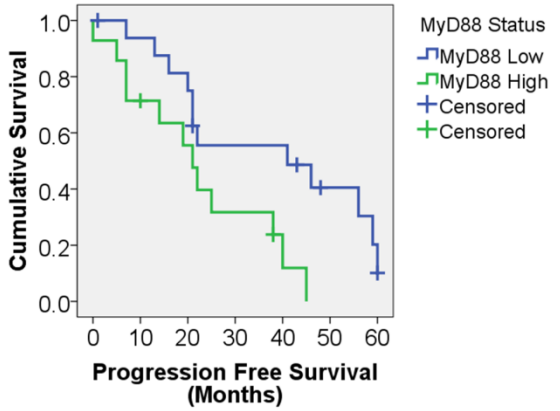

	MyD88 Low	MyD88 High	Significance
No. of Cases	17	14	0.018
No. of cases censored	5	2	
Mean Survival	38	23	
Median Survival	41	21	

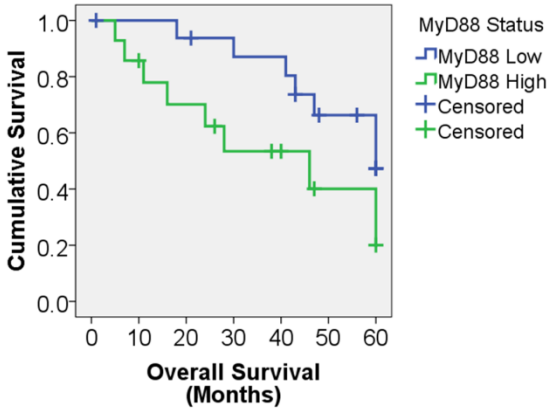

	MyD88 Low	MyD88 High	Significance
No. of Cases	17	14	0.062
No. of cases censored	10	6	
Mean Survival	52	38	
Median Survival	60	46	

MyD88 expression in patients with low MAD2 expression and its effect on patient prognosis. Patients who had a high MyD88 immunostaining score in low MAD2 expression group had a significant reduction in their DFI and PFS, They also exhibited a reduction in their OS, but this was not significant, *p<0.05.

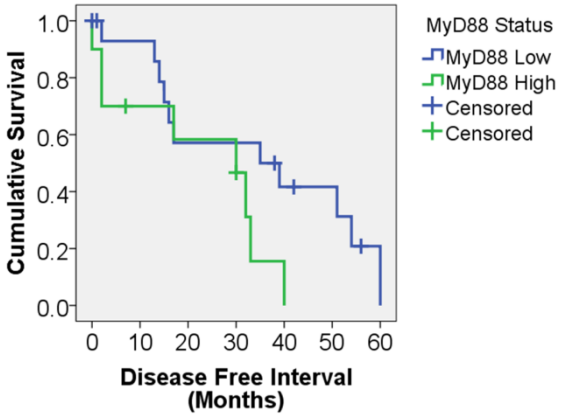

	MyD88 Low	MyD88 High	Significance
No. of Cases	16	10	0.094
No. of cases censored	5	2	
Mean Survival	34	22	
Median Survival	35	30	

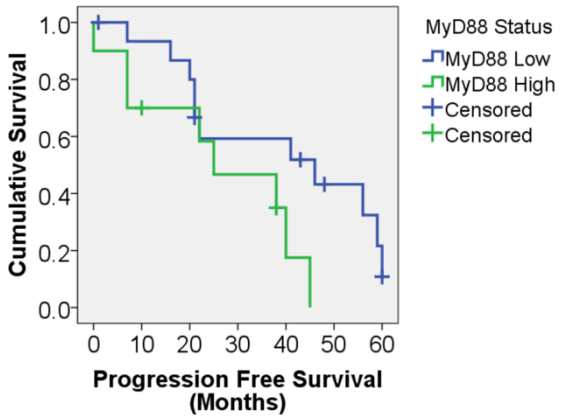

	MyD88 Low	MyD88 High	Significance
No. of Cases	16	10	0.062
No. of cases censored	5	2	
Mean Survival	40	26	
Median Survival	46	25	

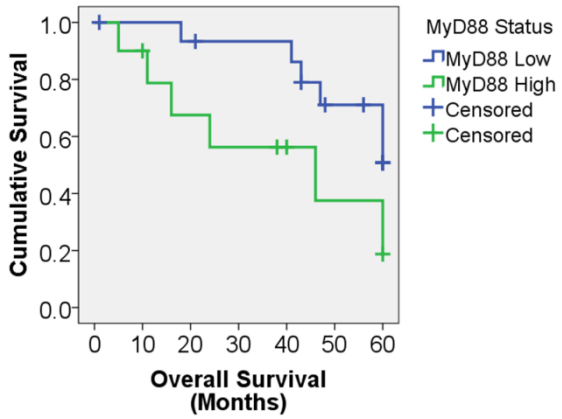

	MyD88 Low	MyD88 High	Significance
No. of Cases	16	10	0.048
No. of cases censored	10	4	
Mean Survival	54	37	
Median Survival	60	46	

MyD88 expression in patients with low MAD2 and low TLR4 expression and its effect on patient prognosis. Patients who had a high MyD88 immunostaining score in the low MAD2 and low TLR4 expression group had a significant reduction in their PFS, They also exhibited a reduction in their DFI, OS, but this was not significant, *p<0.05.

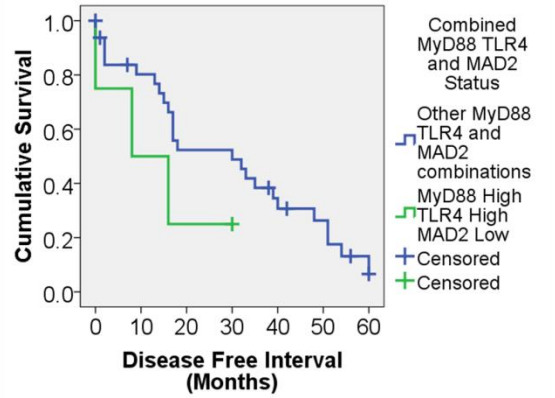

	Other MyD88 TLR4 MAD2 combinations	MyD88 High TLR4 High MAD2 Low	Significance
No. of Cases	32	4	0.197
No. of cases censored	7	1	
Mean Survival	30	14	
Median Survival	30	8	

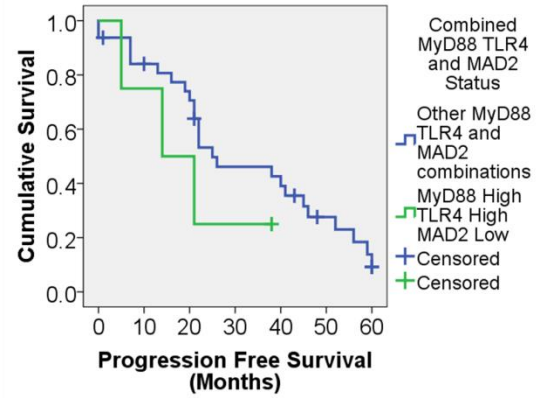

	Other MyD88 TLR4 MAD2 combinations	MyD88 High TLR4 High MAD2 Low	Significance
No. of Cases	32	4	0.288
No. of cases censored	7	1	
Mean Survival	32	20	
Median Survival	25	14	

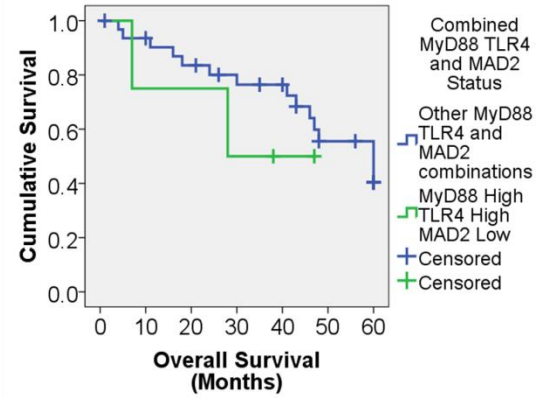

	Other MyD88 TLR4 MAD2 combinations	MyD88 High TLR4 High MAD2 Low	Significance
No. of Cases	32	4	0.435
No. of cases censored	17	2	
Mean Survival	47	32	
Median Survival	60	28	

MyD88, TLR4, MAD2, and patient prognosis. Patient samples within the TMA cohort were stained for MyD88 and TLR4. Patients who had a high MyD88, High TLR4 and Low MAD2 immunostaining score exhibited a reduction in both their mean and median DFI, PFS and OS, although this was not significant.

Additional Kaplan-Meir Curves: PMR Cohort

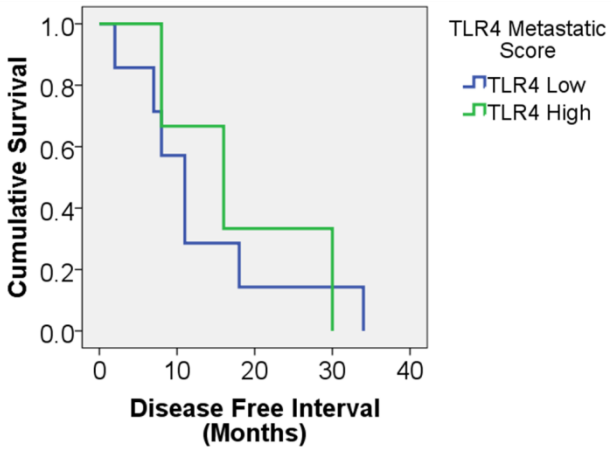

TLR4 Metastatic Score	TLR4 Low	TLR4 High	Significance
No. of Cases	7	3	0.782
No. of cases censored	0	0	
Mean Survival	13	18	
Median Survival	11	16	

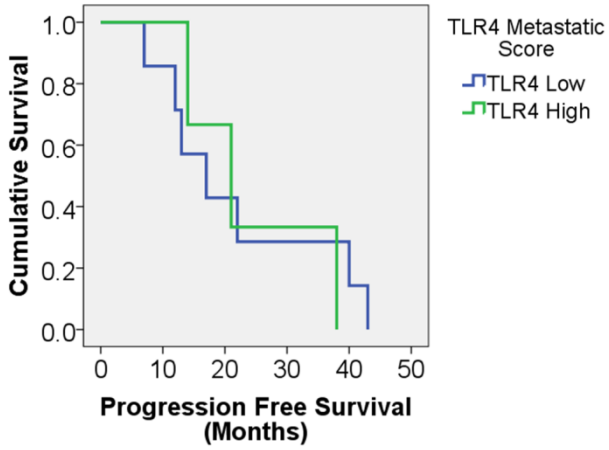

TLR4 Metastatic Score	TLR4 Low	TLR4 High	Significance
No. of Cases	7	3	0.854
No. of cases censored	0	0	
Mean Survival	22	17	
Median Survival	24	21	

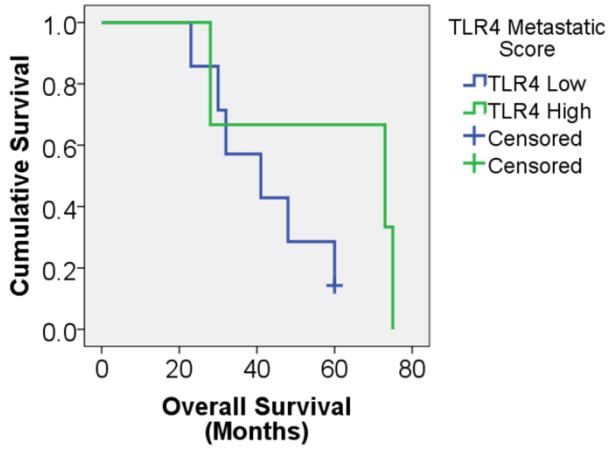

TLR4 Metastatic Score	TLR4 Low	TLR4 High	Significance
No. of Cases	7	3	0.258
No. of cases censored	1	0	
Mean Survival	42	59	
Median Survival	41	73	

TLR4 expression during metastasis and patient prognosis. Patient samples within the PMR study cohort were stained for TLR4. TLR4 expression patterns in metastatic omentum were then correlated with patient prognosis. In metastatic omental disease patients who had a high TLR4 immunostaining score exhibited minor reduction in their median PFS, compared to those with high TLR4 score, however patients with TLR4 low score had a slight reduction in their mean and median DFI and OS.

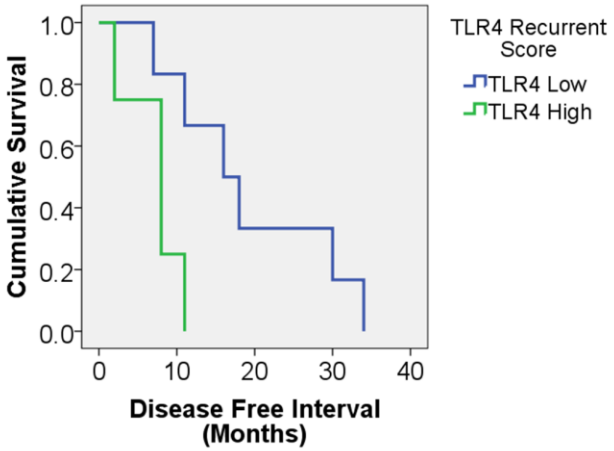

TLR4 Recurrent Score	TLR4 Low	TLR4 High	Significance
No. of Cases	6	4	0.036
No. of cases censored	0	0	
Mean Survival	19	7	
Median Survival	16	8	

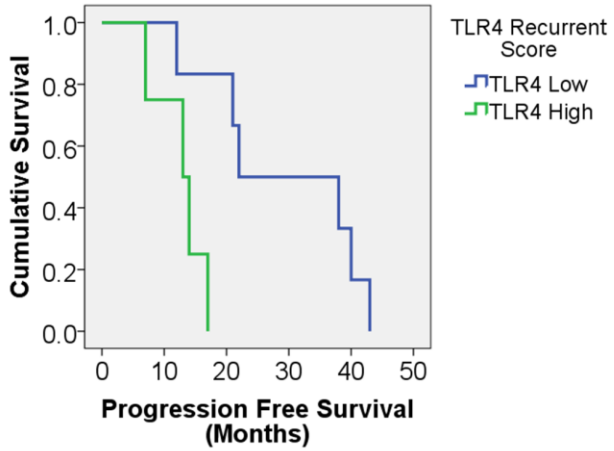

TLR4 Recurrent Score	TLR4 Low	TLR4 High	Significance
No. of Cases	6	4	0.017
No. of cases censored	0	0	
Mean Survival	29	13	
Median Survival	22	13	

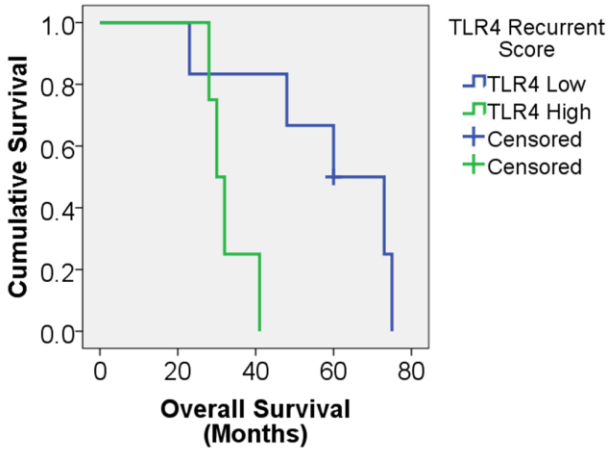

TLR4 Recurrent Score	TLR4 Low	TLR4 High	Significance
No. of Cases	6	4	0.024
No. of cases censored	1	0	
Mean Survival	59	33	
Median Survival	60	30	

TLR4 expression during disease recurrence and patient prognosis. Patient samples within the PMR study cohort were stained for TLR4. TLR4 expression patterns during disease recurrence were then correlated with patient prognosis. In recurrent disease patients who had a high TLR4 immunostaining score exhibited significant reductions in their mean and median DFI, PFS and OS compared to those with high TLR4 score, p,<0.05.

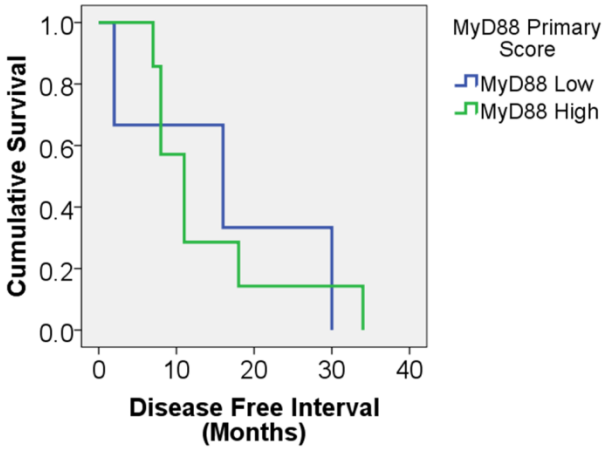

MyD88 Primary Score	MyD88 Low	MyD88 High	Significance
No. of Cases	3	7	0.987
No. of cases censored	0	0	
Mean Survival	16	14	
Median Survival	16	11	

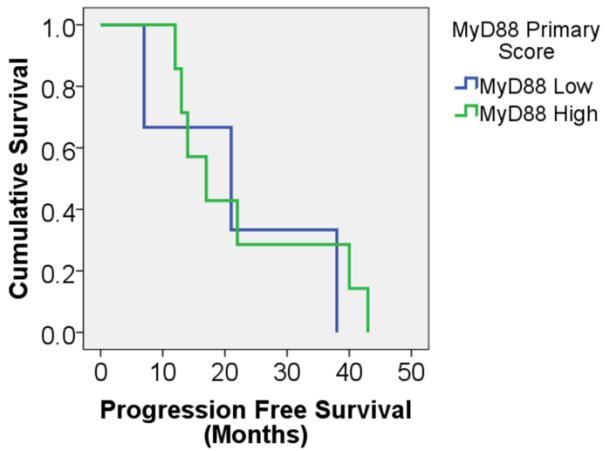

MyD88 Primary Score	MyD88 Low	MyD88 High	Significance
No. of Cases	3	7	0.626
No. of cases censored	0	0	
Mean Survival	22	23	
Median Survival	21	17	

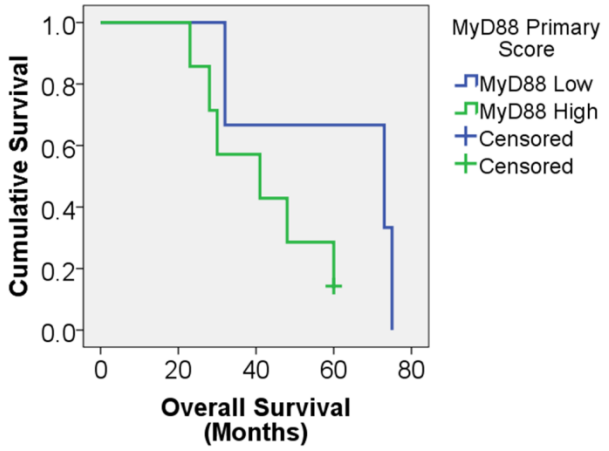

MyD88 Primary Score	MyD88 Low	MyD88 High	Significance
No. of Cases	3	7	0.190
No. of cases censored	0	1	
Mean Survival	60	41	
Median Survival	73	41	

MyD88 expression and primary disease. Patient samples within the PMR study cohort were stained for MyD88. MyD88 expression patterns during primary disease were then correlated with patient prognosis. Patients who had a high MyD88 immunostaining score exhibited reductions in their mean and median DFI, PFS and OS compared to those with low MyD88 score.

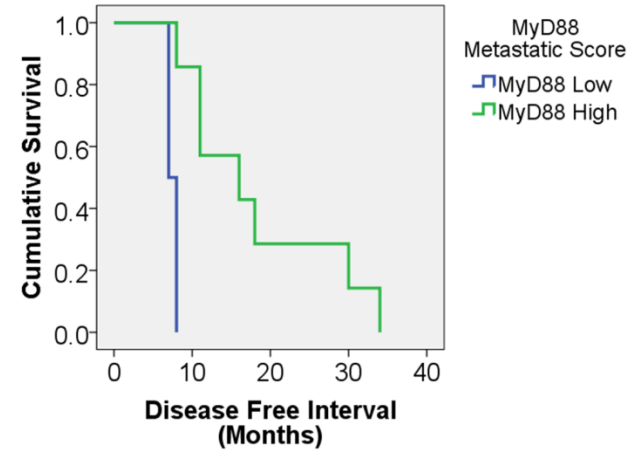

MyD88 Metastatic Score	MyD88 Low	MyD88 High	Significance
No. of Cases	2	7	0.011
No. of cases censored	0	0	
Mean Survival	8	18	
Median Survival	7	16	

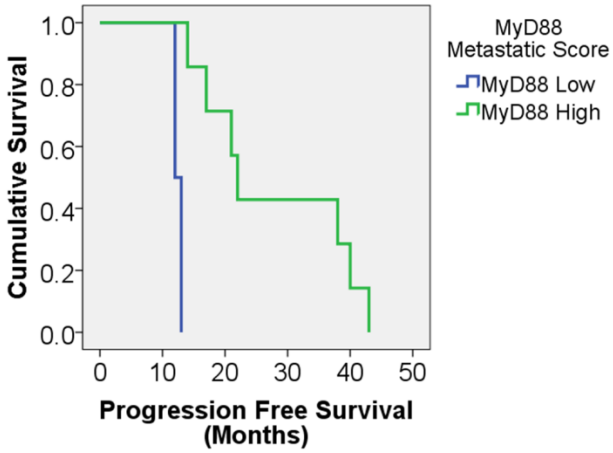

MyD88 Metastatic Score	MyD88 Low	MyD88 High	Significance
No. of Cases	2	7	0.002
No. of cases censored	0	0	
Mean Survival	13	28	
Median Survival	12	22	

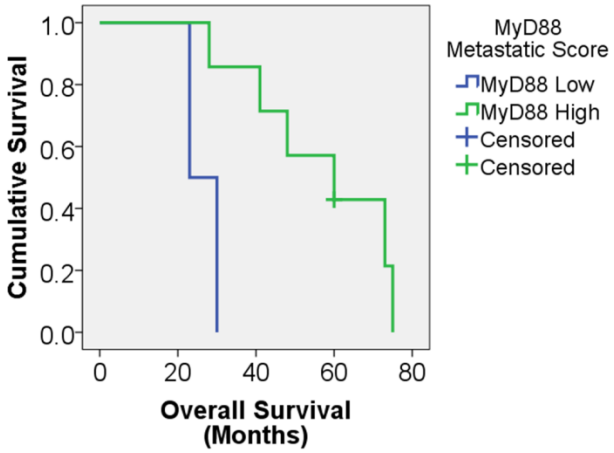

MyD88 Metastatic Score	MyD88 Low	MyD88 High	Significance
No. of Cases	2	7	0.018
No. of cases censored	0	1	
Mean Survival	27	57	
Median Survival	23	60	

MyD88 expression and metastatic disease. Patient samples within the PMR study cohort were stained for MyD88. MyD88 expression patterns during metastatic disease were then correlated with patient prognosis. Patients who had a low MyD88 immunostaining score exhibited reductions in their mean and median DFI, PFS and OS compared to those with a high MyD88 score, *p<0.05, **p<0.01.

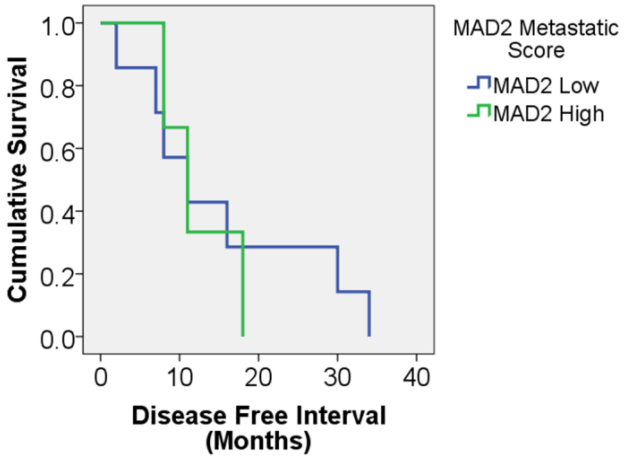

MAD2 Metastatic Score	MAD2 Low	MAD2 High	Significance
No. of Cases	7	3	0.772
No. of cases censored	0	0	
Mean Survival	15	12	
Median Survival	11	11	

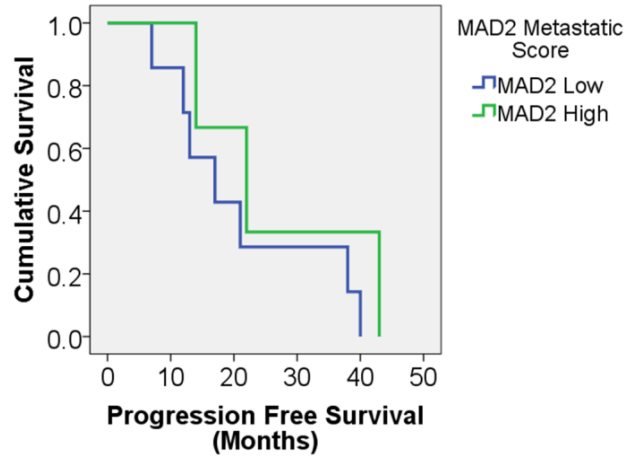

MAD2 Metastatic Score	MAD2 Low	MAD2 High	Significance
No. of Cases	7	3	0.299
No. of cases censored	0	0	
Mean Survival	21	26	
Median Survival	17	22	

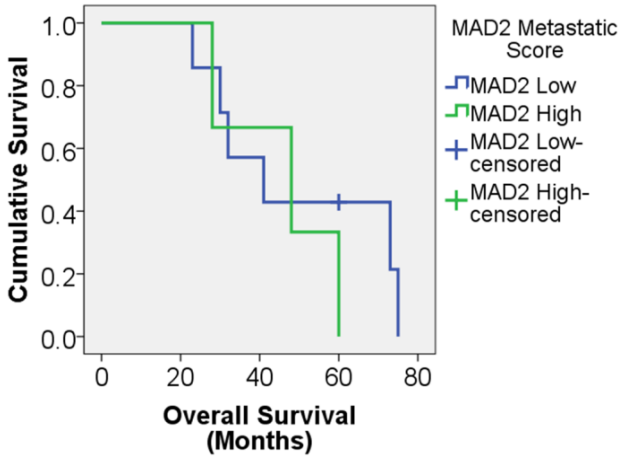

MAD2 Recurrent Score	MAD2 Low	MAD2 High	Significance
No. of Cases	3	7	0.084
No. of cases censored	0	0	
Mean Survival	14	27	
Median Survival	13	22	

MAD2 expression during metastasis and patient prognosis. Patient samples within the PMR study cohort were stained for MAD2. MAD2 expression patterns during omental metastasis were then correlated with patient prognosis. In metastatic omental disease patients who had a low MAD2 immunostaining score had exhibited minor reduction in their median DFI, PFS and OS compared to those with high MAD2 score.

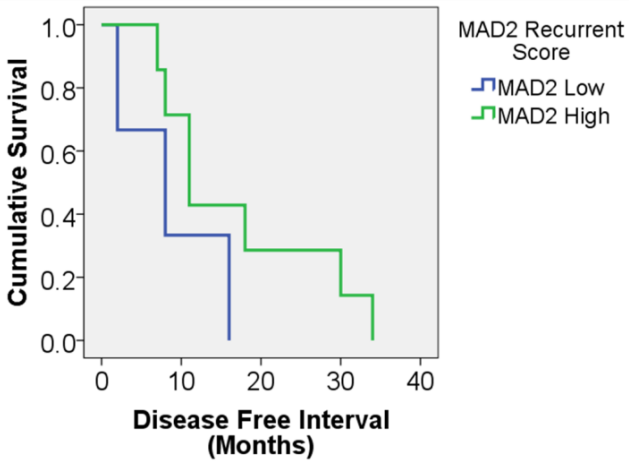

MAD2 Recurrent Score	MAD2 Low	MAD2 High	Significance
No. of Cases	3	7	0.186
No. of cases censored	0	0	
Mean Survival	9	17	
Median Survival	8	11	

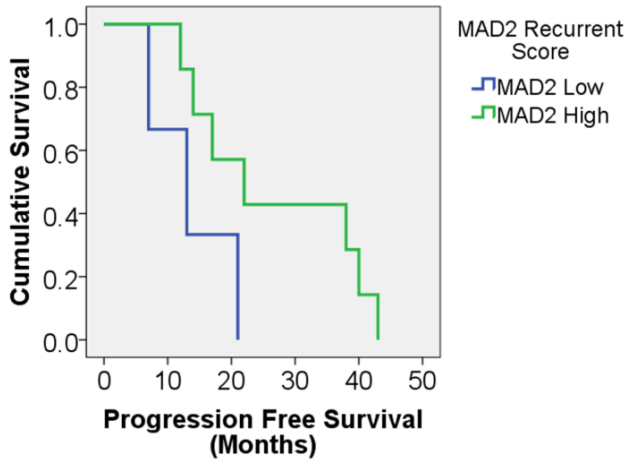

MAD2 Recurrent Score	MAD2 Low	MAD2 High	Significance
No. of Cases	3	7	0.084
No. of cases censored	0	0	
Mean Survival	14	27	
Median Survival	13	22	

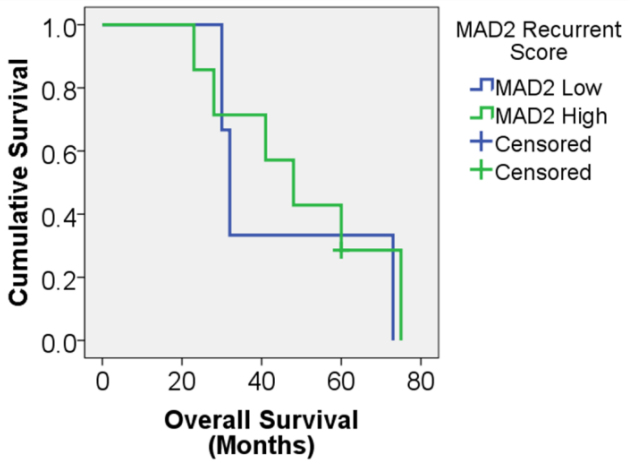

MAD2 Recurrent Score	MAD2 Low	MAD2 High	Significance
No. of Cases	3	7	0.642
No. of cases censored	1	0	
Mean Survival	45	50	
Median Survival	32	48	

MAD2 expression during recurrent disease and patient prognosis. Patient samples within the PMR study cohort were stained for MAD2. MAD2 expression patterns during disease recurrence were then correlated with patient prognosis. In recurrent disease patients who had a low MAD2 immunostaining score exhibited small reductions in their mean and median DFI, PFS and OS compared to those with high MAD2 score.